UNIVERSITY OF SOUTHAMPTON

FACULTY OF NATURAL AND ENVIRONMENTAL SCIENCES

Ocean and Earth Science

2016/2017

STABLE ISOTOPE ANALYSIS OF FISH EYE LENSES: RECONSTRUCTION OF ONTOGENETIC TRENDS IN SPATIAL AND TROPHIC ECOLOGY OF ELASMOBRANCHS AND DEEP-WATER TELEOSTS

by

Katie Quaeck

Thesis for the degree of Doctor of Philosophy

August 2017

Abstract

Studying ontogenetic trends in diet and habitat use of endangered sharks and deep-water teleosts is logistically challenging and expensive, due to the remote and inaccessible nature of the pelagic realm, and the extent of many marine migrations. Chemical analysis of inert, organic, incrementally formed tissues represents a window to retrospectively study whole life-history ecology, however these tissues are rare or absent in many fishes.

The fish eye lens is a unique tissue, formed via the sequential deposition of protein-filled fiber cells, which undergo no subsequent remodelling once formed. Despite having great potential to record chemical variations reflecting foraging behaviour, lenses have received relatively little analytical attention. In this thesis I have explored the suitability of fish lenses for recovery of retrospective ontogenetic chemical information, focusing particularly on pre-birth and early juvenile life histories in elasmobranchs.

I have confirmed consistent relationships between the body size and lens diameter of four study species (*Aphonopus carbo*, *Coryphaenoides rupestris*, *Lamna nasus* and *Squalus acanthias*), which allows recovery of a body size-referenced lens samples. Growth relationships reveal that a large proportion of lens tissue in elasmobranchs is deposited pre-birth, opening a previously unrecognised opportunity to study maternal provisioning from tissues of the offspring as adults. I have confirmed that transects of stable isotope compositions across lenses show bilateral symmetry, reflecting the sequential deposition of eye lens tissue. Muscle-lens tissue offsets were examined in *S. acanthias* and *C. rupestris*, identifying the potential for species-specific differences, possibly driven by variability in taxon-specific lens protein expression.

I have then applied the validated lens sampling protocol to recover cross-generational life history movement and diet ecology information in three study species. Focusing on pre-birth ecology requires some understanding of the isotopic relationship between maternal and embryonic tissues. With access to gravid female spiny dogfish, isotopic spacing between maternal and offspring tissues was investigated. However, the measured mother-embryo isotopic offsets are confounded by migration across isotopic provinces, introducing considerable temporal de-coupling between nutrient assimilation fuelling maternal tissue remodelling and yolk sac provisioning, particularly in species with a long gestation period.

For the spiny dogfish *Squalus acanthias* recovered from the North Sea, lens-derived isotope histories revealed that, whilst the southern and central North Sea represent important foraging areas during mature life history, the northern North Sea is more important during gestation, pupping, and early life history.

Similarly, porbeagle (*L. nasus*) lens chemistry indicates that the mothers of individuals caught in the Celtic Sea region forage over a wide area of the north Atlantic. Attracting mothers from a wide geographical area, this nursery area is likely to be important for the conservation of the endangered northeast Atlantic population, where mitigating discarding is a priority to fisheries managers.

The isotopic variability of sequential *A. carbo* lens samples was also investigated in order to address trends in foraging and location throughout individual life history. Lens data provide further evidence of ontogenetic depth and latitudinal movements, consistent with the species' ontogenetic migration theory.

Obtaining a near whole life history record of information relating to an individual's trophic and spatial ecology using traditional tagging methods is challenging, if not impossible. The lens therefore represents a valuable chemical repository for high-resolution ecological information that can be analysed retrospectively.

Contents

CHAPTER 2: TELEOST AND ELASMOBRANCH EYE LENSES AS A TARGET FOR ONTOGENETIC STABLE ISOTOPE ANALYSES

CHAPTER 3: STABLE CARBON AND NITROGEN ISOTOPE FRACTIONATION BETWEEN MATERNAL AND OFFSPRING TISSUES IN AN APLACENTAL SHARK, SQUALUS ACANTHIAS: IMPLICATION FOR RECOVERY OF CROSS-GENERATIONAL TROPHO-SPATIAL INFORMATION

List of Tables

List of Figures

CHAPTER 1

CHAPTER 2

DECLARATION OF AUTHORSHIP

I, KATIE QUAECK

declare that this thesis and the work presented in it are my own and has been generated by me as the result of my own original research.

STABLE ISOTOPE ANALYSIS OF FISH EYE LENSES: RECONSTRUCTION OF ONTOGENETIC TRENDS IN INSPATIAL AND TROPHIC ECOLOGY OF ELASMOBRANCHS AND DEEP-WATER TELEOSTS

I confirm that:

1. This work was done wholly or mainly while in candidature for a research degree at this University;
2. Where any part of this thesis has previously been submitted for a degree or any other qualification at this University or any other institution, this has been clearly stated;
3. Where I have consulted the published work of others, this is always clearly attributed;
4. Where I have quoted from the work of others, the source is always given. With the exception of such quotations, this thesis is entirely my own work;
5. I have acknowledged all main sources of help;
6. Where the thesis is based on work done by myself jointly with others, I have made clear exactly what was done by others and what I have contributed myself;
7. None of this work has been published before submission

Signed:

Date: August 19th, 2017

Acknowledgements

First and foremost, I would like to thank my supervisor, Dr. Clive Trumean, for his continuous support throughout my PhD studies. I am eternally grateful to him for his guidance, encouragement and patient perseverance. Many thanks are also due to my second supervisor, Dr. Kirsteen MacKenzie, for her advice and insightful comments, and to Prof. Martin Palmer and Prof. Gavin Foster for their direction during the early stages of my research.

I would like to express my gratitude to NERC for funding the research, and to Cefas for providing essential samples and Seedcorn funding. Thanks also to Victoria Bendall, for her expertise.

I am also hugely indebted to all the those in the SUMIE research group, for their support and advice: Sarah Magozzi, Ming-Tsung Chung, Rhiannon Meier, Diana Shores, Rui Pedro Vieira, Christopher Bird, Clare Prebble, Katie St John Glew and Matthew Cobain. To the technical and support staff at the National Oceanography Centre, including Matt O'Shaughnessey, Nicola Pratt and Dan Dornan, thank your for putting up with my tireless nagging! Bob Jones and John Ford deserve a special mention. Thank you for your practical and moral support, and the coffee!

It gives me great pleasure to acknowledge the people who mean the world to me. A very special thanks is reserved for my wonderful parents, for their emotional, practical and financial support over the years. Thank you for believing in me and allowing me to realize my potential. To my husband, Rich, thank you for all you've sacrificed to allow me to do what I love. Finally, to my mischievous boy, Hari, thank you for putting the biggest smile on my face, every single day.

Chapter 1: Thesis introduction

1.1 An introduction to spatial and trophic ecology

A species' distribution in the natural world is neither uniform nor random, resulting in the occurrence of spatial trends and patterns, or patchiness (Legendre & Fortin, 1989). Biogeography (or spatial ecology) refers to the study of the driving forces and consequences of this distribution (over time and space), uniting the fields of population biology and ecosystem science (Levin, 1992). Focussing on understanding how individual movement patterns affect communities, populations and ecosystems (Hastings *et al.* 2011), the analysis of spatial trends has been applied to the fields of wildlife management and conservation (Yahner, 1988; Riley, 2006), carbon sequestration (Field *et al*. 1998; Trueman *et al.* 2014) and population ecology (Homes *et al*. 1994; Tilman *et al*. 1997), to name but a few.

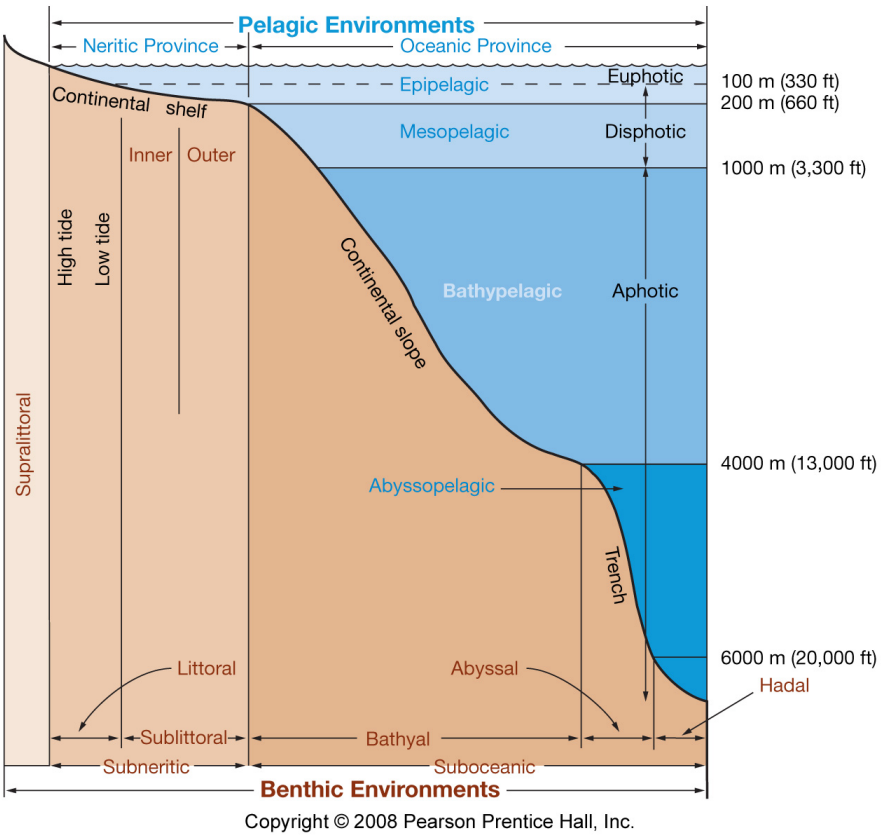

Figure 1.1 - Horizontal and vertical zonation in the pelagic environment (Source: Pearson Prentice Hall).

Given that nature rarely conforms to a set order, observational data are preferable to modelled output in order to address spatial ecology questions (Perry *et al*. 2002). Identification of the spatial extent of a species' distribution allows determination of whether specific movement patterns occur over a local, regional or global scale. In reality, achieving benchmark survey data is extremely challenging, particularly in the field of marine science, where there is potential for large-scale movements and distribution. Moreover, in the pelagic realm (Figure 1.1), direct observation is unfeasible, due to the remoteness of the open ocean, and the inaccessible nature of the deep-sea. These challenges combined with financial restrictions and project time constraints, makes the direct observation of a species' spatial distribution difficult. Whilst advances in tagging technology (Block *et al.* 2011) permit reconstruction of accurate and precise movements tracks, failed data transmission and premature detachment are persistent problems (e.g. Aaerstrup *et al.* 2009; Bendall *et al*. 2013; Biais *et al*. 2017). Relying on locating individuals in the first instance (which is notoriously challenging in the case of elusive pelagic sharks), electronic tags are typically deployed for a period of <1 year, and thus only provide a snap-shop of ontogenetic movements. Moreover, the cost of electronic tags often prevents the tagging of a large number of individuals (Hussey *et al*. 2015).

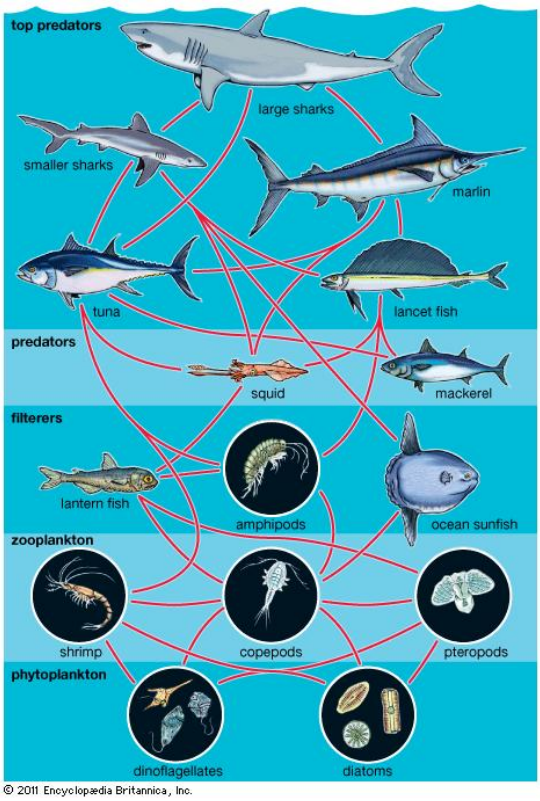

Figure 1.2 – Example of marine food web (Source: britannica.com)

The field of trophic ecology concerns the study of feeding relationships between organisms within an ecosystem, involving the reconstruction of diets (Minson *et al*. 1975; Tieszen *et al*. 1983; Samelius *et al*. 2007), assignment of species to trophic positions within food webs (e.g. Figure 1.2) (Minagawa & Wada, 1984; Fry, 1991; Post, 2002), elucidation of trends in resource location, acquisition and allocation (O'Brien *et al*. 2000; Cherel *et al*. 2005; Waas *et al*. 2010), and niche characterization (Genner *et al*. 1999; Bearhop *et al*. 2004; Newsome *et al*. 2007).

Ontogenetic shifts in spatial and trophic dynamics are ubiquitous in the natural world (Morris, 2003), as life-history requirements drive changes in location and foraging behavior (Carlisle *et al.* 2012). Habitat use and diet are therefore closely coupled. For example, habitat selection does not occur independently of resource availability, quality and competition (Fretwell & Lucas, 1970; Rosenzweig, 1981; Morris, 1988). Risk of predation may also play a role in structuring a species' distribution (Brown, 1988; 1992; Abrahams & Dill, 1989; Lima & Dill, 1990; Kotler & Blaustein, 1995; Brown *et al*. 1999). Life histories cannot evolve detached from the habitats they occupy (McNamara & Houston, 1992; Morris, 1998) and the fields of trophic and spatial ecology are thus intertwined.

1.2 Migratory species

1.2.1 Pelagic sharks

Migratory species, including pelagic sharks, have the potential to impact upon nutrient and energy flow within the marine environment; connecting otherwise discrete food webs (McCauley *et al*. 2012; Bauer & Hoye, 2014; Roff *et al*. 2016; Ruppert *et al*. 2016) and exerting top-down control (Holdo *et al*. 2011; Heupel *et al*. 2014; Roff *et al*. 2016; Ruppert *et al*. 2016), predatory species play a key role in structuring ecosystems.

Marine apex predators have declined in abundance by >90% in recent decades, driven by unsustainable harvest and their appearance as by-catch (Pauly *et al.* 1998; Myers & Worm 2003; Hutchings & Baum 2005; Baum & Worm, 2009; Estes *et al*. 2011). Whilst the impact of the removal of top predators is somewhat unclear (Heupel *et al*. 2014; Grubbs *et al*. 2016; Ruppert *et al*. 2016), possible ecosystem-level

responses may include trophic cascades (Myers *et al*. 2007), reduced ecosystem resilience (Polis *et al*. 1997; Lundberg & Moberg, 2003; McCann *et al*. 2005) and behavioural modifications of prey (Heithaus *et al*. 2007; 2008). Managing and conserving remaining pelagic shark stocks is therefore essential in order to maintain healthy ecosystems, requiring improved understanding of the movements and foraging behaviour of these fishes, and the identification of critical habitats (Salzman, 1990).

1.2.2 Deep-water teleosts

Highly migratory deep-water species also play an important role in facilitating energy transfer from epi- and mesopelagic zones to the near bottom zone, via diel vertical migration (Vinogradov, 1997; Bergstad *et al*. 2003). Moreover, in species that also undertake large-scale latitudinal movements, the potential for redistribution of this energy is great, resulting in the connection of otherwise spatially segregated regions of our oceans. However in recent decades, as the biological resources of coastal waters have diminished globally, fisheries have responded to the continually rising demand by expanding offshore (Christensen *et al*. 2003) and into deeper waters (Koslow *et al*. 2000; Gianni, 2004). Deep-sea fisheries are now exploiting one of the last remaining refuges for commercial species (Morato *et al*. 2006). Changes in ecosystem structure, energy transfer and carbon sequestration (Trueman *et al.* 2014) associated with the over-exploitation of deep-water fishes and the destructive fishing techniques employed, are of grave concern. Once again, effective management of remaining stocks is required in order to prevent irreversible damage to deep-sea ecosystems.

1.2.3 Life-history traits

Many elasmobranchs and teleosts demonstrate common ontogenetic shifts is spatial and trophic behavior, often reflecting changes in dispersal potential and resource partitioning throughout life history. Juveniles and sub-adults tend to direct energy toward growth, in order to maximize survival, whereas mature individuals optimize reproduction (Werner & Gillam, 1984; Heupel *et al*. 2007; Carlisle *et al*. 2015). This strategy may serve to reduce intraspecific competition (Munoz-Chapuli, 1984), and often results in sexual and size-based segregation in many species (e.g. Mucientes *et al.* 2009; Holt *et al.* 2013; Dell'Apa *et al.* 2014) driving complex spatial structure.

For example, with increasing size and developing maturity, the sevengill shark (*Notorynchus cepedianus*) undergoes a dietary shift from teleosts to chondrichthyans, with marine mammals becoming increasingly important prey in larger sharks (Ebert, 2002). This trend for larger, higher nutritional quality valuable prey is common in size-structured marine systems, where feeding interactions are strongly governed by individual size. Spatial segregation between large and small size classes, reflected in the reduced dietary overlap between large and small sharks, may also reduce conspecific competition, enhancing survivorship of young sharks that are vulnerable to predation (Ebert 1991a, 1991b, 2002).

Improved understanding of these ontogenetic movement patters (and associated trophic ecology) would allow characterization of critical habitats throughout life history (Vandeperre *et al.* 2014; 2016). This, in turn, could improve management, potentially reducing fishery-interactions and by-catch, mitigating discarding where survivorship is poorly understood.

1.3 Critical habitats

According to the Endangered Species Act (ESA) of 1973 (U.S. Legislation), a critical habitat is a geographic area that contains features crucial to the continued viability and conservation of an endangered species (Salzman, 1990), which may itself require special protection or management.

Both abiotic and biotic factors required for life processes, specifically reproduction, are considered during the assignment of critical habitats. For example, space for population growth, shelter and cover, and resource availability (including food, water, air, light, minerals etc.). Critical habitat legislation also aims to protect sites for breeding and rearing offspring (Salzman, 1990). For example, 12 major haulout sites of the Steller Sea lion (*Eumetopias jubatus*) in Alaska were designated as critical habitats in 1993 (NMFS, 2008) in order to protect the species during the summer breeding season, with the ultimate aim of reducing mortality by minimizing potential harassment and disturbance which could interfere with sea lion behavior. Similarly, 45 specific areas occupied by Atlantic salmon (*Salmo salar*) in the state of Maine, spanning 19,571 km of perennial river, stream and estuary habitat and 799 km^2 of lake habitat, was protected under Critical Habitat legislation in order to preserve

physical and biological features essential for the conservation of the species (NMFS, 2009).

Critical habitat assignment therefore helps to protect areas, both occupied and unoccupied, that area essential to conserve the endangered species in question (Rosenfeld & Hatfield, 2006). These areas do not necessarily provide refuge or sanctuary, but serve as a tool to guide management.

In the case of elasmobranchs, pupping and nursery grounds represent typical critical habitats (Heupel *et al*. 2004; Carraro & Gladstone, 2006; Wiley & Simpfendorfer, 2007; Knip *et al*. 2010; Espinoza *et al*. 2011; Heupel *et al.* 2007; Norton *et al*. 2012). Habitats utilized by mature females during egg sac provisioning (in aplacental viviparous sharks) may also be important to the conservation of a species. Given that regions exploited by mature females during egg sac provisioning differ in their habitat requirements to those selected for their suitability as pupping and nursery grounds, understanding the connectivity between the two has the potential to aid in the management and conservation via the protection of mature and gestating females. However, identifying these sites is inherently challenging, due to the elusive nature of large females sharks and the difficulties associated with directly observing them in the wild.

1.4 Logistical challenges associated with studying movements and diet

Studying the behaviour of individual fish in the marine environment is logistically challenging and expensive. Direct observation of latitudinal and depth movements and foraging behaviour is near impossible, due to the remote and inaccessible nature of the pelagic realm (Figure 1.1), and the extent of many marine migrations. To date, much of what we know about the spatial and trophic ecology of pelagic sharks and deep-water teleosts is gleaned from fisheries catch data, tagging studies and stomach content analysis (Trueman *et al.* 2012).

Fisheries-dependent data is, by nature, spatially and temporally biased, with the distribution of capture information reflecting fleet activity rather than the true extent of species' range, and individual movement (Bolle *et al.* 2005). In marine systems,

where tagged fish have a very low chance of recapture (ICES, 2009b), passive tagging programmes must also be extensive in order to produce enough data to allow confident interpretation. For example, early salmon tag-recapture studies involving the tagging of 4657 of individuals in waters off West Greenland saw only 325 recaptures, both within and beyond the homewater fisheries of Greenland (Jensen, 1980). Even then, passive tagging provides no information relating to individual habitat use between tagging and re-capture locations, and there may again be an element of tempo-spatial biasing associated with fisheries recaptures. Conversely, active tags provide high-resolution, often fisheries-independent data relating to the movements and habitat use of individual fish. However, active tags (e.g. archival tags, smart tags, pop-up satellite tags) are relatively expensive and, whilst tag technology is improving, many still fail to transmit, or release prematurely. Accounting for these caveats therefore requires considerable financial outlay, and project funding may therefore restrict the number of individuals that can be tagged. For example, even the international TOPP project (Census of Marine Life) was limited to tagging fewer than 5000 individuals (Block *et al*. 2011).

The trophic level and diet of fishes has traditionally been studied via stomach content analysis (Hyslop, 1980; Cortés, 1999) however, this method is not without limitations. The primary caveat is that this technique provides only a snapshot of relatively recently consumed prey items, and does not provide a time-integrated picture of foraging (Pinnegar & Polunin, 1999). Stomach content analysis also relies upon accurate identification and quantification of prey items, which are often partially digested, leading to a further bias towards more robust items, relative to soft-bodied prey (Bergstad *et al*. 2010). In the case of pelagic sharks, insufficient sample numbers across all size classes, spanning the species' geographical range, also hinders investigation of diet and trophic dynamics. Many predators are also recovered with empty stomachs (either as a result of natural feeding behaviour or regurgitation caused by capture stress), and it is therefore necessary to sacrifice a large number of individuals in order to characterize diet (Arrington *et al*. 2002). This is not ideal given the conservation concerns associated with so many marine apex predators. Similarly, in the case of deep-dwelling species, stomach eversion in response to pressure changes associated with being brought to the surface is problematic. However, stomach content analysis does offer high taxonomic resolution

and assessment of the size composition of the diet (Pinnegar and Polunin, 1999), where accurate identification is possible.

1.5 Natural chemical tags

Spatial and trophic ecology can also be studied retrospectively, via the analysis of natural chemical tags. Natural chemical tags refers to the incorporation of natural occurring variations in chemical compositions, relating to ambient water conditions or the local food web (Trueman *et al.* 2012), into consumer tissues. Where the chemical composition of consumer tissues reflects environmental conditions, these tissues can be analysed in order to gain information pertaining to diet and/or movement, thus serving as a complementary approach to traditional tagging methodologies and stomach content analysis applied to the study of spatial and trophic ecology. Furthermore, where inert, incrementally formed tissues exist, analysis of natural chemical variations of individual increments can also allow reconstruction of ontogenetic trends in location and diet.

1.5.1 Stable isotope analysis

Stable isotope analysis (SIA) refers to the study of naturally occurring, non-radioactive isotopes. The suite of techniques associated with SIA has provided insight into the dietary and spatial ecology of many species of bird, mammal and fish. Stable isotope ratios are expressed as δ values with per mil (‰) units, which represent the measured isotope value relative to an international standard, for example:

$$\delta X = \left(\frac{Rsample}{Rstandard} - 1\right) \times 1000 \qquad \text{(eq. 1.1)}$$

where *X* is the isotope of interest, and *R* is the corresponding ratio of heavy to light isotope. Thus, the more positive the δ value, the more enriched the sample is in the heavier isotope. For the purpose of this study, ^{13}C and ^{15}N are the two isotopes of interest, and are expressed relative to their standards: Vienna Pee Dee Belemnite and air, respectively.

Isotopic variation within the biosphere occurs largely as a result of kinetic isotope fractionation. Heavier isotopes have reduced mobility compared to light isotopes, and

generally have higher binding energies. Thus, the product in the biochemical reaction is usually depleted in the heavier isotope, as equilibrium is rarely achieved. In living organisms, this process results in the organism's tissues being isotopically heavier than the diet (DeNiro & Epstein 1978, 1981). This is referred to as isotopic enrichment, or tissue-diet spacing. SIA therefore works on the principal of "you are what you eat". Developing upon the work of Smith & Epstein (1970), Minson *et al*. (1975), Minagawa & Wada (1984) and Haines (1976), who observed that consumer tissues are isotopically enricher relative to their dietary sources, Fry *et al*. (1978) and DeNiro & Epstein (1978, 1981) noted consistent differences between the isotopic signatures of consumers and their food, reporting that the isotopic enrichment is estimated to have a mean of 1‰ for ^{13}C and 3.4‰ for ^{15}N, per trophic level. However, these values are highly variable and are dependent upon taxa, mode of excretion, growth rate, tissue, amino acid composition, diet quality and nutritional status (Hogberg, 1998; Vanderklift and Ponsard, 2003).

1.5.1.1 Carbon

There are three naturally-occurring carbon isotopes; ^{12}C, ^{13}C and ^{14}C. Only ^{12}C and ^{13}C are stable, and occur at natural proportion of 99:1. $\delta^{13}C$ values in marine plant and animal tissues reflect the isotopic composition of primary production at the base of the food web (Wada *et al.* 1991). Isotopic variability in particulate organic matter (POM) is controlled by a number of biological, chemical and physical factors including the isotopic composition of dissolved CO_2 and nitrogen source, phytoplankton growth rate, phytoplankton species and cell geometry (Wong & Sackett, 1978; Fry & Wainright, 1991; Francois *et al*. 1993; Goericke *et al*. 1993; Bidigare *et al*. 1997; Popp *et al*., 1999; Maranon, 2009; Lara *et al*. 2010).

At low sea surface temperatures (SST) the concentration of dissolved CO_2 is relatively high, contributing to relatively negative $\delta^{13}C$ values of POM due to preferential uptake of the lighter isotope. Similarly, SST impacts upon phytoplankton growth rate: growth is reduced in cooler waters relative to warmer conditions, provided nutrients are not limiting (Popp *et al.* 1998; Hofmann *et al.* 2000; Ngochera & Bootsma, 2011). This results in negative $\delta^{13}C$ in cooler waters relative to warm conditions, as lighter, more mobile ^{12}C isotopes are preferentially incorporated into tissues. Finally, small-celled phytoplankters dominate in warmer, stratified and eutrophic regions, while larger

celled phytoplankters (especially diatoms) are common in colder waters. Larger phytoplankton species also exhibit lower levels of fractionation relative to small-celled nanoplankton, and therefore display more possitive $\delta^{13}C$ values (Popp *et al*. 1998). Thus, warm surface temperatures results in the combination of reduced CO_2 concentrations and small-celled phytoplankters with increased growth rates, contributing to elevated $\delta^{13}C$ values. Stratification, often induced by warm temperatures, fast phytoplankton growth rates, and subsequent nutrient utilization, can also influence isotopic signatures.

SST can therefore be considered a master controller, influencing dissolved CO_2 concentrations, growth rates, and the dominant phytoplankton taxa, which contribute to isotopic variability (Sackett *et al.* 1965; O'Leary, 1981; Rau *et al.* 1989; Fry & Wainright, 1991; Freeman & Hayes, 1992; Goericke *et al.* 1993; Goericke & Fry, 1994; Laws *et al.* 1995; Popp *et al.* 1998; Sigman & Casciotti, 2001; Montoya, 2007). This consequently produces latitudinal gradients in $\delta^{13}C$ values, with cool high latitude waters producing phytoplankton with relatively low $\delta^{13}C$, and warmer lower latitude regions producing phytoplankton enriched in ^{13}C, resulting in a relatively positive $\delta^{13}C$ (Lorrain *et al.* 2009). In addition to this latitudinal pattern in POM $\delta^{13}C$ values, in areas where a thermocline persists and primary production is nutrient-limited (e.g. oligotrophic sub-tropical gyres), plankton $\delta^{13}C$ values tend to be relatively negative as slow growth favours ^{12}C uptake.

The species of primary producer at the base of the food web can also confound isotopic signatures, as different taxa utilize different enzymes during ammonium uptake: ammonium becomes increasingly important as a source of nitrogen as blooms progress (Trueman *et al.* 2012). It is assumed that these enzymes are less discriminative in their carbon uptake compared to the enzymes associated with the RuBisCo cycle, and have been shown to result in relatively positive $\delta^{13}C$ values in diatoms and dinoflagellates (Lara *et al*. 2010). Additionally, diatoms are considered to be a fast growing group of phytoplankton, which also drives ^{13}C enrichment resulting in relatively positive $\delta^{13}C$ values (Trueman *et al.* 2012).

1.5.1.2 Nitrogen

Two naturally-occurring non-radioactive nitrogen isotopes exist (Högberg, 1997); ^{15}N, which occurs at ~0.366 aton % in atmospheric N_2, with the remainder comprising ^{14}N (Junk & Svec, 1958; Mariotti, 1983).

Variability in POM nitrogen isotope δ values is controlled by the nutrient source at the base of the web, the mechanisms by which nitrogen is integrated into tissues, and the size of the nutrient pool (Mullin *et al*. 1984; Mann & Lazier 1996; Trueman *et al*. 2012). In most marine environments, nitrate (NO_3^-) fuels primary production. Here, the isotopic signature of the dissolved nitrate supplied to the euphotic zone, (particularly via upwelling (Graham *et al*. 2010)), and the amount of nitrate utilization determines the isotopic composition of the phytoplankton (Graham *et al*. 2010; Trueman *et al.* 2012). Complete NO_3^- uptake results in the annually integrated $\delta^{15}N$ value of primary production equalling the $\delta^{15}N$ value of nitrate inputs (Eppley & Peterson 1979). Where direct nitrogen fixation occurs (e.g. by diazotrophs), $\delta^{15}N$ values in POM are low as the isotopic signature of fixed N_2 is close to zero and little discrimination, or fractionation, takes place during this process.

In regions where the nitrate pool is large, and uptake is incomplete, lighter ^{14}N isotopes are preferentially utilized, producing relatively reduced $\delta^{15}N$ values (Graham *et al*. 2010). This also occurs in areas such as the Southern Ocean, where iron availability limits primary production (Graham *et al*. 2010). Under these conditions, nitrate assimilation is incomplete, thus ^{14}N is preferentially incorporated leading to relatively low $\delta^{15}N$ values. The opposite occurs where nitrate limits growth, as isotopic uptake is indiscriminative. Additionally, in low oxygen conditions, where bacterial respiration results in the removal of ^{15}N depleted nitrate, the remaining water is enriched in the heavier isotope and results in higher $\delta^{15}N$ values of POM (Voss *et al*. 2001).

1.5.1.3 Isotopic gradients

The carbon and nitrogen δ values in POM vary considerably across the globe. To some extent, this variability can be explained by large scale SST and circulation features which drive predictable latitudinal isotopic gradients (Figure 1.3) (Hofmann *et al.* 2000; Tagliabue & Bopp, 2008; Graham *et al.* 2010; Longmore *et al.* 2014). $\delta^{13}C$

variability can therefore be used to characterize water masses, as $\delta^{13}C$ values reflect primary production at the base of the food web, which is strongly related to temperature. Nitrate availability is also linked to SST, and so influences $\delta^{15}N$ values, however coastal proximity, pollution (terrestrial runoff and atmospheric input) and trophic dynamics play a more important role in driving variations in nitrogen isotope ratios (Cabana and Rasmussen, 1996; Cole *et al.* 2004). This makes baseline $\delta^{15}N$ values harder to predict than $\delta^{13}C$ values.

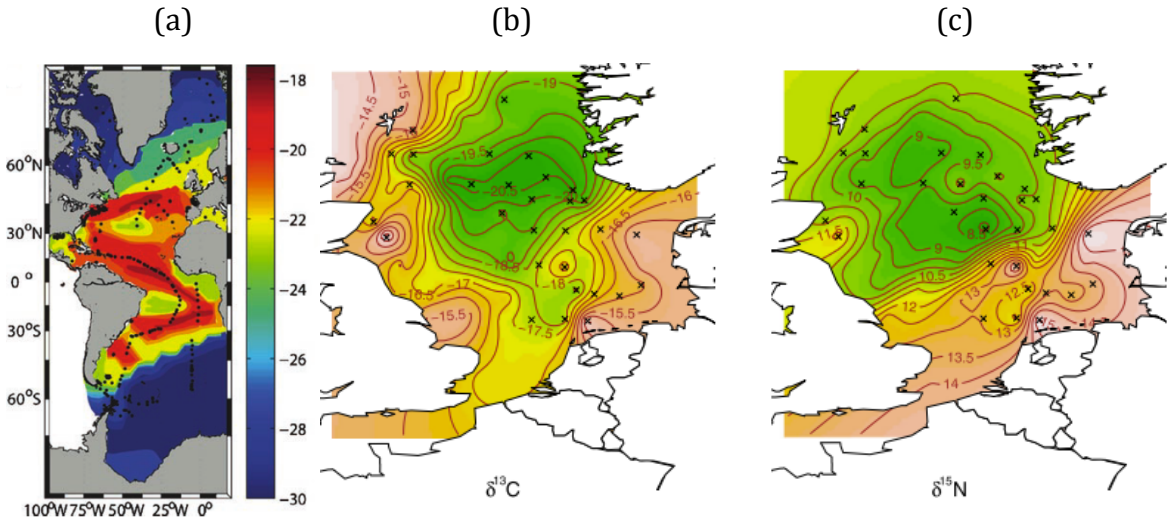

Figure 1.3 – (a) Contour plot of isoscape values in the Atlantic Ocean from meta-analysis of published data, displaying latitudinal patterns in $\delta^{13}C$ (Graham *et al.* 2010) and mapped North Sea isoscape models for (b) $\delta^{13}C$ values and (c) $\delta^{15}N$ values in jellyfish mesoglea tissues (MacKenzie *et al*. 2014).

Baseline carbon and nitrogen δ values also vary spatially and temporally. Thus, super-imposed upon latitudinal gradients are variations in isotope signatures associated with seasonal, annual and decadal climate cycles (Rolff, 2000; Hofmann *et al.* 2000; Tagliabue & Bopp, 2008; Graham *et al.* 2010; Newsome *et al*. 2010; Trueman *et al.* 2012).

Offshore gradients in $\delta^{15}N$ values also occur in many regions, attributed to coastal proximity and associated anthropogenic inputs and terrestrial runoff. For example, anthropogenic nitrogen sources causing enrichment in nitrogen δ values of freshwater systems (McClelland *et al*. 1997) can lead to marked offshore gradients (Jennings & Warr 2003; Jennings *et al.* 2008). Offshore pelagic systems generally receive less anthropogenic nitrogen sources. In these open ocean regions, variations

in $\delta^{15}N$ values caused by bloom size and phytoplankton taxonomy are often smaller than variations associated with trophic dynamics (DeNiro & Epstein, 1981).

1.5.1.4 Trophic Enrichment

The sources of carbon and nitrogen in marine food webs ultimately sets baseline isotopic signatures, which are subsequently transformed via isotopic fractionation during assimilation (Peterson & Fry, 1987). These signatures are then transferred through marine food webs, undergoing trophic enrichment in consumer tissues, which is characterized by a stepwise increase in δ values with trophic level (Hobson & Smith, 2007). This occurs due to the preferential excretion of lighter isotopes owing to reaction kinetics, leaving consumer tissues enriched in the heavier isotope (Figure 1.4) (Gaebler *et al*. 1966; DeNiro and Epstein, 1981; Minagawa and Wada, 1984; Owens, 1987; Smit, 2001; Vanderklift & Ponsard, 2003).

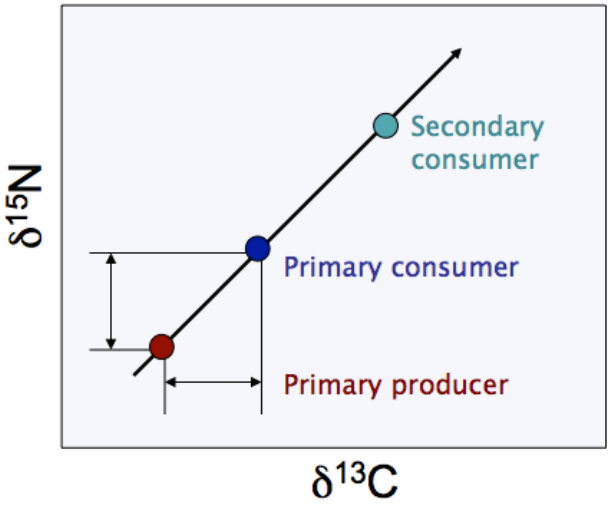

Figure 1.4 - Schematic demonstrating trophic enrichment of $\delta^{13}C$ and $\delta^{15}N$ values in a marine food-web.

Numerous studies have addressed this enrichment (or tissue-diet spacing) and have produced "average" values of approximately ~3‰ and ~1‰ for nitrogen and carbon, respectively (Minagawa & Wada, 1984; Fry & Sherr, 1984; Peterson & Fry, 1987). Due to the trophic fractionation of nitrogen isotopes, $\delta^{15}N$ values can provide information relating to trophic level of an individual. Whilst $\delta^{15}N$ scaling with trophic position is not fully understood at a biochemical level, NH_4^+ excretion, associated with considerable isotopic fractionation, drives the isotopic enrichment of a consumer's tissue relative to its food (Bada *et al*. 1989; Gannes *et al*. 1997). However, trophic

fractionation of carbon isotopes is less pronounced, and therefore lends itself to the study of a species' spatial distribution, as variations in $\delta^{13}C$ values are tied to SST, oceanographic conditions and latitude (Popp *et al*. 1998; Hofmann *et al*. 2000; Ngochera & Bootsma, 2011). However, interpretation of isotopic variability is confounded by the spatial and temporal variability of baseline values (Hofmann *et al*. 2000; Tagliabue & Bopp, 2008; Graham *et al*. 2010; Newsome *et al*. 2010). It is therefore recommended that isotope studies should be "anchored" by a reference organism that integrates this variability in primary producers (often benthic invertebrate species with an assumed trophic level of ~2) (Cabana & Rasmussen, 1996, Vander Zanden & Rasmussen, 1999; Jennings *et al*. 2008), such as filter-feeding bivalves (Goering *et al*. 1990, Lorrain *et al*. 2002). Thus, where the isotopic composition of the anchor species is known, the trophic level of consumers within the same food web can then be estimated via the isotopic distance between them and the anchor species (Hobson & Welch, 1992; Vanderklift & Ponsard, 2003).

The amino acid composition of organic tissues can also introduce considerable variability in $\delta^{15}N$ values; McClelland & Montoya (2002) revealed that $\delta^{15}N$ of 15 amino acids studied ranged over 13.6‰. The type of amino acid can also influence isotope ratios. Essential amino acids are generally conserved between food/prey and consumer tissues and undergo little fractionation (discrimination), resulting in comparable $\delta^{15}N$ values (Hare *et al.* 1991; McMahon *et al.* 2015). Conversely, non-essential amino acids undergo substantial processing and fractionation via transformation and deamination altering the original isotopic signature (Hare *et al.* 1991; McMahon *et al.* 2015). These processes lead to tissue- and taxon-specific variations in isotopic signatures associated with differential fractionation due to the disparities in the amino acid composition different tissues (MacKenzie, 2010). However, McClelland & Montoya (2002) revealed that a combination of essential and non-essential amino acids were incorporated into the tissues of herbivorous zooplankton with little modification of $\delta^{15}N$ values, when fed a known algal diet. This study revealed that some amino acids that are considered "non-essential" undergo little fractionation during incorporation into consumer tissues (e.g. serine), while some essential amino acids experience considerable trophic enrichment (e.g. leucine, isoleucine and valine). Thus, the classic essential vs. non-essential amino acid categorization does not accurately describe the differences in enrichment associated

with trophic dynamics. However, McClelland & Montoya (2002) did reveal that the isotopic signature of some amino acids does reflect $\delta^{15}N$ values at the base of the food web (e.g. glycine), and are now often referred to as "source" amino acids (Karasov & Martínez del Rio, 2007; McMahon *et al.* 2013).

1.5.1.5 Other sources of isotope variability

Mode of excretion further complicates the interpretation of $\delta^{15}N$ values. For example, the more complex the mode of converting nitrogenous waste from ammonia to urea/uric acid, the more elevated the $\delta^{15}N$ values become. This is due to increased fractionation in the consumer's body, resulting in isotopically light waste product and relatively heavy tissue (Vanderklift & Ponsard, 2003).

Nutritional stress can also impact upon the isotopic signature of an organism's tissues (Hobson *et al*. 1993). In these cases, self-catabolizing can lead to enrichment in $\delta^{15}N$ values (Doucett *et al*. 1999). Similarly, the persistence of maternal signatures in neonate or inert, incrementally formed tissues may also influence $\delta^{15}N$ values (Pilgrim, 2007), potentially reflecting foraging at a trophic level that exceeds that of the mother (Jenkins *et al*. 2001; Frankel *et al*. 2012).

1.5.1.6 Isotope summary

In summary, baseline $\delta^{13}C$ values vary temporally and spatially in relation to SST and primary production. Carbon isotopes therefore contain information relating to the state of productivity at a given location, at a particular time. Although $\delta^{15}N$ values are also impacted by SST, these isotopes undergo strong dietary fractionation, offering a tool to study trophic level. Thus, analysis of the variations in stable carbon and nitrogen isotope ratios can potentially allow retrospective reconstruction of feeding location and trophic dynamics, provided that other sources of isotope variability, associated with tissue type, mode of excretion etc., are taken into consideration.

1.6 Sclerochronology

Sclerochronology refers to the study of variations in the physical and chemical characteristics of incrementally grown tissues. Growth bands relate to daily, seasonal and annual patterns, and occur in the hard tissues of numerous marine and aquatic phyla including mammalian teeth, molluscan shells, coral skeletons and fish otoliths

(Campana & Thorrold, 2001). The suite of techniques associated with sclerochronological study have become invaluable to fisheries researchers, allowing assessment of age, growth and maturity, alongside the study of spatial and trophic ecology throughout ontogeny.

1.6.1 Otoliths

Developing from Reibisch's original examination of otolith annuli in 1889 (Jackson, 2007), there has been increasing interest in the use of otolith structure in determining the age of individual fish. Otoliths have since become an invaluable "timekeeper" for fisheries scientists, as collection of individual growth, population age structure and life history data are essential prerequisites for accurate stock assessment and fisheries management (Lorance *et al.* 2003).

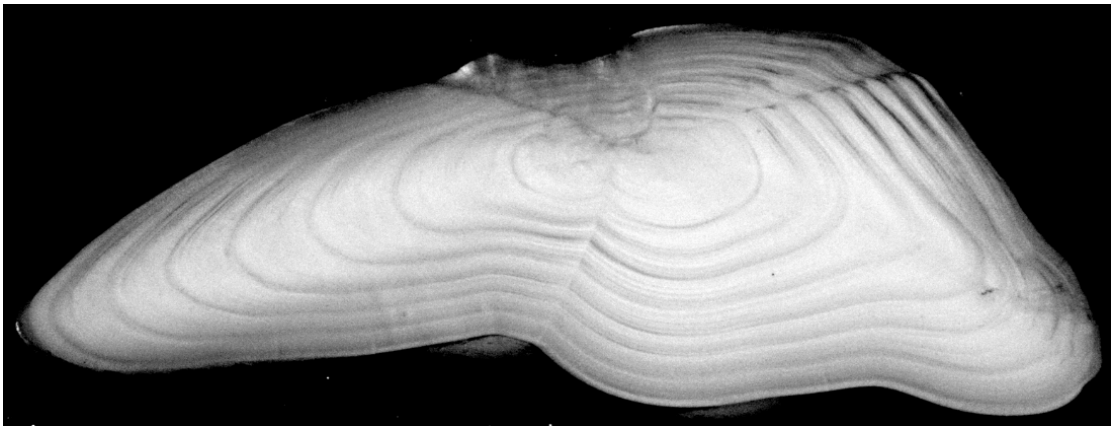

Figure 1.5 - Sectioned cod (*Gadus morhua*) otolith displaying annual growth bands.

Otoliths are paired calcified structures found in the cranium of all teleost fish, associated with balance and/or hearing (Campana, 1999), and unlike the majority of calcified skeletal structures, they demonstrate continual growth (Campana & Thorrold, 2001) which appears to be maintained even when somatic growth ceases (Maillet & Checkley, 1990). Although growth bands materialize in the calcified structures of several marine phyla (Campana & Thorrold, 2001), otoliths offer the most accurate method of age determination (Secor *et al*. 1995). Each growth band, or annulus, comprising an opaque and translucent zone (Figure 1.5), usually relates to fast and slow growth, respectively (the opposite is true in some species). Because of the periodicity of their formation, otoliths are used in age determination studies (Pannella, 1971), and estimates have been repeatedly validated by sensitive assays

such as bomb radiocarbon and ^{210}Pb:^{226}Ra techniques (Campana, 1999), which confirm their accuracy (referred to as validation studies).

1.6.1.1 Chemical analysis of otoliths

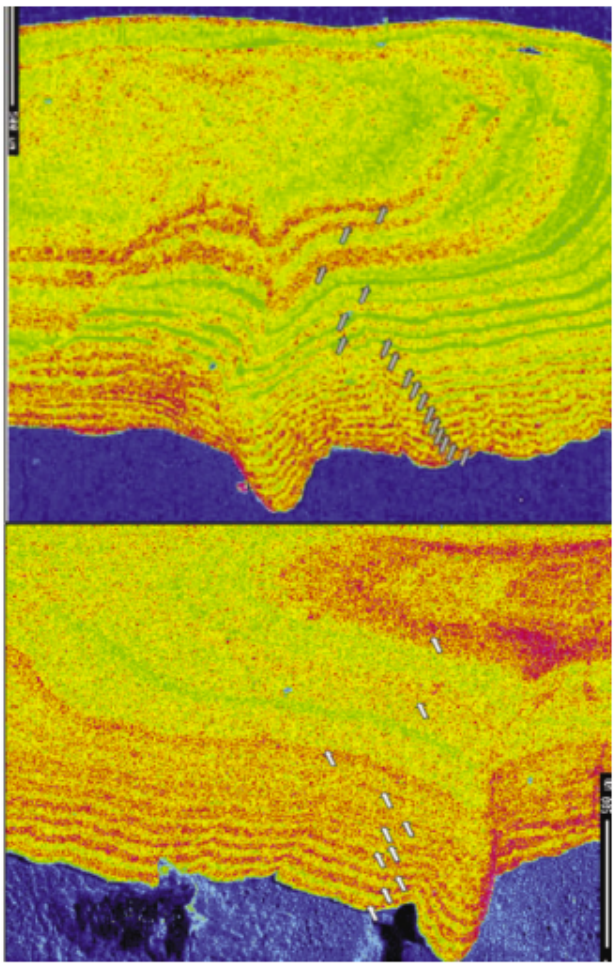

Figure 1.6 - X-ray composition maps of strontium (Sr) concentrations in the otolith for two female striped bass (*Morone saxatilis*) collected in Chesapeake Bay in 2000. Arrows indicate annuli. Red and orange colours represent regions with higher Sr concentrations whereas yellow and green represent regions with lower Sr concentrations. Composition maps show the coincidence of strontium banding patterns with banding patterns of annuli, indicative of annual anadromous migrations from high to low salinity waters. From Secor & Piccoli (2007).

The unique properties that allow otolith annuli to be retained also results in the preservation of chemical signals within the calcium carbonate structure, relating to aspects of the environment that the fish is exposed to (Campana, 1999). Otoliths therefore record time-resolved chemical information associated with the ontogeny of an individual, and these increments can be analysed to examine whole-life environmental histories, as chemical fingerprints are maintained within the tissue

microstructure (Sturrock *et al.* 2012). For example, analysis of orange roughy (*Hoplostethus atlanticus*) otolith increment chemistry helped elucidate down-slope ontogenetic migration via examination of oxygen and carbon stable isotope ratios, which are influenced by water temperature and metabolism, respectively (Trueman *et al.* 2013). Similarly, x-ray composition maps of the surface of sectioned Hudson River striped bass (*Morone saxatilis*) otoliths reveal alternating high and low strontium concentrations (Figure 1.6), relating to annual migration from high to low salinity waters (Secor & Piccoli, 2007).

1.6.1.2 Limitations

The chronological properties of otoliths are considered unparalleled in the animal world (Campana & Thorrold, 2001). Despite this, their predominantly inorganic calcium carbonate composition prevents analysis of organically derived chemical signatures. Although recent studies have successfully isolated and analysed the organic protein contained within the inorganic $CaCO_3$ structure (Grønkjær *et al.* 2013), sequential sampling of individual growth bands is difficult due to the mass requirements of analysis (~0.5mg organic material; organic protein comprises 0.2-10% of otolith mass (Degens *et al.* 1969; Hüssy *et al.* 2004)). Therefore, it is currently not feasible to study the chemical properties of the collagen contained within individual otolith annuli. Consequently, it is impossible to investigate ontogenetic shift associated with spatial and trophic ecology via analysis of otolith chemistry.

1.6.2 Vertebrae

Elasmobranchs do not possess large calcified otoliths. Vertebrae present an alternative tissue for study, and are one of the few structures in sharks that are known to produce periodic growth bands (Figure 1.7). Vertebrae are commonly used in order to study shark ecology, revealing information pertaining to the age, migratory behaviour and trophic dynamics of individual animals (e.g. Campana *et al.* 2002; Estrada *et al*. 2006; Kerr *et al*. 2006; Porter *et al*. 2006; Natanson *et al*. 2013; Hamady *et al*. 2014; Carlisle *et al*. 2015). Similar to otoliths, vertebrae present opaque and translucent banding patters (Figure 1.7). However, validation of vertebrate-derived age estimates is inherently difficult, as each species of interest must be addressed separately. Based upon tag-recapture experiments using oxytetracycline (OTC), the vertebral banding of sexually immature porbeagle sharks (*Lamna nasus*)

has been demonstrated to form annually (Natanson *et al.* 2002). Validation of growth bands in mature porbeagles has yet to be conducted, and is complicated by the potential for resorption and remodeling in older sharks, along with the difficulty associated with interpreting growth bands in older individuals where banding becomes narrow (Campana *et al.* 2002). Under-aging mature adults is therefore common, and obtaining an accurate estimate of age is further complicated by the fact that not all sharks produce interpretable growth bands (Campana *et al.* 2006) and estimates derived from different positions along a vertebral column can also vary (Officer *et al*. 1996). Using bomb radiocarbon dating, Hamady *et al*. (2014) compared the ^{14}C content of the white shark vertebrae (*Carcharodon carcharias*) with $\Delta^{14}C$ reference chronologies, confirming age estimates from vertebrae band counts, and so publishing the first age-validation study for this species. However, accurate aging using this technique is limited to relatively old individuals that were born prior to (or during) a period of thermonuclear device testing during the 1950s and '60s (e.g. Kalish, 1993; Campana *et al*. 2002; Hamady *et al*. 2014).

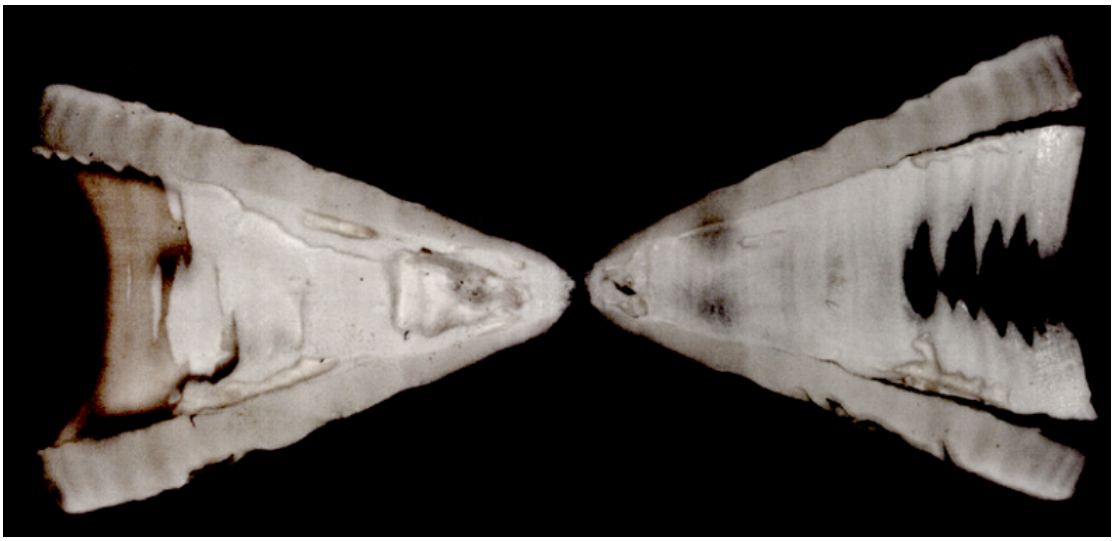

Figure 1.7 - Sectioned porbeagle (*Lamna nasus*) vertebrae displaying growth bands along corpus calcareum (From Stephanie Lavelle's Masters research, *unpublished*).

1.6.2.1 Chemical analysis of vertebrae

As with otoliths, chemical information contained within vertebral growth bands is retained, and vertebrae can also be sampled incrementally to investigate ontogenetic changes in chemical composition. Elasmobranch vertebrae comprise partially ossified cartilage with a mineral composite consisting of hydroxyapatite within the collagen

matrix. The proportion of collagen exceeds that observed in otoliths (~11-27% (Porter *et al.* 2006; Kim & Koch, 2012; Christiansen *et al.* 2014) and therefore vertebrae better lend themselves to the study of spatial and trophic ecology. For example, Estrada *et al.* (2006) revealed enrichment of $\delta^{15}N$ isotopes along the radius of white shark (*Carcharodon carcharias*) vertebral centra, relating to two distinct ontogenetic trophic shifts following parturition and at a total length exceeding 341cm (Figure 1.8). Similarly, Kim *et al*. (2012b) identified individuality in diet preference and foraging behaviours via examination of isotope ratios from sequentially formed vertebrae tissue of *C. carcharias*. Comparable methodologies have also been employed in order to explore habitat use by bull sharks (*Carcharhinus leucas*), highlighting habitat shift in sub-adults occupying the waters off northeast Queensland (Werry *et al.* 2011). Thus, by exploiting the sequential growth and organic content of the vertebrae, it is possible to investigate variations in the chemical content of the tissue throughout the whole ontogeny, relating to the ecology of the individual.

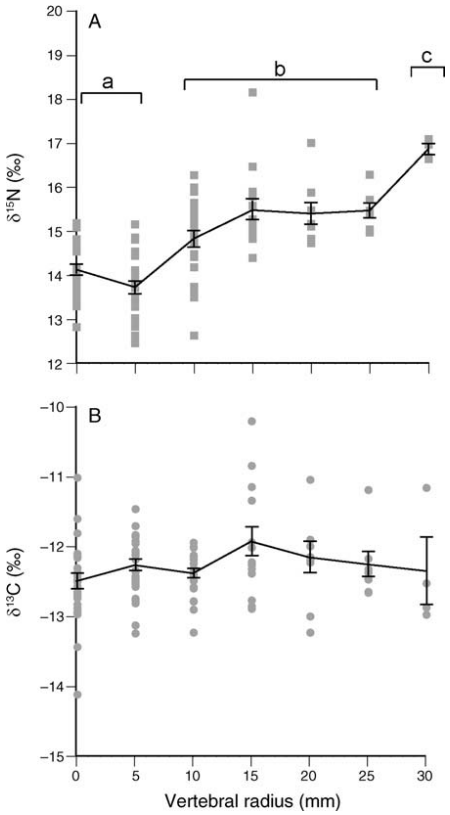

Figure 1.8 – Stable carbon and nitrogen isotope values ($\delta^{13}C$ and $\delta^{15}N$) of white shark vertebral tissue vs. vertebral radius (mm). (a), (b) and (c) indicate groups that differ significantly from one another based on isotopic composition of the vertebral tissue. Squares (A) and circles (B) relate individual values; the solid lines connect means (± SE). From Estrada *et al.* (2006).

1.6.2.2 Limitations

The inorganic hydroxyapatite portion of shark vertebrae may differ in isotopic composition to protein (collagen), necessitating isolation of the organic collagen component prior to isotope analysis. Typically, demineralization is achieved via addition of either hydrochloric acid (HCl) (Tuross *et al.,* 1988) or ethylene diamine tetra-acetic acid (EDTA) (Kim & Koch, 2012) to powdered or solid vertebrae samples. However, few studies have investigated (a) whether or not demineralization is required, and (b) the impact that treatment has upon the chemical properties of the resultant sample. Moreover, the mass requirements of stable carbon and nitrogen isotope analysis (~0.5mg organic material) combined with the narrowing of growth bands with increasing age ultimately limits temporal resolution.

1.6.3 Eye lenses

Vertebrate and cephalopod eye lenses possess the same structural characteristics that make otoliths and vertebrae suitable for sclerochronological interpretation: they form incrementally and are not remodeled.

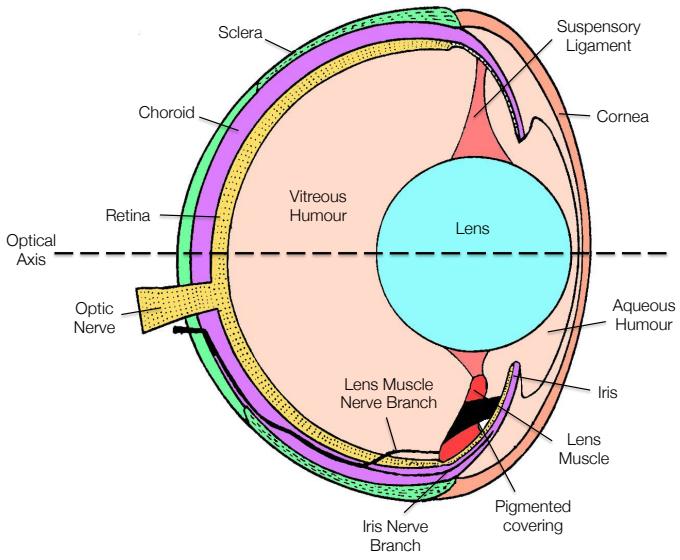

Figure 1.9 - Schematic of teleost eye, adapted from Nicol (1989).

Despite evolving to suit numerous ecological niches, the cellular structure of the vertebrate eye lens is conserved across taxa (Blundell *et al.* 1981). Serving as a focusing device allowing images to form on the retina (Bloemendal *et al.* 2004), lenses must be transparent and have a high refractive index (Bloemendal *et al.* 2004; Kröger,

2013), and it is these requirements that has resulted in the evolution of the structural characteristics that make lenses suitable for sclerochronological investigation.

Unlike in air, the cornea provides no refractive power in water (de Busserolles *et al*. 2013), and the lens, generally spherical or sub-spherical in fishes (Nicol, 1989) (Figure 1.9), is solely responsible for light refraction and is therefore required to have a refractive gradient from core to edge. Lens growth begins during early embryonic development (Grainger, 1992), and stems from the ectoderm that overlies the optic cup, which subsequently inverts and pinches off to form a hollow vesicle (Bassnett & Beebe, 1992; Bloemendal *et al.* 2004). The lens comprises densely packed, protein-filled fiber cells, and growth is achieved via sequential deposition of fiber cells, arranged in concentric layers. Primary fiber cells are produced via the elongation of cells occupying the posterior region of the lens capsule (Bloemendal *et al.* 2004). Secondary fiber cells envelop primary cells, and are formed via division of epithelial cells, arranged in a monolayer anterior to the lens equator (Bloemendal *et al.* 2004). Thus, older cells occupy the central core region, and younger cells subsequently added on top (Bloemendal *et al.* 2004; Kröger, 2013). This process continues throughout the lifetime of all vertebrates, resulting in a continuous increase in tissue volume (Bassnett & Beebe, 1992).

Varying from ~0.13 g ml^{-1} at the outer edge to 1.05 g ml^{-1} at the core (Bloemendal *et al.* 2004), fish lens fiber cells have an unusually high protein content. All vertebrate lenses contain α, β and γ crystalline proteins, commonly known to as the classic or ubiquitous crystallins (Bloemendal *et al.* 2004; Lynnerup *et al.* 2008), however, other taxon-specific proteins also occur within the lens (Bloemendal *et al.* 2004). The variable refractive gradient from lens edge to core is associated with the water content and protein concentration of the fiber cells, controlled by regulation and post-translational modification of aquaporin-0 (Ball *et al.* 2004; Hedfalk *et al*. 2006; Törnroth-Horsefield *et al*. 2010; Gutierrez *et al*. 2011). Owing to it's high protein and low water content (Bloemendal *et al.* 2004), the lens core is hard, and often incompressible (Fernald, 1985). The core therefore has a relatively high refractive index (Fernald, 1985). Once the proteins have obtained this high concentration, they are generally not re-soluble (Bloemendal *et al.* 2004) and the nucleus achieves a uniform refractive index (Fernald, 1985). Moving toward the lens edge (outer cortex),

cytosolic protein concentration decreases (Philipson, 1969), and water content increases, resulting in the reduction in the refractive index. This gradient is essential in order to maintain visual functioning in fishes. Lens proteins therefore exist both in a concentrated solid state in the core, and a gelatinous solution at the outer cortex (Lynnerup *et al.* 2008), resulting in the formation of a tissue comprising two physically distinct zones (Fernald, 1985). The shape of the outer cortex is maintained by the lens capsule (Fernald, 1985), whereas the central core region is a dense, stable structure. The hydrated protein composition of eye lenses also lends itself to stable carbon and nitrogen analysis, as no lipid extraction or demineralization is needed (Parry, 2003; Onthank, 2013; Wallace *et al*. 2014).

During fiber cell differentiation, degradation of all membrane bound organelles occurs, in a process which closely resembles the early stages of apoptosis (Bassnett, 2002). The purpose of this is to remove light-scattering particles (to achieve transparency), however as an upshot, lens fiber cells can no longer synthesize or degrade proteins (Bloemendal *et al*. 2004) and the protein-filled cells must persist throughout the organism's lifetime (Bloemendal *et al*. 2004). The lens therefore serves as a chronological repository for chemical information (Parry, 2003; Onthank, 2013; Wallace *et al*. 2014) relating to the individuals entire life history.

With their predominantly organic (protein) composition, lenses have great potential to record chemical variations pertaining to the spatial and trophic ecology of an individual, throughout its lifetime. Despite this, lenses have received relatively little analytical attention, with only a handful of published articles relating to the chemical composition of eye lenses in relation to ecology (Parry, 2003; Onthank, 2013; Wallace *et al*. 2014).

1.7 Aims and objectives

The research presented in this thesis focuses on recovering ontogenetic stable isotope records from the eye lenses of elasmobranch and teleost fishes. Developing upon what is known about the morphology and growth of vertebrate (and cephalopod) lenses, ontogenetic trends in lens chemistry are examined, and tissue-specific offsets and maternal-offspring isotopic spacing addressed.

The specific aims of the project are to:

- Apply novel and established lens-based protocols to investigate isotopic variability in incrementally formed eye lenses. Comparing and contrasting lens data from the spiny dogfish (*Squalus acanthias*), the northeast Atlantic porbeagle shark (*Lamna nasus*) and deep-water teleosts, *Aphanopus carbo* and *Coryphaenoides rupestris*, findings are discussed in relation to the spatial and trophic ecology of case-study species.

- Corroborate lens data with the known spatial and trophic ecology of case study species in order to examine whether the lens records "sensible" trends in isotope composition.

- Examine species-specific tissue isotopic offsets (i.e. lens-muscle) allowing comparison of the chemical composition of lesser-studied lens tissue with that of more commonly analysed muscle.

- Examine maternal-offspring tissue isotopic spacing, and address the impact that reproductive (placental vs. aplacental viviparity) strategy has upon the chemical composition of lens tissue formed *in utero* (elasmobranchs only).

Chapter 2: Teleost and elasmobranch eye lenses as a target for ontogenetic stable isotope analyses

Chapter 2 is a manuscript in preparation, to be submitted in August 2017: "Teleost and elasmobranch eye lenses as a target for ontogenetic stable isotope analyses. K. Quaeck-Davies, K. MacKenzie, V. Bendall, C. Trueman." Written by Katie Quaeck, including feedback from all co-authors.

2.1 Abstract

Incrementally grown, inert tissues such as fish otoliths, provide biochemical archives of behaviour and physiology over the whole life of the individual. Organic tissues are particularly useful as the stable isotope composition of the organic component can provide information about diet, trophic level and location. Unfortunately, inert, incrementally grown organic tissues are rare, particularly in elasmobranchs. The vertebrae eye lens is formed via sequential deposition of protein-filled fibre cells, which are subsequently metabolically inert. Lenses therefore have the potential to serve as a biochemical log of life-long dietary and spatial ecology, but have been largely overlooked as a target for retrospective analyses. Basic morphological and methodological details relevant to the recovery of ontogenetic stable isotope records are therefore difficult to find.

Here the structure and formation of eye lenses is reviewed, and lens morphology compared across different teleost and elasmobranch species. The trade-offs between alternative lens handling and sampling techniques are also discussed, and the complexities associated with interpreting isotopic data from lenses of fishes with varied reproductive strategies addressed. We present relationships between the body size and lens diameter of four study species (*Aphonopus carbo*, *Coryphaenoides rupestris*, *Lamna nasus* and *Squalus acanthias*), confirming that recovery of a body size-referenced sample is possible. Transects of stable isotope compositions across eye lenses of *A. carbo* were symmetrical around the lens core, reflecting sequential deposition and subsequent stability of lens proteins. The isotope composition of the lens core varied among species, consistent with known trophic ecology; $\delta^{15}N$ values increase from the zooplanktivorous *C. rupestris* to the piscivorous *A. carbo*, with the

highest values observed in the lenses of the viviparous shark, *L. nasus*. Finally, the isotopic offset between lens protein and white muscle tissue for the spiny dogfish *Squalus acanthias* is quantified. Lens protein carbon and nitrogen was slightly but significantly isotopically depleted relative to muscle proteins, however the measured isotopic differences between lens and muscle proteins are close to analytical uncertainty.

2.2 Introduction

2.2.1 Natural chemical tags

Stable isotope analysis of incrementally formed tissues provides a window to study aspects of the ecology of an individual throughout its life history, serving as natural biochemical tags. These chemical markers present a complementary approach to study trophic and spatial ecology, which can be used alongside traditional tagging, representing a particularly useful tool to study elusive marine animals such as deep-water fishes, pelagic sharks and migratory marine mammals (Iken *et al*. 2001; Polunin *et al*. 2001; Michener & Kaufman, 2007). Sclerochronological tissues suitable for retrospective assessment of movements and diet include otoliths, baleen, vibrissae, vertebral collagen and lenses (e.g. Schell *et al*. 1989; Hobson & Schell, 1998; Parry, 2003; Estrada *et al.* 2006; Kerr *et al*. 2006; Newsome *et al*. 2010; Longmore *et al*. 2011; Onthank, 2013; Wallace *et al*. 2014; Carlisle *et al*. 2015).

The isotopic composition of carbon and nitrogen in incrementally grown organic tissues such as hair, baleen, and vertebral collagen provides additional information concerning ontogenetic life history patterns in spatial and trophic ecology. Exploiting strong geographic isotopic gradients ($\delta^{13}C$) between different water masses and latitudes, and via the sequential sampling of inert, incrementally formed baleen, Best & Schell (1996), Hobson & Schell (1998) and Lee *et al.* (2005) identified repeated seasonal migrations between breeding and feeding grounds of bowhead whales (*Balaena mysticetus*) and southern right whales (*Eubalaena australis*). Similarly, the isotopic composition of serially sampled pinniped vibrissae has unveiled previously unknown multi-year foraging strategies in male Antarctic fur seals (*Arctocephalus gazelle)* (Cherel *et al.* 2009). Elasmobranch vertebral collagen also forms incrementally, and has been analysed in order to address Pacific white shark foraging

behavior (Kim *et al.* 2012b) identifying a high degree of individual specialization in diet.

The inorganic chemistry of otolith aragonite has also been used extensively to provide a chronological chemical record of the water the fish inhabited (Kalish, 1991; Thorrold *et al.* 1997; Campana, 1999; Høie *et al.* 2004), addressing topics such as Atlantic bluefin tuna (*Thunnus thynnus*) stock mixing and nursery origin (Schloesser *et al.* 2010), ontogenetic depth migration in the roundnose grenadier (*Coryphaenoides rupestris*) (Longmore *et al.* 2011), and migration in Atlantic salmon (*Salmo salar*) (Hanson *et al.* 2013). Recently, isotopic analyses of the organic component of otoliths have provided retrospective reconstruction of feeding and spatial ecology of fishes (Grønkjær *et al.* 2013).

Thus, retrospective chemical analysis of inert, incrementally formed tissues has the potential to provide new insights into the ecology of elusive marine animals, identifying behaviours that would otherwise be difficult to study using traditional tagging methods. The vertebrate eye lens is an incrementally grown, metabolically inert proteinacous tissue (Nicol, 1989), and is therefore also suitable for retrospective recovery of life history biochemical data. The vertebrate eye lens has the potential to reveal new information about foraging and habitat use in species that are traditionally difficult to study, particularly elasmobranchs that do not posses otoliths, and open ocean or deep water fishes that are difficult to study using conventional tags (Nielsen *et al.* 2016).

2.2.2 Structure and formation of the vertebrate eye lens

Despite evolving to suit numerous ecological niches, the cellular structure of the vertebrate eye lens is conserved across taxa (Blundell *et al.* 1981). Within the eye, lenses serve as a focusing device allowing images to form on the retina (Bloemendal *et al.* 2004). In order to fulfill this role, lenses must be transparent and have a high refractive index (Bloemendal *et al.* 2004; Kröger, 2013). The crystalline protein composition and mechanism of lens growth achieves these requirements, and also results in an incrementally grown, metabolically inert tissue that possesses the key pre-requisites for retrospective stable isotope analysis.

In water, the cornea provides no refractive power (de Busserolles *et al*. 2013). Consequently the lens, with its variable refractive gradient from core to edge, is solely responsible for light refraction, and is generally spherical or sub-spherical in fishes (Nicol, 1989) (Figure 2.1). Growth of the lens begins during early embryonic development (Grainger, 1992) and stems from the ectoderm that overlies the optic cup, which subsequently inverts and pinches off to form a hollow vesicle (Bassnett & Beebe, 1992; Bloemendal *et al.* 2004). Cells occupying the posterior region of the lens elongate to form primary lens fibre cells, which subsequently fill the vesicle (Bloemendal *et al.* 2004). The anterior region of the lens comprises a monolayer of epithelial cells which divide in a region located anterior to the equator (Bloemendal *et al.* 2004). Newly formed cells elongate forming secondary fiber cells which overlay the primary fibers (Bron *et al.* 2000; Kröger, 2013). Cells in the same layer connect at the poles of the lens in an area referred to as the suture plane. Suture planes result in some light scattering even in healthy lenses, and are believed to serve as pathways of extracellular transport (Vaghefi *et al.* 2012).

Fiber cells are densely packed and arranged in concentric layers with older cells occupying the central core region, and younger cells subsequently added on top (Bloemendal *et al.* 2004, Kröger, 2013). This process continues throughout the lifetime of all vertebrates, including humans (Augusteyn, 2010), resulting in a continuous increase in tissue volume (Bassnett & Beebe, 1992), although growth rate is variable (Bron *et al.* 2000).

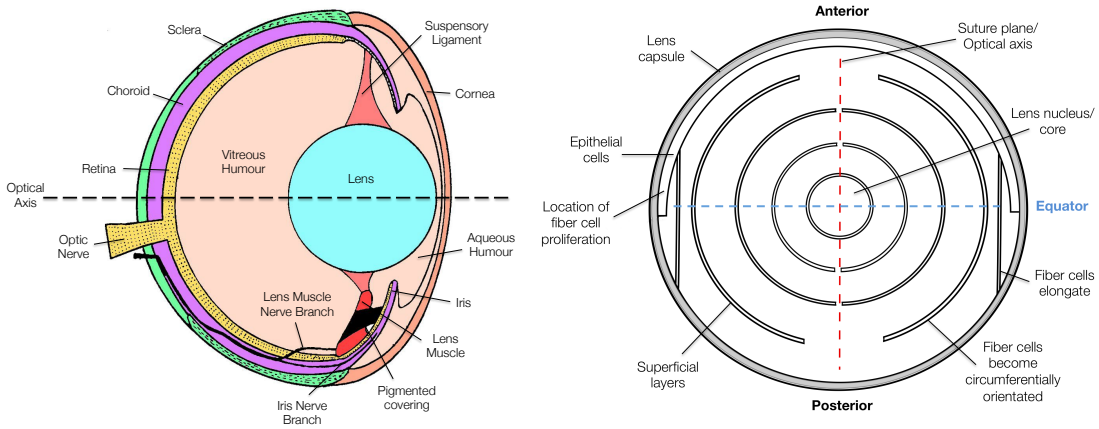

Figure 2.1 - Schematic of teleost eye (left) and lens (right), adapted from Nicol (1989).

During fiber cell differentiation, protein-coding genes are expressed in a regular manner resulting in variable relative proportions of proteins between the core/nucleus and outer cortex (Bloemendal *et al.* 2004). These soluble proteins are collectively referred to as the crystallins.

During the last phase of fiber cell differentiation, degradation of the membrane bound organelles occurs in a process which closely resembles the early stages of apoptosis (Bassnett, 2002). Loss of nuclei, mitochondria and ribosomes removes potential light scattering objects, and is necessary for the lens to achieve transparency (Bassnett & Beebe, 1992; Bassnett, 2002; Bloemendal *et al.* 2004). After the loss of organelles, fiber cells can no longer synthesize or degrade proteins, and crystalline proteins therefore persist throughout the organism's lifetime (Bloemendal *et al.* 2004).

Primary fiber cells are the first to lose their organelles, resulting in an organelle free zone (OFZ) (Bassnett, 2002). As development proceeds, the OFZ also envelops secondary fiber cells at a rate of roughly 20 cell widths per day (Bassnett, 2002). In fishes, the depth horizon of fiber cell denucleation is approximately 90% of the lens radius (Schartau *et al.* 2009). Beyond the OFZ, in the outer c.10% of the lens radius, the process of cell denucleation is incomplete.

2.2.3 Lens proteins.

Lens fiber cells have an unusually high cytosolic protein content which, in fish, varies from approximately 0.13 g ml^{-1} at the outer edge to 1.05 g ml^{-1} at the core (Bloemendal *et al.* 2004). All vertebrate lenses contain α, β and γ crystalline proteins, commonly known to as the classic or ubiquitous crystallins (Bloemendal *et al.* 2004; Lynnerup *et al.* 2008). Other crystalline proteins exist within the lens, however these are taxon-specific (Bloemendal *et al.* 2004). The increasing refractive gradient from lens edge to core is associated with the water content and protein concentration of the fiber cells. Water content is controlled by regulation and post-translational modification of aquaporin-0 (Ball *et al.* 2004; Hedfalk *et al*. 2006; Törnroth-Horsefield *et al*. 2010; Gutierrez *et al*. 2011). The core region of the lens is often hard and incompressible (Fernald, 1985), owing to its high protein and low water content (Bloemendal *et al.* 2004). The core consequently has a relatively high refractive index (Fernald, 1985). Once the proteins have obtained this high concentration, they are generally not re-soluble (Bloemendal *et al.* 2004) and the nucleus achieves a uniform

refractive index (Fernald, 1985). Moving away from the core, cytosolic protein concentration decreases (Philipson, 1969), and water content increases, resulting in the reduction in the refractive index. Close to the lens surface, cytosolic protein concentration decreases rapidly (Kröger, 2013). This results in a steep refractive gradient between the outer edge of the core region, and the outer cortex (Fernald, 1985). This gradient is essential in order to maintain visual functioning in fishes. Proteins must therefore exist both in a concentrated solid state in the core, and a gelatinous solution at the outer cortex (Lynnerup *et al.* 2008), producing a tissue consisting of two physically distinct zones (Fernald, 1985). The shape of the outer cortex is maintained by the lens capsule (Fernald, 1985), whereas the central core region is a dense, stable structure. The hydrated protein composition of eye lenses also lends itself to stable carbon and nitrogen analysis, as no lipid extraction or demineralization is needed (Parry, 2003; Onthank, 2013; Wallace *et al*. 2014).

Once deposited, cells are highly specialized and do not undergo re-modelling (Kjeldsen *et al*. 2010). In the eye, the epithelial basement membrane completely encloses the lens, resulting in the absence of blood vessels (Lynnerup *et al.* 2008). Desquamation of ageing cells is therefore restricted as no metabolites are transported to the lens, preventing cell degradation (Beebe, 2003). Thus, the protein-filled lens fiber cells are not remodeled throughout ontogeny.

The eye lens thus represents a sequentially-formed, metabolically-inert organic tissue, suitable for sclerochronological investigation and stable carbon and nitrogen analysis. Lenses offer an ontogenetic record of biochemical history, the isotopic composition of each layer varying with the trophic and spatial ecology of the individual at time of tissue formation.

2.2.4 The use of eye lenses to study elasmobranch ecology

Elasmobranchs do not possess large calcified otoliths suitable for age determination and ontogenetic investigation (Secore *et al*. 2005; Campana *et al*. 2002), consequently the life histories of elasmobranchs are generally poorly understood, relative to those of teleosts. Elasmobranch vertebrae (Cailliet, 1990) and fin spines (Brennan & Cailliet, 1989) grow incrementally, and can offer sclerochronological detail, providing most of the known methods to age elasmobranchs. However, many elasmobranchs do

not possess fin spines, and poorly mineralized vertebrae present many challenges for accurate and precise age determination. Vertebrae do offer a medium for retrospective isotopic analysis (e.g. Kim *et al*. 2012(b)), but many species possess small vertebrae, and the mass requirements of analysis (~0.5mg of organic material) limits the number of samples available for ontogenetic study, ultimately reducing temporal resolution. Incrementally grown tissues such as eye lenses also contain tissue formed during early development (Parry, 2003; Onthank, 2013; Wallace *et al*. 2014). Functioning eyes are highly adaptive in pelagic animals, and there is therefore selective pressure to develop eyes early in ontogeny. Consequently eye lenses may be particularly well suited to the reconstruction of early life history ecology in fishes. In many elasmobranchs, the yolk or placenta provides nourishment to the developing pup prior to emergence from the egg case (oviparous) or birth (viviparous/aplacental viviparous). Thus, nutrient assimilation driving embryonic development is characterized by the chemical properties of the prey of mature females during gestation or the period of yolk sac formation, and can provide information pertaining to maternal behaviour immediately prior to gestation. The eye lens therefore represents a unique tissue with the potential not only to allow retrospective investigation of whole life history ecology, but also examination of behaviour in pregnant females, and potentially consistency in behaviour across generations. This is particularly exciting as mature female elasmobranchs are often elusive, and therefore difficult to observe and study using traditional techniques.

2.2.5 Eye lenses as archives of biochemical information

The inert, organic, and incrementally-formed nature of the fish eye lens is analogous to the otolith, encouraging the exploration of the suitability of the lens for aging, fisheries stock discrimination, and trophic ecology, particularly in elasmobranchs. In the late 1990's, the trace element content of fish eye lenses was compared to that of otoliths and other tissues in the context of potential indicators of fish stock discrimination (Dove & Kingsford, 1998; Kingsford & Gillanders, 2000; Gillanders, 2001). These studies noted differences in absolute and relative trace element composition between lens, otolith and other biomineralised tissues, as expected based on the protein compared to biomineral matrix. Overall, lenses performed relatively poorly in stock discrimination trials, limiting further studies in this area, despite a call to consider lenses as suitable targets particularly for covalently-bound

metals (Gillanders, 2001). The stable isotope composition of carbon and nitrogen in lens proteins from squid has been explored in an attempt to reconstruct feeding chronologies (Parry, 2003; Hunsicker *et al.* 2010; Onthank, 2013). By peeling off sequential layers of lens tissue, Parry (2003) identified an increasing trend in $\delta^{15}N$ values with body size in two study species (*Ommastrephes bartramii* and *Sthenoteuthis oualaniesis*), suggesting that ontogenetic trophic shifts are reflected and preserved within eye lens chemistry. Whilst Onthank (2013) identified no common ontogenetic trend in stable isotope composition among squid in his study, individual specimens did exhibit shifts in lens stable nitrogen isotope composition, suggesting changes in diet over the individual's lifetime. Hunsicker (2010) applied similar methodologies to study the commander squid (*Berryteuthis magister*) in the eastern Bering Sea, identifying an increase of ~1 trophic position between juvenile and adult life stages. A similar approach was adopted to demonstrate recovery of whole life stable isotope records from teleost fishes (Wallace *et al.* 2014). Red grouper (*Epinephelus morio*), gag (*Mycteroperca microlepis*), red snapper (*Lutjanus campechanus*), and white grunt (*Haemulon plumierii*) lenses were examined, showing consistency between left and right eye lenses, and increasing $\delta^{15}N$ values from lens nucleus (core) to cortex, as expected given anticipated increases in trophic position with size/age.

The inert nature of lens core proteins formed in early juvenile periods also opens the potential for radiocarbon-based age estimation. Lynnerup *et al*. (2008) and Kjeldsen *et al*. (2010) both reported successful application of bomb radiocarbon dating to human eye lenses. More recently, Nielsen *et al.* (2016) attempted to radiocarbon date the eye lens nuclei of 28 female Greenland sharks (*Somniosus microcephalus*) estimating longevity to be in the order of hundreds of years.

The brief review above demonstrates that:

1. Vertebrate (and cephalopod) eye lenses are inert, undergoing no remodeling or replacement. Consequently, the chemical content of lens tissue at the time of formation is preserved.

2. Lens tissue consists primarily of protein and water. Thus, lenses are organic structures and their carbon and nitrogen stable isotope content can be sampled in order to address questions relating to distribution, movement/migration, trophic dynamics and juvenile ecology.

3. Lenses are incrementally grown and therefore have the potential to serve as a chronological record of chemical information (stable isotopes, trace elements, radiocarbon etc.), with each sequential laminae recording chemical signatures relating to the ecology of the species at time of tissue formation.

To improve the potential for lens protein as a useful target for stable isotope based investigation across a wide range of fish taxa, several additional factors should be addressed:

(1) The relationship between lens diameter and body size should be tested across taxa, allowing back-calculation of an estimate of the size of the individual at the time of lens tissue formation.

(2) The structure of lenses should be compared between taxa, and a consistent sampling methodology should be determined.

(3) Isotopic variability expected between and within individuals should be demonstrated across a range of taxa.

(4) Any potential isotopic offset between lens and muscle tissue should be calculated across taxa, allowing comparison of the chemical composition of lesser-studied lens tissue with that of more commonly analysed muscle (also reflecting contrasting incorporation rates).

In this study we address the points above using lens tissues from elasmobranch and teleost fishes.

2.3 Materials and Methods

2.3.1 Sample collection

Growth relationships between lens and body size were recovered from two teleosts, the black scabbard (*Aphanopus carbo*) and the roundnose grenadier (*Coryphaenoides rupestris*), and two elasmobranchs, the porbeagle shark (*Lamna nasus*) and spiny dogfish (*Squalus acanthias*). Lens and body measurements for *A. carbo* (n=19) and *C. rupestris* (n=29) were obtained from individual fish recovered using scientific dual-warp bottom trawls with rock-hopper ground gear during the 2012 and 2013 deep-water surveys of the west Scotland continental slope, onboard the MRV Scotia (survey methods reported in Neat *et al*. 2010). Lenses from a sub-set of individuals of both species were also processed for stable isotope analysis (n= 11 and n=11, for *A. carbo* and *C. rupestris*, respectively).

Lamna nasus (n=30) lenses and associated body size data were collected from sharks by-caught in a commercial gill-net fishery in the Celtic Sea between 2011 and 2014, and landed under dispensation in association with the Neptune Scientific Fishery (Cefas/Defra). Lenses from a sub-set of 7 individuals were processed for stable isotope analysis. Lenses and body size data were recovered from *Squalus acanthias* (n=101) caught off the Lowestoft coast during 2014. Lens and muscle tissue were also extracted from the embryos of gravid females (n = 11 and 19, respectively).

Lenses were extracted from cod (*Gadus morhua*, n=2), haddock (*Melanogrammus aeglefinus*, n=2), hake (*Merluccius merluccius*, n=4) and conger eels (*Conger conger*, n=2) obtained from commercial fishermen operating in the English Channel and North Atlantic. Monkfish (*Lophius americanus*, n=4) lenses were provided by The School for Marine Science and Technology (SMAST), at the University of Massachusetts (Dartmouth). Oceanic white-tip shark (*Carcharhinus longimanus*, n=2) lenses were obtained from a by-caught specimen caught off Wallis and Futuna in the South Pacific, in 2012, whilst blue shark (*Prionace glauca*, n=30) samples were from individuals caught by Spanish and Portuguese long-lining vessels operating off the Canary Islands in 2014.

2.3.2 Tissue preparation

One lens was extracted from each fish by making an incision along the length of the cornea, allowing the lens to be removed using forceps. To test growth relationships, the diameter of the lens was measured to the nearest 0.25mm with calipers. Once excised, the lenses were frozen at -80°C overnight, before being freeze-dried. Once freeze-dried, lenses were embedded in Epoxy resin (EpoFix).

To compare lens core permeability between species, eye lenses extracted from a range of teleost and elasmobranch species were freeze-dried and embedded in blue dyed Epoxy resin. Penetration of the blue dye provides a relative measure of lens permeability to a viscous, hydroscopic fluid after lyophilisation.

Embedded lenses were sectioned using two diamond wafering blades (0.3mm thick) mounted upon a low-speed precision saw (Isomet-Buehler), separated by a 2mm spacer. The double blade system was used to produce a thin section, measuring ~2mm thick, with one of the blades running through the absolute core of the lens. This produced a section revealing the lens structure. Dye-embedded lenses were also sectioned using the same instrument set-up, and the resultant thin section imaged using a Panasonic Lumix FZ200 Bridge Camera.

In preparation for stable isotope analysis, a second section was made across the surface of the exposed lens produced by the first double-blade cut, producing a section of lens, approximately 2mm thick and 2mm wide with the lens core at its centre. The lens strip was then sequentially sectioned by removing slivers of lens material, measuring approximately 0.5mm in width, using a scalpel. Sub-sampled segments of dried lens tissue were then weighed (~ 0.5 mg) and stored in tin capsules, prior to stable isotope analysis. Samples of pure resin were also submitted for analysis. Whole embryonic lenses (n = 11) were also dried, weighed and submitted for analysis.

White muscle samples were extracted from the region located anterior to the dorsal fin of 19 *Squalus acanthias* embryos. In order to remove any free ammonia, samples were rinsed ten times in deionized water, centrifuged for 10 minutes, before being

rinsed a further ten times. The muscle samples were then frozen, lyophilized, and weighed prior to analysis.

Where the lipid content of samples submitted for stable isotope analysis is high, the resultant $\delta^{13}C$ value is negatively biased (Reum, 2011). According to Post (2002), C:N ratios exceeding 3.5 are indicative of high lipid content in the tissues of aquatic organisms. Embryonic and maternal muscle tissue C:N ratios range from 5.58 to 9.18 (mean = 6.79 ± 0.71) and 3.57 to 8.83 (mean = 5.36 ± 0.94), respectively. *Squalus acanthias* muscle data therefore required retrospective correction for lipid content. The two-parameter model developed by Fry (2002) was used:

$$\Delta \delta^{13}C = D - DF(R_{CN})^{-1} \quad (2)$$

Here, D represents the protein-lipid $\delta^{13}C$ offset, and F the lipid-free C:N ratio, set at 3.16 (± 0.07) (Reum, 2011). R_{CN} represents the C:N ratio of the bulk sample submitted for analysis.

2.3.3 Analytical methods

Stable carbon and nitrogen isotope ratios of teleost and *L. nasus* lens samples were determined at OEA Laboratories Ltd. Laboratory standards (USGS40) were analysed for every ~10 unknown samples in each analytical sequence. Isotope ratios are expressed in δ notation (‰), relative to the international standards of V-Pee dee belemnite and air for carbon and nitrogen, respectively. Experimental precision (standard deviation of replicate USGS40 standards) for *C. rupestris* and *L. nasus* sample analysis was 0.21‰ for carbon and 0.27‰ for nitrogen. Experimental precision for *A. carbo* sample analysis was 0.12‰ and 0.16‰ for carbon and nitrogen, respectively.

All *S. acanthias* lens and embryo muscle samples were analysed at the NERC Life Sciences Mass Spectrometry Facility in East Kilbride, using a Pyrocube Elemental Analyzer (2013, Elementar, Hanau, Germany) and Delta XP (Thermo Electron) mass spectrometer (2003). The same in-house laboratory standards (USGS40) were

analysed every 10 samples. Experimental precision was 0.14‰ for carbon and 0.13‰ for nitrogen (standard deviation of laboratory standard replicates).

To account for inter-lab variability, replicate glutamic acid standards from the University of Southampton were analysed at both facilities. Mean $\delta^{15}N$ and $\delta^{13}C$ reported for standards analysed at OEA Laboratories Ltd. are -3.72 (± 0.26) and -12.87 (± 0.18) (*A. carbo* lens analysis), -3.73 (± 0.84) and -12.74 (± 0.31) (*L. nasus* & *C. rupestris*) for carbon and nitrogen, respectively. Mean $\delta^{15}N$ and $\delta^{13}C$ reported from standards analysed at NERC Life Sciences Mass Spectrometry Facility are -3.86 (± 0.15) and -13.01 (± 0.21) for nitrogen and carbon, respectively. The reported isotopic composition of glutamic acid standards analysed at each facility do not differ significantly, with mean $\delta^{15}N$ and $\delta^{13}C$ values within 1 standard deviation of each other.

2.4 Results

2.4.1 Relationship between lens and somatic growth

The relationship between total length (TL, mm) and lens diameter (LD, mm) was linear across the size range sampled (Figure 2.2). The best-fit linear relationships between body length and lens diameter are:

Aphonopus carbo LD = -3.713 (±1.279) + 0.185 (±0.013) *TL (2.1)

Coryphaenoides rupestris LD = -0.369 (±0.142) + 0.108 (±0.003) *TL (2.2)

Lamna nasus LD = 4.461 (±0.733) + 0.070 (±0.004) *TL (2.3)

Squalus acanthias LD = 0.479 (±0.181) + 0.109 (±0.002) *TL (2.4)

In the case of the roundnose grenadier and both shark species, a near-full size range of individuals was sampled. *C. rupestris* specimens as small as 50mm were obtained, representing the larval life history stage of this species. Similarly, a juvenile porbeagle shark measuring 1130mm was captured (size at birth = ~800-900mm (Aasen, 1963)). A rare opportunity to sample developing *Squalus acanthias* embryos was also available, as gravid females were obtained from the Neptune Scientific Fishery. Thus,

for the aforementioned species, the growth equations (eq. 2.2-4) are deemed to accurately reflect the relationship between lens diameter and body size.

An analysis of covariance (ANCOVA) revealed that individual size (TL) and species has a significant effect upon lens diameter ($F_{1,189}$ = 9275.18, p=<0.001 and $F_{3,189}$ = 264, P = <0.001, respectively) as does the interaction of these variables ($F_{3,189}$ = 38.79, p = <0.001). Thus, the slopes and intercepts of equations 1-4 differ from one another, and the relationship between body size and lens diameter varies across species.

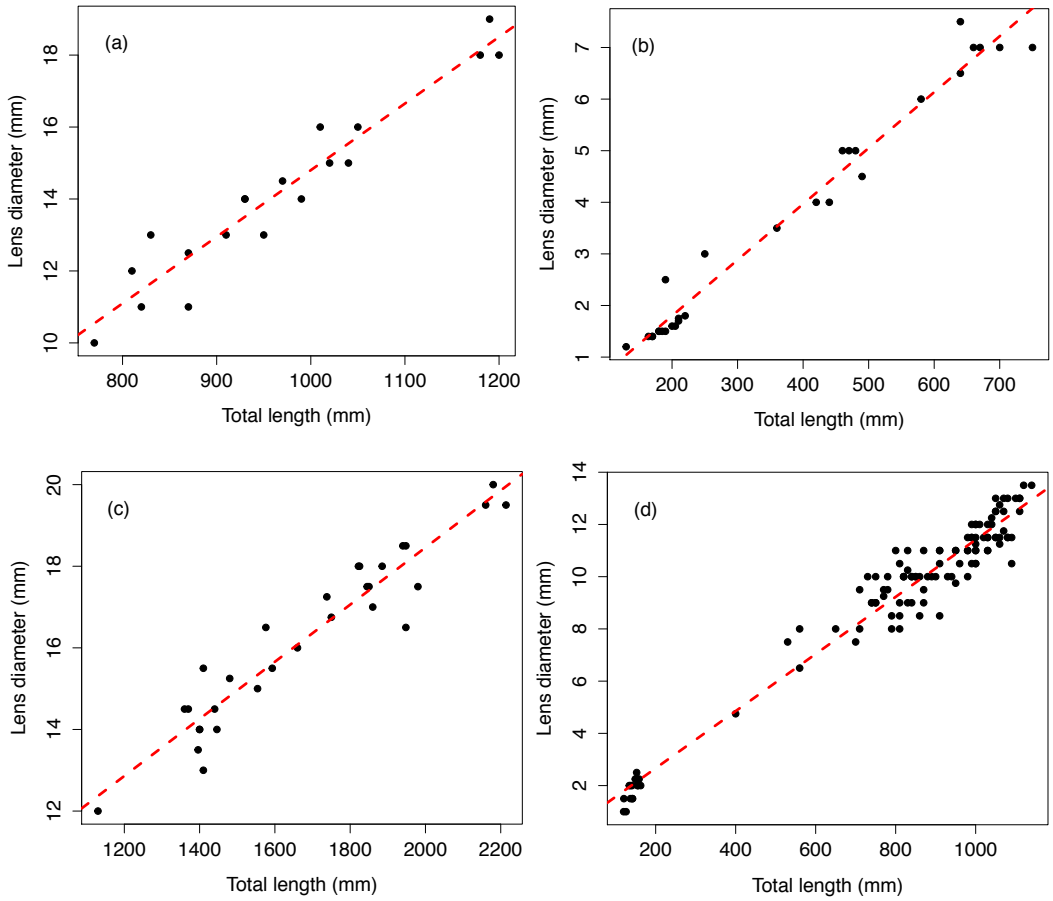

Figure 2.2 - The relationship between total length (TL) and lens diameter (LD) for (a) the blackscabbard fish, *Aphonopus carbo*, (n = 19, r^2=0.917, p < 0.001), (b) the roundnose grenadier, *Coryphaenoides rupestris*, (n = 29, r^2 = 0.973, p < 0.001), (c) the porbeagle shark, *Lamna nasus* (n = 30, r^2 = 0.901, p <0.001), and (d) the spiny dogfish, *Squalus acanthias* (n= 119, r^2 = 0.959, p < 0.001).

2.4.2 Comparison of lens morphology and permeability

Sectioned teleost lenses reveal well-defined, concentric banding, which is enhanced during freeze-drying, as weaknesses between fiber cell layers promote concentric fractures (Figure 2.3). Distinct differences in lens morphology and the structural response of the lens to freeze-drying are seen between species. Cod (*Gadus morhua*, Fig. 2.3.c), conger eel (*Conger conger*, Fig. 2.3.d), and monkfish (*Lophius americanus*, Fig. 2.3.b) lenses all possess clear, concentric bands throughout, radiating from the lens core to edge (outer cortex). Hake (*Merluccius merluccius*, Fig. 2.3.e), haddock (*Melanogrammus aeglefinus*, Fig. 2.3.f), and black scabbard (*Aphonopus carbo*, Fig. 2.3.a) lenses also display clear concentric banding throughout the solid core region of the lens, but with no clear structure within the hydrated outer cortex region. Here, the uniform region surrounding the solid lens core and extending to the lens membrane represents the gelatinous outer cortex. In some cases, the gelatinous region remains structurally stable following freeze-drying, enveloping the core evenly (e.g. *M. merluccius* & *A. carbo*, Fig. 2.3. e & a) with the solid core sitting centrally within the gelatinous outer cortex. Conversely, in the case of *M. aeglefinus* (Fig. 2.3.f), the process of handling and freeze-drying appears to have de-stabilized the structure of the outer cortex, and thus, the solid core is not positioned centrally within the outer cortex portion of the lens. Hake (*M. merluccius*, Fig. 2.3.e), haddock (*M. aeglefinus*, Fig. 2.3.f), and black scabbard (*A. carbo*, Fig. 2.3.a) lenses were relatively hydrated compared to cod and conger eel lenses, and required careful handling to avoid puncturing the lens membrane, which would result in the loss of the gelatinous outer cortex material.

All elasmobranch lenses included in this comparison presented difficulties associated with handling prior to freeze-drying, due to the large proportion of gelatinous material. In the case of the porbeagle shark (*Lamna nasus*, Fig. 2.3.g) and oceanic white tip (*Carcharhinus longimanus*, Fig. 2.3.j), the outer cortex was gelatinous and sticky, comprising less than one third of lens volume. Conversely, the outer cortex of blue shark (*Prionace glauca*, Fig. 2.3.i) lenses comprised approximately half of the lens volume, and the highly hydrated region was less viscous. Spiny dogfish (*Squalus acanthias*, Fig.2.3.h) lenses were intermediate between porbeagle/oceanic white tip and blue shark lenses in terms of relative hydration (Figure 2.3).

The core region of all elasmobranch lenses examined here was generally less dense than that of the teleosts. Elasmobranch lenses also show less concentric banding, and increased hydration relative to teleost lenses (Figure 2.3). Whilst some faint banding is identifiable within the thin section of oceanic white-tip (*C. longimanus*, Fig. 2.3.j) and spiny dogfish (*S. acanthias*, Fig. 2.3.h) lenses, porbeagle (*L. nasus*, Fig. 2.3.g) lenses display no clear concentric structuring. The blue shark (*P. glauca*, Fig. 2.3.i) is the only elasmobranch species included in this comparison that displays clear concentric banding in the core region, however much of the outer cortex material was lost during the process of freeze-drying and sectioning. The hydrated elasmobranch lenses are also more susceptible to fracturing, due to the increased water content. Although fracturing is most evident in the blue shark (*P. glauca*, Fig. 2.3.i), the oceanic white-tip (*C. longimanus*, Fig. 2.3.j) also displays a large fissure radiating from outer cortex to the edge of the core.

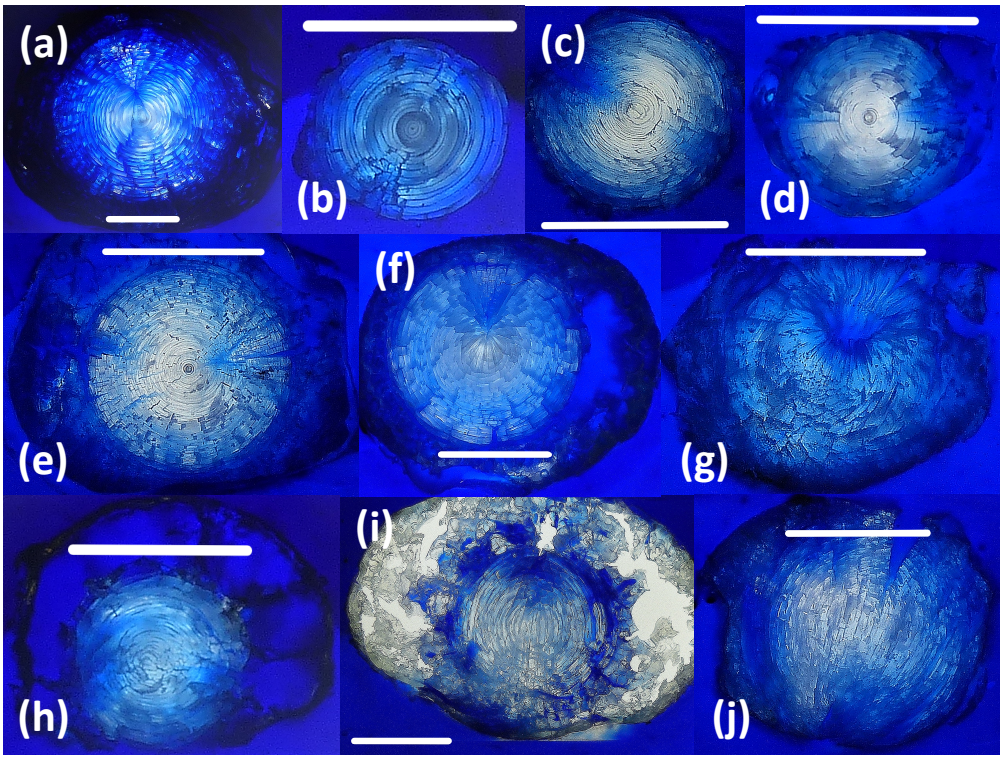

Figure 2.3 – Thin sections of teleost and elasmobranch lenses embedded in pigmented Epoxy resin. Penetration of resin into the lens results in blue staining. Labels represent individual lenses from (a) black scabbardfish (*Aphonopus carbo*), (b) monkfish (*Lophius amaericanus*), (c) cod (*Gadus morhua*), (d) conger eel (*Conger conger*), (e) hake (*Merluccius merluccius*), (f) haddock (*Melanogrammus aeglefinus*), (g) porbeagle (*Lamna nasus*), (h) spiny dogfish (*Squalus acanthias*), (i) blue shark (*Prionace glauca*), and the (j) Oceanic white-tip shark (*Carcharhinus longimanus*), respectively. White lines represent 5mm scale bars.

The relative penetration of dyed resin into the lens differs according to the species examined. For example, the lenses of cod (*G. morhua*, Fig. 2.3.c), conger eels (*C. conger*, Fig. 2.3.d), and hake (*M. merluccius*, Fig. 2.3.e) are relatively impermeable to resin. Conversely, in species such as the porbeagle shark (*L. nasus*, Fig. 2.3.g), oceanic white-tip (*C. longimanus*, Fig. 2.3.j), haddock (*M. aeglefinus*, Fig. 2.3.f), and monkfish (*L. americanus*, Fig. 2.3.b), resin penetrated up to the core of the lens, possibly via the fractures produced during freeze-drying. In the case of the black scabbard (*A.carbo*, Fid. 2.3.a) and spiny dogfish (*S. acanthias*, Fig. 2.3.h), some resin contamination was observed in the outer cortex, but the core appears to be resin-free. A qualitative ranking of susceptibility to resin contamination, was (most susceptible first): *P. glauca* > *L. nasus* > *L. americanus* > *M. aeglefinus* > *S. acanthias* > *A. carbo* > *C. longimanus* > *M. merlucuius* > *C. conger* > *G. morhua*.

2.4.3 Resin contamination

Embedding lenses in Epoxy resin has been shown to introduce resin-derived carbon and nitrogen to lens tissue (to a varying degree), subsequently impacting upon the isotopic signature of the sample. A mass balance approach was used to estimate the relative proportion of resin per sub-sample submitted for analysis, allowing retrospective correction where contamination is low, and rejection of samples from the dataset where contamination is high:

$$\delta^{13}C_s = A * \delta^{13}C_r + B * \delta^{13}C_l \quad (2.5)$$

Here, $\delta^{13}C_s$ represents the isotopic composition of the potentially mixed sample (i.e. lens and resin), $\delta^{13}C_r$ represents the isotopic composition of carbon in the pure resin and $\delta^{13}C_l$ represents the isotopic composition of carbon in a pure lens sample (estimated from core values for each species). A and B represent the relative proportion of resin and lens in each sample, respectively. The equation above assumes that core and edge $\delta^{13}C$ values do not differ significantly compared to the isotopic difference between resin and lens protein.

Following estimation of the relative proportion of resin per sample, an arbitrary threshold of 20% was set to distinguish between samples with high and low levels of contamination. Where the percentage of resin within a particular sample was less

than threshold (<20%), the degree of contamination was corrected for using the following equation:

$$\delta^{13}C_C = \frac{(\delta^{13}C_s * CN_s) - (\delta^{13}C_r * (CN_s - 3.7)}{3.7} \quad (2.6)$$

Here, subscript "s" and "r" represent individual samples and resin, respectively. 3.7 reflects the C:N ratio of a pure protein.

Where the proportion of resin estimated in a given sample exceeded the threshold, the sample in question was rejected from the dataset. Nitrogen isotope compositions were not corrected to account for contamination, in order to avoid error propagation.

The isotopic composition of pure resin differs considerably from lens protein (Epoxy resin: $\delta^{13}C$ = -29.49‰, $\delta^{15}N$ = -2.28‰). Whilst the occurrence of Epoxy resin is generally reduced in the lens nucleus, core samples from the study species comprise up to ~10% resin, with high variability in the case of *L. nasus*.

C. rupestris lenses were most susceptible to resin contamination with 39% of all samples containing >20% resin, followed by *L. nasus* with 36% of samples exceeding the 20% contamination threshold. Relatively little resin contamination was observed in *A.carbo* lenses, and only 13% of samples were omitted from data set due to contamination. This allowed correction and subsequent production of cross-lens profiles detailing isotopic variability (Figure 2.4).

2.4.4 Ontogenetic trends in stable isotope compositions across lenses

Symmetrical ontogenetic trends centered around the lens core were recovered for both $\delta^{15}N$ and $\delta^{13}C$ values in *Aphanopus carbo* lenses. The total length associated with each lens sub-sample was calculated using equation 2.1 and the corresponding distance from lens core (mm). In general $\delta^{15}N$ and $\delta^{13}C$ values increase with body size in *A. carbo* with a sharp isotopic excursion associated with the lens core (Figure 2.4).

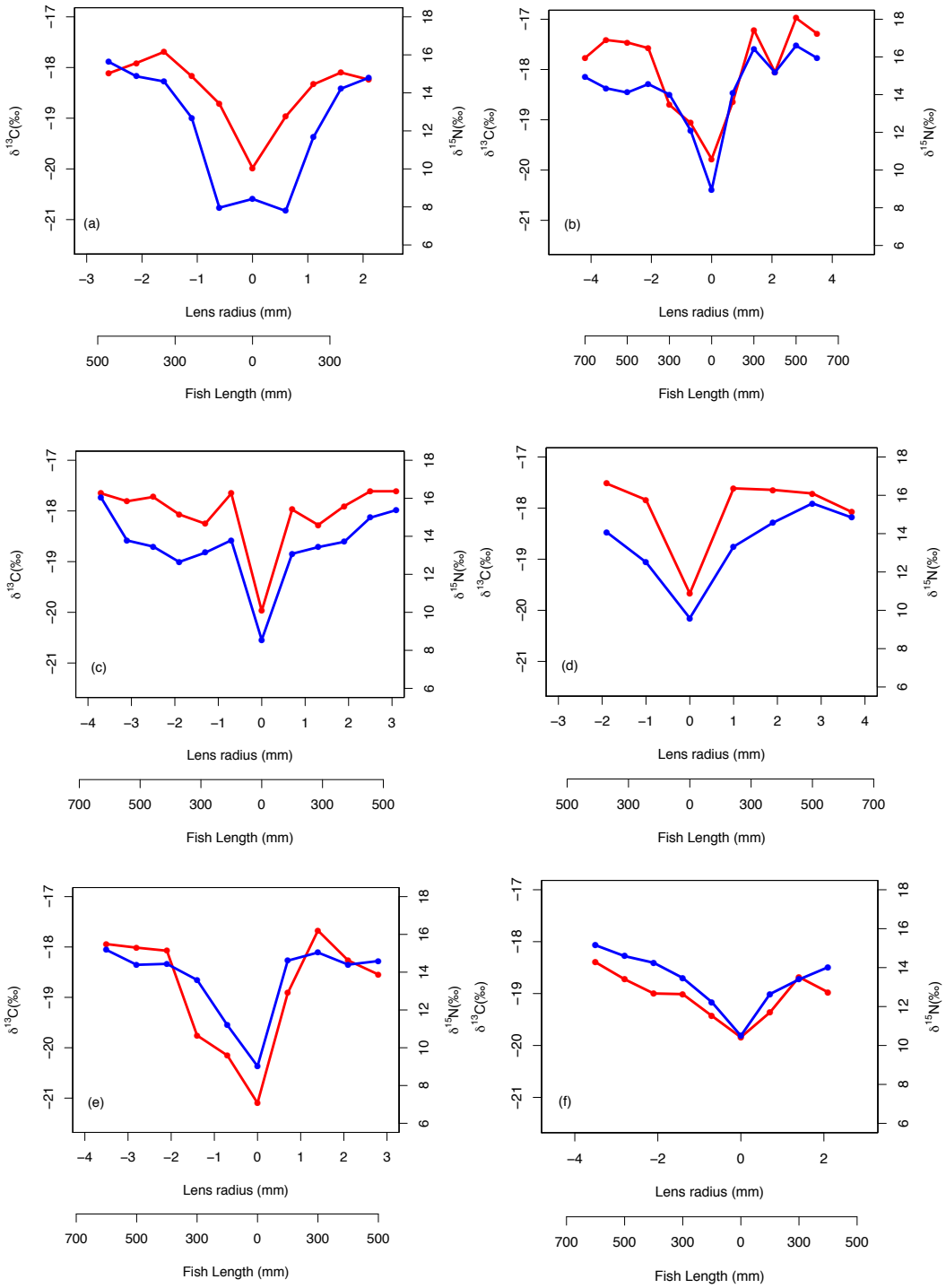
(a)
(b)
(c)
(d)
(e)
(f)
δ13C(‰)
δ15N(‰)
Lens radius (mm)
Fish Length (mm)

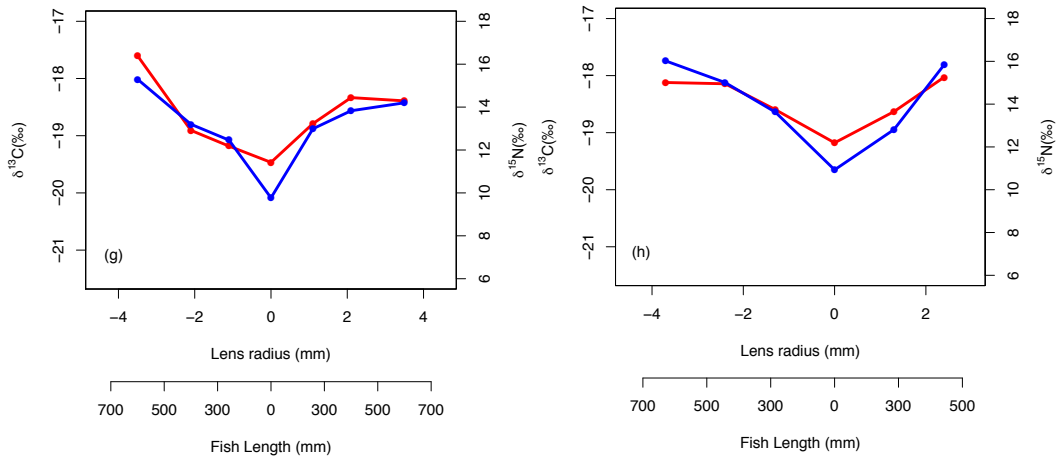

Figure 2.4 – Bivariate plots of $\delta^{15}N$ (blue) and $\delta^{13}C$ (red) variability through *Aphonopus carbo* lenses. The corresponding size-estimate of individual fish at time of tissue formation was recovered from relationship reported in Figure 2.2(a), and the location of the sample from the lens transect.

2.4.5 Between-species comparisons of lens isotope compositions

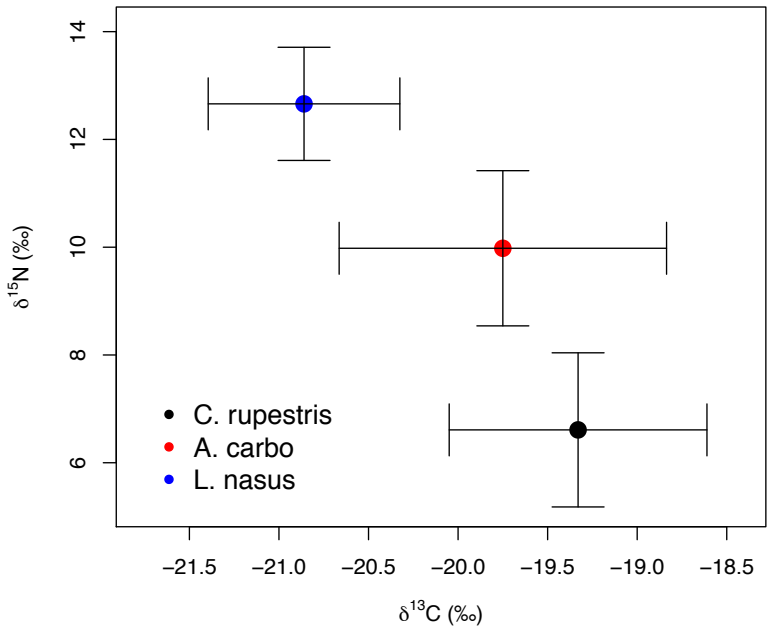

Figure 2.5 - Comparison of mean core $\delta^{13}C$ and $\delta^{15}N$ values for *Coryphanoides rupestris*, *Aphonopus carbo* and *Lamna nasus*. Error bars display standard deviation.

Due to the high resin content of sequential lens samples, only isotope values from the core, representing early juvenile compositions, are compared between species. The isotopic compositions of the lens core of the three sampled species are distinct (Figure 2.5) (one-way ANOVA, $F_{2,26} = 8.01$, $p = 0.001$ and $F_{2,26} = 44.13$, $p = <0.001$, for carbon and nitrogen, respectively). Post-hoc comparison (Tukey test) confirmed a

significant difference between *L. nasus* and *C. rupestris* ($p < 0.01$ for carbon and nitrogen), and between *A. carbo* and *L. nasus* lens tissue ($p = 0.02$ & $p < 0.01$ for carbon and nitrogen, respectively). Whilst a significant difference was also identified between *A. carbo* and *C. rupestris* lens $\delta^{15}N$ ($p < 0.01$), $\delta^{13}C$ values are comparable between the two species ($p = 0.43$). Lowest mean nitrogen isotope ratios are seen in the grenadier (mean = 7.95 ‰ ± 1.68), followed by the black scabbard (mean = 11.58‰ ± 1.23) and porbeagle shark (mean = 15.22‰ ± 1.81). Lens core carbon isotope compositions for *C.rupestris* and *L.nasus* are distinct, however there is considerable isotopic overlap between *A. carbo*, and both *C.rupestris* and *L.nasus*.

2.4.6 Isotopic fractionation between lens and muscle tissue

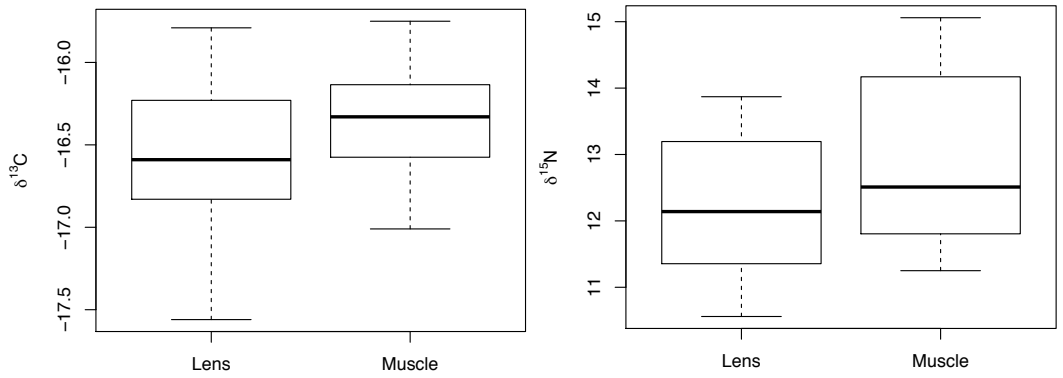

Figure 2.6 – Comparison of embryonic lens and muscle $\delta^{15}N$ and $\delta^{13}C$ values from 11 *Squalus acanthias* specimens.

The isotopic composition of lens and muscle samples from spiny dogfish (*Squalus acanthias*) embryos was compared (n = 11 and 19, respectively), under the assumption that lens and muscle tissue formed *in utero* are derived from the same nutrient source (egg yolk) and have similar isotopic incorporation times, not exceeding the species' gestation period. Due to the small size of pup lens samples, whole lenses were analysed. Reum's (2011) lipid correction model was applied to the muscle data. The isotopic compositions of lens protein from *S. acanthias* show similar variability in both $\delta^{15}N$ and $\delta^{13}C$ values to muscle (Figure 2.6). Muscle tissue was enriched in both ^{13}C and ^{15}N relative to lens protein (paired t-test, mean offset in nitrogen, = 0.66 ± 0.38 ‰, p=<0.01: mean offset in carbon = 0.18 ± 0.23 ‰, p=<0.01), but the mean offset in carbon was similar to analytical precision.

Finally, $\delta^{15}N$ and $\delta^{13}C$ values from the lens core of mature *Coryphaenoides rupestris* were compared with existing measurements of $\delta^{15}N$ and $\delta^{13}C$ values of muscle tissue from early juvenile *C. rupestris* specimens measuring ≤ 50mm, recovered from the same region (Figure 2.7). Lens tissues were more varied in both $\delta^{15}N$ and $\delta^{13}C$ values compared to muscle and while lenses were again generally depleted in ^{13}C and ^{15}N, mean $\delta^{15}N$ and $\delta^{13}C$ values did not differ significantly between lens and muscle proteins ($\delta^{15}N$ – t = 0.495, p = 0.332, $\delta^{13}C$ – t = -1.001, p = 0.332).

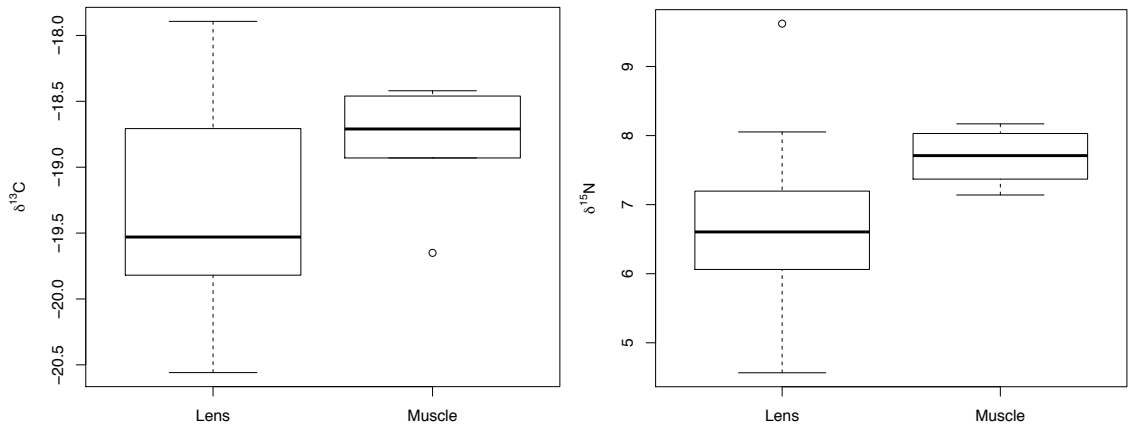

Figure 2.7 – Comparison of lens core and muscle $\delta^{15}N$ and $\delta^{13}C$ values from *Coryphaenoides rupestris* specimens measuring ≤ 50mm. Eye lenses and muscle samples were obtained from specimens caught during the deep-water survey onboard MRV Scotia; lenses were excised from fish caught in 2012, and the muscle originates from specimens caught during the 2013 cruise.

2.5 Discussion

Before eye lens tissues can be considered as an effective host for ontogenetic stable isotope analyses, the following issues must first be addressed:

(1) The relationship between lens diameter and body size should be tested across taxa
(2) The structure of lenses should be compared between taxa, and a consistent sampling methodology should be determined.
(3) Isotopic variability expected between and within individuals should be demonstrated across a range of taxa.
(4) The isotopic offset between lens and muscle tissue should be calculated across taxa.

Below, each issue is addressed in turn.

2.5.1 Relationship between lens and body size

Lens accretion occurs in linear proportion to the somatic growth in each of the four species studied. Linear growth between lens radius and body size indicates that the lens presents a near whole-life chronology of chemical information with greater temporal resolution during periods of rapid body size growth. Linear growth allows retrospective estimation of the approximate size of the fish corresponding to a particular location within the lens. The slope and intercepts of the lens to body size relationship differ between species, requiring this to be estimated for each new study species, at least until sufficient species have been assessed to develop generalised predictive relationships.

2.5.2 Lens structure and sampling methodology

Lenses are relatively difficult tissues to handle due to their partially hydrated, gelatinous exterior, hard internal core and spherical shape. Two alternative sampling processes have been proposed, 'peeling' layers from the lens developed by Parry (2003), and later applied by Wallace *et al*. (2014), and embedding and sectioning comparable to more standard sclerochronological sampling methods. The peeling technique represents a simple and attractive method to sample eye lenses, but sequential peeling techniques are difficult to apply where lenses are either highly crystalline or highly gelatinous. Additionally, it is relatively difficult to accurately control the depth of each sequential layer peeled from a lens, making cross-referencing to age models inaccurate. Embedding lenses in a resin medium and sectioning could provide a more reliable handling technique, but embedding methods bring the tissue under study into contact with a potential contaminant (the resin embedding medium). Therefore permeability of the lens to the embedding medium is a critical concern. High interspecific diversity in permeability to epoxy resin among lenses was observed (Figure 2.3), however teleost lenses are generally denser and less hydrated relative to elasmobranchs. The extent of contamination as assessed by carbon isotope mass balance was also highly variable between species, ranging from <15% for dense lenses of *A. carbo*, and core regions in other species, to more than 30% in the hydrated outer portions of *Lamna nasus* and *Coryphaenoides rupestris*

lenses. Visual assessment of resin contamination similarly suggested that the susceptibility to contamination corresponds to the degree of hydration of the lens, and freeze-drying appears to enhance resin contamination during embedding possibly because of the development of fractures that penetrate circumferential lamellae. The degree of hydration ultimately influences the ability to sample lenses accurately and precisely via both peeling and sectioning.

Lens size may be a driving factor of the relative hydration of lenses and, consequently, the suitability of a particular lens to resin embedding and sectioning. For example, blue shark, oceanic white-tip shark, haddock and black scabbard lenses are both the largest lenses included in this study, and also the most hydrated (*a priori* observations). Increased porosity or hydration in large lenses may be associated with the demand for lenses to remain transparent and reduce light refraction. With increasing size, comes an increase in the path length that light must travel through the lens, which, in turn increases the potential for light scattering. Thus, maximum protein concentration may be limited in larger lenses to a level lower than that of smaller lenses (Kröger, 2013), in order to reduce light scattering.

The structure of a particular lens will ultimately determine the methodology used, and each species must be addressed on a case-by-case basis. The "peeling" technique developed by Parry (2003) and implemented by Wallace *et al*. (2014) represents a high-resolution, contamination-free technique, and should be the first choice method. Where "peeling" is not possible, or where accurately resolved distances across the lens are required, the resin-embedding method represents an alternative approach, but only for relatively dense lenses, and the potential for contamination must be assessed. In the case of highly gelatinous lenses, neither methodology discussed in this paper is suitable at least for recovering sequential samples across the lens.

2.5.3 Recovery of expected isotopic differences within and between species

Transects of $\delta^{15}N$ and $\delta^{13}C$ values across whole lenses of *Aphonopus carbo* show a high degree of bilateral symmetry, i.e. different locations of roughly equal radial distance from the core record similar isotopic signals. All *Aphonopus carbo* specimens analysed in this study exhibit progressive enrichment in $\delta^{15}N$ values consistent with *a priori* expectations of increasing trophic level with body size in this species (Trueman

et al. 2014), and agree with published trends in the lens nitrogen isotope values of teleosts (Wallace *et al.* 2014). The one exception is the presence of elevated core $\delta^{15}N$ value in one *A.carbo* specimen (Figure 2.4(a)). This is attributed to the presence of a maternal signal at the absolute core, which may elevate the $\delta^{15}N$ value of this sample relative to adjacent tissue.

$\delta^{15}N$ and $\delta^{13}C$ ratios in the lens core differed significantly between the three sampled species (Figure 2.5). $\delta^{15}N$ values increase from the zooplanktivorous *C.rupestris* to the piscivorous *A.carbo* and are highest in the vivaporous *L. nasus*, consistent with the expected relative trophic position of the juveniles of these species. *A. carbo* and *C. rupestris* specimens were both sampled from the North East Atlantic continental slope west of Scotland, but genetic and microchemical data indicate that *C. rupestris,* is a lifelong resident species, whilst *A. carbo* individuals spend their earliest life stages in southern waters around Madeira (Longmore *et al.* 2014). $\delta^{13}C$ values successfully distinguish the resident *C.rupestris* from the migratory *A.carbo*. Between-species variation in the isotopic composition of lens core protein is thus greater than among-individual variation, as expected for these functionally distinct species.

2.5.4 Potential for isotopic offset between lens and muscle protein

Estimates of isotopic fractionation between tissues are generally performed across tissues in the same individual. This methodology is relatively difficult for eye lens proteins as (a) turnover times for muscle and lens protein are unknown and (b) outer portions of lenses are hydrated, gelatinous and difficult to sample accurately. Consequently we took two complimentary approaches: comparisons of lens and muscle tissues within developing embryos, and comparing lens and muscle between different individuals but at similar life stages.

Tissues of embryonic sharks form over relatively similar timescales, are sustained from a single isotopically constant nutrient source and have no isotopic memory associated with tissue turnover. Embryonic sharks therefore provide a uniquely constrained opportunity to determine potential isotopic offset effects associated with tissue composition. Within individual embryos of spiny dogfish (*Squalus acanthias*) lens protein was slightly but significantly depleted in both $\delta^{15}N$ and $\delta^{13}C$ values

compared to muscle protein (mean difference = 0.66 ± 0.38 ‰, p=<0.01, and 0.18 ± 0.23 ‰, p=<0.01, for nitrogen and carbon, respectively) (Figure 2.6).

For teleosts, we compared lens protein values in the core regions from adult fish with those of juvenile fish of equivalent sizes. Therefore we compare across individuals from different year classes, but of equivalent size (Figure 2.7). Mean $\delta^{13}C$ and $\delta^{15}N$ values in eye lens proteins were again depleted relative to muscle tissue from *Coryphaenoides rupestris* specimens. However the absolute offset is small and effectively obscured by the additional variance associated with un-matched individuals. Consequently, lens protein appears to be depleted in both $\delta^{15}N$ and $\delta^{13}C$ values compared to muscle protein for both elasmobranchs and teleosts, but the isotopic differences are less than 0.75% and 0.25% respectively and likely to be obscured by between-individual variation and analytical error.

2.5.5 Additional complexities associated with lens-based methodologies

The data presented above, together with previous published studies (Parry, 2003; Onthank, 2013; Wallace *et al*. 2014), clearly demonstrate that eye lenses of teleosts and elasmobranchs can provide retrospective, whole life records of isotopic compositions. These life history records can be exploited to study spatial and trophic ecology particularly relating to early juvenile life stages.

The application of lens-based methodologies to investigate elasmobranch ecology, however, is complicated by the reproductive strategies adopted by members of this subclass. Sharks, rays and skates expend a large amount of energy producing relatively few, well developed offspring, via oviparous or viviparous (placental/aplacental) strategies. Embryos are maternally nourished either directly (viviparity) or indirectly via the yolk sac (oviparity/aplacental viviparity), thus the chemical composition of tissue formed during embryonic development reflects the diet of mature females during egg sac provisioning (aplacental) or the foraging behaviour of gestating mothers (placental). Whilst this provides a potentially exciting opportunity to study the movements of mature and pregnant females via analysis of lens core chemistry, there are several factors that must first be addressed. The duration of maternal nourishment varies considerably between species, with gestation ranging from months to years (Koob & Callard, 1999). Thus, the relative

proportion of the lens representative of maternal nourishment varies according to species, an estimate of which is required in order to isolate lens tissue formed pre-birth from that representative of exogenous feeding in the juvenile life history stage. Where size-at-birth data are available, this information can be used alongside the growth relationship parameters in order to isolate lens tissue formed pre-birth from lens tissue accreted post-parturition.

In viviparous species, isotopic variability within the pre-birth portion of the lens is likely to reflect changes in diet and/or location of the gestating female. However, in oviparous and aplacental viviparous species, the pre-birth lens tissue reflects maternal nutrient assimilation during egg sac formation. Given that yolk capsules may be laid down prior to the initiation of embryo growth (Wood *et al*. 1979), there is potential for considerable temporal decoupling between maternal feeding fuelling yolk sac production, and the subsequent utilization and incorporation of this material into the tissues of the embryo. Furthermore, in aplacental viviparous species, the potential for pre-birth omnivory in the developing embryo presents an additional complication. Consumption of unfertilized eggs (oophagy) formed at different times may further complicate the issue of temporal decoupling, whilst consumption of un-hatched embryos (embryophagy) could introduce an additional trophic offset, similar to that associated with maternal partitioning.

Thus, whilst lens-based methodologies offer a novel way to retrospectively investigate whole life history ecology, interpretation of lens-hosted isotope data, particularly in the pre-birth portion of the lens requires further investigation.

2.6 Conclusions

Many researchers have exploited the unique structural characteristics of the vertebrate eye lens, and applied this to aging studies, investigations into fisheries stock discrimination and isotope ecology. Here we show that eye lens tissue also serves as a repository for chemical information relating to whole life-history of an individual, allowing retrospective investigation of ontogenetic trophic history and habitat use through stable isotope analyses.

This novel lens-based technique has the potential to aid elucidation of the movements and trophic dynamics of otherwise inaccessible migratory species. However, the structure and mechanical properties of the fish lens differs markedly between species, and can present problems associated with handling. It is therefore important to assess lens morphology on a case-by-case basis, and to develop handling and preparation protocols that can be adapted accordingly to suit different species.

Further research is also required in order to elucidate the issues associated with the interpretation of lens tissue formed *in utero* in elasmobranchs. Sharks, rays and skates require special attention, and given the range of reproductive strategies, the associated maternal nourishment, and variable gestation period, each species should be addressed on a case-by-case basis. In conclusion, the eye lens represents a promising target for biochemical reconstruction of life-long diet and spatial ecology.

Chapter 3: Stable carbon and nitrogen isotope fractionation between maternal and offspring tissues in an aplacental shark, *Squalus acanthias*: implications for recovery of cross-generational tropho-spatial information.

This Chapter is a manuscript in preparation, to be submitted in Spring 2017. Written by Katie Quaeck, including feedback from Clive Trueman.

3.1 Abstract

Tissues formed before birth are built from carbon and nitrogen atoms derived from the mother, and thus the isotopic composition of these tissues provides information on the trophic and spatial ecology of the individual's mother during egg production/gestation. Accessing this information demands a clear understanding of the potentially complex isotopic relationship between maternal and offspring tissues.

Here the isotopic relationship between mother and offspring pairs in muscle and eye lens tissues from the spiny dogfish *Squalus acanthias* caught in the North Sea is assessed. The isotopic composition of carbon and nitrogen in muscle tissue was relatively consistent between embryos in a single brood (mean $d^{13}C$ = -16.27‰ ± 0.35, mean $d^{15}N$ = 13.48‰ ± 1.02), but still exceeded analytical uncertainty in 2 of 5 sampled broods, implying that mothers foraged across isotopic gradients during growth of eggs.

The isotopic composition of muscle tissue from 20 gravid female sharks caught in a single location varied between individuals (mean $d^{13}C$ = -17.03‰ ± 0.31; mean $d^{15}N$ 12.96‰ ± 0.67) reflecting individual variation in tropho-spatial ecology during the timescale of muscle turnover. Between-individual variation in the isotopic composition of nitrogen was greater in embryonic muscle than in maternal muscle tissue, implying that the slow turnover rate of adult muscle obscured short duration migrations

across isotopic gradients that were captured in faster growing egg tissues and passed to embryos.

Estimating likely isotopic offsets between maternal and embryonic tissues in wild sharks is complicated by the temporal mismatch in tissue growth and migration across isotopic gradients. Here, maternal-embryonic lens nitrogen isotope spacing is attributed to both tissue growth dynamics and migration across isotopic gradients, with eggs reflecting isotopically light (northern) maternal foraging. Whilst ruling out additional trophic effects is difficult, the systematic maternal-embryonic carbon isotope offset recorded in muscle and lens tissue, considered within the context of the North Sea and it's isoscape, provides further evidence for systematic maternal-offspring isotopic offset.

3.2 Introduction

Stable isotope analysis (SIA) is a routine tool in trophic and spatial ecology (Hobson, 1999). At the base of the food chain, carbon and nitrogen isotope values vary spatially (Rubenstein & Hobson, 2004; Graham *et al*. 2010; MacKenzie *et al*. 2014), and this variability is incorporated into the tissues of animals moving through, and foraging within, isotopic provinces (Hobson, 1999; Graham *et al.* 2010; Hobson *et al.* 2010). Preferential excretion of light isotopes during respiration leads to systematic isotopic enrichment of predators compared to their prey, forging the basis for isotopic diet analysis (Smith & Epstein, 1970; Minson *et al*. 1975; Haines, 1976; DeNiro & Epstein, 1978; Fry *et al*. 1978; DeNiro & Epstein, 1981).

The use of SIA is particularly appealing in environments where direct observation of predator-prey interactions, or spatial movements, is challenging, and consequently SIA has been widely applied in marine systems (e.g. Hobson *et al*. 1992; Best & Schell, 1996; Parry, 2003; Lee *et al*. 2005; Estrada *et al*. 2006; Jaeger *et al*. 2010; MacKenzie, 2010; Hussey *et al*. 2011; Trueman *et al*. 2012; Onthank, 2013; Wallace *et al*. 2014). One distinct advantage of SIA is the ability to sub-sample incrementally grown tissues such as shells, otoliths and vertebrae to gain a retrospective view of trophic and spatial ecology through the whole lifetime of an individual

(Trueman *et al*. 2013). During gestation, the resources fuelling embryonic development are derived from the mother, either by a direct mother-embryo link (placental) or via yolk tissue (aplacental). Following birth and upon the onset of independent foraging, the chemical composition of neonatal tissue, previously reflecting maternal provisioning, is slowly restructured, remodelled and replaced by independent post-partum feeding habits (Frankel *et al*. 2012). However, where inert, incrementally formed tissues occur, for example, the vertebrate eye lens, the chemical composition of tissue fuelled by maternal provisioning is preserved, providing information relating to maternal foraging directly from offspring. This information source could, for instance, identify covariances between differential maternal foraging ecologies and offspring fitness (e.g. maternal effects on offspring survivorship).

Accessing and interpreting maternal-origin biochemical signals in incrementally grown tissues first requires a thorough understanding of the biochemical relationship between the tissues of the developing offspring and it's mother. Given that the isotopic composition of an organism is generally enriched relative to its diet (DeNiro & Epstein, 1978; Minagawa & Wada, 1984; Post, 2002), and assuming that mothers and embryos are comparable physiologically, the tissues of neonates are frequently anticipated to appear isotopically enriched relative to their mothers (Jenkins *et al*. 2001; McMeans *et al*. 2009), with offspring appearing as though they are "feeding on mum". This phenomenon is expected to persist within neonate tissues until independent *post-partum* feeding habits restructure and replace maternal signals (McMeans *et al.* 2009).

In aplacental animals, the isotopic composition of yolk (and thus also pre-partum offspring tissues) reflects that of the mother's diet during yolk formation. In some species yolk formation occurs many months before fertilization and embryonic development (Ketchen, 1972), and thus may occur in locations with differing chemical baselines. The rate of growth of yolk tissue is likely to be much greater than the rate of isotopic turnover in commonly sampled tissues such as muscle (Vander Zanden *et al*. 2015),

particularly in adult females partitioning resources towards reproduction. The isotopic composition of yolk (and embryonic tissue) may therefore differ from other maternal tissues if the mother migrates across isotopic gradients, or feeds on isotopically varying prey through time (Frankel *et al*. 2012). The isotopic systematics and temporal dynamics of maternal-embryonic nourishment must therefore be considered (Vaudo *et al.* 2010). Whilst the production of "uterine milk" (histotroph) represents an additional source of nourishment to the developing embryos of some elasmobranchs (notably false catsharks, *Pseudotriakidae*), histotrophy does not contribute to *S. acanthias* embryo growth (Hamlett & Hysell, 1998).

3.2.1 Embryonic nutrition in elasmobranchs

Table 3.1 – Table of literature data detailing maternal-embryonic isotopic offset factors of three placentatrophic elasmobranch shark species. NB Data from aplacental species unavailable.

Study	**Species**	**Reproductive mode**	**Tissue**	**Embryo-maternal offset**	
				Carbon	Nitrogen
McMeans *et al*. (2009)	*Rhizoprionodon terraenovae*	Placentatrophic	Muscle	1·5‰	1·4‰
			Liver	1·5‰	1·7‰
			Vertebral collagen	−1·01‰	1·1‰
Vaudo *et al*. 2010	*Sphyrna lewini*	Placentatrophic	Muscle	1.01‰	0.82‰
	Carcharhinus limbatus			−0·26‰	0.88‰

The range of reproductive strategies adopted by elasmobranchs (see Wourms, 1977, 1981; Wourms *et al*. 1988; Koob & Callard, 1991; Hamlett and Koob, 1999) introduces additional complexities when interpreting data relating to neonate and juvenile sharks, particularly when incrementally formed tissues are studied. In placentatrophic (viviparous)

elasmobranch species, embryos initially feed upon yolk from an external yolk sac. Once exhausted, the sac fuses with endometrial tissues, forming a direct placental link to the mother, supplemented in some species by histotrophy ("uterine milk") (Hamlett & Hysell, 1998). Thus, sclerochronological tissues isolated from the offspring of placentatrophic species, and formed *in utero*, have the potential to record the foraging history of the mother not only during initial yolk sac production, but also during later gestation once the placental link is formed.

In oviparous species, nutrition is supplied to the embryo via yolk sacs, which are laid in collagenous cases. In oviparous elasmobranchs, much of the early development occurs outside the mother's body, and growth is fuelled solely by yolk tissue. Conversely, aplacental viviparous species retain soft egg cases until development is complete, giving birth to live young. In both cases, once the egg sac is laid down, the embryo receives no further nourishment from the mother. Thus, the chemical composition of embryonic tissues is representative of the foraging habits of the mother at the time of yolk sac formation, assuming no biasing of nutrients occurs during transfer from mother to offspring. Where oophagy occurs, and embryos feed on unfertilized ova once their own yolk sac is depleted, there is potential for additional isotopic nutrient sources if ova are produced continually while mothers migrate across isotopic gradients. In extreme cases, siblings may conduct in-uterine cannibalism, potentially introducing an additional trophic enrichment (Hamlett & Hysell, 1998).

Maternal-embryonic offsets in stable isotope compositions have been investigated in several placentatrophic elasmobranchs. For example, McMeans *et al.* (2009) compared the stable carbon and nitrogen isotope compositions of mother and embryo Atlantic sharpnose (*Rhizoprionodon terraenovae*) tissues. $\delta^{13}C$ and $\delta^{15}N$ values in the muscle and liver of embryos were elevated relative to their mothers, however whilst embryo vertebral collagen $\delta^{15}N$ was similarly elevated, $\delta^{13}C$ values appear depleted relative to their mothers (McMeans *et al.* 2009)) (Table 3.1). Similar results were also observed when maternal and embryonic scalloped

hammerhead (*Sphyrna lewini*) and blacktip shark (*Carcharhinus limbatus*) muscle tissue were compared (Vaudo *et al.* 2010), as embryos of both species were enriched in $\delta^{15}N$ relative to their mothers (Table 3.1). However, the direction and extent of $\delta^{13}C$ offsets differ, with embryonic *S. lewini* appearing enriched, and *C. limbatus* depleted, relative to maternal tissue. Mother–offspring nitrogen offset ($\Delta^{15}N$) of muscle, liver and vertebral collagen range from 0.82 to 1.7‰ in placentatrophic sharks (McMeans *et al*. 2009; Vaudo *et al*. 2010), with embryos generally appearing enriched relative to their mothers. Carbon offsets ($\Delta^{13}C$) appear to be more variable, possibly highlighting tissue- and species-dependant effects.

In aplacental sharks, mother-offspring differences in the isotope composition of muscle and liver tissue have been determined in two species: *Squalus megalops* and *Centrophorus moluccensis* (Le Bourg *et al.* 2014). Muscle and liver tissues of *S. megalops* offspring display similar $\delta^{13}C$ values to their mothers, while offspring $\delta^{15}N$ values where similar in liver, but lower in muscle, compared to their mothers (absolute isotope ratios unavailable). Conversely, whilst maternal and embryonic isotope ratios were similar in *C. moluccensis* muscle, embryonic liver tissue was elevated in $\delta^{13}C$, and depleted in $\delta^{15}N$, relative to their mothers (Le Bourg *et al.* 2014). Isotopic fractionation thus appears to differ considerably between placentatrophic and aplacental sharks, with some interspecific variability within the two reproductive modes. Furthermore, tissue-specific effects also appear to influence the direction and extent of fractionation. However, with limited data available on the subject, reported mother-offspring discrimination factors must be applied with caution, and ideally addressed for each species of interest.

In addition to isotopic offsets associated with tissue composition, the isotopic offset between maternal and embryonic tissues in aplacental elasmobranchs potentially depends on the foraging location of the mother during egg production and subsequently, isotopic gradients between these foraging locations and the rates of formation of egg proteins and other maternal tissues. Muscle is a metabolically active tissue, and in adult animals with limited somatic growth, the

isotopic composition of muscle varies through metabolic tissue turnover. The rate of isotopic turnover of muscle in adult elasmobranchs can be crudely estimated based on statistical relationships between body size and isotopic half life across vertebrate ectotherms (Vander Zanden *et al*. 2015). Ectotherms weighing between 10^3 and 10^4 grams are estimated to have isotopic half-lives between 50 and 150 days and thus broadly equilibrate to diets over a timescale of months to a year. By contrast growth of the egg sac is likely to occur over a relatively short timeframe (Koob & Callard, 1999). Consequently maternal-offspring tissue comparisons also compare tissues forming within the mother over long (adult muscle) and short (egg) timeframes.

3.2.2 Case study species and area

This study is based on spiny dogfish (*Squalus acanthias*) recovered from the eastern North Sea. *S. acanthias* is a small (<120cm total length, TL; Hammond & Ellis, 2004), long-lived and slow growing squaliform shark (Holden & Meadows, 1962; Tucker, 1985; Campana *et al*. 2006). Believed to have once been the most abundant living shark and a nuisance species (Tallack & Mandelman, 2009), it is now listed as endangered in the Northeast Atlantic. During the first half of the 20th century, spiny dogfish landings increased in the northeast Atlantic due to the demand for its liver oil and meat. Target fisheries began operating within Norwegian waters, and the North and Celtic Seas by 1963, and landings of >60,000 t were reported (ICES, 2009a). However, landings fell steadily throughout the latter half of the 20th and into the 21st centuries, with the exception of a brief increase in the 1980s associated with the development of new directed fisheries off Ireland and in the Irish Sea (de Oliveira *et al*. 2013).

Commonly associated with coastal waters and the continental shelf (Burgess, 2002; Shepherd *et al*. 2002), spiny dogfish are known to segregate by sex and size (Ebert *et al*. 2013), with adult females schooling in relatively shallow inshore waters, while adult males are found offshore in deeper waters (Shepherd *et al*. 2002; Ebert *et al*. 2013). *S. acanthias* are also known to undertake seasonal migrations (Hisaw *et al*. 1947; Holden, 1965; Burgess, 2002; Stenberg, 2005; Francis *et al*. 2007), and occasional trans-Atlantic migrations have also been documented (Templeman, 1976).

The distribution of *S. acanthias* in the Northeast Atlantic has long been of interest to fisheries ecologists, and there have been many investigations into the movements of spiny dogfish since the 1950s (Aasen, 1964; Holden, 1967; Hjertenes, 1980; Vince, 1991). Once widespread and abundant throughout the region, spiny dogfish now occur more commonly in the western North Sea and off the isles of Orkney and Shetland, with large catches of juveniles occurring off the northern coast of Scotland (Ellis *et al*. 2012). Thus, whilst the North Sea represents a known component of spiny dogfish distribution, the relative importance of this coastal sea in terms of the species' (critical) habitat use and residency, with particular reference to gravid females, is unknown.

Spatial variations in the stable isotope composition of carbon and nitrogen in the marine food chain of the North Sea have been well characterised (Jennings & Warr, 2003; Barnes *et al*. 2009; MacKenzie *et al*. 2014; Trueman *et al*. 2016). The isotopic composition of nitrogen in North Sea ecosystems is systematically more positive in the shallow south and particularly the south-eastern basin, with a $\delta^{15}N$ range exceeding 8‰ (Trueman *et al.* 2016). The isotopic composition of carbon shows a distinct minimum in the central southern North Sea basin, with a total range in $\delta^{13}C$ values exceeding 5‰ (Trueman *et al.* 2016). The broad distribution of stable isotope values across the North Sea has remained stable for at least 10 years (MacKenzie *et al*. 2014), reflecting underlying controls related to hydrology and geography rather than dynamic biological control. Animals moving between the northern and southern North Sea basins therefore traverse strong and predictable isotopic gradients.

The purpose of this investigation is to examine the isotopic relationship between maternal and embryonic muscle and eye lens proteins in the aplacentally viviparous, migratory spiny dogfish, *Squalus acanthias*, to determine any isotopic offset related to tissue composition, and infer the extent that migration across isotopic gradients during and subsequent to egg production influences maternal-embryo isotopic spacing.

3.3 Materials and Methods

Squalus acanthias samples were collected from sharks landed in association with the Neptune Scientific Fishery (Cefas/Defra). Muscle tissue was extracted from the dorsal region of twenty pregnant *S. acanthias* specimens, from a seized catch by the Marine Management Organisation off Southwold, caught by long-liner (<10metre). Muscle tissue was also extracted from the dorsal region of one embryo from each mother. Five of the mothers were selected randomly, and muscle tissue from an additional four embryos was sampled in order to compare intra-brood isotopic variability.

One eye lens was extracted from each of the twenty pregnant females by making an incision along the length of the cornea, allowing the lens to be removed using forceps. Once excised, whole lenses were subsampled using the technique developed by Parry (2003), core tissue and samples originating from the outermost region of the lens were isolated from gravid females. Whole lenses were also extracted from one embryo from each of the adult *S. acanthias* specimens. An additional subset of 45 lens cores, selected at random from adult specimens, were submitted for stable isotope analysis (totalling 65 lens cores, including the 20 samples isolated from pregnant females).

Once extracted, muscle tissue was rinsed with deionised water ten times in order to remove any labile nitrogenous material (e.g. urea or ammonia). Samples were then centrifuged for 10 minutes, before a further ten rinses were conducted. It was not necessary to rinse lens tissue prior to analysis as they are isolated within the lens capsule. Muscle and lens samples were frozen overnight prior to lyophilisation. The tissue was then weighed (~0.5mg) and stored in tin capsules in preparation for analysis.

Stable isotope ratios of embryonic samples were determined at the NERC Life Sciences Mass Spectrometry Facility in East Kilbride, using a Pyrocube Elemental Analyzer (2013, Elementar, Hanau, Germany) and Delta XP (Thermo Electron) mass spectrometer (2003). Stable carbon and nitrogen isotope ratios of adult *Squalus acanthias* muscle samples were determined at OEA Laboratories Ltd. In-house laboratory standards (USGS40) were analysed in order to account for and

correct instrument drift. Experimental precision was 0.29‰ and 0.17‰ for carbon and nitrogen, respectively (standard deviation for replicates of standards). The same laboratory standard was analysed at the beginning and end of every analytical run of 155 samples at the NERC Life Sciences Mass Spectrometry Facility. Additional in-house standards were also analysed every 10 samples to allow identification of any instrument drift. Experimental precision here was 0.09‰ for carbon and 0.17‰ for nitrogen (standard deviation for replicates USGS40 standards).

Glutamic acid (GA) standards from The University of Southampton were also analysed at both laboratories, nested within the samples. Mean $\delta^{15}N$ and $\delta^{13}C$ reported for standards analysed at OEA Laboratories Ltd. are -3.99‰ (± 0.23) and -12.99‰ (± 0.27) for nitrogen and carbon, respectively. Mean $\delta^{15}N$ and $\delta^{13}C$ reported from standards analysed at NERC Life Sciences Mass Spectrometry Facility are -3.84‰ (± 0.16) and -13.03‰ (± 0.24) for nitrogen and carbon, respectively. Absolute isotopic delta-values for the University standard were consistent within error between the two laboratories.

Isotope ratios are expressed in δ notation (‰), relative to the international standards of V-Pee dee belemnite and air for carbon and nitrogen, respectively. Given that no lipid extraction was performed prior to the stable isotope analysis, Reum's (2011) lipid correction model was applied to all muscle data. Due to the loss of one sample during analysis, only 19 mother-embryo pairs are available for comparison.

The isotopic difference between maternal and offspring tissues was calculated as a maternal-offspring offset (Δ), where the isotopic composition ($\delta^{15}N$ and $\delta^{13}C$ value) of tissue from each replicate embryo was subtracted from the maternal isotope value.

3.4 Results

3.4.1 Embryonic tissue – muscle

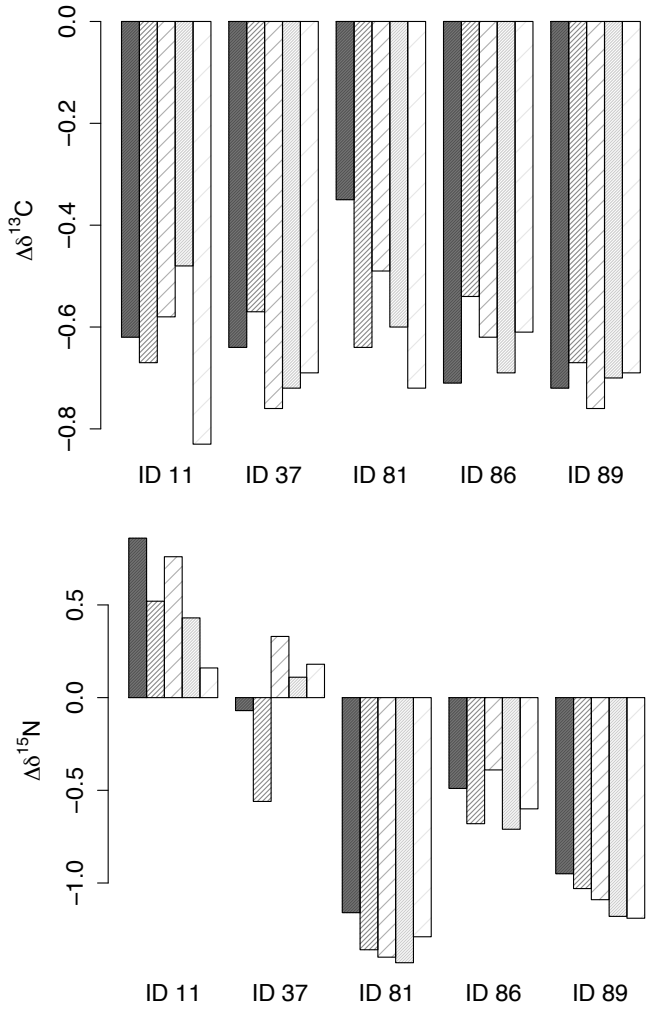

Figure 3.1 – Distribution of the maternal-offspring isotope offsets (Δ) for muscle tissue of individual *Squalus acanthias* embryos from 5 broods.

Where the lipid content of samples submitted for stable isotope analysis is high, the resultant $\delta^{13}C$ value is negatively biased (Reum, 2011). According to Post (2002), C:N ratios exceeding 3.5 are indicative of high lipid content in the tissues of aquatic organisms. Embryonic and maternal muscle tissue C:N ratios ranged from 5.58 to 9.18 (mean = 6.79 ± 0.71) and 3.57 to 8.83 (mean = 5.36 ± 0.94), respectively. *Squalus acanthias* muscle data therefore required retrospective correction for lipid content. The two-parameter model developed by Fry (2002) was used:

$$\Delta \delta^{13}C = D - DF(R_{CN})^{-1} \quad (2)$$

Here, D represents the protein-lipid $\delta^{13}C$ offset (8.39 ± 0.74), and F the lipid-free C:N ratio, set at 2.71 (± 0.14) (Reum, 2011). R_{CN} represents the C:N ratio of the bulk sample submitted for analysis.

Corrected embryonic muscle $\delta^{13}C$ values range from -16.90‰ to -15.67‰ (mean = -16.27‰ ± 0.35). $\delta^{15}N$ values range from 11.62‰ to 14.51‰ (mean = 13.48‰ ± 1.02). All corrected stable isotope data are reported in the Appendix (B).

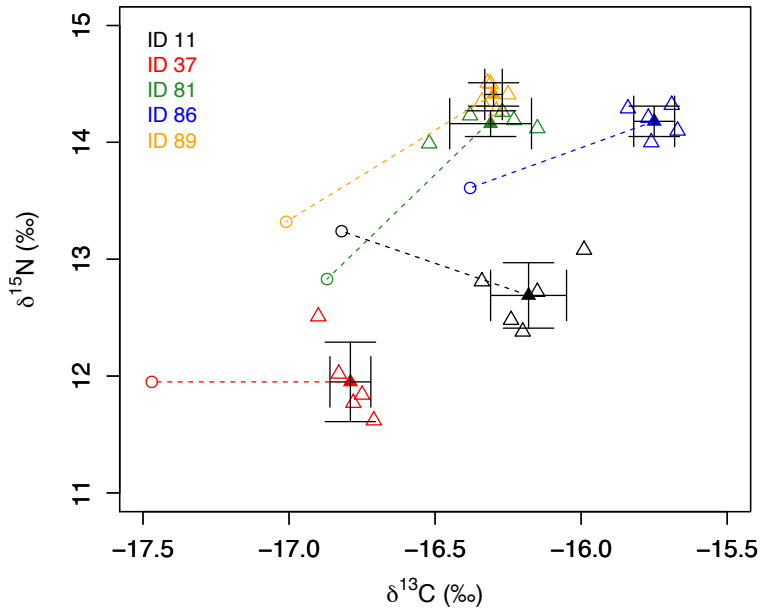

Figure 3.2 – Muscle stable carbon and nitrogen isotope values from *Squalus acanthias* mothers (circles) and 5 embryos (triangles) from five different broods, identified by colour. Mean brood $\delta^{13}C$ and $\delta^{15}N$ values, and associated standard deviations, are represented by filled triangles and error crosses.

Intra-brood muscle carbon isotope variability is low, with standard deviations within the range of analytical error (0.03-0.14 ‰; standard deviation of replicate USGS40 samples) (Figure 3.1). Nitrogen isotope values are more variable within broods, relative to carbon (Figure 3.1, Table 3.2), however the associated standard deviations are again within the range of analytical error (0.10-0.34 ‰) (Table 3.2). Embryos from the same litter are therefore deemed isotopically comparable. Thus, in order to avoid pseudoreplication, where multiple embryos per litter were

sampled, one embryo per litter was selected at random to reflect the entire brood.

Embryonic tissue is elevated relative to corresponding maternal muscle tissue for $\delta^{13}C$, producing consistent negative maternal-offspring offsets (Δ); all $\Delta\delta^{13}C$ values from individual mother-embryo pairs are negative (Figure 3.1 & 3.2) and the mean $\Delta\delta^{13}C$ value of each of the 5 broods ranges from -0.71 to -0.56‰ (Table 3.2). $\Delta\ \delta^{13}C$ values therefore display low inter-brood variability, and an ANOVA revealed that mother ID has no significant impact upon the maternal-offspring offset (Δ) of individual mother-embryo pairs ($p = 0.88$). This is mirrored by the low standard deviation associated with the mean $\Delta\ \delta^{13}C$ value when data from all broods are combined: ± 0.28 ‰.

Table 3.2 – Mean isotopic composition ($\delta^{15}N$ and $\delta^{13}C$), associated standard deviation (S.D.), and maternal-offspring offset (Δ) of muscle tissue from five *Squalus acanthias* broods (n=5).

Mother/ Brood ID	Mean brood $\delta^{15}N$	Mean brood $\delta^{13}C$	Mean $\Delta_{m\text{-}e}$ $\delta^{15}N$	Mean $\Delta_{m\text{-}e}$ $\delta^{13}C$
11	12.69 ± 0.28	-16.18 ± 0.13	-0.55	-0.64
37	11.95 ± 0.34	-16.79 ± 0.07	0.00	-0.68
81	14.16 ± 0.11	-16.31 ± 0.14	1.33	-0.56
86	14.18 ± 0.13	-15.75 ± 0.07	0.57	-0.63
89	14.41 ± 0.10	-16.30 ± 0.03	1.09	-0.71

Mean $\delta^{15}N$ values for each of the 5 broods ranges from 11.95 ‰ (± 0.34) to 14.41‰ (± 0.10). Inter-brood nitrogen isotope variability therefore exceeds intra-brood variability (Figure 3.1) and leads to a large standard deviation associated with the mean offset when data from all broods are pooled ($\Delta\ \delta^{15}N$ = -0.13 ± 0.85 ‰). An ANOVA confirmed that mother ID has a significant effect upon nitrogen isotope values ($p=<0.001$, $F_{1, 23} = 83.36$), and is thus responsible for the high variability in the global $\Delta\ \delta^{15}N$. Post-hoc comparison (Tukey test) confirmed a significant difference

between all mothers, when paired individually ($p<0.01$), with the exception of ID 89 and 81, which are isotopically similar with regards to nitrogen ($p=0.43$).

Figure 3.1 highlights the variability in the direction and extent of isotopic spacing ($\Delta\ \delta^{15}N$) from individual mother-embryo pairs, across broods. Embryonic muscle tissue from Brood 81, 86 & 89 is elevated relative to corresponding maternal tissue with regards to mean brood nitrogen isotope value. A negative maternal-offspring nitrogen isotope difference is observed for Brood 11, and a similar mean $\delta^{15}N$ value is reported for embryonic tissue relative to the mother in Brood 37, also reflected in Figure 3.2. Higher within-brood variance in $\delta^{15}N$ values therefore appears to be associated with relatively negative mean maternal-offspring nitrogen isotope offset terms (Figure 3.1).

3.4.2 Embryonic tissue – lens

Embryonic lens tissue $\delta^{13}C$ and $\delta^{15}N$ values range from -17.56‰ to -15.79‰ (mean = -16.56‰ ± 0.49) and 10.56‰ to 13.60‰ (mean = 12.06‰ ± 1.04), respectively.

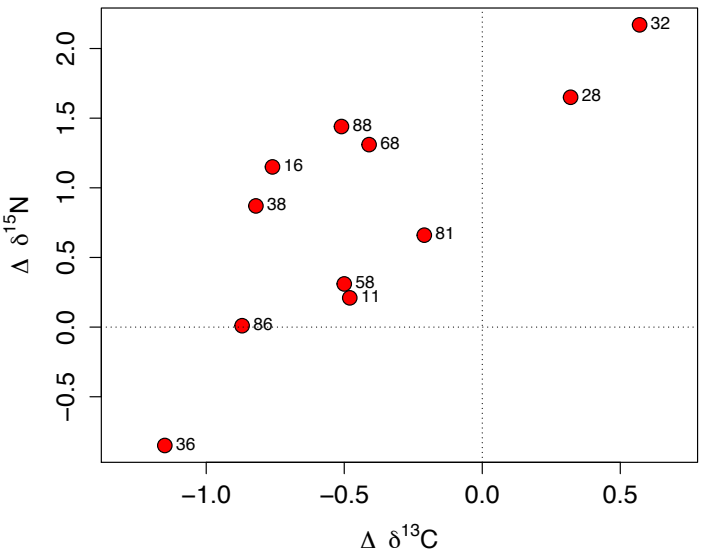

Figure 3.3 – Biplot of eye lens maternal-offspring isotopic spacing (Δ) from 11 spiny dogfish (*Squalus acanthias*) mother-embryo pairs. Dotted lines represents no maternal-offspring spacing, or Δ=0, for carbon (vertical) and nitrogen (horizontal).

Isotopic lens maternal-offspring spacing (Δ) for individual mother-embryo pairs is presented in Figure 3.3 Δ $\delta^{13}C$ and Δ $\delta^{15}N$ values range from -1.15‰ to 0.57‰ and -0.85‰ to 2.17‰, respectively. Generally, embryonic tissue is elevated relative to corresponding maternal lens tissue with regards to carbon, with all but 2 mother-embryo pairs (ID 28 & 32) falling to the left of the dotted line in Figure 3.3, representing no isotopic offset (Δ $\delta^{13}C = 0$). Conversely, maternal tissue is generally elevated relative to the corresponding embryonic lens with regards to nitrogen, highlighted in Figure 3.3, with all but 2 mother-embryo pairs (ID 36 & 86) falling above the dotted line representing no nitrogen-specific isotopic offset (Δ $\delta^{15}N= 0$). This indicates a positive maternal-embryonic offset.

The distribution of $\delta^{15}N$ values from embryonic lens core samples (n=20) is broadly representative of a larger population of 65 adult spiny dogfish lens cores (Figure 3.4). A slight negative skew is observed in the distribution of adult $\delta^{15}N$ values, relative to embryonic data.

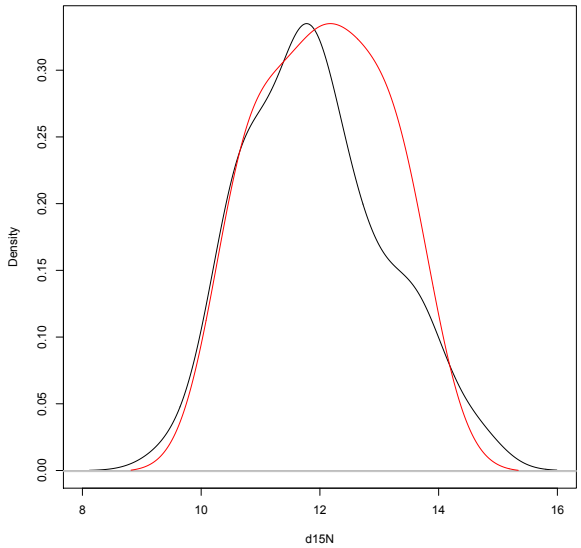

Figure 3.4 - Probability density functions for distributions of $\delta^{15}N$ values of eye lens cores of 65 adult (n=65) *Squalus acanthias* (black) and the embryos (n=20) sampled in this study (red).

3.4.3 Maternal tissue

Isotopic ratios of maternal muscle tissue range from -17.66‰ to -16.38‰ (mean = -17.03‰ ± 0.31) and 11.95‰ to 14.4‰ (mean = 12.96‰ ± 0.67) for carbon

and nitrogen, respectively (n=19). The range of maternal outer lens tissue $\delta^{13}C$ and $\delta^{15}N$ values is similar to that of muscle; carbon range = -17.68‰ to -16.45‰ (mean = -17.00‰ ± 0.37), nitrogen range = 11.71‰ to 13.96‰ (mean = 12.87‰ ± 0.64) (n = 11).

Isotopic spacing between maternal muscle and embryonic lens tissue ranges from -1.38 to 0.24 ‰ (mean = -0.51‰, ± 0.42) and -0.87 to 1.94 ‰ (mean = -0.51‰, ± 0.42), for carbon and nitrogen, respectively. Figure 3.5 highlights that maternal muscle is generally depleted in $\delta^{13}C$ relative to corresponding embryonic lens tissue. Conversely, elevated $\delta^{15}N$ values are commonly recorded in the mother's muscle, compared to the lens of the offspring. Again, the maternal muscle-embryonic lens offset (Δ) is more predictable in direction in the case of carbon, and with the exception of one mother-embryo pair (ID 32), all individual $\Delta\delta^{13}C$ values are negative (Figure 3.5). However, the extent of the offset (Δ) remains variable, ranging from -1.38 to -0.07‰. In the case of nitrogen, $\Delta\delta^{15}N$ values are again variable in both direction and extent (Figure 3.5).

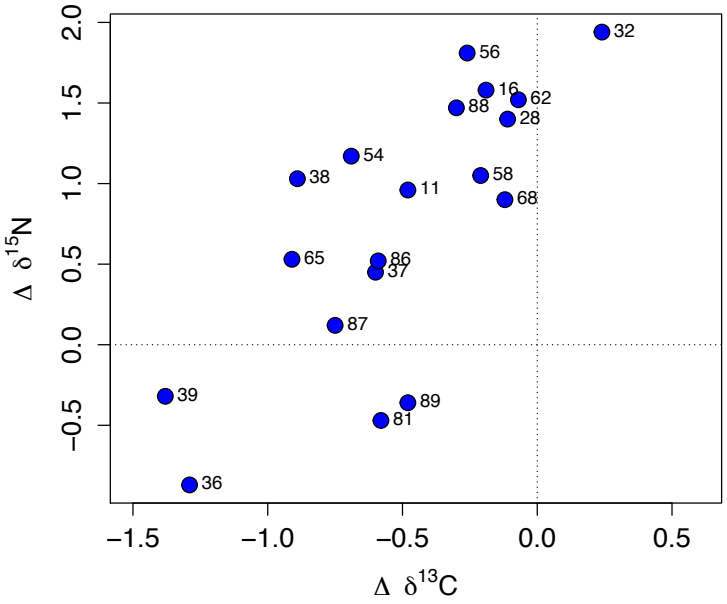

Figure 3.5 – Maternal muscle-offspring lens offset (Δ) from 19 spiny dogfish (*Squalus acanthias*) mother-embryo pairs. Dotted lines represents no maternal-offspring spacing, or Δ=0, for carbon (vertical) and nitrogen (horizontal).

3.4.4 Offset comparison

The isotopic composition of nitrogen in embryonic muscle tissue is more variable than the isotopic composition of the mothers (Figure 3.6). Embryonic muscle $\delta^{15}N$ values range from 11.25-15.06‰, compared to 11.95-14.4‰ in maternal tissue.

Mean embryonic muscle $\delta^{13}C$ values are elevated relative to maternal muscle tissue (-16.34 ± 0.37‰ and -17.03 ± 0.31‰, respectively (Figure 3.6)), and a paired t-test confirmed that the difference between the carbon isotope compositions is significant (mean difference = 0.68‰ ± 0.39, p=<0.01). Conversely, mean $\delta^{15}N$ values are elevated in the maternal tissue, relative to the embryo: 12.96 ± 0.67‰ and 12.83 ± 1.22‰, respectively (Figure 3.6). No significant systematic mother-embryo $\delta^{15}N$ offset was found.

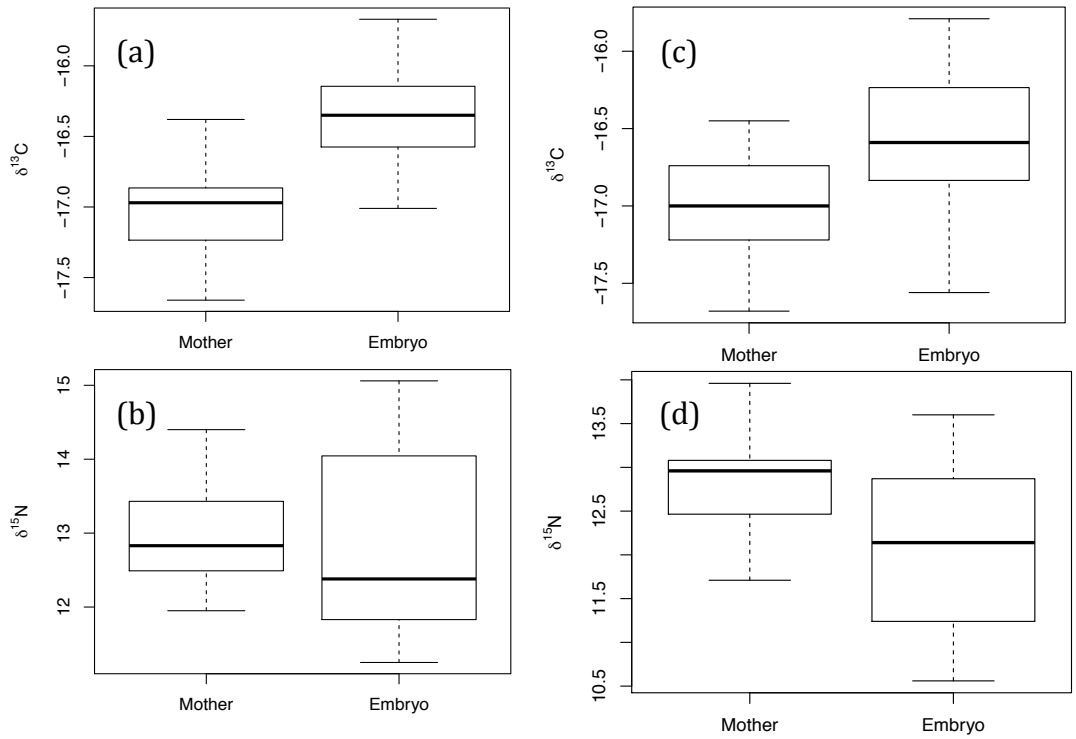

Figure 3.6 – Boxplots comparing the isotopic composition of *Squalus acanthias* embryonic and maternal muscle (left; a & b) (n = 19) and lens (right; c & d) (n = 11) tissue across mother-embryo pairs.

Mean embryonic lens $\delta^{13}C$ value is significantly elevated relative to maternal lens tissue: -16.56 ± 0.49‰ and -17.00 ± 0.37‰, respectively (Figure 3.6), as confirmed by paired t-tests: mean difference (Δ) = -0.44 ±

0.51‰ (p=<0.05, t= 2.85). However, unlike muscle, the mean $\delta^{15}N$ value of maternal lens (12.87 ± 0.64‰) is significantly elevated relative to the embryo lens (12.06 ± 1.04‰), paired t-test (p=<0.05, t= -3.14). Consequently the apparent mean $\delta^{15}N$ offset (Δ) between maternal and embryonic lens is -0.81± 0.86 ‰ (p=<0.05, t= -3.14). Large standard deviations (relative to the mean difference) are reported for both carbon and nitrogen, reflecting the variability in both the extent and direction of individual offset (Figure 3.6).

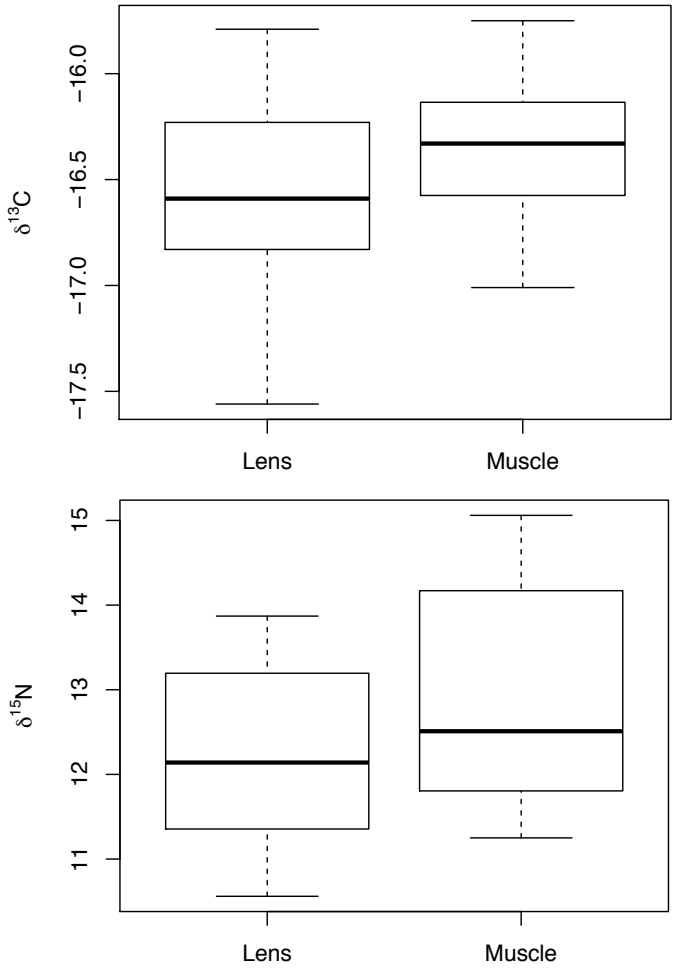

Figure 3.7 – Comparison of embryonic lens and muscle $\delta^{15}N$ and $\delta^{13}C$ values from 11 *Squalus acanthias* specimens.

Figure 3.7 compares the isotopic composition of paired embryonic lens and dorsal muscle samples. Lens protein is slightly but significantly depleted in both $\delta^{15}N$ and $\delta^{13}C$ values compared to muscle protein (paired t-tests - for $\delta^{15}N$, p=<0.01, t=-3.42, mean difference = 0.66 ± 0.38 ‰, and for $\delta^{13}C$ p=<0.01, t=-7.56, mean difference = 0.18 ± 0.23 ‰).

Paired t-tests also indicate that the isotopic composition of maternal muscle and embryonic lens tissue differs significantly (p=<0.05, t=4.17 and p=<0.05, t=5.30 for carbon and nitrogen, respectively). The reported offset (Δ) is -0.51 ± 0.41 ‰ and 0.76 ± 0.83‰ for carbon and nitrogen, respectively.

3.5 Discussion

Embryonic tissues of aplacental species are assimilated from a single, assumed isotopically homogenous, nutrient source (in this case the yolk sac), therefore the embryo acts as a controlled feeding study allowing determination of isotopic offsets between tissues, driven by differences in protein composition. Within individual embryos, lens protein was slightly but significantly depleted in both $\delta^{15}N$ and $\delta^{13}C$ values compared to muscle protein (mean difference = 0.66 ± 0.38 ‰, p=<0.01, and 0.18 ± 0.23 ‰, p=<0.01, for nitrogen and carbon, respectively), Figure 3.6. The relatively minor isotopic offset identified between the two tissues implies that any subsequent significant differences identified between the isotopic composition of maternal muscle and embryonic lens or muscle tissue can be attributed to spatio-temporal effects associated with maternal foraging across isotopic gradients and/or differential rates of tissue formation.

3.5.1 Intra-brood isotopic variance

Across the 5 sampled broods, mean intra-brood muscle carbon isotope variability was within the range of analytical error (0.03-0.14 ‰). This suggests that embryos within a particular litter are provisioned from eggs formed at the same time, which is consistent with the known reproductive biology of the species (Hisaw & Albert, 1947; Koob & Callard, 1989; Jones & Ugland, 2001), and is supported by the comparable developmental stage of all embryos within a single litter (*a priori* observation). However, two of the five broods did record between-embryo isotopic differences that exceeded analytical precision. The intra-brood and inter-brood nitrogen isotope variability observed for Litter 11 and 37 is therefore likely to reflect maternal foraging over an isotopic gradient during yolk sac

production. By extension, we assume that the movements of mothers 81, 86 & 89 were limited during egg production.

Increased within-brood variability in embryonic $\delta^{15}N$ values appears to be associated with more negative maternal muscle $\delta^{15}N$ values (e.g. Brood 11 and 37). In the context of the North Sea, where elevated $\delta^{15}N$ values are generally encountered in the southeast relative to the northwest (MacKenzie *et al*. 2014; Trueman *et al.* 2016), we may infer that that mothers 81, 86 & 89 foraged primarily in the southwest during the period of yolk sac production, whereas mothers 11 and 37, displaying elevated intra-brood $\delta^{15}N$ variability and more depleted $\delta^{15}N$ values, may have been moving between, and foraging within, the north and south during egg development.

The isotopic data present no clear evidence for the embryonic consumption of continually produced unfertilized eggs (oophagy) or inuterine cannibalism, both of which would by likely to result in increased isotopic variability between different embryos within a single brood. Once again, this is consistent with the current understanding of *Squalus acanthias* reproduction (Koob & Callard, 1999).

3.5.2 Relationship between isotopic variability in mothers and embryos

In addition to the confounding effects of maternal movement during yolk sac production, poor temporal coupling presents another potential source of tissue isotope variability. It has been suggested that mature female *Squalus acanthias* lay down egg cases up to 4 years prior to parturition (i.e. ~2 years prior to fertilization) (Wood *et al*. 1979). If this is the case, the nutrient assimilation fuelling yolk sac production may be temporally decoupled from foraging that drives maintenance and growth of adult tissues. In a wide ranging species like the spiny dogfish, this decoupling has the potential to introduce considerable spatio-temporal variability, as maternal and embryonic tissues are likely to be characterised by foraging over different time scales, in isotopically distinct regions. This is of particular relevance in the North Sea, where spiny dogfish are known to

migrate across strong baseline nitrogen isotope gradients (Holden, 1965; Stenberg, 2005).

Muscle stable isotope compositions in the 19 sampled adult female spiny dogfish varied by more than analytical precision (Figure 3.1) indicating foraging across isotopic gradients during muscle tissue turnover. Isotopic variability was significantly greater in nitrogen compared to carbon (σ of δ values = 0.31‰ and 0.68‰ respectively), consistent with the greater spatial isotopic variability in nitrogen in the North Sea (MacKenzie *et al*. 2014; Trueman *et al*. 2016). However, the range of $\delta^{15}N$ values expressed in maternal muscle tissues is relatively small compared to the c.8‰ potential spatial range. Variation in $\delta^{15}N$ and to a lesser extent $\delta^{13}C$ values between individual females is lower in adult muscle tissue than in embryo muscle tissues (Figure 3.1). The isotopic composition of a consumers tissue reflects the averaged composition of all prey consumed over the timescale of tissue assimilation or turnover. Where movements within isotopically varied environments are rapid with respect to tissue assimilation, the isotopic expression of these movements will be reduced and individuals will trend towards a weighted average value. Faster growing tissues have more potential to record between-individual variation related to differential short-term movements. Consequently it is inferred that embryo muscle and lens tissues reflect relatively fast growth of egg cases compared to turnover rates of adult muscle. Thus, embryonic tissues more faithfully capture the isotopic expression of adult movements across isotopic gradients in the North Sea.

3.5.3 Maternal-embryo offsets

In the case of nitrogen, it is likely that the observed apparent negative spacing between mother and embryo reflects migration across isotopic gradients and growth dynamics (as above), with eggs more closely reflecting the contribution of isotopically light (northern) maternal foraging. Whilst we cannot rule out the possibility of an additional systematic 'trophic style' offset between maternal and embryonic tissues (as in Table 3.1 with offsets as + 0.8: +1.5 ‰), this would imply more extreme separation between maternal muscle and egg foraging grounds.

$\delta^{13}C$ values are systematically enriched in both embryonic muscle and lens tissue compared to maternal values. Considered alongside the limited systematic spatial gradient in $\delta^{13}C$ values within the North Sea (Trueman *et al*. 2016), this provides additional evidence for systematic maternal-offspring isotopic spacing, however the mean observed spacing is c. 0.5‰, lower than reported in Table 3.1.

3.5.4 Implications for ecology of spiny dogfish

In an attempt to examine the relative importance of the north and southern North Sea to the provisioning of embryos, the probability density functions of $\delta^{15}N$ distribution from core lens samples of 65 adult spiny dogfish and 11 embryos was compared. The isotopic composition of lens cores from the embryos sampled in this study are broadly representative of the larger population of lens cores sampled from 65 adult spiny dogfish (Figure 3.4). The distribution of $\delta^{15}N$ values in the lens core form the larger population spans a similar range indicating maternal provisioning in northern and southern areas. The mean $\delta^{15}N$ value is relatively low, and the distribution is negatively skewed suggesting that foraging in the northern North Sea may be more important for maternal provisioning than foraging from the southern North Sea (characterised by elevated $\delta^{15}N$ values). A smaller sub-population of adult cores suggests that southern foraging areas are used for maternal provisioning for a subset of the spiny dogfish population. Three of the five mothers sampled in our study belong to this group, inferred from the probability distribution figure (Figure 3.4).

3.6 Conclusion

Tissues formed *in utero* comprise carbon and nitrogen atoms derived from maternal foraging. The isotopic composition of embryonic tissues therefore provides information on the trophic and spatial ecology of the mother during egg production. Identifying regions that are important during egg sac provisioning in mature females, which contribute to the successful offspring population, is important for the conservation of endangered sharks, including the spiny dogfish. However, accessing this

information requires a clear understanding of the complex relationship between maternal and offspring tissue chemistry.

This investigation represents the first study to examine lens-specific mother-offspring isotope offsets. Here, tissue-specific differences in isotopic offsets (Δ) are revealed, and different Δ $\delta^{13}C$ and Δ $\delta^{15}N$ values and trends reported for lens and muscle tissue. Introducing the confounding factor of maternal movements, we discuss the effect that this has on the isotopic variability of embryonic tissue, and the impact that this has upon estimating mother-offspring isotopic offsets.

This study also highlights the additional complexities associated with establishing the temporal comparability of tissue formation. For example, despite sharing the same biochemical composition, differences in isotopic composition of maternal and embryonic lens (and muscle) tissue may occur irrespective of trophic offset if the period of nutrient assimilation fuelling the growth and remodelling of these tissues is not coupled. However, we believe that this is likely to pose a lesser problem in placentatrophic species, where maternal nourishment is replenished throughout gestation, and in species with shorter gestation periods.

Small sample sizes represents a common problem associated with mother-offspring offset studies, and highlights some of the difficulties associated with lethal sampling of elasmobranchs, particularly species that are a conservation concern. Furthermore, this study highlights some of the risks associated with applying generalised tissue-specific trends in maternal-offspring offsets to other aplacental and placentatrophic shark species, revealing that both the extent and direction of isotopic offset (Δ) varies considerably between species. It is therefore recommended that mother-offspring isotope offsets be addressed on a case-by-case basis, and considerable consideration should be made for the impact of spatial effects.

Chapter 4: How I met your mother: Cross-generational records of tropho-spatial ecology revealed from isotopic analyses of eye lens proteins in the aplacental spiny dogfish, *Squalus acanthias*.

This Chapter is a manuscript in preparation, to be submitted in April 2017. Written by Katie Quaeck, including feedback from Clive Trueman.

4.1 Abstract

Spiny dogfish (*Squalus acanthias*) may have once been the most abundant living shark species, but is now listed as vulnerable on the IUCN Red List, and endangered in the Northeast Atlantic. Management and conservation of the species depends on reliable data concerning life-long movements and distributions. Here stable isotope compositions of sequentially-grown tissues (eye lenses) are examined in order to reconstruct life-long and cross-generational movement patterns in spiny dogfish from the North Sea, comparing with relatively recent foraging behaviour (revealed via geographic assignment of dorsal muscle tissue).

Geographic assignment of dorsal muscle samples and recently formed lens tissue ($\delta^{13}C$ and $\delta^{15}N$ values) reveals that the southern and central North Sea represent important foraging areas during mature life history. Conversely, the northern North Sea appears to be an important ecoregion during gestation, pupping, and early life history, identified via analysis of lens tissue formed *in utero* and during juvenile life history.

The eye lens therefore serves as a unique tissue, not only allowing retrospective investigation of whole life history spatial and trophic ecology, but also permitting examination of maternal signals relating to habitat use in pregnant females.

4.2 Introduction

4.2.1 Spiny Dogfish

The spiny dogfish (*Squalus acanthias*) is a small (<120cm total length, TL; (Hammond & Ellis, 2004) squaliform shark that displays antitropical distribution in the Atlantic and Pacific oceans. Spiny dogfish are commonly associated with coastal regions and the continental shelf (Burgess, 2002; Shepherd *et al*. 2002; Ebert *et al*. 2013), and are long-lived and slow growing [max age estimated at 40 years (Nammack, 1982)] (Holden & Meadows, 1962; Tucker, 1985; Campana *et al*. 2006). Age at maturity is estimated at approximately 6-14 and 12-23 years, for males and females respectively. *S. acanthias* reproduce via aplacental viviparity (Hammond & Ellis, 2004), display low fecundity (1-17 pups per litter (Holden & Meadows, 1962; Ketchen, 1972), and have the longest gestation period of any known vertebrate (up to 24 months (Ketchen, 1972; Jones & Ugland, 2001)). These traits make the spiny dogfish susceptible to, and slow to recover from, overexploitation.

Once considered a nuisance species, spiny dogfish landings in the Northeast Atlantic increased during the first half of the 20th century due to the demand for liver oil, and meat for human consumption (Pawson *et al*. 2009). By 1963, target fisheries began operating within the Norwegian, North and Celtic Seas, and landings of >60,000 t were documented (ICES, 2009a). Subsequently, apart from a brief increase in landings in the 1980s related to the development of new directed fisheries in the Icelandic and Irish Seas, landings fell steadily throughout the latter half of the 20th, and into the 21st century, falling to 1700 tons in 2008 (de Oliveira *et al*. 2013). Once widespread and abundant throughout the region, spiny dogfish are now more commonly found in the western North Sea and off the isles of Orkney and Shetland (Ellis *et al*. 2012), with large catches of juveniles occurring off the northern coast of Scotland (Ellis *et al*. 2005).

Effective management of vulnerable, migratory fish requires a thorough understanding of lifelong movements, particularly related to feeding and reproduction. The long lifespan of *S. acanthias* complicates study of ontogenetic

movement ecology. Spiny dogfish display sexual and size-based segregation (Conradt, 2005; Ebert *et al*. 2013), with adult females schooling in relatively shallow inshore waters, while adult males occupy deeper waters offshore (Shepherd *et al*. 2002; Compagno *et al*. 2005). *S. acanthias* also undertakes seasonal migrations (Hisaw *et al*. 1947; Holden, 1965; Stenberg, 2005).

4.2.2 Movement ecology of *Squalus acanthias* in the Northeast Atlantic and North Sea

Understanding the distribution and movement of spiny dogfish in the northeast Atlantic has long been of interest to fisheries biologists. In the late 1950's, British and Norwegian scientists independently tagged several thousand individuals in order to examine the movements and migration of this commercially important species (e.g. Aasen, 1964; Holden, 1967). However, the interpretation of these investigations differed. Aasen (1964) postulated that a single, widely distributed spiny dogfish stock existed in the northeast Atlantic, with a population centre occurring in ICES areas IVa and VIa (Aasen 1960). Conversely, Holden (1967) suggested that several discrete stocks exist within European waters, but also identified regional movements from the English Channel into the North Sea in summer (Holden, 1965). Despite their conflicting conclusions, both investigations identified a seasonal pattern in distribution between Northern Scotland/Shetland and the Norwegian coast. However, the disparity in recapture rates of both experiments was attributed to differences in fishing pressure, with the majority of recaptures occurring in regions where the major fisheries of the time were operational (Gauld & MacDonald, 1982 Hammond & Ellis, 2004), thus highlighting the spatial and temporal bias associated with this technique.

In 1980, Hjertenes suggested that spiny dogfish migration patterns had changed in the North Sea within the ~15 years between studies, and observed a north-south migration occurring seasonally from a "winter area" north of Scotland, to a "summer/autumn area" in the southern North Sea. Publication of this study also coincided with a shift in the fishing grounds from previously productive Norwegian coastal waters, to the Dogger Bank (Gauld & MacDonald, 1982).

In the northeast Atlantic, recent tagging experiments have revealed that *S. acanthias* migrate all around the British Isles, suggesting the existence of a single Northeast Atlantic stock (Vince, 1991). Trans-oceanic basin migrations have also been documented for *S. acanthias*, highlighting its high dispersal potential (Holden, 1967; Templeman, 1976) however recent molecular studies have ruled out global panmixia (Verissimo *et al*. 2010). This is supported by the infrequency of transatlantic recaptures relative to the thousands of tags deployed in the 1960's. Thus, northwest and northeast Atlantic spiny dogfish are considered two distinct stocks (Holden, 1967; Vince, 1991; Pawson & Ellis, 2005).

The spatial distribution of individual sharks may also be influenced by site fidelity, defined as the return to a previously occupied location (Switzer 1993). Philopatry, for example, is defined as the return of an individual to its birthplace (Mayr, 1963), a phenomenon previously identified in Pacific white sharks (*Carcharodon carcharias*) (Jorgensen *et al*. 2010) and oceanic whitetips (*Carcharadon longimanus*) (Howley-Jordan *et al*. 2013). *S. acanthias* are known to display strong aggregative behaviour associated with reproductive cycles, with females occurring in large numbers within the Celtic Sea in order to parturate during winter and spring (Pawson, 1995). Whilst this may provide some evidence for natal homing in the species, further information is required in order to confirm philopatry, and aid in the identification of critical habitats essential for the management and conservation of the species.

Although the large-scale longline *S. acanthias* fisheries operational in the 1980s and 1990s have ceased, and the current TAC is the Northeast Atlantic is zero (Fordham *et al*. 2006), spiny dogfish continue to appear as incidental by-catch (current landings data unavailable). The aggregation behaviour of the species, particularly in mature females, increases their susceptibility to fisheries interactions. Despite this, since the tagging work of the last century (Aasen, 1964; Holden, 1967; Vince, 1991), few studies have examined the habitat use of Northeast Atlantic spiny dogfish. Effective management of target and by-caught marine species relies upon understanding habitat use throughout life history. Identification of critical habitats that facilitate survival, for example breeding

and nursery grounds, has therefore become a key area in fisheries research (Salzman, 1990). Obtaining this information is particularly important in shark management and conservation (e.g. Heupel *et al*. 2004; Carraro & Gladstone, 2006; Wiley & Simpfendorfer, 2007; Knip *et al*. 2010; Espinoza *et al*. 2011; Heupel *et al.* 2007; Norton *et al*. 2012), where species are susceptible to both direct and indirect fishing, and are often slow to recover from exploitation. Historic distribution studies of *S. acanthias* focus primarily on tag-recapture methods to examine the movements of individual fish. These methods are poorly suited to assessment of critical habitats, as they provide no data between the tagging and recapture locations, and are often spatially and temporally biased (Block *et al*. 2011). The application of alternative and complementary techniques, allowing investigation of spiny dogfish movement throughout ontogeny, are therefore required in order to improve understanding of habitat use and residency.

4.2.3 Isotopes & Isoscapes

Natural chemical tags, such as stable isotopes, present an alternative method to retrospectively investigate spatial (and trophic) ecology. Where the composition of fish tissues reflects that of the ambient water and the local food web (Trueman *et al*. 2012), this can provide information on fish location, presenting an attractive complementary method to study movement.

Sea temperature can be considered the master controller of stable carbon isotope ratio variability. Temperature regulates dissolved CO_2 concentrations, and influences the dominant phytoplankton group, along with their cell size, geometry, growth rate, etc. (e.g. Richardson & Schoeman, 2004). These variables, in turn, impact upon isotopic fractionation during photosynthesis, resulting in temporally and spatially variable $\delta^{13}C$ values (Zohary *et al*. 1994; Barnes *et al*. 2009; Graham *et al*. 2010). Variability in stable nitrogen isotope ratios ($\delta^{15}N$) is driven by nutrient source, subsequent biological transformation (e.g. N-fixation) and trophic fractionation (Dugdale & Goering, 1967; Mullin *et al*. 1984; Owens, 1985). Baseline carbon and nitrogen isotope compositions are subsequently transferred along food webs, undergoing enrichment with each trophic level.

Geographic assignment of an individual based on the chemical composition of its tissues is often complicated by the difficulties associated with the construction and validation of reference maps, detailing the distribution of isotope values across ocean basins, known as isoscapes (West *et al.* 2010; Bowen *et al.* 2005; Bowen & West, 2008; Wunder & Norris, 2008; Bowen, 2010; Graham *et al.* 2010; Wunder, 2010; Trueman *et al.* 2012). The isotopic values at the base of the food web are both spatially and temporally variable. Thus, measuring and monitoring isotopic variability in the marine environment is logistically demanding and expensive. However, where the drivers of isotopic variability are temporally stable and spatially predictable, isoscapes can be modelled, validated and subsequently applied to studies of spatial distribution (e.g. Schell *et al.* 1989; Best & Schell, 1996; Cherel *et al.* 2000; Jaeger *et al.* 2010).

4.2.4 The Eye Lens

Incrementally formed, inert tissues offer an ontogenetic record of body isotopic composition, providing a biochemical archive of behaviour and physiology over the entire lifetime of an individual. Organic tissues of this nature are particularly useful, as their stable isotope composition can provide information pertaining to diet, trophic level and location, and can retrospectively be analysed to address trophic and spatial ecology in marine organisms (Schell *et al.* 1989; Best & Schell, 1996; Cherel *et al.* 2000; Jaeger *et al.* 2010). If the incremental tissue begins formation during early embryonic development, then its chemical composition in the earliest formed portion offers insight to maternal behaviour during gestation/yolk production, allowing trans-generational study of habitat use during critical life-history stages. Thus, analysis of stable carbon and nitrogen isotope signatures can potentially provide information relating of movement and diet throughout life history, from embryonic development to the time of capture.

The vertebrate eye lens fulfils the criteria above; it is organic (proteinaceous), metabolically inert, and forms incrementally (Bassnett & Beebe, 1992; Bron *et al.* 2000; Bloemendal *et al.* 2004; Kroger, 2013;). Its hydrated crystalline protein structure lends itself to stable isotope analysis (Onthank, 2003; Parry, 2003; Hunsicker *et al*. 2010), and has been identified as a suitable target for chemical

analysis and investigation of spatial and trophic ecology (Wallace *et al.* 2011). Furthermore, a linear relationship exists between lens diameter and somatic growth, and the lens therefore serves as a size-referenced chemical repository for whole life-history information, which can be sequentially sampled in order to examine patterns in movement and trends in diet, throughout ontogeny (as discussed extensively in Chapter 2).

4.2.5 Aims & Objectives

Here, muscle and sequential eye lens samples from individual spiny dogfish are geographically assigned to feeding grounds within the North Sea, using regional temporally stable isoscapes. The relationship between spiny dogfish body size and lens diameter is quantified, in order to back-calculate size at time of lens tissue formation, and reconstruct potential ontogenetic trends in stable isotope variability.

The aim of this work is to identify regions on the North Sea that are important for assimilation of food in adults (using recently formed muscle tissue), and explore ontogenetic variations in stable isotope compositions from eye lens tissue, with a particular focus on reconstructing migration patterns. The resulting information may aid fisheries management for *S. acanthias* either as a target species or in by-catch mitigation. It is hypothesysed that adult muscle tissue will be re-assigned to the central-southwest North Sea, reflecting capture location. Given the sexual and size-based aggregation behaviour of spiny dogfish, we also anticipate that ontogenetic lens samples of comparable life history stage will be assigned to similar areas within the North Sea, resulting in the identification of distinct geographical pockets of distribution relating to different developmental stages. Geographical assignment of maternal and embryonic core lens samples also allows philopatry to be addressed for this long-lived species.

4.3 Materials & Methods

Lens and body measurements were obtained from 101 sharks landed in association with the Cefas/Defra Neptune Scientific Fishery. All specimens were

by-caught in a seized catch by Marine Management Organisation off Southwold (long-liners <10m) from June-September, 2014. Individuals ranged in size from 40-113cm, with females representing >85% of the samples, >40% of which were pregnant. Dorsal muscle was sampled from all 101 sharks, and lenses extracted from 19 individuals selected at random (10 males, 9 females). The embryos of 20 randomly selected gravid female sharks were also sampled, and embryonic lens and body measurements recorded.

4.3.1 Tissue preparation

One lens was extracted from each fish via an incision along the length of the cornea. The diameter at the equator of each lens was measured to the nearest 0.25mm using callipers. Sequential laminae were then removed using a scalpel and fine-tipped forceps (Wallace *et al*. 2014). Tissue was peeled from pole to pole, and the lens diameter following each subsequent peel was re-measured. In an attempt to standardise laminae depth, the thinnest layer of lens tissue possible was removed during each peel. This process was repeated until no further layers of tissue could be removed, and the entire lens, from outer cortex to nucleus, had undergone delamination. Individual laminae were stored in Eppendorf tubes and frozen for 12 hours, prior to lyophilisation.

Dorsal muscle was also extracted from 101 individual spiny dogfish, and 20 embryos. A small sample, ~1cm^3, was removed from the region anterior to the first dorsal fin. The skin was removed and the remaining tissue stored in Eppendorf tubes. Samples were then rinsed ten times in deionised water, centrifuged, and rinsed a further 10 times in order to remove free ammonia. Dorsal muscle samples were then frozen and lyophilised.

Dried lens and muscle tissue was homogenised, weighed to ~0.5mg, and stored in tin capsules in preparation for stable isotope analysis.

4.3.2 Analytical Methods

Stable carbon and nitrogen isotope ratios of adult *Squalus acanthias* muscle samples were determined at OEA Laboratories Ltd. In-house laboratory standards (USGS40) were analysed in order to account for and correct

instrument drift. Experimental precision was 0.29‰ and 0.17‰ for carbon and nitrogen, respectively (standard deviation for replicates of standards). All lens and embryonic (muscle and lens) samples were analysed at the NERC Life Sciences Mass Spectrometry Facility in East Kilbride, using a Pyrocube Elemental Analyzer (2013, Elementar, Hanau, Germany) and Delta XP (Thermo Electron) mass spectrometer (2003). The same laboratory standard was analysed at the beginning and end of every analytical run of 155 samples. Additional in-house standards were also analysed every 10 samples to allow identification of any instrument drift. Experimental precision was 0.09‰ for carbon and 0.17‰ for nitrogen (standard deviation for replicates USGS40 standards). Glutamic acid (GA) standards from The University of Southampton were also analysed at both laboratories, nested within the samples. Mean $\delta^{15}N$ and $\delta^{13}C$ reported for standards analysed at OEA Laboratories Ltd. are -3.99‰ (± 0.23) and -12.99‰ (± 0.27) for nitrogen and carbon, respectively. Mean $\delta^{15}N$ and $\delta^{13}C$ reported from standards analysed at NERC Life Sciences Mass Spectrometry Facility are -3.84‰ (± 0.16) and -13.03‰ (± 0.24) for nitrogen and carbon, respectively. Absolute isotopic delta-values for the in-house standard were therefore consistent within error between the two laboratories. Isotope ratios are expressed in δ notation (‰), relative to international standards of V-Pee dee belemnite and air for carbon and nitrogen, respectively.

4.3.3 Isoscape

The reference isoscape used to geographically assign individual spiny dogfish samples to feeding locations within the North Sea was developed by Trueman *et al.* (2016), and based on earlier work from MacKenzie *et al*. (2014). *Cyanea capillata* mesoglea tissue was sampled from from 66 individuals, caught at 52 stations around the North Sea in 2015, during the International Bottom Trawl Survey on board RV Cefas Endeavour. Isoscapes were developed using Linear Kriging, producing models of the spatial variation of the isotopic composition of jellyfish tissue (lipid and size-corrected) (Figure 4.1, Trueman *et al*. 2016).

The resultant isoscapes reveal an area of relatively negative $\delta^{13}C$ values in the central southern North Sea, surrounded by waters characterised by increasing $\delta^{13}C$ values with increasing proximity to the coast. Predicted nitrogen isotope

variability effectively divides the North Sea into two distinct regions: the northern North Sea and southern North Sea, characterised by relatively negative and positive $\delta^{15}N$ values, respectively. An area characterised by high $\delta^{15}N$ values is also associated with continental Europe in the southeast North Sea.

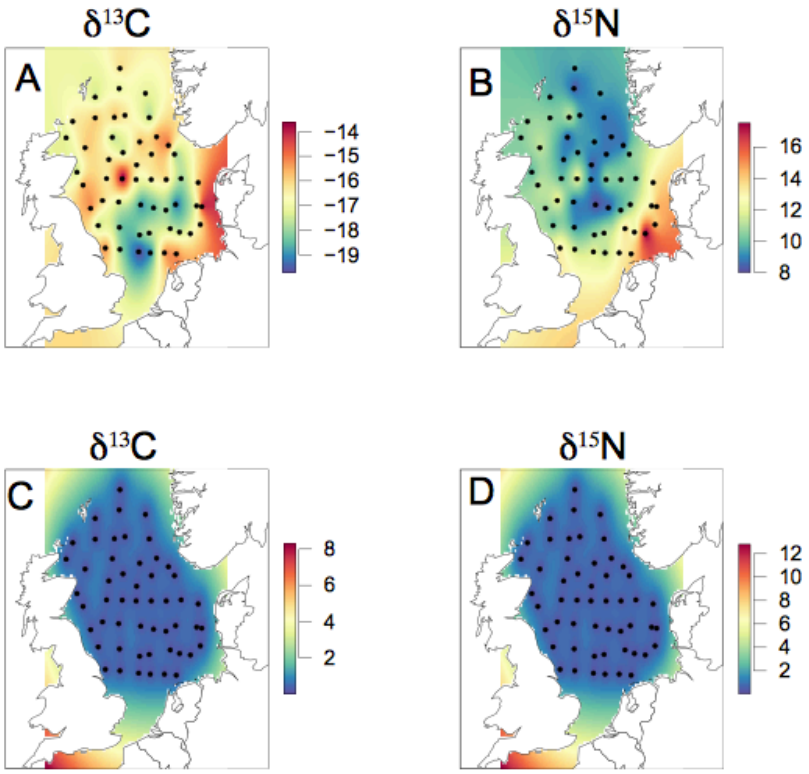

Figure 4.1. – Isoscape models (A and B) and associated variances (C and D) for $\delta^{13}C$ (A and C) and $\delta^{15}N$ (B and D) based on Cynea capillata, sampled in September, 2011 (Trueman *et al*. 2016). Filled circles indicate sampling stations.

The broad-scale trends in isotopic variability across the region are similar to those identified by Jennings *et al*. (2003), Barnes *et al*. (2009), MacKenzie *et al*. (2014), and Jennings & van der Molen (2015), suggesting long-term stability in isotopic gradients. Moreover, these trends appear to be conserved between benthic and pelagic feeders. Thus, the hydrodynamic and biogeochemical processes driving isotopic variability in this region are temporally stable (MacKenzie *et al.* 2014). We are therefore confident that the isoscape developed by Trueman *et al*. (2016) is suited to the geographic assignment of North Sea spiny dogfish tissues.

4.3.4 Assignment

The assignment approach outlined by Vander Zander *et al*. (2015) was followed in order to assign lens and muscle tissue to the North Sea isoscape produced by Trueman *et al*. (2016). Each cell in the isoscape is assigned a likelihood of origin based on the isotopic difference between the measured tissue and the isoscape cell compared to the multi-variate normal distribution of all $\delta^{15}N$ and $\delta^{13}C$ values comprising the isoscape. A critical odds ratio threshold is established and all cells with a probability of origin greater than this threshold are considered as likely origin. A threshold odds ratio of 1.43 (representing 30% of all cells in the North Sea with the highest probability values) was selected as in validation studies using queen scallop tissue (*Aequipecten opercularis*) from known locations this provides the best compromise between accuracy and precision (>70% accuracy, assigning to cells comprising 30% of the possible area Trueman *et al*. 2016).

The reference organism used to construct isoscapes *(Cyanea capillata)* is a mid trophic level animal, feeding primarily upon zooplankton and icthyoplankton (Fancett, 1988, Fancett & Jenkins, 1988, Brewer, 1989, Båmstedt *et al*. 1997, Hansson, 1997, Purcell & Sturdevant, 2001; Purcell, 2003). In order to geographically assign higher trophic level spiny dogfish samples to a jellyfish-derived isoscape, the trophic offset between these species must be addressed. Mackinson & Daskalov (2007) estimated that gelatinous zooplankton and juvenile spiny dogfish occupy trophic level 3.6 and 4.29 respectively, with adult spiny dogfish feeding at trophic level 4.34. An offset of 0.75 and 0.5 (± 1.00) was therefore applied to account for the likely trophic distance between *C. capillata* and adult and juvenile *S. acanthias*, respectively. In order to account for the trophic enrichment associated with tissue formed *in utero* and fuelled by maternal foraging, an offset of 0.75 (± 1.00) was similarly applied to embryonic samples. The conservative standard deviation associated with this estimate also accounts for error related to changes in trophic distance with increasing spiny dogfish size. The isotopic offset is subsequently accounted for by multiplying trophic level offset by 3 and 1, representative of the enrichment factor per trophic level for carbon and nitrogen, respectively (Smith & Epstein, 1970;

Minson *et al*. 1975; Haines, 1976; Fry *et al*. 1978; DeNiro & Epstein, 1978; DeNiro & Epstein, 1981).

C. capillata and *S. acanthias* tissues are also likely to differ in their biochemical composition, potentially introducing additional isotope offsets which must be addressed. Unaware of any studies that compare the isotopic composition of jellyfish bell tissue and spiny dogfish muscle, a tissue discrimination factor was identified by applying the smallest possible offset term to allow all samples to be geographically assigned within the study area, making the assumption that all specimens were foraging within the North Sea at the time of tissue formation. An offset of -1‰ (σ = 0.5) for $\delta^{13}C$ and -3‰ (σ = 0.5) for $\delta^{15}N$ values was therefore applied. Given that the muscle-lens tissue discrimination factor has been identified for this species (See Chapter 2), this information was also incorporated into the offset term when assigning lens tissue ($\delta^{13}C$ = -0.2‰, σ = 0.5 and $\delta^{15}N$ = -3.66‰, σ = 0.5).

4.4 Results

4.4.1 Relationship between lens and body size

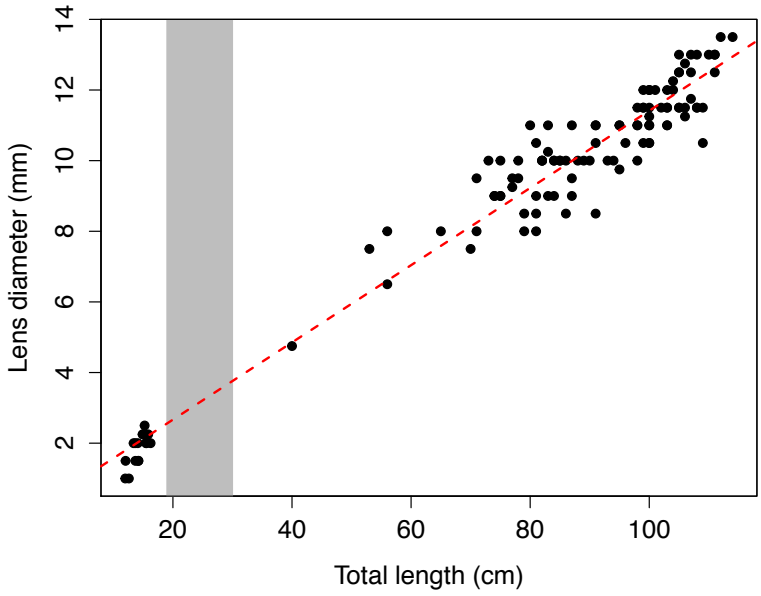

Figure 4.2 - The relationship between total length (TL) and lens diameter (LD) for the spiny dogfish, *Squalus acanthias* (n= 101, r^2 = 0.959, p = <0.001). The grey region represents size at birth (19-30cm) (Gauld, 1979).

The growth relationship between total length (TL) and lens diameter (LD) is linear for *Squalus acanthias* (Figure 4.2), and the corresponding equation is represented as:

$$y = 0.479\ (\pm 0.181) + 0.109\ (\pm 0.002)\ x \qquad (4.1)$$

Here, y represents the lens diameter (mm) and x represents the total length (cm) of the fish. The grey area highlighted in Figure 4.2 represents *Squalus acanthias* size range at birth: 19-30cm (Gauld, 1979). Using equation 4.1, an estimate of total length, corresponding to each sequential lamina, is back calculated from the measured diameter following each subsequent peel. This allows lens tissue formed pre- and post-birth to be distinguished according to total length, using 19cm as the conservative upper limit of tissue formed in utero (Gauld, 1979). Similarly, back-calculation of total length allows a size-referenced ontogenetic series to be produced, per shark. Lens size ultimately limits the number of laminae removed. In this investigation, 6-13 layers of lens tissue were extracted per individual.

4.4.2 Lipid correction

Where lipid content of tissues submitted for stable isotope analysis is high, the resultant $\delta^{13}C$ value is negatively biased (Reum, 2011). According to Post (2002), C:N ratios exceeding 3.5 are indicative of high lipid content in the tissues of aquatic organisms.

Figure 4.3 displays the relationship between the C:N ratio and $\delta^{13}C$ values for 99 spiny dogfish muscle samples (2 samples failed during analysis), demonstrating that the relationship between the two parameters is highly constrained. Elevated C:N ratios are associated with relatively negative $\delta^{13}C$ values.

Mean C:N ratios of muscle samples submitted for isotope analysis were 5.36 (± 0.94) and 6.79 (± 0.71) for adults and embryos, respectively. Thus, all *Squalus acanthias* muscle data required retrospective correction for lipid content. The two-parameter model developed by Fry (2002) was used:

$$\Delta \delta^{13}C = D - DF(R_{CN})^{-1} \quad (4.2)$$

Here, D represents the protein-lipid $\delta^{13}C$ discrimination factor (8.39 ± 0.74), and F the lipid-free C:N ratio, set at 2.71 (± 0.14) (Reum, 2011). Due to the low lipid content of lens tissue (C:N < 3.5), no correction was required (mean CN = 2.85 ± 0.18).

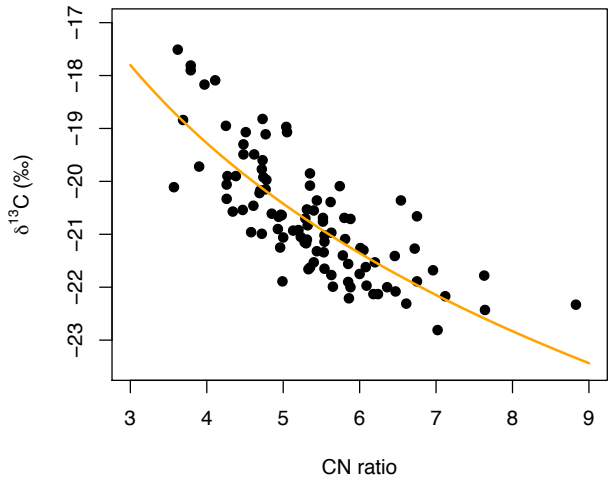

Figure 4.3 – Relationship between dorsal muscle $\delta^{13}C$ and C:N ratio for 99 spiny dogfish (*Squalus acanthias*). Orange trend line represents logarithmic function.

4.4.3 Isotope data & assignment

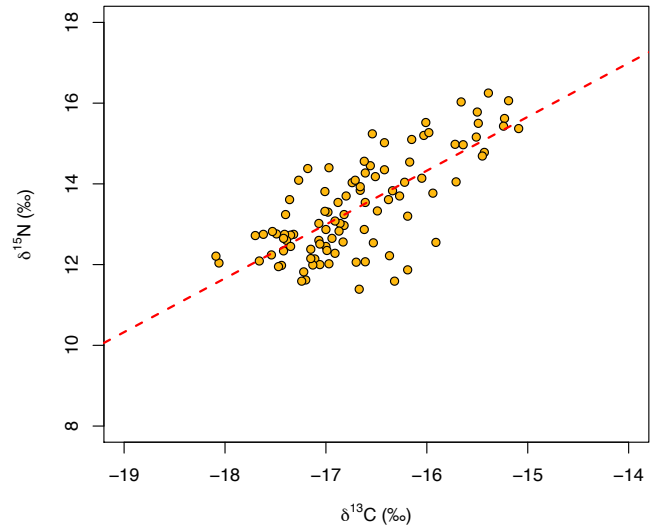

Figure 4.4 – Biplot of $\delta^{15}N$ values and lipid-corrected $\delta^{13}C$ values (Fry, 2002) of dorsal muscle samples from 99 adult *Squalus acanthias* specimens caught in the North Sea between June and Spetember, 2014. Dotted red line represents positive regression ($F_{(1,97)} = 118.4$, $p < 0.01$, $R^2 = 0.55$).

Figure 4.4 displays all corrected dorsal muscle data from free-living specimens (embryonic samples excluded) (raw data in Table 4.1). $\delta^{13}C$ values range from -18.09 to -15.09 ‰ (mean = -16.68 ± 0.68 ‰). $\delta^{15}N$ values range from 11.39-16.25 ‰ (mean = 13.42 ± 1.23 ‰). A positive linear relationship exists between $\delta^{13}C$ and $\delta^{15}N$ values: $F_{(1,97)} = 118.4$, $p < 0.01$, $R^2 = 0.55$.

The overlain assignment probabilities of all 99 spiny dogfish dorsal muscle samples are displayed in Figure 4.5, with increasing colour intensity representing increasingly common assignment areas. Although there is some assignment of muscle samples throughout the North Sea, most samples are assigned to an area within the central and southern North Sea (south and northwest of Dogger Bank).

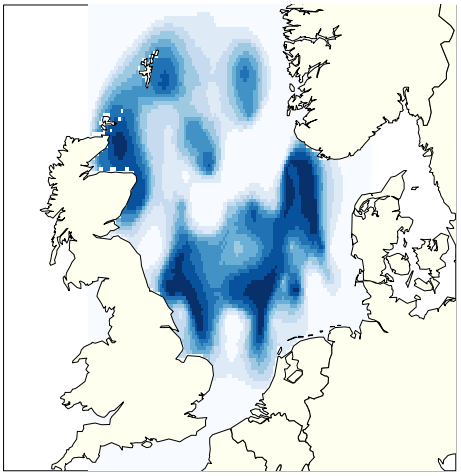

Figure 4.5 – Geographic assignment of spiny dogfish, based upon the isotopic composition ($\delta^{13}C$ and $\delta^{15}N$ values) of adult dorsal muscle samples (n= 99 - 11 male, 88 female). The coloured region represents the overlain assignment probabilities for all samples, with increasing intensity representing more common assignment region.

Figure 4.6 displays all lens data, including sequential samples (5-11 per lens) from 25 adult spiny dogfish (12 male, 13 female). Raw data are presented in Table 4.2. Lens isotope values span a greater range compared to muscle data: 9.18 to 15.64‰ (mean = 12.02 ± 1.29 ‰) and -18.95 to -14.91‰ (mean = -16.83 ± 0.77 ‰) for nitrogen and carbon, respectively.

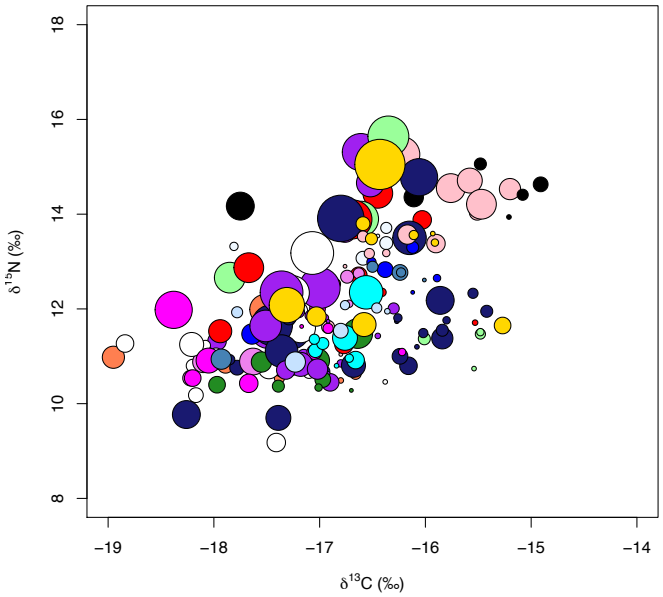

Figure 4.6 – Biplot of sequential lens $\delta^{15}N$ values and $\delta^{13}C$ values (up to 11 subsamples per lens), from a subset of 25 adult spiny dogfish. Colour represents individual shark ID, and relative size corresponds to lens diameter measurement.

In order to examine lens isotope composition throughout ontogeny, the data were separated according to the back-calculated estimate of size (total length). This low-resolution comparison allowed investigation of differences in the isotopic composition of lens tissue formed during juvenile and mature life history stages, whilst also permitting examination of pre-birth/maternal signals. Based on the measured linear relationship between lens diameter and body size (Figure 4.2), a conservative upper size limit of 20cm was applied in order to isolate pre-birth data (*S. acanthias* size at birth estimated at 19-30cm (Gauld, 1979)), whilst data from the mature portion of the lens were selected by applying a lower cut-off limit of 55cm and 74cm total length (Pawson & Ellis, 2005), corresponding to size at maturity for males and females, respectively. Lens tissue formed during juvenile life history was limited to samples with an associated total length of 30-55 cm (males) and 30-73cm (females). A repeated measures analysis of variance (ANOVA) revealed significant differences in nitrogen isotope ratios between the three categories ($F = 9.31_{2, 144}$, $p < 0.001$). Conversely, carbon isotope ratios are comparable across categories ($p = 0.125$).

Table 4.1 – Muscle carbon ($\delta^{13}C$) and nitrogen ($\delta^{15}N$) isotope data from 99 spiny dogfish (*Squalus acanthias*). $\delta^{13}C$ values are corrected for lipid content.

ID	$\delta^{15}N$	$\delta^{13}C$	Sex	TL (cm)	ID	$\delta^{15}N$	$\delta^{13}C$	Sex	TL (cm)
1	16.06	-15.19	F	87	**57**	11.82	-17.22	F	103
2	14.45	-16.56	F	110	**58**	13.7	-16.8	F	99
3	15.62	-15.23	M	77	**59**	13.24	-17.4	F	105
5	15.78	-15.5	M	65	**60**	14.97	-15.64	F	105
6	14.27	-16.61	F	107	**61**	11.59	-17.24	M	74
11	13.24	-16.82	F	93	**62**	13.08	-16.91	F	100
13	15.52	-16.01	M	73	**63**	15.2	-16.03	F	104
13	14.98	-15.72	F	104	**64**	11.59	-16.32	F	71
14	12.75	-17.62	F	83	**65**	14.4	-16.97	F	106
15	12.45	-17	F	89	**66**	12.28	-16.91	F	100
16	12.14	-17.11	F	56	**67**	12.76	-17.49	F	106
17	12.55	-15.91	M	87	**68**	12.65	-16.94	F	108
18	15.43	-15.24	F	78	**69**	14.38	-17.18	F	105
19	12.87	-16.62	F	80	**70**	15.1	-16.15	F	99
20	15.16	-15.51	M	79	**71**	15.37	-15.09	F	102
21	12.87	-17	F	91	**73**	15.02	-16.42	F	94
22	11.62	-17.2	F	81	**74**	13.3	-16.98	F	111
23	12.97	-16.82	F	90	**75**	16.03	-15.66	F	91
24	13.2	-16.19	F	81	**76**	14.03	-16.74	F	100
25	13.81	-17.01	F	70	**77**	13.02	-17.07	F	99
26	16.25	-15.39	F	88	**78**	14.78	-15.43	F	56
27	12.02	-16.97	F	107	**79**	12.65	-17.42	F	109
28	13.54	-16.88	F	96	**80**	14.69	-15.45	F	111
29	11.98	-17.44	F	100	**81**	12.83	-16.87	F	102
30	14.56	-16.62	F	95	**82**	14.04	-16.22	F	108
32	12.75	-17.32	F	100	**83**	12.45	-17.35	F	98
33	13.84	-16.66	F	103	**84**	12	-17.06	F	81
34	13.61	-17.36	F	103	**85**	12.04	-18.06	F	85
35	12.72	-17.7	F	95	**86**	13.61	-16.38	F	112
36	12.73	-17.35	F	98	**87**	13.93	-16.66	F	111
37	11.95	-17.47	F	103	**88**	12.38	-17.15	F	108
38	12.6	-17.07	F	95	**89**	13.32	-17.01	F	100

39	12.09	-17.66	F	106	**90**	12.24	-17.54	F	82
40	13.7	-16.27	F	99	**91**	12.21	-18.09	M	75
41	14.14	-16.05	F	91	**92**	14.09	-17.27	F	81
42	14.18	-16.51	F	109	**93**	12.07	-16.61	M	75
43	12.56	-16.83	F	85	**94**	11.99	-17.13	F	86
44	12.65	-17.41	F	71	**95**	15.27	-15.98	F	84
45	11.87	-16.19	F	75	**96**	13.83	-16.34	F	73
46	11.39	-16.67	F	74	**97**	12.15	-17.15	M	61
47	12.6	-17.39	F	86	**98**	15.24	-16.54	F	114
48	14.05	-15.71	F	81	**99**	13.77	-15.94	F	101
49	14.54	-16.17	M	82	**103**	13.33	-16.49	F	100
50	12.75	-17.41	F	91	**104**	14.09	-16.71	F	86
51	12.51	-17.06	F	83	**105**	12.82	-17.53	F	87
52	12.06	-16.7	M	71	**106**	15.5	-15.49	F	105
53	12.54	-16.53	F	79	**108**	13.54	-16.61	F	77
54	12.34	-17.42	F	98	**110**	12.35	-16.99	F	84
55	14.35	-16.42	F	107	**111**	12.22	-16.37	F	105
56	13.02	-16.86	F	103					

Table 4.2 – Carbon ($\delta^{13}C$) and nitrogen ($\delta^{15}N$) isotope data for sequential eye lens samples from 25 spiny dogfish (*Squalus acanthias*). Sub-ID relates to each delamination stage, with A representing the outermost layer of lens tissue removed.

ID	**Sub ID**	**$\delta^{15}N$**	**$\delta^{13}C$**	**Lens Diameter**	**Sex**
3	A	15.26	-16.22	9.5	M
3	B	14.55	-15.76	7.75	M
3	C	14.71	-15.58	6.75	M
3	D	14.53	-15.20	5.75	M
3	E	14.04	-15.51	4.25	M
3	F	11.62	-16.92	3.5	M
3	G	11.41	-17.62	2	M
3	H	11.04	-16.80	1	M
5	A	14.44	-16.45	8	M
5	B	13.88	-16.03	5	M
5	C	12.71	-16.63	4.5	M
5	D	12.45	-16.54	3.5	M

5	E	12.53	-16.85	2.75	M
5	F	12.35	-16.41	2.25	M
5	G	12.45	-16.51	1.25	M
10	A	12.30	-17.27	7.5	M
10	B	12.01	-17.02	4.25	M
10	C	11.60	-17.19	3.25	M
10	D	11.59	-16.92	2.75	M
10	E	11.52	-16.74	1.5	M
10	F	12.29	-16.66	0.75	M
13	A	15.31	-16.61	10	M
13	B	14.66	-16.52	7.5	M
13	C	13.64	-16.76	6	M
13	D	11.32	-17.97	5	M
13	E	12.37	-16.58	3.5	M
13	F	12.01	-16.30	3	M
13	G	11.43	-16.45	1.5	M
17	A	11.57	-17.46	6.5	M
17	B	11.95	-17.20	5	M
17	C	13.07	-16.59	3.75	M
17	D	13.39	-16.37	3.5	M
17	E	13.71	-16.37	3	M
17	F	13.32	-17.81	2.25	M
17	G	13.54	-16.45	1	M
20	A	15.64	-16.35	11	M
20	B	13.90	-16.61	9.5	M
20	C	12.66	-17.85	8.25	M
20	D	12.31	-17.34	5.5	M
20	E	12.37	-17.12	4.75	M
20	F	11.80	-17.32	4.25	M
20	G	11.82	-17.24	3.75	M
20	H	11.37	-16.01	3.25	M
20	I	11.47	-15.48	2.75	M
20	J	11.51	-15.48	2	M
20	K	10.74	-15.54	1.25	M
21	A	11.99	-17.52	8	F
21	B	10.98	-18.95	6	F

21	C	10.82	-17.89	4.5	F
21	D	10.79	-17.22	4	F
21	E	10.63	-16.66	3	F
21	F	10.54	-17.38	2.75	F
21	G	10.49	-16.80	1.5	F
24	A	11.54	-17.27	10	F
24	B	10.85	-17.27	6.5	F
24	C	10.76	-17.78	4	F
24	D	10.89	-17.12	3.75	F
24	E	10.68	-16.96	3.25	F
24	F	10.93	-17.85	2.75	F
24	G	11.03	-17.16	2.25	F
24	H	11.20	-16.08	1.25	F
26	A	14.17	-17.75	7.5	F
26	B	14.36	-16.11	5.25	F
26	C	14.63	-14.91	4	F
26	D	15.06	-15.48	3.25	F
26	E	14.41	-15.08	3	F
26	F	14.27	-15.53	2.25	F
26	G	13.94	-15.21	1.25	F
30	A	13.89	-16.69	10.5	F
30	B	12.87	-17.67	8	F
30	C	11.53	-17.94	6.25	F
30	D	11.25	-16.77	5	F
30	E	10.76	-17.44	4	F
30	F	10.71	-17.36	3.75	F
30	G	11.52	-17.31	3	F
30	H	11.71	-15.53	1.5	F
38	A	12.44	-17.00	11	F
38	B	11.52	-17.49	9	F
38	D	10.45	-16.90	4.75	F
38	E	11.01	-17.15	3.5	F
38	G	10.85	-16.80	2	F
38	H	10.64	-16.92	1	F
49	A	14.78	-16.06	10	M
49	B	13.50	-16.15	9	M

49	C	12.18	-15.86	7.5	M
49	D	10.81	-16.68	6.5	M
49	E	11.38	-15.84	5.75	M
49	F	10.80	-16.16	4.75	M
49	G	11.00	-16.24	4.25	M
49	H	11.95	-15.42	3.25	M
49	I	12.33	-15.55	2.75	M
49	J	11.76	-15.80	2	M
49	K	11.74	-16.27	1.25	M
52	A	11.47	-17.64	5.5	M
52	B	12.83	-16.38	4.25	M
52	C	13.30	-16.12	3.25	M
52	D	12.99	-16.51	2.5	M
52	E	12.65	-15.89	2	M
52	F	12.35	-16.12	1	M
59	A	13.18	-17.07	11.5	F
59	B	12.34	-17.26	9.25	F
59	C	11.60	-17.18	8	F
59	D	10.75	-17.48	5.75	F
59	E	9.18	-17.41	5	F
59	F	10.18	-18.17	4	F
59	G	10.80	-18.20	3.5	F
59	H	11.23	-18.08	2.75	F
59	I	11.22	-18.24	1.5	F
61	A	11.91	-17.37	9	M
61	B	10.89	-17.63	7.25	M
61	C	10.88	-18.10	5.75	M
61	D	10.54	-18.22	4.25	M
61	E	12.68	-16.74	3.5	M
61	F	12.75	-16.63	3	M
61	G	12.11	-16.72	2	M
64	A	11.48	-16.64	8	F
64	B	10.91	-17.02	6.5	F
64	C	10.88	-17.55	5.5	F
64	D	10.40	-17.97	4.5	F
64	E	10.51	-16.97	4.25	F

64	F	10.37	-17.39	3.25	F
64	G	10.34	-17.01	2	F
64	H	10.28	-16.70	1	F
74	A	13.91	-16.80	12.5	F
74	B	11.66	-17.45	11	F
74	C	11.11	-17.36	8.75	F
74	D	9.77	-18.26	7.5	F
74	E	9.70	-17.39	6.75	F
74	F	11.82	-17.29	4	F
74	G	11.55	-15.84	3.25	F
74	H	11.49	-16.02	2.5	F
74	I	11.81	-16.26	2.25	F
78	A	14.21	-15.47	8	F
78	B	13.57	-16.17	5.25	F
78	C	13.38	-15.90	5	F
78	D	13.53	-16.59	3	F
78	E	13.17	-16.53	2.75	F
78	F	13.18	-16.37	2	F
78	G	12.90	-16.76	1	F
84	A	11.25	-18.21	6.5	F
84	B	11.27	-18.84	4.75	F
84	C	11.02	-17.98	4	F
84	D	10.66	-17.10	3.25	F
84	E	10.72	-17.33	3	F
84	G	10.46	-16.38	1.25	F
85	A	11.98	-18.38	10	F
85	B	10.91	-18.05	6.75	F
85	C	10.43	-17.67	5	F
85	D	10.54	-18.20	4.5	F
85	E	11.09	-17.05	4	F
85	F	11.09	-16.22	2	F
85	G	11.63	-17.17	1	F
88	A	12.35	-17.36	11.5	F
88	B	11.64	-17.51	8.5	F
88	C	10.83	-17.18	6.5	F
88	D	10.73	-17.02	5.5	F

88	E	10.71	-17.32	5	F
88	F	11.85	-17.04	3.75	F
88	G	11.94	-17.20	3.25	F
88	H	11.86	-17.09	2.75	F
88	I	11.81	-16.95	2	F
88	J	11.74	-16.92	1	F
91	A	10.94	-17.93	5.5	M
91	B	12.77	-16.24	4.25	M
91	C	12.89	-16.50	3	M
91	D	12.77	-16.23	2.5	M
91	E	12.61	-16.01	1	M
93	A	12.35	-16.56	9	M
93	B	11.39	-16.76	6.75	M
93	C	10.92	-16.66	4.75	M
93	D	11.12	-17.04	3.75	M
93	E	11.27	-16.97	3.25	M
93	F	11.36	-17.05	2.75	M
93	G	10.96	-16.72	2.25	M
93	H	10.80	-16.84	1.25	M
97	A	10.88	-17.23	5.5	M
97	B	11.54	-16.80	4	M
97	C	11.93	-17.78	3	M
97	D	12.02	-16.46	2.75	M
97	E	12.08	-16.76	2.5	M
97	F	11.95	-16.36	1.5	M
98	A	15.05	-16.43	13.5	F
98	B	12.08	-17.31	9.5	F
98	C	11.67	-16.58	6.5	F
98	D	11.84	-17.03	5.25	F
98	E	11.65	-15.27	4.5	F
98	F	13.80	-16.59	3.75	F
98	G	13.48	-16.51	3.25	F
98	H	13.56	-16.11	2.5	F
98	I	13.40	-15.91	2	F
98	J	13.59	-15.93	1.25	F

Table 4.3 – Summary of lens isotope data grouped according to back-calculated estimate of total length: pre-birth (n=45) = 0-20cm, juvenile (n=73) = 30-54cm (males) and 30-73cm (females), mature (n=32) = >55 cm (males), >74 cm (females).

	Pre-birth		**Juvenile**		**Mature**	
	$\delta^{15}N$	**$\delta^{13}C$**	**$\delta^{15}N$**	**$\delta^{13}C$**	**$\delta^{15}N$**	**$\delta^{13}C$**
Min	10.28	-18.24	9.18	-18.95	10.81	-18.38
Max.	14.27	-15.21	14.63	-14.91	15.64	-15.58
Mean	11.97	-16.46	11.64	-17.12	13.00	-16.86
St. Dev.	1.02	0.61	1.24	0.83	1.47	0.65

$\delta^{13}C$ values were more positive in the pre-birth portion of the lenses (mean = -16.46 ± 0.61 ‰), and more negative in the juvenile region (mean = -17.12 ± 0.83 ‰). $\delta^{15}N$ values were higher in the mature portion of spiny dogfish lenses (mean = 13.00 ± 1.47 ‰), and lower in the immature (juvenile) region (mean = 11.64 ± 1.24 ‰).

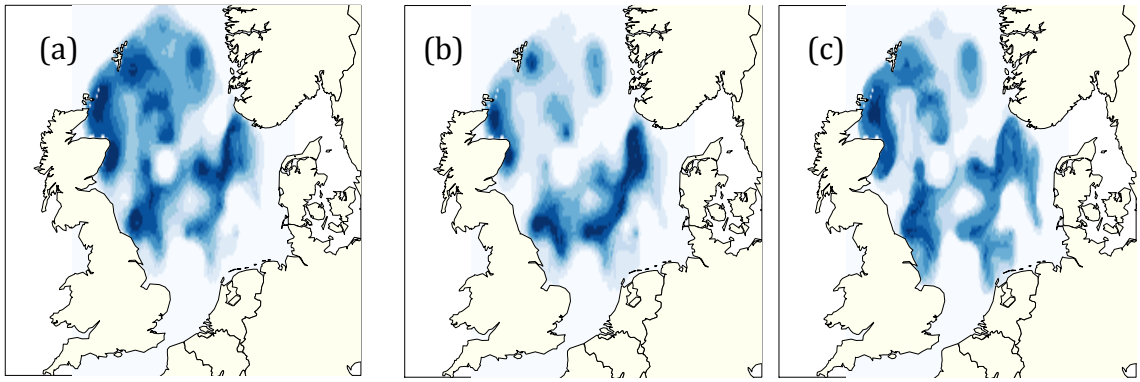

Figure 4.7 - Geographic assignment of sequential samples relating to the (a) pre-birth, (b) immature & (c) mature portion of spiny dogfish lenses (13 female, 12 male). The coloured region represents the overlain assignment probabilities for all samples, with increasing intensity representing more common assignment region.

Figure 4.7 highlights the shift in geographic assignment of lens samples reflecting distinct life-history stages. Lens tissue formed pre-birth and during juvenile life history is commonly assigned to the central and northern North Sea (Fig. 4.11.a & b). In Figure 4.7 (c) there remains some assignment to the

northern North Sea, however there is evidence of a shift in foraging location to south, and lens tissue formed during adult life history is commonly assigned to the southern North Sea, closely representing the geographic assignment plot for muscle tissue (Figure 4.5).

In order to address potential philopatry, the isotopic composition of lens nucleus tissue extracted from pregnant females was compared to that of their pups. The resultant assignment output (Figure 4.8) highlights similar geographic assignment; both sample sets reflect foraging throughout the North Sea, with an emphasis on northern regions.

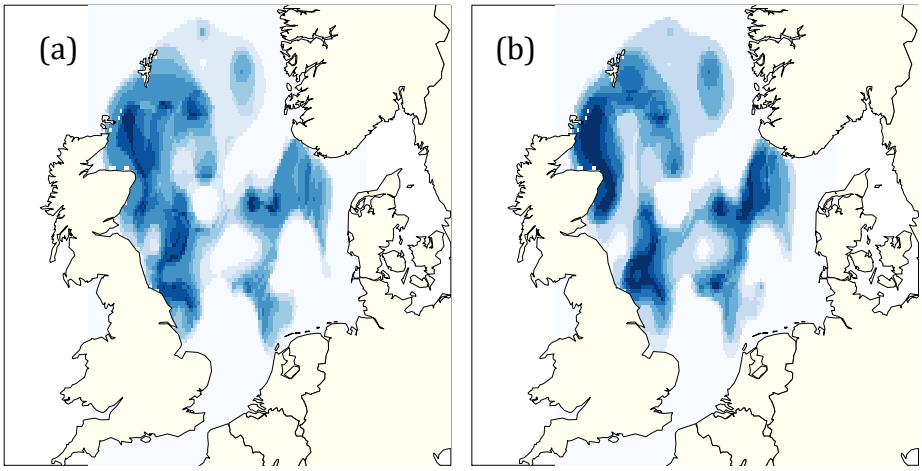

Figure 4.8 - Geographic assignment of spiny dogfish core lens tissue from pregnant females (a) and their embryos (n = 11). The coloured region represents the overlain assignment probabilities for all samples, with increasing intensity representing more common assignment region.

Figure 4.9 displays the difference between the geographic assignment of muscle tissue from pregnant *Squalus acanthias* specimens (4.9.a) and their embryos (4.9.b). Here very different common assignment areas are revealed, with embryonic tissue isotope compositions indicative of foraging throughout the North Sea (north and south of Dogger Bank), whilst muscle tissue from their pregnant mothers appears to reflect nutrient assimilation in the southern North Sea (Figure 4.9.a).

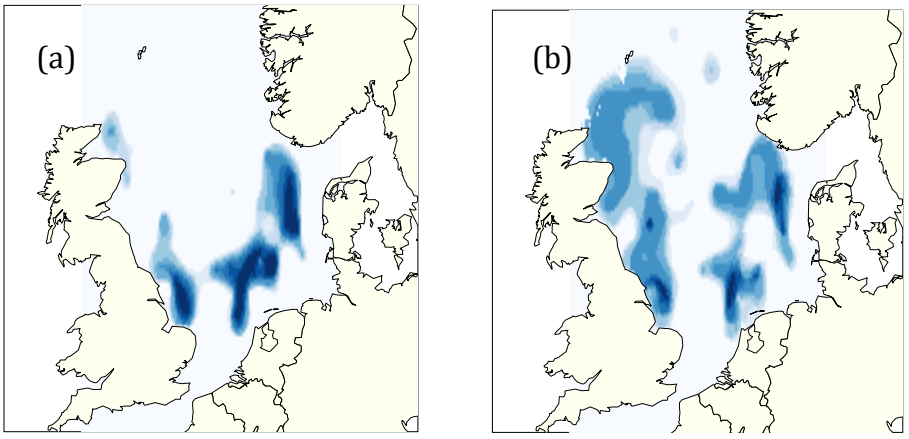

Figure 4.9 - Geographic assignment of spiny dogfish muscle from (a) pregnant females and (b) their embryos (n = 19). The coloured region represents the overlain assignment probabilities for all samples, with increasing intensity representing more common assignment region.

4.4.4 Isotopic Life Histories

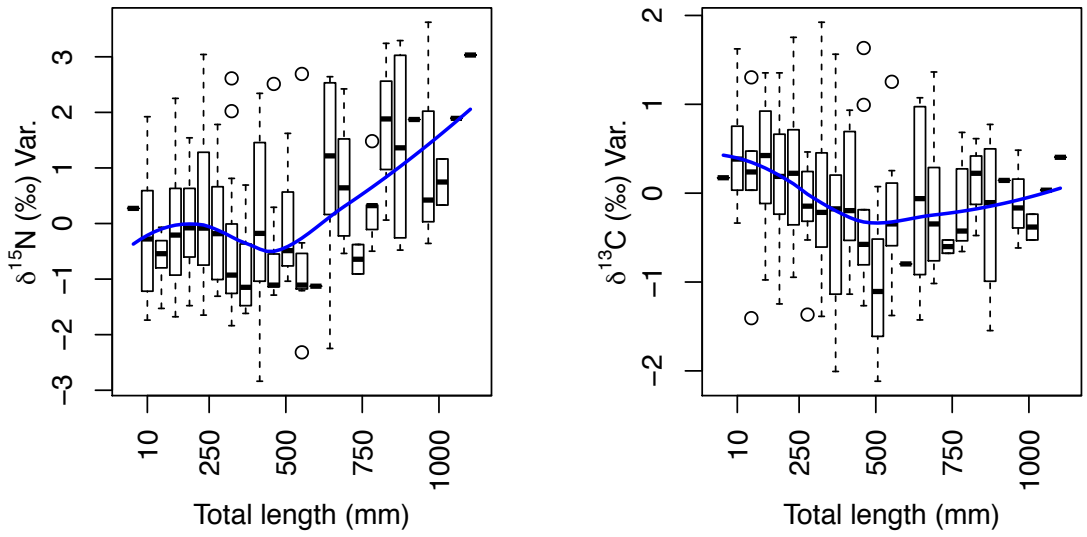

Figure 4.10 - Distribution of normalised $\delta^{13}C$ and $\delta^{15}N$ of lens samples from spiny dogfish (*Squalus acanthias*) for sequential 0.5mm diameter bins. Isotopic variance is plotted against the corresponding back-calculated total length at time of tissue formation. Blue lines represent loess smoothing.

Lens data grouped into individual 0.5mm diameter bins (corresponding TL reported) were normalised, by subtracting the mean of each size bin from the

global average, for both carbon and nitrogen. This allows comparison of common isotopic traits with increasing lens diameter. A distinct change in isotopic composition is subsequently seen at body lengths between 500-700mm (Figure 4.10), approximately equivalent to the length at maturity. Whole-life normalised $\delta^{15}N$ values are generally more positive after maturity, consistent with increasing trophic level, and increased use of isotopically-heavy resources from the southern North Sea basin (Trueman *et al*. 2016). Whole life averaged carbon isotope compositions fall steadily through juvenile time periods before stabilising around the age of maturity (Figure 4.10).

Table 4.4 - Summary of sharks (ID) assigned to nitrogen clusters (n = 3) identified by time-series cluster analysis of nitrogen isotope values, following application of a loess smooth function, using the Euclidean distance method. Across-lens transects of sharks assigned to Cluster 1 are characterised by high $\delta^{15}N$ values, whilst Cluster 2 transects display intermediate to high $\delta^{15}N$ values, decreasing with beyond lens diameters corresponding to size at birth. The lens transects of sharks assigned to Cluster 3 display low to intermediate, relatively stable $\delta^{15}N$ values.

Shark ID	Cluster ID	Shark ID	Cluster ID
3	1	**52**	2
5	3	**59**	3
10	3	**61**	2
13	3	**64**	3
17	2	**74**	3
20	3	**78**	1
21	3	**85**	3
24	3	**88**	3
26	1	**91**	2
30	3	**93**	3
38	3	**97**	3
49	3	**98**	2

Following identification of significant differences between the isotopic compositions of the three life history categories (Table 4.3), high-resolution transects, detailing isotopic variability from lens nucleus to edge, were produced for each of the 25 sharks examined. 6-13 subsamples were extracted per lens. The number of samples obtained from the delamination process was ultimately governed by the size of the lens. Thus, larger specimens yield more samples than smaller individuals.

Lens transects were grouped according to the shape of trends in $\delta^{15}N$ values ($\Delta\ \delta^{15}N$) from the pre-birth and maximum size at birth (30cm TL). To test for the (dis)similarity in the isotopic composition of the pre-birth lens tissue of individual sharks, a loess smooth function was first applied to all samples with an associated diameter ≥1.5mm, ≤4.5mm. This resulted in the production a smooth line through the pre-birth portion of each lens transect, allowing subsequent identification of common trends in the data via time-series cluster analysis using the Euclidean distance method. Due to insufficient data, shark ID 11 was omitted from the cluster analysis. Three clusters were identified, characterised by (1) high $\delta^{15}N$ values (n=3), (2) intermediate to high $\delta^{15}N$ values, decreasing through lens diameters corresponding to size at birth (n=5), and (3) low to intermediate, and relatively stable $\delta^{15}N$ values (n=16). Table 4.4 summarises the cluster assigned to each individual.

The transects displayed in Figure 4.11 reveal high cross-lens isotope variability, particularly in $\delta^{15}N$ values. Although three distinct transect types (Cluster ID 1, 2 and 3) have been identified, one feature common in most individuals is the presence of an increasing trend in $\delta^{15}N$ values throughout the region of the lens relating to exogenous feeding in free-living individuals. This trend is observed in all specimens where the lens was of a sufficient size to allow extraction of multiple lens samples from the juvenile and mature life-history stages (18 of the 25 spiny dogfish lenses), and is highlighted when lens values are normalised to the global mean (Figure 4.10(a)).

$\delta^{13}C$ values are less variable (see Table 4.3), and it is difficult to identify any clear trends to distinguish between groups. Moreover, as nitrogen isotope variability is more informative in terms of spatial ecology and movements in the North Sea, due to the strong north-south $\delta^{15}N$ gradients, cluster analysis of pre-birth lens carbon chemistry was not conducted.

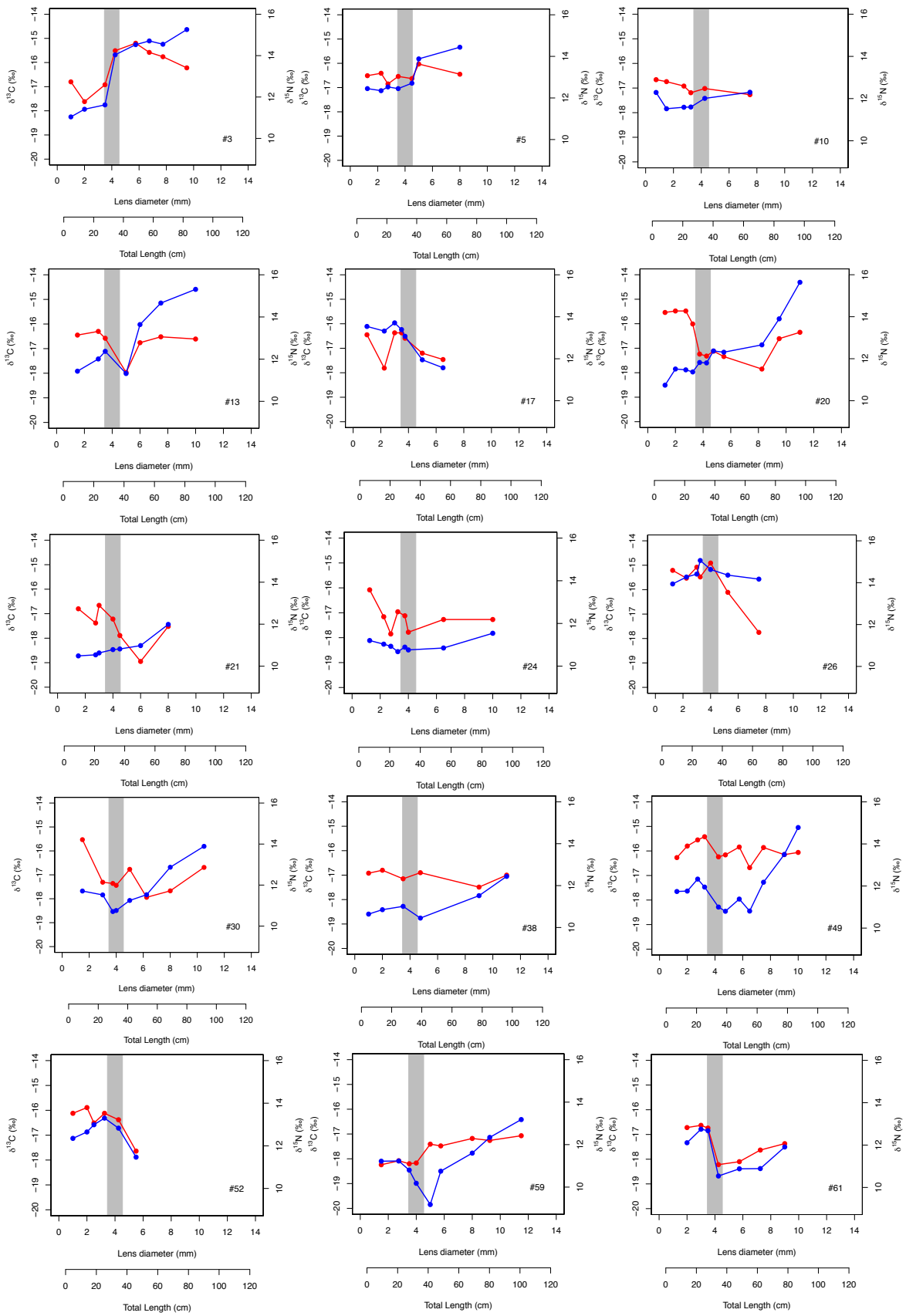
#3
#5
#10
#13
#17
#20
#21
#24
#26
#30
#38
#49
#52
#59
#61
δ13C (‰)
δ15N (‰)
Lens diameter (mm)
Total Length (cm)

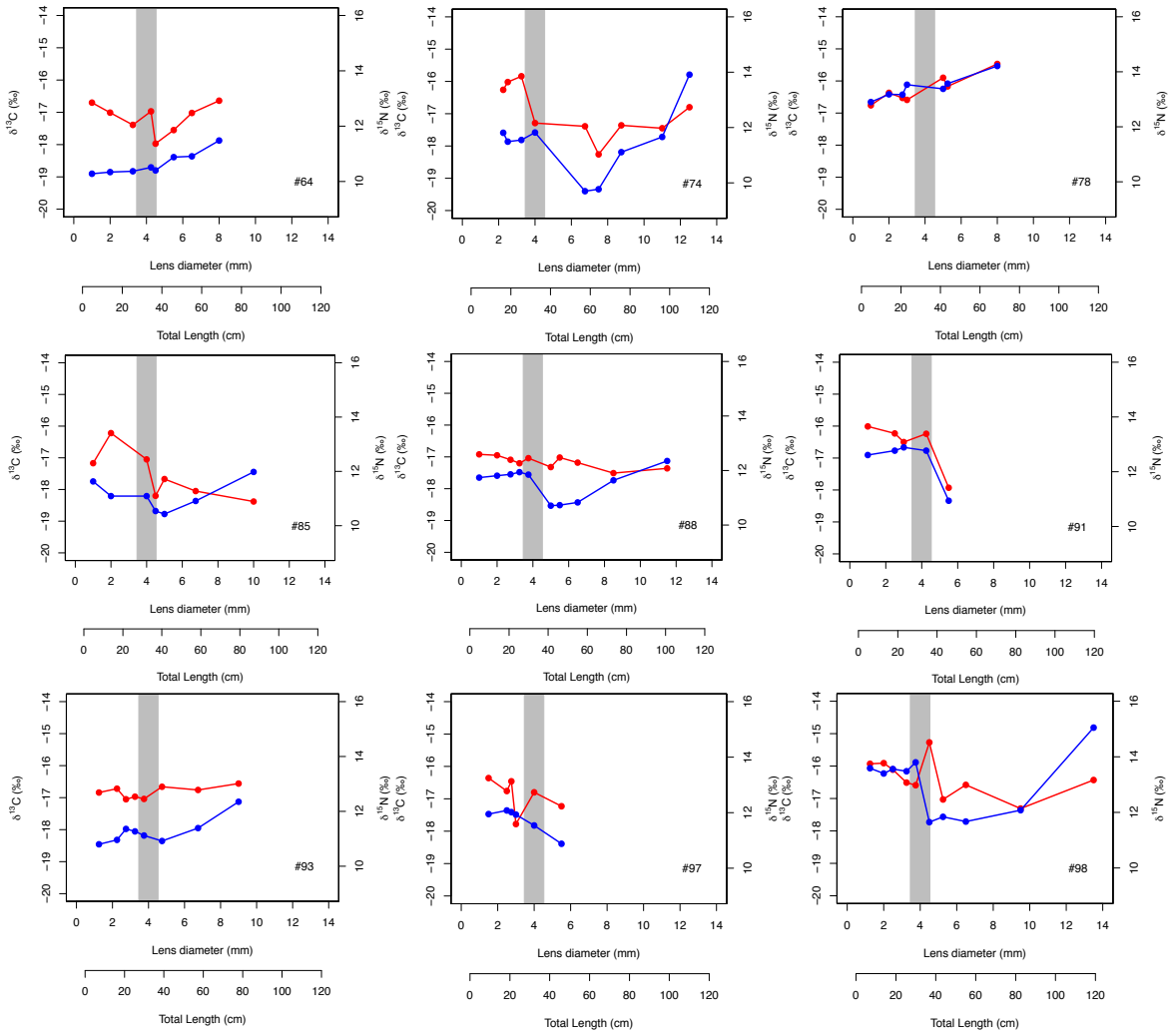

Figure 4.11 – Biplots highlighting cross-lens variability in carbon (red) and nitrogen (blue) isotope compositions. Grey bars represent *Squalus acanthias* size range at birth (19-30cm, Gauld 1979).

4.5 Discussion

4.5.1 Geographic assignment

Comparison of lens and muscle data, and the resulting assignment plots, highlights that different areas within the North Sea play important roles in the ecology of the spiny dogfish (*Squalus acanthias*) throughout its ontogeny. Whilst the southern and central North Sea represent important foraging areas within the relatively recent life history of the species, revealed via the geographic assignment of muscle and adult lens data, the northern North Sea appears to be an important ecoregion during gestation, pupping, and early life history.

4.5.2 Foraging areas of mature adults

Muscle samples obtained from male and female spiny dogfish, spanning a wide size range (56-114cm) are commonly assigned to the central and southern North Sea (Figure 4.5). Tissue turnover is slower in mature individuals relative to juveniles (Vander Zanden *et al*. 2015), and it is estimated that isotopic variability is incorporated into *S. acanthias* muscle over a period of months to years in individuals of the aforementioned size range.

Similarly, lens samples relating to mature life history (Figure 4.7.c.) are more commonly assigned to the central and southern North Sea, closely resembling muscle assignment plot of Figure 4.5. Given that lens fiber cell deposition and somatic growth are tightly coupled (Figure 4.2), it is assumed that lens and muscle tissue formed or remodelled during mature life history will have comparable, relatively slow isotopic incorporation rates, and that the chemical composition reflects nutrient assimilation over a similar temporal scale. The assignment areas identified for these tissues (Figure 4.5 & 4.7.c) supports this assumption, indicating that the southern North Sea region is an important foraging area for mature individuals of the species.

4.5.3 Foraging areas during egg sac provisioning

Here, further evidence supporting maternal philopatry in *Squalus acanthias* is presented. Figure 4.8 compares the geographic assignment of lens nucleus data derived from pregnant spiny dogfish, and their embryos, highlighting that the pregnant females forage within areas characterised by similar isotopic compositions as their mothers did, during the period of yolk sac formation. Moreover, the assignment of lens core samples (formed *in utero*) to the central and northern North Sea suggests that this area is an important ecoregion for mature females during egg sac provisioning.

4.5.4 Reconstructing movements post-partum

Geographic assignment of sequentially formed lens samples reveals shifts in *Squalus acanthias* foraging area throughout ontogeny. Assignment of tissue formed pre-birth and during juvenile life history, relating to maternal nutrient

assimilation and exogenous feeding post-partum, suggests that the northern North Sea is an important foraging area for mature/pregnant females and immature individuals (Figure 4.7.a. & 4.7.b). This also corresponds to regions where high numbers of juvenile spiny dogfish are caught (Ellis *et al*. 2005).

Time-series cluster analysis of high-resolution lens data associated with the transition from maternal provisioning to exogenous feeding in offspring categorised individual sharks into one of three groups according to nitrogen isotope variability (Table 4.4).

Individual spiny dogfish assigned to Cluster 1 display high $\delta^{15}N$ values in the pre-birth portion of the lens, suggesting that mothers of these individuals were foraging in waters characterised by high nitrogen isotope values, similar to those encountered in the southern North Sea. Cross-lens transects of individuals assigned to Cluster 2 are characterised by a sharp decrease in $\delta^{15}N$ values at lens diameters corresponding to size at birth. This suggests that the mothers of these individual sharks fed in areas characterised by very different baseline stable nitrogen isotope conditions, compared to their offspring. Furthermore, the decreasing trend suggests that the pregnant females are assimilating nutrients in southern regions, relative to their offspring. Spiny dogfish assigned to Cluster 3 display no sharp shifts in lens $\delta^{15}N$ values around the time of birth. Nitrogen isotope ratios remain stable throughout the transition zone, suggesting that the mother and pup are feeding and assimilating nutrients in areas characterised by similar isotopic compositions.

The classification of individual sharks to one of three nitrogen clusters suggests that juvenile foraging behaviour is variable, relative to maternal foraging during yolk sac provisioning. Exogenous feeding post birth exposes individual sharks to a much wider range in isotopic variability, driven by prey item, location and trophic level. Thus, the differences in pre- and post-birth lens isotope variability are also supported by the reproductive strategy of the species.

One key assumption was made prior to geographically assigning spiny dogfish muscle and lens samples: all individuals included in this investigation were

foraging within the North Sea during the period of tissue formation/isotopic incorporation. Given the potential for movement and migration in the species, it is entirely possible that some individuals foraged outside this geographical area at some stage during ontogeny, and the isotopic composition of tissue formed or remodelled during these forays will therefore reflect baseline isotopic conditions beyond the North Sea. However, given that no validated spatial isotope data currently exists for the English Channel, Irish Sea, Scottish waters and other regions occupied by spiny dogfish, this assumption was required in order to assign samples to the isoscape region. This caveat must therefore be considered when discussing the geographic assignment and evidence for ontogenetic movements in the species. Nevertheless, retrospective geographical assignment of juvenile lens tissue does coincide with the known distribution of juvenile spiny dogfish (Ellis *et al*. 2005), and assignment of tissues formed during mature life history also encompasses the capture location of adults sampled in this study.

4.5.5 Temporal decoupling

One disparity identified by this study is associated with differences in the geographic assignment of muscle tissue originating from gravid spiny dogfish, and that of their embryos. Despite investigating the same tissue, the isotopic composition of muscle derived from pregnant females and their pups differs considerably, thus resulting in very different geographic assignment (Figure 4.9). The conflicting assignment regions may be associated with the time lag observed between yolk sac formation and embryonic development. If egg development begins up to 4 years prior to parturition (Wood *et al*. 1979) and no subsequent replenishment of yolk matter occurs during gestation, then the isotopic variability associated with feeding prior to fertilization is likely averaged within the tissue. This would not only explain the low intra-individual variability in pre-birth lens isotope data, but would also result in a considerable temporal offset between formation of the yolk material fuelling embryo growth, and maternal foraging driving muscle turnover and lens formation in the mother (~ 2 years). Thus, if this is the case, it is unsurprising that the resultant assignment output plots seen in Figure 4.9, relating to embryo and mother assignment, display strong disparity. Nevertheless, the northerly shift in

assignment of embryonic tissue relative to maternal muscle suggests that the northern North Sea is an important ecoregion exploited by mature female spiny dogfish during yolk sac provisioning.

Whilst teasing out the complexities associated with yolk sac formation in aplacental viviparous species is beyond the scope of this work, based on the comparison of the chemical composition of lens tissue formed pre-birth and during juvenile and mature life-history, considerable shifts in spiny dogfish distribution within the North Sea appears to occur throughout ontogeny.

4.5.6 Isotopic offset

DeNiro & Epstein (1978) revealed that the various biochemical fractions of the diet are subject to differential fractionation processes, subsequently impacting upon the incorporation of isotopic compositions into consumer tissues. Pinnegar & Polunin (1999) identified that the degree of fractionation is also affected by the relative distribution and proportion of individual fractions. For example, vertebrae collagen displays elevated $\delta^{13}C$ relative to muscle (Estrada *et al*. 2006; Kim *et al*. 2012a), attributed to the high glycine content of collagen, which is enriched in ^{13}C relative to other amino acids. Moreover, lens proteins are comprised of α, β, δ and other taxon-specific crystalline proteins, which vary in their relative proportions according to species (Bloemendal *et al.* 2004; Lynnerup *et al.* 2008). Tissue-specific isotopic offsets must therefore be addressed on a case-by-case basis. Muscle-lens isotopic spacing has previously been addressed for this species (discussed at length in Chapter 3): muscle-lens offset = 0.66‰ and 0.18‰ for nitrogen and carbon, respectively. This information was incorporated into the offset term prior to the geographic assignment of all lens tissue.

In order to examine potential maternal isotopic offset, muscle extracted from mothers and their embryos were compared (Chapter 3). A significant difference was identified between embryonic and maternal muscle $\delta^{13}C$ values, with embryos appearing elevated relative to the mother. No significant difference in $\delta^{15}N$ values was identified. However, due to the uncertainties associated with the comparability of maternal and embryonic muscle tissue from matched pairs

(due to the potential for temporal decoupling, previously discussed), we avoided applying the carbon isotope offset when assigning embryonic tissue.

Untangling the intricacies associated with yolk sac formation and subsequent assimilation and incorporation into the tissues of developing embryos can only be achieved via long-term captive feeding experiments of mature and pregnant females. This is logistically challenging and ultimately requires sacrifice of the study organism and is therefore unsuitable for spiny dogfish.

4.5.7 Management implications

The identification and subsequent safeguarding of critical habitats offers a tool by which fisheries managers can facilitate the recovery of the northeast Atlantic *S. acanthias*. This study suggests that the northern North Sea represents an important foraging area during the gestation, pupping and the early life history of the spiny dogfish, and may represent a potential nursery area for this endangered species. Protecting pregnant females and juvenile sharks that are vulnerable to fishing is imperative. Fisheries managers should therefore consider limiting fishing activity within the northern North Sea, possibly via the introduction of closed seasons corresponding with the occurrence of gravid female and neonate/juvenile spiny dogfish north of Dogger Bank.

4.6 Conclusion

This study highlights the value of the lens as a host tissue for ecological investigation. Here, analysis and subsequent geographic assignment of muscle data alone would only identify the southern North Sea as a key foraging area, providing only a snapshot of relatively recent location of feeding and nutrient assimilation in this species. Conversely, examination of eye lens chemistry relating to different life history stages reveals ontogenetic shifts in foraging behaviour and habitat use of spiny dogfish. Obtaining this information via traditional tagging methods would be near impossible.

Chapter 5: Maternal foraging behaviour revealed from offspring eye lens chemistry: the role of the Celtic Sea as nursery grounds for the porbeagle shark (*Lamna nasus*).

This Chapter is a manuscript in preparation, to be submitted in April 2017. Written by Katie Quaeck, including feedback from Clive Trueman.

5.1 Abstract

Due to their elusive nature and general scarcity, studying the movements of pelagic sharks presents many challenges to ecologists. Sequentially formed, inert eye lenses serve as a life-long repository of chemical information relating to an individual's entire life history, including a "pre-birth" tissue formed in utero. Analysis of eye lenses therefore allows reconstruction of the isotopic expression of maternal foraging behaviour from offspring tissue. Here the lens chemistry of 51 porbeagle sharks (*Lamna nasus*) is examined and the findings discussed in relation to maternal foraging, and associated management and conservation implications.

Isotopic data recovered from sequentially formed porbeagle eye lenses indicates that the mothers of juveniles and sub-adults in this region demonstrate high variability in foraging behaviour, reflecting foraging across a wide geographical area. The Celtic Sea nursery area may therefore represent a critical habitat for the species, and thus is important for the conservation of the northeast Atlantic porbeagle population.

5.2 Introduction

Studying the individual behaviour of pelagic sharks presents many challenges to fisheries researchers, due to their elusive nature, their potential for large-scale movements, the logistical challenges of working in the open ocean environment, and the general scarcity of high trophic level predators (Grubbs, 2010; MacKenzie *et al.* 2011; Trueman *et al.* 2012; McMahon *et al.* 2013).

The porbeagle shark (*Lamna nasus*) is a cold-temperate, fast-swimming pelagic shark, considered one of the top marine predators in the North Atlantic and southern hemisphere (Francis *et al*. 2008; Pade *et al*. 2009). A member of the Lamnidae family, porbeagle are known to thermoregulate, and occur in waters ranging from 2-23°C (Campana & Joyce, 2004). Its relatively slow growth rate, low fecundity and late maturity make this species, like many other pelagic sharks, vulnerable to over-fishing. Prized for its meat and fins, porbeagle sharks have been caught by targeted and non-targeted fisheries in the Northeast Atlantic since the 1930s (Campana *et al*. 2008). Norwegian and Faroese fleets heavily fished the species north of the British Isles (Aasen 1963), and landings initially peaked at 3,884 t in 1993 (DFO, 2005). Upon the reopening of the fishery following World War II in 1947, 6,000 tonnes of porbeagle sharks were taken by Norwegian vessels, however a steady fall in landings was observed to 1,900 t in 1960 (DFO, 2005). The collapse of the northeast Atlantic fishery resulted in the displacement of Norwegian and Faroese fishing efforts to the western north Atlantic.

Directed porbeagle fisheries were opened by French and Spanish longliners in the 1970s, however a similar decline in landings from the Celtic Sea and the Bay of Biscay was documented over the following years, from 1,092 tonnes in late 1970s to 300-400 tonnes in the late 1990s (DFO, 2005). Porbeagle sharks were also opportunistically fished by Spanish vessels at this time although landings appear to vary seasonally (Mejuto, 1985; Lallemand-Lemoine, 1991). More recently, longliners operational in the Bay of Biscay, targeting blue sharks (*Prionace glauca*), landed ~30 tonnes of porbeagle (and some shortfin mako, *Isurus oxyrunchus*) between 1998 and 2000.

Porbeagle are now listed as “Critically Endangered” in the northeast Atlantic by the International Union for Conservation of Nature (IUCN), and the European Commission introduced a zero total allowable catch (TAC) in EU waters in 2010 (Bendall *et al*. 2014). Despite their conservation status, these sharks still appear as incidental bycatch in gillnet fisheries operating in the Celtic Sea.

Juvenile porbeagle sharks occur sporadically and seasonally in the Celtic Sea and the western approaches to the English Channel, however mature individuals are

less frequently encountered (Bendall *et al*. 2012). Analysis of catch length data from French vessels lead Hennache & Jung (2010) to propose that Saint Georges Channel is a likely nursery area for porbeagle in the northeast Atlantic (length <170cm for 90% of catches, <125cm for 25%). Assuming this deduction is correct, the relationship between nursery area and foraging grounds remains poorly understood: we do not know whether this nursery serves a localized UK slope foraging population, or the entire northeast Atlantic porbeagle stock.

Recent tracking via pop-up satellite archival tagging (PSATs) allowed the reconstruction of the movements of sub-adult and adult porbeagle sharks caught along the Bay of Biscay shelf break (Biais *et al*. 2017). The study revealed similar migration patterns for nine tagged sharks, with individuals moving northward away from the Bay during late summer, returning in the following spring, providing some evidence of site fidelity following large-scale forays >2000km (Biais *et al*. 2017). The movements reported by Biais *et al*. (2017) are also consistent with those reported for porbeagle tagged elsewhere in the Northeast Atlantic (Pade *et al*. 2009; Saunders *et al*. 2011), providing evidence for complex spatial dynamics, incorporating wide-scale latitudinal movements through pelagic and coastal regions, resulting in exposure to variable fishing pressures. While, satellite tagging has revolutionised spatial ecology of large migratory animals (Block *et al.* 2011), the equipment costs and high failure rate often results in poor coverage, limited individual sample numbers (Trueman *et al*. 2012) and requires substantial financial investment. Moreover, tagging juveniles with the aim of studying their movements into mature life history is near impossible, as satellite tag technology rarely allows tracking over multiple years (Hamady *et al*. 2014).

More detailed knowledge of the movements of porbeagle is needed to limit fisheries interactions and reduce the risk of bycatch mortality. In particular, understanding the reason for the species' sporadic occurrence in the Celtic Sea, and juvenile behaviour has the potential to aid the management and conservation of northeast Atlantic porbeagle, providing further ecological information where data are currently lacking.

Inert, incrementally grown tissues provide an alternative technique to study ecology retrospectively, recording and preserving chemical information relating to the spatial and trophic dynamics of the individual, throughout life history (Cailliet *et al*. 2004). The stable carbon isotope composition of organic tissues reflects the carbon isotope signature at the base of the food web. Carbon isotope fractionation is controlled by temperature, which impacts upon the local phytoplankton community (e.g. dominant species, growth rate, geometry, cell size etc.) and the concentration of dissolved CO_2, driving spatial trends in baseline carbon isotope composition (Wong & Sackett, 1978; Fry & Wainright, 1991; Francois *et al*. 1993; Goericke *et al*. 1993; Bidigare *et al*. 1997; Popp *et al.* 1998; Popp *et al*. 1999; Hofmann *et al.* 2000; Maranon, 2009; Lara *et al*. 2010; Ngochera & Bootsma, 2011).

This chemical signature is subsequently incorporated into the tissues of consumers, subject to trophic enrichment (~1‰, per trophic level (DeNiro & Epstein, 1978; DeNiro & Epstein, 1981; Peterson & Fry, 1987)), which is attributed to the reaction kinetics that leave consumer tissues enriched in the heavier isotope, relative to the prey. Similarly, $\delta^{15}N$ values vary spatially, with baseline variability primarily driven by nitrification-denitification reactions, and the relative proportion of newly-fixed compared to remineralised nitrogen assimilated into primary production (Graham *et al*. 2010). The trophic enrichment of nitrogen isotopes is around ~3‰ per trophic level (DeNiro & Epstein, 1978; DeNiro & Epstein, 1981; Peterson & Fry, 1987), and an ontogenetic step-wise increase in $\delta^{15}N$ values is commonly observed in marine organisms, where feeding interactions are strongly driven by individual body size. Thus, nitrogen isotope composition is commonly used to study trophic dynamics.

Via analysis of sequentially formed eye lenses, the isotopic expression of juvenile behaviour from individual porbeagle that appear as bycatch in the western English Channel is reconstructed. The inert incrementally grown eye lens serves as a life-long log of chemical information relating to the individual's entire life history, including "pre-birth" tissue formed *in utero*, reflecting maternal foraging. Isotopic life history traits are examined in order to establish whether common trends are recorded within eye lens tissue of different sharks. This data is also interpreted with respect to foraging patters (e.g. onshore vs. offshore feeding).

The possibility that adult females from a wide area pup in the English Channel is also examined, and discussed in the light of the population's vulnerability to fishing activity and changes in ocean regimes.

5.3 Materials & Methods

Lamna nasus (n=50) lenses and associated body size data (total length measurements) were collected from sharks by-caught in a commercial gill-net fishery (targeting hake, pollock, ling, haddock, saithe and cod) in the Celtic Sea between 2011 and 2014, and landed under dispensation in association with the Neptune Scientific Fishery (Cefas/Defra). An additional sample was obtained from a single individual caught off the Faroe Islands, donated by a fisherman in 2014. One eye lens was extracted from each of the 51 sharks by making an incision along the length of the cornea, allowing the lens to be removed using forceps. Once excised, the diameter at the equator of each lens was measured to the nearest 0.25mm using callipers. All lens samples were stored at -20°C prior to processing. Lenses were subsampled using the technique developed by Parry (2003). Sequential laminae were then removed using a scalpel and fine-tipped forceps (Wallace *et al*. 2014). Tissue was peeled from pole to pole, and the lens diameter following each subsequent peel was re-measured. In an attempt to standardise laminae depth, the thinnest layer of lens tissue possible was removed during each peel. This process was repeated until no further layers of tissue could be removed, and the entire lens, from outer cortex to nucleus, had undergone delamination. Individual laminae were stored in Eppendorf tubes and frozen for 12 hours, prior to lyophilisation. Dried lens tissue was homogenised, weighed to ~0.5mg, and stored in tin capsules in preparation for stable isotope analysis.

All samples were analysed at the NERC Life Sciences Mass Spectrometry Facility in East Kilbride, using a Pyrocube Elemental Analyzer (2013, Elementar, Hanau, Germany) and Delta XP (Thermo Electron) mass spectrometer (2003). In-house standards were analysed every 10 samples to allow identification of any instrument drift. Experimental precision was 0.14‰ for carbon and 0.13‰ for nitrogen (standard deviation for replicate standards).

5.4 Results

The relationship between total length (TL) and lens diameter is linear for porbeagle sharks (*Lamna nasus*) (Figure 5.1.). The corresponding growth equation is represented by:

$$y = -3.71\ (\pm 1.28) + 0.19\ (\pm 0.01)\ x \qquad \text{(eq. 5.1)}$$

Where y represents the lens diameter (mm), and x represents the total length (mm). This equation was applied in order to back-calculate the estimated total length corresponding to each layer of lens tissue, using the diameter measurements recorded following each subsequent delamination stage. A size-referenced ontogenetic series was subsequently produced, per fish (e.g. Figure 5.5). The number of laminae removed per lens is ultimately controlled by the lens size and relative hydration. Here, 4-14 layers of lens tissue were extracted per specimen.

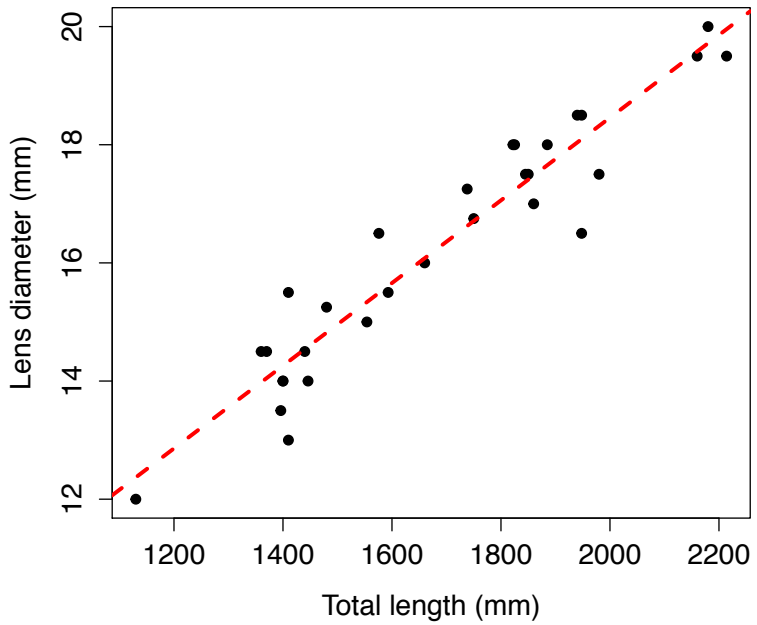

Figure 5.1 - The relationship between total length (TL) and lens diameter for the porbeagle shark, *Lamna nasus* (n= 30, $r^2 = 0.90$, p = <0.001).

Lens data grouped into individual 0.5mm diameter bins (corresponding TL reported) were normalised, by subtracting the isotopic composition of each sample from the global average of all sharks, allowing comparison of common

isotopic traits with increasing lens diameter. The variance of each size class is presented as a boxplot in Figure 5.2. Figure 5.2 reveals that both carbon and nitrogen isotope variability decreases with increasing distance from the nucleus, with a sharp decrease in variability in size bin with a corresponding back-calculated total length exceeding 1000mm.

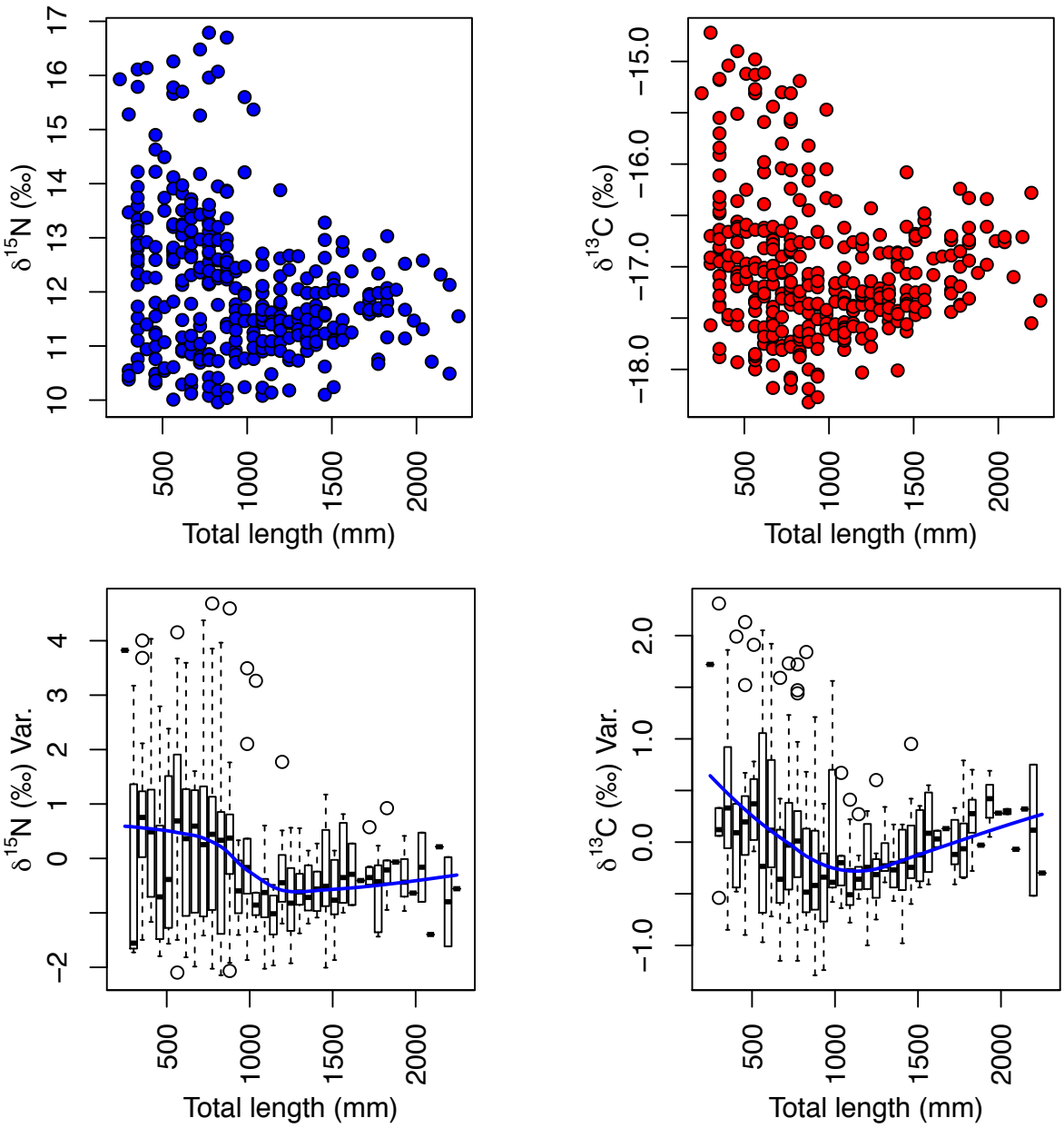

Figure 5.2 – Distribution of absolute (upper pane) and normalised (lower pane) $\delta^{13}C$ and $\delta^{15}N$ of lens samples from porbeagle (*Lamna nasus*) for sequential 0.5mm diameter bins. Isotopic variance is plotted against the corresponding back-calculated total length at time of tissue formation. Blue lines represent loess smoothing.

Porbeagle size-at-birth is estimated at 600-900 mm total length (TL) (Aasen, 1963; Jensen *et al*. 2002). 600 mm therefore represents the conservative cut-off for tissue formed pre-birth. Increased isotopic variability in the pre-birth portion of the lens is reflected in Figure 5.3, demonstrating that lens tissue reflecting maternal foraging records a greater range in both carbon and nitrogen isotope values, relative to tissue formed post-partum, representing exogenous feeding.

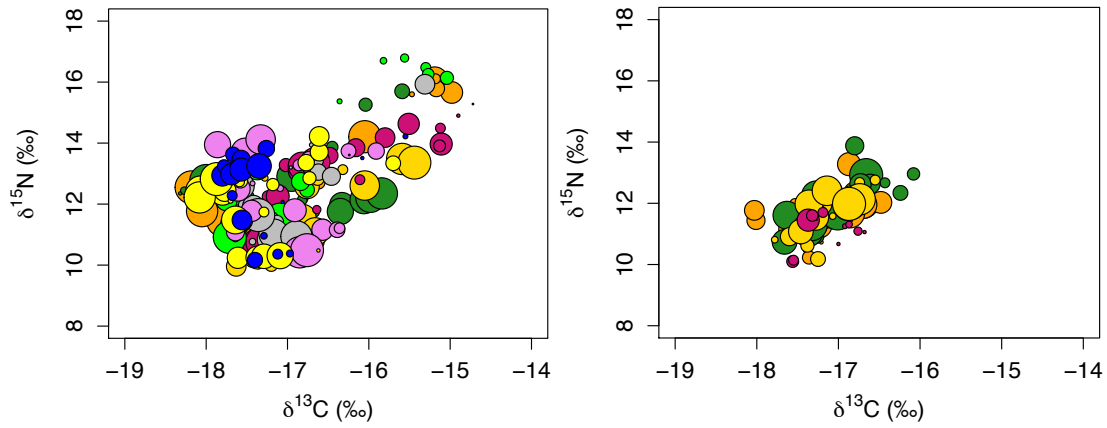

Figure 5.3 – Stable carbon and nitrogen isotope variability of sequentially sampled porbeagle shark (*Lamna nasus*) eye lenses (n = 670), divided into tissue formed pre-birth (left) and post-partum (right). Symbol size represents relative total length of individual sharks at the time of tissue formation, and symbol colour reflects shark ID (n = 51).

A low-resolution comparison of lens tissue isotope composition was conducted by separating lens tissue into 4 distinct categories representing tissue formed pre-birth, and during juvenile, sub-adult and adult life history (Figure 5.4). Tissue was assigned to these groups according to the back-calculated total length estimates associated with each sample. Male and female porbegale sharks attain maturity at ~190 cm and ~220 cm, respectively (Hennache & Jung ,2010), and these size estimates represent the lower threshold for lens tissue formed during adult life history (n = 6). Attaining lengths of 170cm TL at roughly 5-6 years (Natanson *et al*. 2002), lens samples with associated back-calculated TL estimates that exceed 170cm, but are less than the aforementioned size-at-maturity estimates, are assigned to the sub-adult size category (n = 11). Lens tissue samples with associated total length estimates exceeding 60 cm, but less than 170cm are therefore assigned to the juvenile size category (n = 95). Given that porbeagle size-at-birth is estimated at 600-900 mm total length (TL) (Aasen, 1963; Jensen *et al*. 2002), 600 mm represents the conservative cut-off for tissue formed pre-birth

(n = 228). Fork length (FL) measurements are converted here to total length (TL) using the ratio reported by Campana *et al*. (2013).

The isotopic composition of tissue formed during pre-birth, juvenile, sub-adult and adult life history differs significantly (repeated measures one-way ANOVA, $F_{3, 332} = 3.19$, $p = 0.02$, and $F_{3, 332} = 5.23$, $p < 0.001$, for carbon and nitrogen, respectively). Figure 5.3 highlights that the isotopic composition of lens tissue formed pre-birth is more variable than lens tissue formed post-partum, (mean $\delta^{13}C$ = -16.99‰ ± 0.78, -17.17‰ ± 0.36, -16.77‰ ± 0.30, -16.85‰ ± 0.43, mean $\delta^{15}N$= 12.35‰ ± 1.51, 11.58‰ ± 0.70, 11.87‰ ± 0.56, 11.59‰ ± 0.43, for pre-birth, juvenile, sub-adult and mature size categories, respectively). Moreover, the highest mean $\delta^{15}N$ value is associated with the pre-birth portion of the lens, followed by juvenile and adult size categories. Conversely, the highest mean $\delta^{13}C$ value is associated with the adult portion of the lens, followed by the pre-birth and juvenile size categories (Figure 5.4).

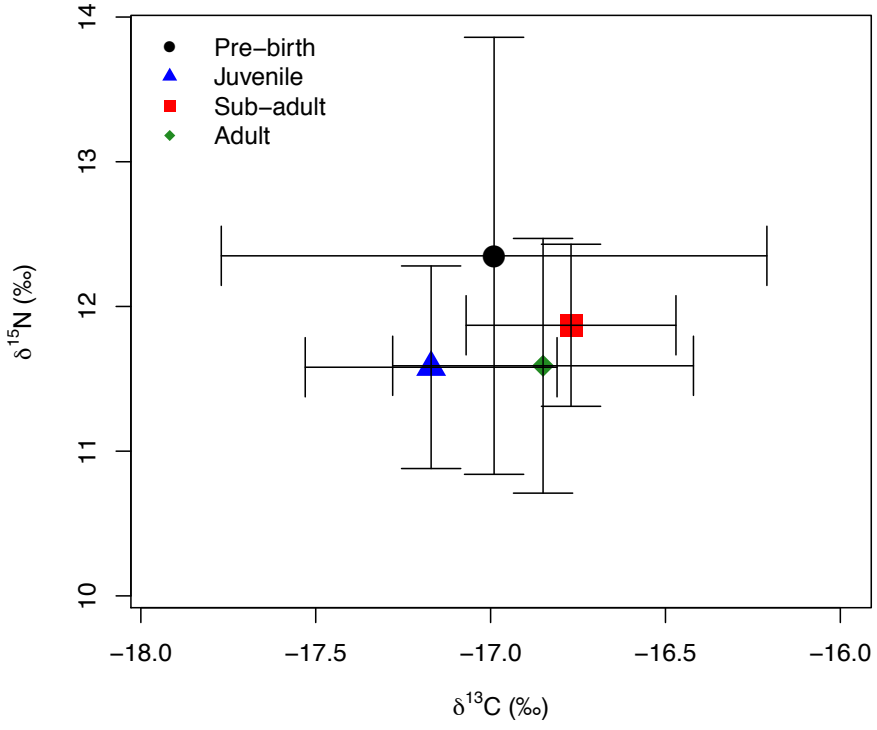

Figure 5.4 - Comparison of the isotopic composition of porbeagle shark (*Lamna nasus*) eye lens samples representative of pre-birth, early juvenile and sub-adult life history. Lens tissue is categorised according to corresponding diameter measurement; pre-birth (≤9 mm), juvenile (9.25 - 15.75 mm), sub-adult (16-17.75 mm) and adult (≥18 mm). Error bars display standard deviations.

5.4.1 Isotopic life history data

To test for the (dis)similarity in the isotopic composition of the pre-birth lens tissue of individual sharks, a loess smooth function was first applied to all samples with an associated diameter ≥3mm, ≤10mm, and the resulting data analysed by time-series cluster analysis using the Euclidean distance method. Due to insufficient data, 3 sharks were omitted from the cluster analysis (ID #14, 44 and 51). For carbon, two clusters were identified. Cluster 1 included 29 of the remaining 47 individuals. Lens transects originating from these individuals display relatively low $\delta^{13}C$ values in the pre-birth portion of the lens, and a shallow decreasing trend observed with increasing distance from the lens nucleus. Conversely, cluster 2 includes 18 sharks whose pre-birth lens chemistry is characterised by elevated $\delta^{13}C$ values (relative to cluster 1 individuals) and a sharp decreasing trend with increasing distance from the nucleus. In the case of nitrogen, three clusters were identified, characterised by (1) high $\delta^{15}N$ values which experience a sharp decreasing trend with increasing distance from the lens nucleus (n=3), (2) relatively low and stable, or steadily increasing, $\delta^{15}N$ values with increasing distance from lens nucleus (n=17), and (3) intermediate and steadily increasing $\delta^{15}N$ values with increasing distance from lens nucleus (n=27). Table 5.1 summarises individuals assigned to each of the carbon and nitrogen clusters.

Table 5.1 – Summary of individual sharks assigned to carbon (2) and nitrogen (3) clusters, identified by time-series cluster analysis of isotope values, following application of a loess smooth function, using the Euclidean distance method

Shark ID	Carbon Cluster	Nitrogen Cluster	Shark ID	Carbon Cluster	Nitrogen Cluster
1	2	1	**30**	2	1
2	2	2	**31**	1	3
3	2	1	**32**	1	2
4	1	3	**33**	1	2
5	1	2	**34**	1	3
6	1	3	**35**	1	2
8	1	2	**36**	2	3
9	1	3	**37**	1	3
10	1	2	**39**	1	2
11	1	3	**40**	2	2
12	1	3	**41**	1	3
13	2	3	**42**	2	3
14	NA	NA	**43**	1	3
15	1	2	**44**	NA	NA
16	2	3	**45**	2	2
17	2	3	**46**	1	3
18	1	3	**47**	1	2
19	1	2	**48**	1	3
20	1	2	**49**	2	3
22	2	3	**50**	1	3
24	2	3	**51**	NA	NA
25	2	3	**52**	1	3
26	2	3	**100**	1	2
28	1	2	**666**	2	3
29	1	2	**999**	1	3

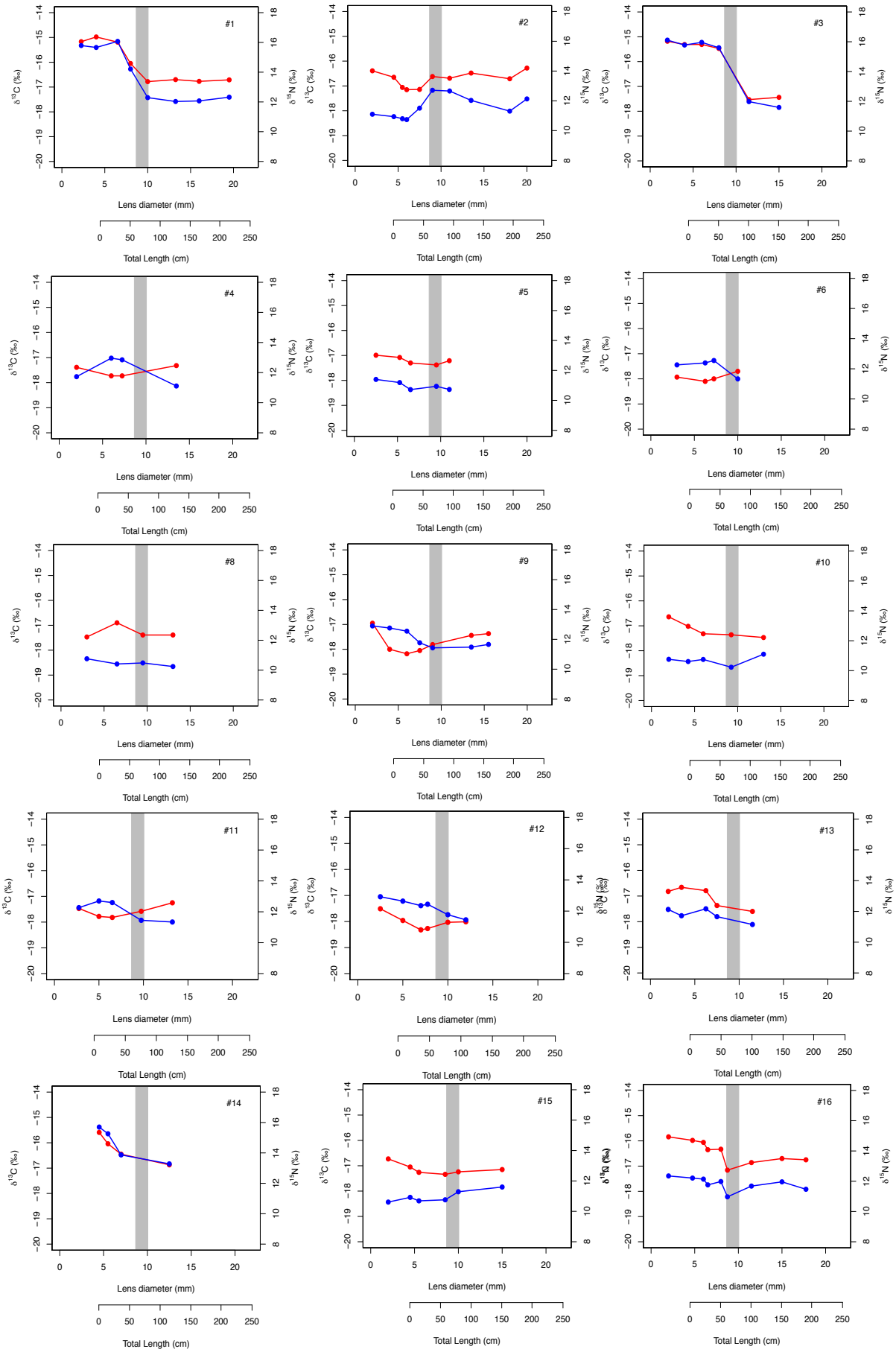
#1
#2
#3
#4
#5
#6
#8
#9
#10
#11
#12
#13
#14
#15
#16
δ13C (‰)
δ15N (‰)
Lens diameter (mm)
Total Length (cm)

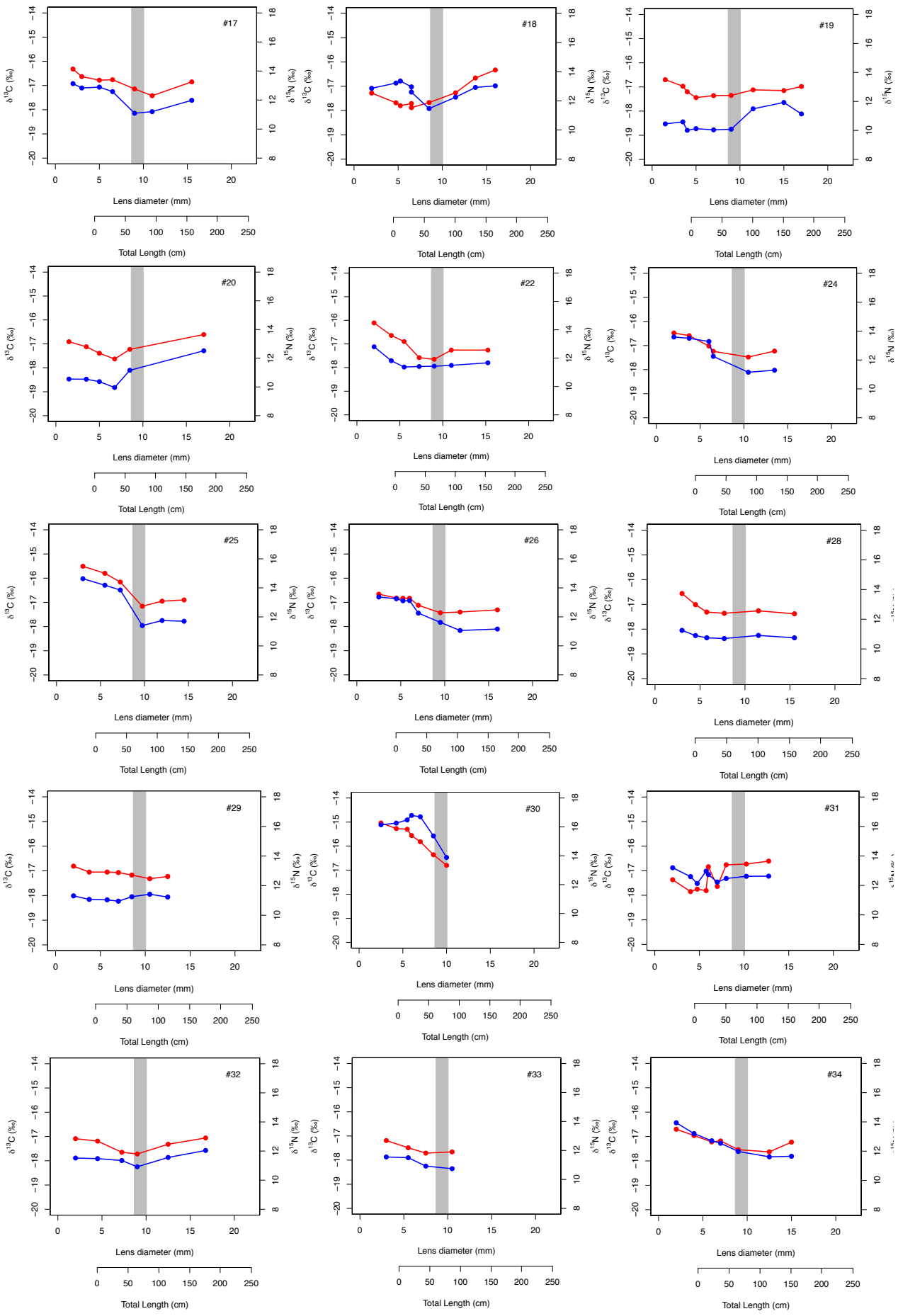
#17
#18
#19
#20
#22
#24
#25
#26
#28
#29
#30
#31
#32
#33
#34
δ13C (‰)
δ15N (‰)
Lens diameter (mm)
Total Length (cm)

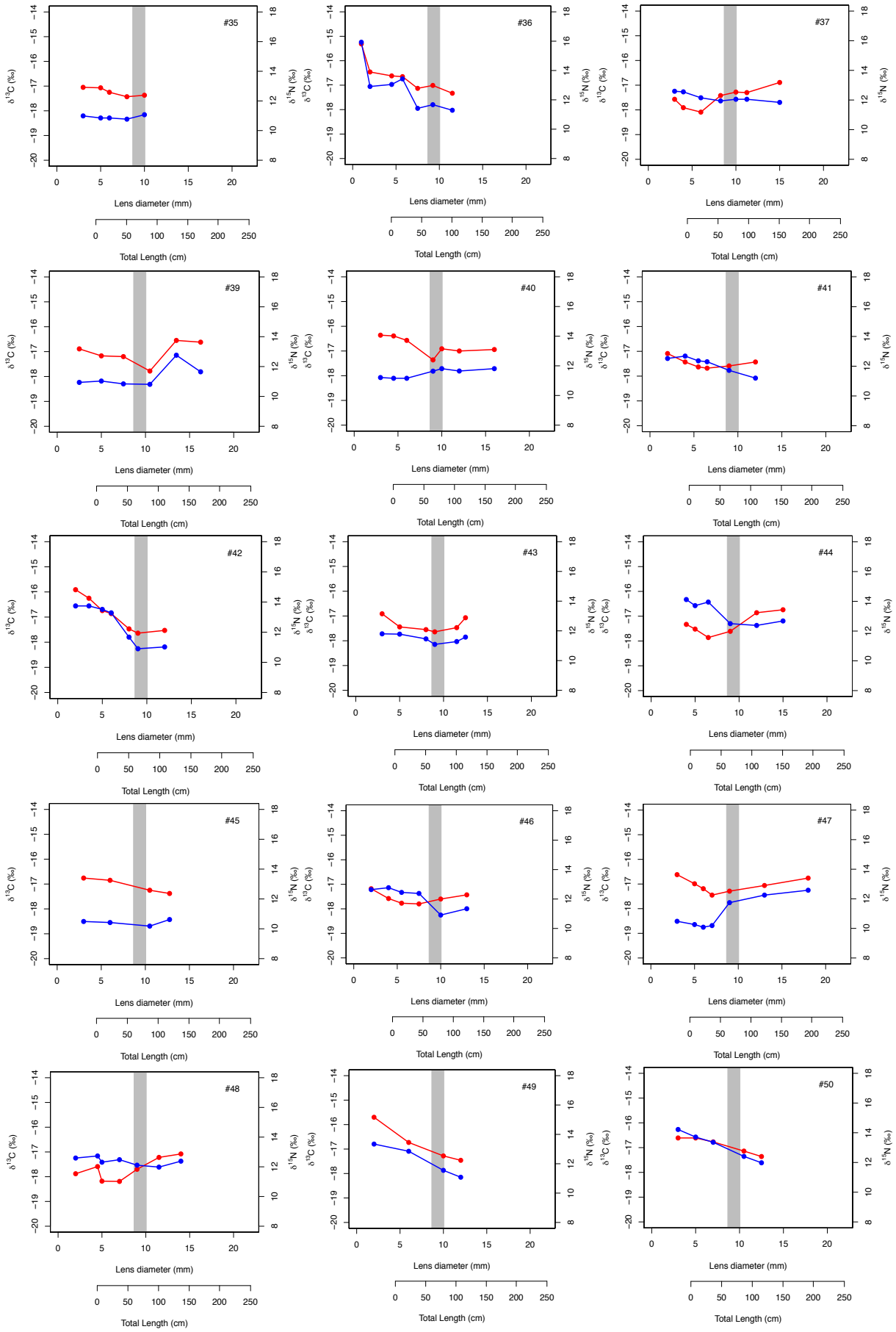
#35
#36
#37
#39
#40
#41
#42
#43
#44
#45
#46
#47
#48
#49
#50
δ13C (‰)
δ15N (‰)
Lens diameter (mm)
Total Length (cm)

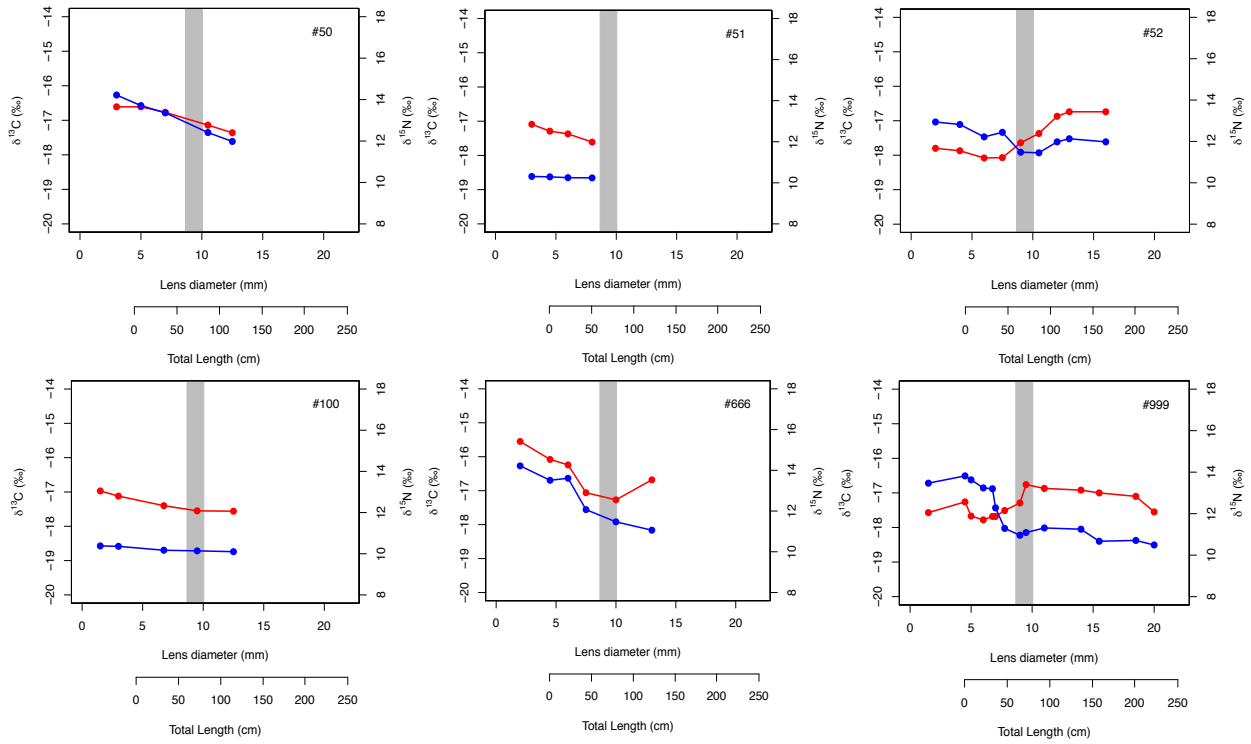

Figure 5.5 –Across-lens transects detailing $\delta^{13}C$ (red) and $\delta^{15}N$ (blue) variability of 51 porbeagle sharks (*Lamna nasus*). Grey bars represent *L. nasus* size range at birth (60-90 cm) (Aasen, 1963; Jensen *et al*. 2002).

5.5 Discussion

Analysis of the chemical composition of 51 porbegale eye lenses reveals that tissue formed pre-birth, relating to maternal foraging, is highly variable between individual sharks (Figure 5.3).

The large range in $\delta^{13}C$ values (~4‰) associated with pre-birth tissue is unlikely explained by foraging in the Celtic Sea alone (Trueman *et al*. 2016), suggesting that the mothers of the sharks sampled during this study were foraging either oceanically, or across a wide range of latitudes during the period of yolk sac formation. Figure 5.6 supports this deduction, highlighting that a 4‰ range in carbon isotope values represents the maximum range that northeast Atlantic porbeagle sharks are likely to be exposed to, given their assumed distribution between the Azores and waters north of Iceland. This observation is also consistent with the apparent absence of large, mature female sharks in the waters of the western approaches to the English Channel. Relatively negative $\delta^{13}C$ values

(~-18‰) recorded in embryonic lens tissue may reflect northerly oceanic foraging, whereas elevated $\delta^{13}C$ values (~-14‰) are more likely to reflect nutrient assimilation at lower latitudes or further offshore, toward the mid-Atlantic ridge (Lorrain *et al*. 2009).

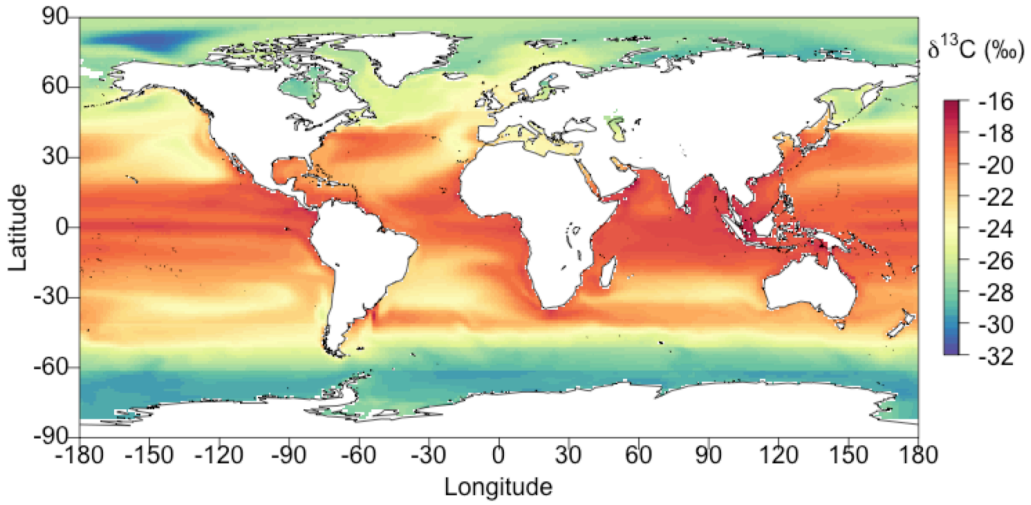

Figure 5.6 - Modelled global annual average phytoplankton $\delta^{13}C$ values (Magozzi *et al*. *in press*).

This high between-individual variability in pre-birth lens isotope ratios can be examined in more detail in Figure 5.4. Cluster analysis of the high-resolution pre-birth isotope data (loess smoother applied) identifies that individual sharks can be categorised into 2 clusters according to trends in carbon isotope variability.

Nitrogen isotope values at the base of the food web also vary spatially. Influenced primarily by nitrogen source, $\delta^{15}N$ values display strong onshore-offshore trends and, when incorporated into consumer tissues, are subject to increased trophic fractionation, relative to carbon. Separating the spatial and trophic components of nitrogen isotope values recorded in consumer tissues is challenging. However, with pre-birth tissues reflecting the feeding behaviour of mature females, we can assume that the difference in trophic level of these large sharks is negligible, and that the differences in $\delta^{15}N$ values are driven primarily by differences in foraging location, or the trophic level of prey items. The 3 nitrogen clusters identified suggest again that mothers of the sharks sampled were assimilating nutrients in regions characterised by very different baseline nitrogen isotope ratios, during the period of egg sac formation.

Our findings support those of Biais *et al*. (2017), who deduce that porbeagle satellite-tagged in the northeast Atlantic demonstrate complex spatial dynamics, incorporating wide-scale latitudinal movements and offshore forays beyond the continental shelf. Differences in pre-birth lens tissue isotope variability of sharks included in this study suggests that the English Channel harbors juvenile sharks whose mothers were exploiting resources from the full latitudinal range of the species within the north Atlantic. Northeast Atlantic porbeagle sharks are currently listed as critically endangered on the IUCN Red List, and protecting this subpopulation is therefore reliant upon safeguarding large females distributed across a wide area of the northeast Atlantic, potentially spanning national boundaries and management zones, posing a considerable management and conservation challenge.

The isotopic compositions of lens tissue formed during juvenile, sub-adult and adult life-history size categories, is less variable relative to tissue formed pre-birth. Tissue formed during juvenile life history spans a range of 2‰ (mean = -17.17‰ ± 0.36,). This reduced between-individual variability relative to tissue formed pre-birth therefore implies minimal movements during early life history, and the existence of a common nursery area, characterized by similar baseline isotope values. It has previously been proposed that the Saint Georges Channel region may be a nursery area for juvenile porbeagle sharks. The proximity of this area to the capture location of the sharks included in this study, and the known spring-summer residency period of large sharks in the Celtic Sea (Biais *et al*. 2017) provides additional anecdotal evidence in support of the existence of a Celtic Sea nursery.

Reduced variability is also associated with tissue formed during sub-adult life history, spanning a range of ~1‰ for carbon (mean = -16.77‰ ± 0.30), possibly reflecting limited latitudinal movements in sub-adult sharks. Due to the low number of lens samples reflecting adult life history, it is impossible to confidently draw any conclusions relating to the movements of mature(ing) sharks caught in the English Channel.

One important caveat associated with lens-based methodologies centres on the growth dynamics of the tissue itself. As an individual matures and somatic growth slows, so does the accretion of lens proteins. Thus, whilst the lens provides as a high-resolution record of chemical information relating to early life history, the temporal resolution of this technique is reduced in older individuals. This must be considered when comparing lens tissue formed during different periods in the organism's development, as reduced variability in isotopic composition may simply be a reflection of the increased incorporation period, thus isotopic variability associated with large-scale foraging may be averaged out within a slow-growing tissue. However, examination of the individual across-lens transects reveals, in the case of individuals assigned to nitrogen cluster 1, a sharp decline in $\delta^{15}N$ values associated with the size of birth, and in the case of carbon cluster 2 individuals, a sharp decline in $\delta^{13}C$ values at birth. This phenomenon is unlikely explained by the masking of high-resolution isotope variability in a slower-growing tissue. We therefore infer that juvenile and sub-adult sharks are exposed to less extreme variations in baseline isotope values, suggesting that large-scale movements are limited during early life history. Moreover, identification of high inter-individual variability in the fast-growing portion of the lens can only be explained by differences in foraging location of mature females.

Reconstructing the movements of individual sharks via geographic assignment of ontogenetic lens tissue samples relies upon the existence of validated reference isotope maps, or isoscapes. Given that the isotopic values at the base of the food web are both spatially and temporally variable, measuring and monitoring this variability in the marine environment is logistically demanding and expensive. Thus, interpreting the exact movements of the individual sharks in question is beyond the scope of this study.

Having identified that the Celtic Sea serves as a nursery, and potential pupping ground, for the entire northeast Atlantic porbeagle population, safeguarding individuals within this area is of critical importance. Minimizing fishing mortality of juveniles in the nursery would serve to protect future generations of sharks, which would eventually leave the region and disperse across the species' geographical range. Similarly, reducing the by-catch of gravid females is also

essential, potentially increasing the numbers of neonates and juveniles in the nursery in the first instance, whilst also maintaining the mature cohort for future reproductive cycles. Moreover, changes in the physical and biological suitability of this area, driven by changing oceanic regimes and habitat destruction, may have a catastrophic impact upon the entire northeast Atlantic porbaegle stock. Thus, protecting sharks within region, and the habitat itself, may have wide-ranging benefits to the northeast Atlantic porbeagle stock, which is currently listed as critically endangered. Fisheries managers should therefore consider re-addressing the regulations associated with commercial gill-netting in the Celtic Sea, possibly limiting fishing activity during the proposed parturition period between May and July (Biais *et al*. 2017) in order to minimize by-catch of gravid females and small juveniles.

5.6 Conclusion

Porbeagle sharks appear commonly (yet seasonally) as by-catch in the gill nets of commercial fishermen in the Celtic Sea and western approaches to the English Channel, an area previously identified as a possible nursery for juveniles of the species. Isotopic data recovered from sequentially formed porbeagle eye lenses indicates that the mothers of juveniles and sub-adults in this region demonstrate high variability in foraging behaviour. Attracting mothers from a wide geographical area, the Celtic Sea nursery area is therefore likely to be important for the conservation of the northeast Atlantic porbeagle population, and mitigating discarding of sharks in the area should be a priority to fisheries managers.

Chapter 6: The use of fish lens isotopes and isotopic life histories to test a migratory hypothesis: Ontogenetic movement of the black scabbardfish, *Aphanopus carbo*.

This Chapter is a manuscript in preparation, to be submitted in April 2017. Written by Katie Quaeck, including feedback from Clive Trueman.

6.1 Abstract

Studying the movements of highly migratory deep-water species presents logistical challenges associated with the inaccessible nature of the environment, and the sensitivity of the organisms to being recovered from depth. Inert, incrementally grown tissues provide an ontogenetic record of information relating to the ecology of an individual, which can be studied retrospectively. Here, the chemistry of organic, sequentially formed black scabbardfish (*Aphanopus carbo*) eye lenses is examined in order to address the species' proposed migration hypothesis.

Black scabbardfish are believed to spawn in the waters surrounding Madeira and the Canary Isles, migrating northward to the sub-adult feeding grounds west of the British Isles before moving southward again toward the coast of continental Portugal where they mature, prior to their return to the southern spawning grounds. Stable isotope analysis of eye lens tissue from black scabbardfish caught in the Rockall Trough and off the coast of Sesimbra (Portugal) revealed that lens tissue formed during early life history is isotopically comparable between the capture locations, and implies feeding in relatively warm, shallow waters. All sampled individuals shared common isotopic life histories, consistent with a single migratory route. At sizes equivalent to the range observed in the Rockall Trough, *A. carbo* lens tissue records a minor, but recognisable isotopic shift, consistent with movement into a new and isotopically distinct feeding area. These findings provide further evidence that support the ontogenetic migration theory of black scabbardfish.

6.2 Introduction

In recent decades the biological resources of coastal waters have diminished globally, and as demand continues to rise, fisheries have responded by expanding offshore and

into deeper waters. Thus, deep-sea fisheries are now exploiting one of the last remaining refuges for commercial species (Morato *et al*. 2006). Changes in ecosystem structure resulting from over-exploitation and destructive fishing techniques are of grave concern (Devine *et al*. 2006), and as fishing continues to pose a major conservation threat (Cheung *et al.* 2005), effective counter-measures are required in order to effectively manage and conserve deep-water stocks (Clark *et al*. 2016). In order to achieve this, it is essential that fisheries scientists understand the life histories and ecology of targeted and by-catch species. However, obtaining information pertaining to deep-water species, particularly relating to individual movements and population connectivity, poses a logistical challenge as the majority of traditional and emerging techniques, such as static or data recording tags, are generally unsuitable. The continental slopes in the northern hemisphere form largely continuous, north-south running features, spanning national boundaries and management zones. This essentially produces an expansive ecosystem characterised by similar physical and biological properties, increasing the potential for large-scale, largely latitudinal, movements of slope fishes. Highly migratory species present additional management complexities, moving through and across different management areas, demanding a cooperative approach in order to conserve fish stocks.

The black scabbardfish is a bathypelagic species with a wide distribution throughout the North Atlantic Ocean. Occurring between 30 and 70°N, it's depth distribution varies according to region; in the northeast Atlantic, *Aphanopus carbo* occur from 200m in the northern reaches of its range (Nakamura & Parin, 1993; Kelly *et al*. 1998) to 2300m around the waters of the Canary Islands (Pajuelo *et al*. 2008), more commonly appearing between 400-1400m west of the British Isles (Ehrich, 1983; Allain *et al*. 2003), and from 800m to 1300m and 1800m in the waters off Madeira and mainland Portugal, respectively (Martins *et al*. 1987; Morales-Nin & Sena-Carvalho 1996). Juvenile *A. carbo* are mesopelagic and adults are bathypelagic, generally associated with demersal fish community (Clarke *et al*. 2016). *A. carbo* occur within a range of habitats, from gentle sedimentary slopes, to steep underwater rises and canyons (Martins *et al*. 1987; ICES, 2012). *A. carbo* is an economically important deep-water fish species. The Madeira black scabbard fishery dates back centuries, and artisanal drifting longliners still operate commercially within the

CECAF area (Fishery Committee for the Eastern Central Atlantic) (Bordalo-Machado *et al*. 2009). An artisanal bottom longlining fleet also targets black scabbardfish within ICES Subarea IXa, off mainland Portugal (Bordalo-Machado *et al*. 2009; ICES, 2012). Moreover, a deep-sea mixed-species trawl fishery, dominated by French and Spanish vessels, operates west of the British Isles, landing approximately 2 million individuals annually (Nakamura & Parin, 1993; ICES, 2012; Clarke *et al*. 2016), ~3000 tons per year landed from ICES Division 5.b. Subareas 6, 7 and 12, between 2009 and 2014 (Clarke *et al*. 2016).

Black scabbardfish are well adapted for fast swimming and efficient predation, possessing a narrow elongated body and pointed head, a long dorsal fin, large eyes and a terminal mouth equipped with sharp fang-like teeth. Based on stomach content analysis, the diet of this top predator is believed to include a wide range of prey items (Zilanov & Shepel, 1975; Nakamura & Parin, 1993; Ribeiro Santos *et al*. 2013), including various teleost species, cephalopods and some crustacea (Du Buit, 1978; Mauchline & Gordon, 1984; Howell *et al*. 2009; Ribeiro Santos *et al*. 2013). Differences in diet according to location have also been documented, and attributed to the seasonal availability of pelagic and mesopelagic fish, such as blue whiting (*Micromesistius poutassou).* However, detailed studies of black scabbardfish diet are scarce, and ultimately complicated by the logistical difficulties associated with sample collection, and the problem of stomach eversion (Ribeiro Santos *et al*. 2013).

Despite numerous studies spanning several decades, the stock structure, life cycle and movements of black scabbardfish remains in question (Farias *et al*. 2013). Combined genetic and otolith microchemical analyses suggest the presence of a single genetically mixed population (Longmore *et al*. 2014) in the Northeast Atlantic, which undertakes a large-scale clockwise ontogenetic migration between the northern and southern reaches of its distribution. Spawning is believed to occur in the waters surrounding Madeira (Morales-Nin & Sena-Carvalho, 1996; Figueiredo *et al*. 2003; Neves *et al*. 2009; Ribeiro Santos *et al*. 2013), the Canary Islands (Pajuelo *et al*. 2008), and possibly further south (Perera, 2008). Black scabbardfish are iteroparous, and spawn in one single event (Pajuelo *et al.* 2008; Ribeiro Santos *et al*. 2013). A northward migration, postulated to involve larvae and juveniles up to ~600mm (Farias *et al*. 2013) is then believed to occur. Examination of research trawl survey

data from cruises conducted around the Rockall Trough by Marine Scotland Science reveals that the smallest *A. carbo* caught in the region measures 810mm (Table 6.1). Despite catching small specimens of other species (e.g. 3cm – *Coryphaenoides rupestris*), no *A. carbo* individuals measuring <800mm were recovered during 7 years of comparative annual surveys (Neat *et al.* 2010). *A. carbo* specimens caught in the Rockall Trough are generally immature, or are in an intermediate maturity stage (Kelly *et al*. 1998). They are also generally smaller (range = 810-1070mm, mean = 898 ± 89mm) than those caught off the coast of continental Portugal (range = 920-1195mm, mean = 1053 ± 68mm), and where individuals are of comparable size, the gonado-somatic index (GSI) is lower than that of individuals caught in Madeira waters (Ribeiro Santos *et al*. 2013). This evidence agrees with the findings of *Swan et al*. and supports the migratory hypothesis, suggesting that the black scabbardfish caught in the Rockall Trough are elsewhere during early life-history, and move from the region before reaching maturity (size at maturity (females) = 1000mm (Figuereido *et al.* 2003)).

Individuals are assumed to remain in northerly regions where they feed and grow, recruiting to the fisheries south of Iceland, around the Faroe Islands, and to the west of the British Isles at 2-3 years old (Farias *et al.* 2013). These fish then move southward toward continental Portugal, where they remain for a further few years and attain size at first maturity (Farias *et al.* 2013). However, spawners have not been observed off mainland Portugal (Swan *et al.* 2001; Bordalo-Machado *et al.* 2009) and individuals here display a lower GSI compared to fish caught in the waters surrounding Madeira (Neves *et al*. 2009). Upon leaving continental Portugal, it is believed that black scabbardfish move south towards Madeira and the Canary Islands, where spawning occurs in November and December (Farias *et al*. 2014).

Several methods have been employed in order to address and clarify *Aphanopus carbo* migration (Figueiredo *et al*. 2003; Swan *et al*. 2003; Pajuelo *et al*. 2008; Longmore *et al*. 2014), but tracking individuals throughout ontogeny is logistically challenging, and evidence supporting a single life history migratory trait shared by all individuals is circumstantial. Here, an emerging method is applied to test for consistent life history migratory traits between individuals based on comparisons of individual ontogenetic trends in stable isotope compositions (isotopic life history

traits). The vertebrae eye lens is an incrementally grown tissue formed of metabolically inert, sequentially deposited, protein-filled fiber cells (Bloemendal *et al*. 2004). Eye lens protein records the isotopic composition of body fluids during assimilation and growth, and sequential analyses allow the reconstruction of isotopic life histories for individual fish. This technique is applied in order to test whether individual *A. carbo* share a common isotopic life history trait consistent with the migratory hypotheses outlined above, and discuss findings in relation to an extensive dataset, characterising the isotopic niche (muscle tissue) of holocephali, teleosts and elasmobranchs in the Rockall Trough (Figure 6.1), allowing comparison with fish caught west of the British Isles, with those caught off the coast of Portugal (Sesimbra).

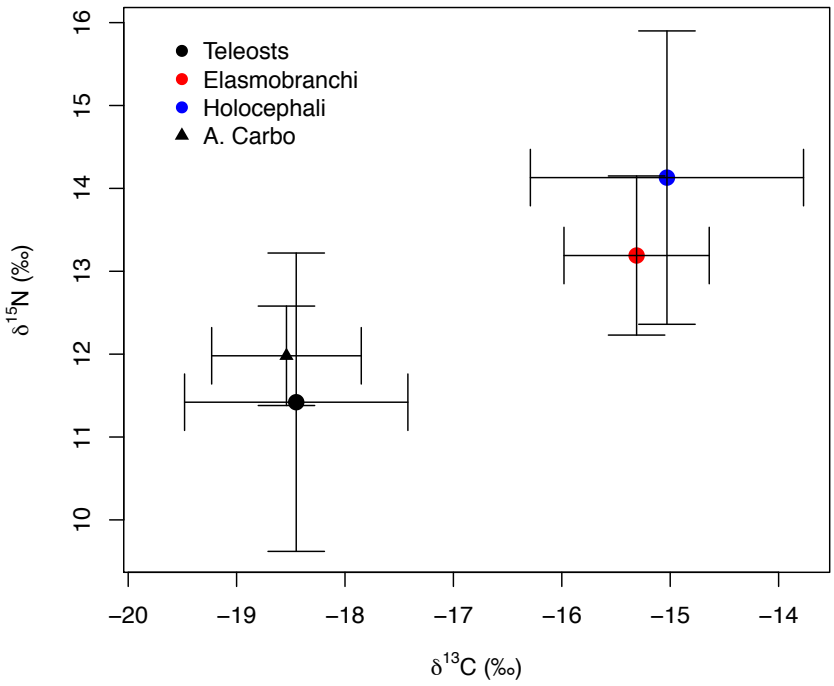

Figure 6.1 - Comparison of the isotopic composition of muscle tissue from teleosts (n=935), elasmobranchs (n=106) and holocephali (chimera) (n=49) sampled off the western coast of Scotland (Rockall Trough) during the 2006-2012 deep-water surveys onboard the MRV Scotia (Neat *et al*. 2010). Mean *Aphanopus carbo* muscle $\delta^{13}C$ and $\delta^{15}N$ values are also plotted. Error bars display standard deviations.

6.3 Materials and Methods

18 black scabbardfish were opportunistically sampled in October 2014 from commercial longliners operating ~30 miles off the coast of Sesimbra, Portugal. The total length of each individual was recorded, and one eye lens was extracted from

each specimen, via an incision made along the length of the cornea with a scalpel. This allowed the lens to be removed easily using forceps. Once excised, the diameter of each lens was measured at the equator, to the nearest 0.25mm, using callipers. Whole lenses were subsampled using the technique developed by Parry (2003). Sequential laminae were removed using a scalpel and fine-tipped forceps. Lens tissue was peeled from pole to pole, and the diameter re-measured following each subsequent peel. The thinnest layer of tissue possible was extracted during each peel, in an attempt to standardise laminae depth. The delamination process was repeated until no further layers could be removed from the lens. Individual laminae were stored in Eppendorf tubes and frozen overnight, prior to lyophilisation. Once dried, the tissue was homogenised, weighed (~0.5mg) and stored in tin capsules in preparation for analysis.

An additional 11 *A.carbo* specimens were obtained from the Rockall Trough during the 2012 deep-water survey onboard the MRV Scotia. Fish were caught using scientific dual-warp bottom trawls with rock-hopper ground gear. Lenses were excised and processed following the aforementioned protocol, however a resin embedding approach was used in order to subsample the lenses (methodology discussed extensively in Chapter 2). Only data from the lens nucleus and mid-lens region are included in this study.

Stable carbon and nitrogen isotope ratios of all samples were determined at OEA Laboratories Ltd. Laboratory standards were analysed every ~10 samples to examine instrument drift. Experimental precision was 0.19‰ for carbon and 0.29‰ for nitrogen (long-term standard deviation for replicates of in-house standard reference materials). Isotope ratios are expressed in δ notation (‰), relative to international standards of V-Pee dee belemnite and air for carbon and nitrogen, respectively.

6.4 Results

The relationship between total length (TL) and lens diameter is linear for *Aphanopus carbo* (Figure 6.2), and the corresponding growth equation is represented by:

$$y = -3.71\ (\pm 1.28) + 0.019\ (\pm 0.001)\ x \qquad \text{(eq. 6.1)}$$

Where y represents the lens diameter (mm), and x represents the total length (mm) of the fish. This equation was applied in order to allow back-calculation of the estimated total length associated with each layer of lens tissue, using the diameter measurements recorded following each subsequent delamination stage. Thus, a size-referenced ontogenetic series can be produced, per fish (Figure 6.4). Lens size and relative hydration ultimately controls the number of laminae removed. In this investigation, 7-13 layers of lens tissue were extracted per specimen.

Eye lens $\delta^{15}N$ values range from 7.16 to 18.19‰ (mean = 13.81 ± 2.49‰), and $\delta^{13}C$ values range from -20.68 to -16.44‰ (mean = -18.32 ± 0.98‰) in Portuguese-caught specimens. $\delta^{15}N$ values from Rockall-caught fish range from 8.50 to 18.34‰ (mean = 13.42 ± 2.92‰), and $\delta^{13}C$ values range from -20.49 to -17.66‰ (mean = -18.83 ± 0.79‰).

Table 6.1 – Isotopic (muscle) and morphometric data from 13 *Aphanopus carbo* specimens sampled during the MRV Scotia deep-water surveys (2006-2012).

Fish ID	**Length (mm)**	**Fishing depth (m)**	**$\delta^{15}N$**	**$\delta^{13}C$**	**CN ratio**
A	920	750	11.56	-18.59	3.37
B	950	750	12.26	-18.78	3.77
C	950	750	12.56	-20.22	4.73
D	1070	750	13.43	-19.77	4.82
E	860	1000	11.42	-18.06	3.20
F	910	1000	12.05	-17.99	3.25
G	810	1000	11.26	-18.10	3.25
H	850	1000	12.04	-18.16	3.26
I	790	1000	11.60	-18.20	3.27
J	780	1000	11.51	-18.39	3.28
K	990	1000	12.09	-18.25	3.28
L	980	1000	12.44	-18.04	3.29
M	810	1000	11.54	-18.44	3.33

A comparison of the mean isotopic composition of *Aphanopus carbo* lens tissue, from individuals caught in the waters of continental Portugal and west of the British Isles, formed during larval, early juvenile, sub-adult and adult life history was conducted. This comparison includes core (larval) data from all 18 specimens caught off Sesimbra, and 11 fish caught in the Rockall Trough. Core tissue was defined as samples with an associated lens diameter of 5mm or less. Samples with an associated diameter of 5.1-11.5mm and 11.6-15.5mm represent early juvenile (<800mm TL, corresponding to fish generally smaller than those recovered from the Rockall Trough) and sub-adult life history (corresponding to the size range of individuals caught at Rockall; ~800-1050mm TL), respectively, and samples with an associated lens diameter greater than 15.5mm were isolated to represent tissue formed during adult life history (>1050mm TL, corresponding to the size of individuals caught off the coast of continental Portugal). Fish caught at Rockall are generally smaller compared to those caught off Sesimbra, and none of the lenses measured >15.5mm in diameter. Contamination associated with the resin embedding technique (unknown at the time of processing) also necessitated that outer lens samples from Rockall caught fish were omitted from the data analysis. Thus, only samples formed during larval and early juvenile life history of Rockall-caught fish are included in the analysis. Multiple samples from the same individual, falling within a given size range, were pooled. The results of the comparison are presented in Table 6.2.

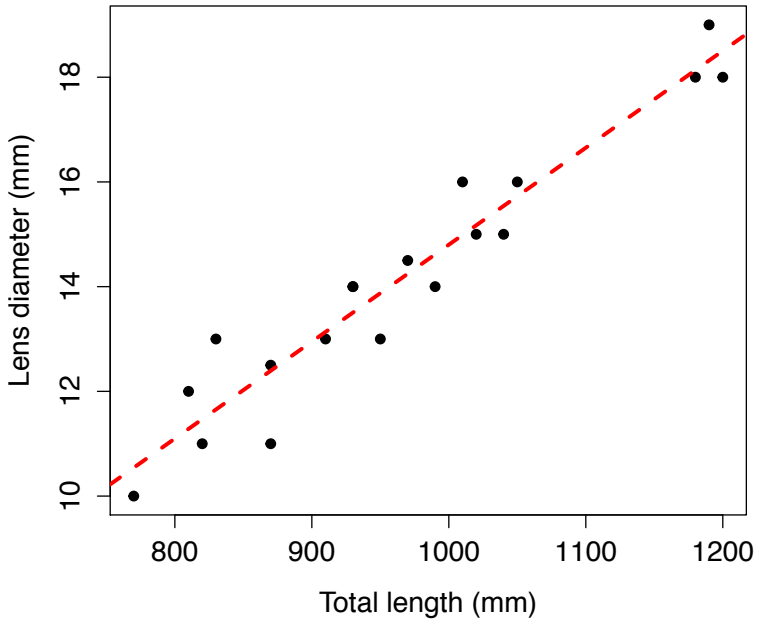

Figure 6.2 - The relationship between total length (TL) and lens diameter for the black scabbardfish, *Aphanopus carbo* (n= 18, r^2 = 0.92, p = <0.001).

A one-way ANOVA revealed that the chemical composition of lens tissue differs significantly between the four size categories, for both Portuguese and Rockall-caught specimens ($F_{(3, 178)}$ = 97.17, p = <0.001 and $F_{(3, 178)}$ = 149.2, p = <0.001, for carbon and nitrogen, respectively; data pooled from multiple laminae, per fish). Post-hoc multiple comparison test (Tukey) confirmed a significant difference between the mean isotopic composition of all lens regions (p<0.01), with the exception of late-adult and juvenile tissue for nitrogen (p=0.99) and carbon (p=0.07). Capture location has no significant effect upon the isotopic composition of core and mid-lens tissue (ANOVA; p= 0.48 and 0.53 for carbon and nitrogen, respectively) and therefore data from Rockall and Sesimbra-caught fishes were subsequently pooled. Figure 6.3 highlights the increasing trend in carbon and nitrogen isotope values from lens core to outer cortex, representative of feeding through larval to adult life history. Mean $\delta^{13}C$ of core lens tissue formed during larval development is -19.28‰ (± 0.79). Tissue representative of early juvenile life history records elevated $\delta^{13}C$ values relative to the core (mean = -18.32‰ ± 0.59), increasing again in the sub-adult region of the lens to -17.41‰ (± 0.42). Outer lens tissue representative of adult foraging records the highest $\delta^{13}C$ values; -16.90‰ (± 0.29).

Table 6.2 – Mean (and standard deviation) carbon and nitrogen stable isotope composition of lens tissue representative of nucleus (<5mm diam.), early juvenile (5-11.4mm), sub-adult (11.5-15.4) and adult (≥15.5mm) life history lens of *Aphanopus carbo* specimens caught in the Rockall Trough and off the coast of Sesimbra, Portugal. No lens samples with a corresponding diameter measurement ≥11.5mm were available for Rockall-caught individuals.

	Rockall Trough		**Portuguese Slope**	
	$\delta^{13}C$	$\delta^{15}N$	$\delta^{13}C$	$\delta^{15}N$
Nucleus	-19.01 ± 0.91	11.73 ± 2.02	-19.43 ± 0.69	10.71 ± 1.45
Early Juv.	-18.15 ± 0.53	14.42 ± 0.86	-18.52 ± 0.60	13.43 ± 1.42
Sub-Adult	NA	NA	-17.41 ± 0.42	16.60 ± 0.78
Adult	NA	NA	-16.90 ± 0.29	16.57 ± 0.82

Figure 6.3 also displays the increasing trend in $\delta^{15}N$ values from core to outer cortex; mean core $\delta^{15}N$ = 11.07‰ (± 1.74), early juvenile = 13.97 ‰ (± 1.24), sub-adult = 16.06‰ (± 0.78), and adult = 16.57‰ (± 0.82).

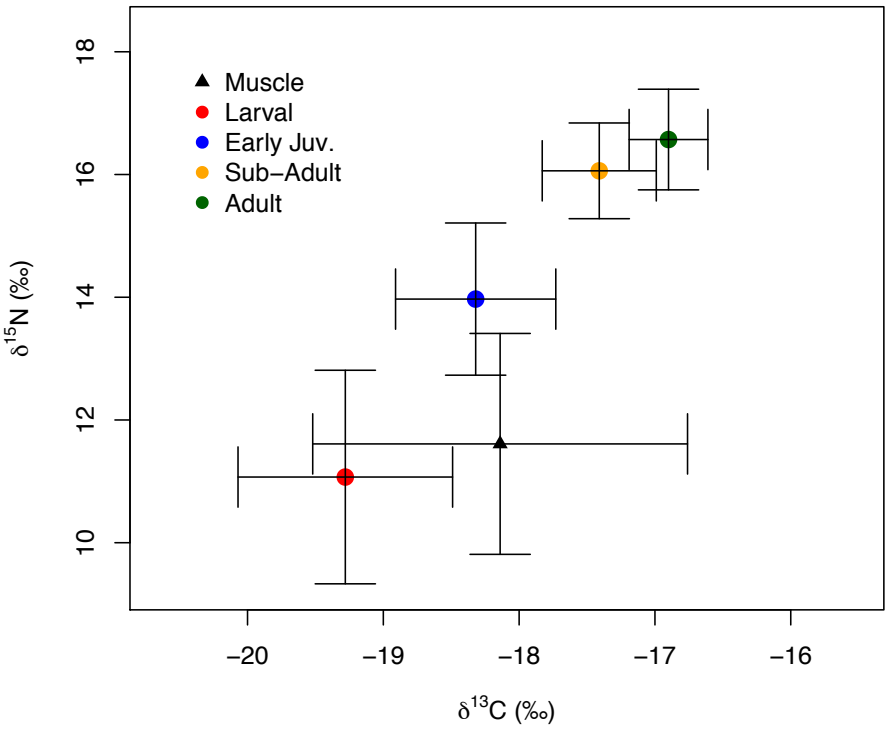

Figure 6.3 - Comparison of the mean isotopic composition of *Aphanopus carbo* eye lens samples representative of larval, early juvenile, sub-adult and adult life history. Data from specimens caught off continental Portugal (n = 13) and the Rockall Trough (n = 11) are pooled following confirmation that capture location does not effect isotopic composition of the four lens regions. Tissue is categorised according to corresponding diameter measurement; larval (≤5mm), early juvenile (5-11.4mm), sub-adult (11.5-15.4) and adult (≥15.5mm). The average isotopic composition of muscle tissue of benthic and pelagic teleost and elasmobranch species caught west of the British Isles between 2006-2012 during the MRV Scotia deep-water surveys is also plotted. Error bars display standard deviations.

A one-way ANOVA confirmed that lens tissue representative of sub-adult and adult life history is isotopically distinct relative to the chemical composition of muscle tissue of benthic and pelagic teleosts and elasmobranchs caught west of the British Isles ($F_{2, 1081}$ = 10.19, p = <0.001 and $F_{2, 1081}$ = 160.5, p = <0.001, for carbon and nitrogen, respectively) (Figure 6.3). However, post-hoc multiple comparison (Tukey test) confirmed that the result is driven by differences between the isotopic composition of the two tissue types, as lens tissue formed during sub-adult and adult

life history is isotopically comparable (p=0.45 and 0.99 for carbon and nitrogen, respectively).

Individual isotopic life histories for the 18 *Aphanopus carbo* caught off the coast of Sesimbra are shown in Figure 6.4. With the exception of fish ID #401 all fish present very similar trends in $\delta^{15}N$ and $\delta^{13}C$ values. An initial rapid increase in nitrogen isotope values occurs with increasing distance from the nucleus, until the lens attains an approximate diameter of 5-10mm (~450-650mm TL). Beyond ~10mm diameter, the rate of $\delta^{15}N$ increase reduces, plateauing in outer lens samples (10-15mm diameter). Carbon isotope ratios present similar trends, displaying an initial rapid increase in $\delta^{13}C$ values with increasing distance from the nucleus. Again, the rate of increase decreases mid-lens (5-10mm), plateauing from ~10-15mm. The isotopic life history for Fish ID 401 [Figure 6.4(p)] differs from all other sampled fish, recording comparatively high $\delta^{15}N$ and $\delta^{13}C$ values throughout the lens, with no rapid increase in either isotope observed. The isotopic composition of the lens tissue of this individual is however within the range observed in the remaining 17 specimens sampled.

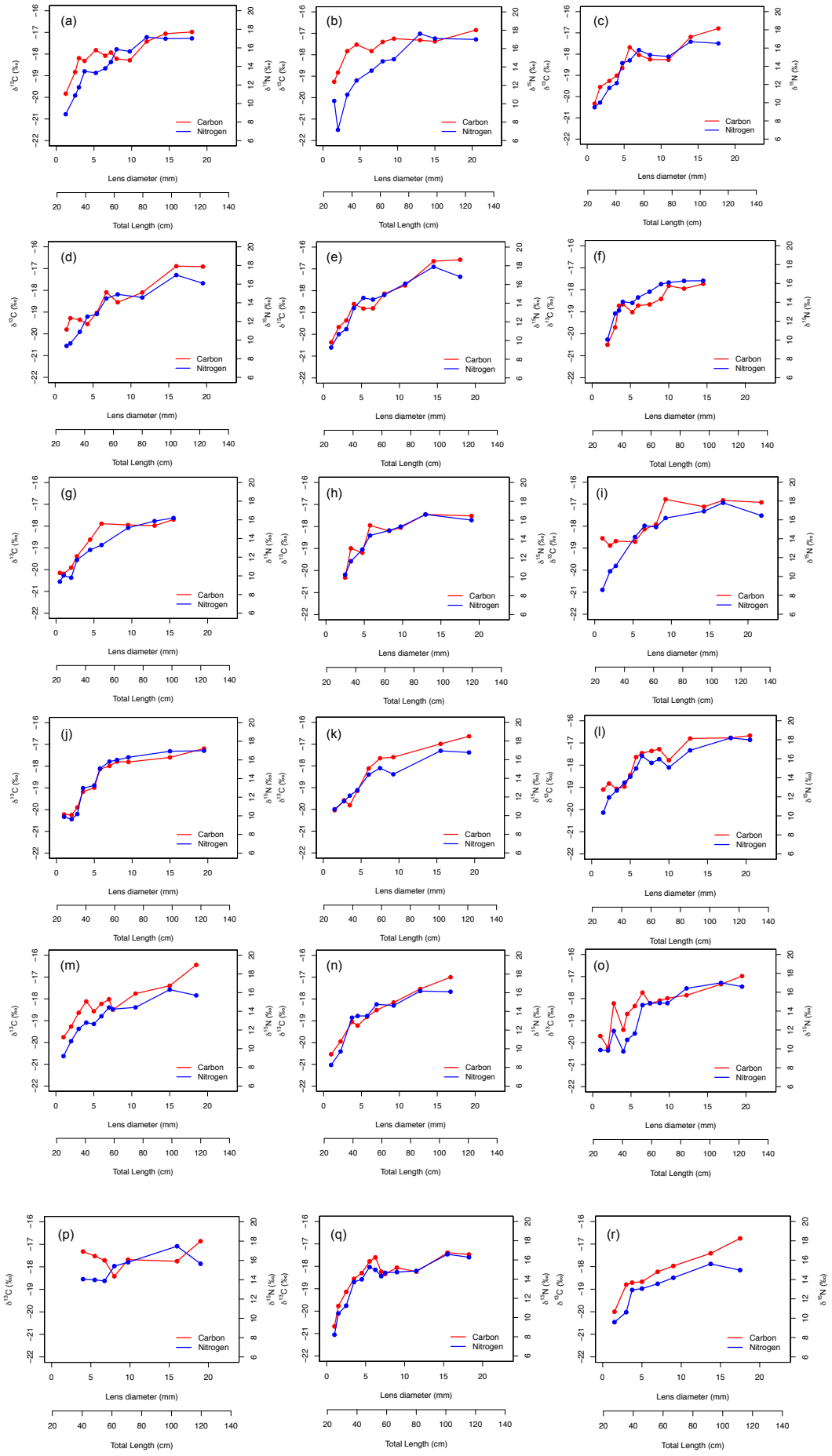
(a)
(b)
(c)
(d)
(e)
(f)
(g)
(h)
(i)
(j)
(k)
(l)
(m)
(n)
(o)
(p)
(q)
(r)
Carbon
Nitrogen
Lens diameter (mm)
Total Length (cm)
δ13C (‰)
δ15N (‰)

Figure 6.4 – Across-lens transects detailing $\delta^{13}C$ and $\delta^{15}N$ variability in 18 *Aphanopus carbo* specimens.

To assess life history trends in isotopic composition between individuals, the time series isotopic values for each individual fish were normalised to the life history mean value for that fish. Lens samples were grouped into 0.5mm diameter size bins (TL reported) and data subtracted from the global average of all fish, allowing assessment of common ontogenetic trends in lens chemistry. The resulting isotopic life history traits are shown in Figure 6.5.

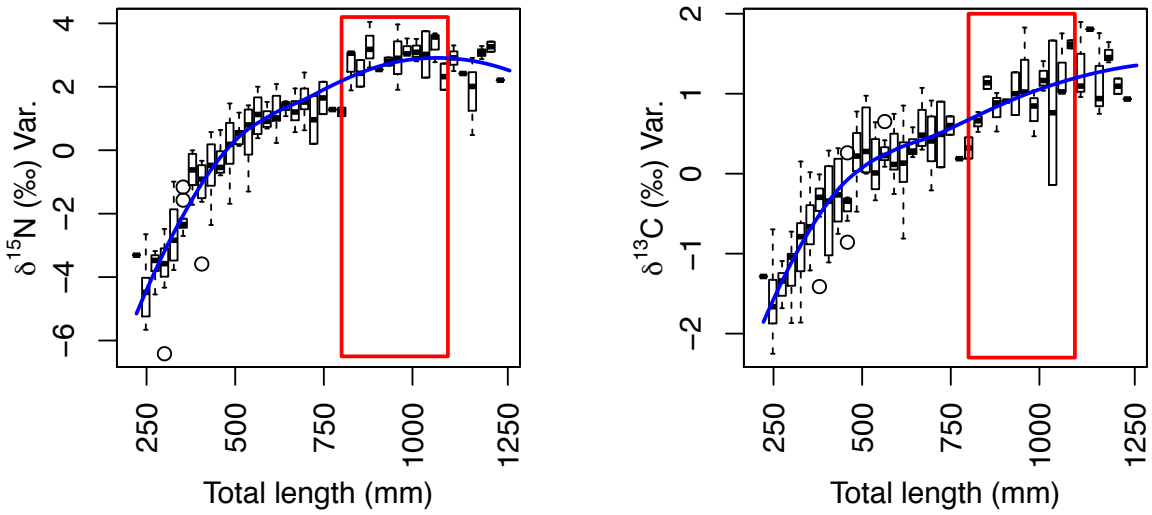

Figure 6.5 - Distribution of normalised $\delta^{13}C$ and $\delta^{15}N$ of lens samples from Portugal slope-caught black scabbardfish (*Aphanopus carbo*) for sequential 0.5mm diameter bins. Isotopic variance is plotted against the corresponding back-calculated total length at time of tissue formation. Blue lines represent loess smoothing and red boxes indicate the approximate size range of individuals recovered west of the British Isles.

Isotopic life histories are characterised by generally increasing $\delta^{13}C$ and $\delta^{15}N$ values (Figure 6.5). $\delta^{15}N$ values increase at approximately three times the rate of $\delta^{13}C$ values (c. 8 per mille increase in $\delta^{15}N$ values and c.2.5 per mille increase between 1 and 10mm diameter). $\delta^{13}C$ values consistently show a plateau at fish lengths equivalent to ~1100mm. Both $\delta^{13}C$ and particularly $\delta^{15}N$ values show a distinct rapid increase around 100mm lens diameter, approximately co-incident with the minimum size of *A. carbo* individuals seen in Rockall surveys. $\delta^{15}N$ and, to a lesser extent $\delta^{13}C$ values,

reach their lifetime maximum around 1000-1100mm, subsequently $\delta^{13}C$ and $\delta^{15}N$ values fall.

6.5 Discussion

Here, the chemical composition of size-referenced eye lens samples, from fish caught in the Rockall Trough and off the coast of Sesimbra (Portugal), is examined in relation to the current ontogenetic clockwise migration theory for black scabbardfish in the north-east Atlantic.

Initially, the isotopic composition during juvenile growth was compared between fish recovered from Rockall and Portugal slope (Table 6.2). A one-way ANOVA confirmed similar isotopic compositions across recovery areas ($p>0.05$). Across-lens transects detailing $\delta^{13}C$ and $\delta^{15}N$ variability of individual fish (Figure 6.4) reveal highly conserved trends in isotopic life history traits. At body sizes of ~450mm (lens diameter c. 5mm) $\delta^{13}C$ values plateau. $\delta^{15}N$ values also level out at around 7.5mm lens diameter (600mm body size). Juvenile life histories are relatively obscure for *A. carbo*, but this early juvenile transition may be associated with a transfer from a predominantly mesopelagic to benthopelagic lifestyle (Perera, 2008; Farias *et al.* 2014). Co-incident isotopic shifts are seen in both $\delta^{13}C$ and $\delta^{15}N$ values at around 750mm body length (11mm lens diameter), approximately equivalent to the smallest body sizes seen in the west of the British Isles. At this life history stage $\delta^{15}N$ values abruptly increase by c. 1 per mille, and $\delta^{13}C$ values show a similar but more variable increase. The consistent isotopic shift strongly suggests a common change in location and/or diet co-incident with size at arrival west of the UK. $\delta^{13}C$ and $\delta^{15}N$ values reach their lifetime maxima at body sizes of approximately 1000mm before declining slightly until their capture west of Portugal. Again this final isotopic life history transition is co-incident with the limit of the size range seen west of the United Kingdom. Isotopic life histories are also characterised by generally increasing $\delta^{13}C$ and $\delta^{15}N$ values throughout ontogeny, a trend commonly observed in marine organisms, where feeding interactions are strongly driven by individual body size.

Lens tissue formed as sub-adults and adults (Portugal slope fishes) record $\delta^{13}C$ and $\delta^{15}N$ values that are elevated beyond the isotopic range preserved in the muscle

tissue of *A. carbo* caught in the Rockall Trough, and is therefore unlikely to reflect foraging there. Similarly, as reflected in the low-resolution analysis presented in Figure 6.3, at lens diameters of ~10mm (total length ~1000mm), $\delta^{15}N$ values increase above 14‰ and remain above this value for the remainder of the individual transects. $\delta^{15}N$ values greater than this threshold are unlikely to reflect foraging within the Rockall Trough, exceeding the isotopic niche of teleost muscle in this region (Figure 6.1). We therefore infer that the isotopic composition of outer lens tissue (>10mm diam.) is characteristic of the waters off the coast of continental Portugal, where the fish in question were caught. The chemical composition of absolute core lens tissue are also beyond the isotopic niche of black scabbardfish caught at the Rockall Trough ($\delta^{13}C$ = ≤-19.5‰, $\delta^{15}N$ = ≤9.5‰), suggesting that fish caught off the coast of Sesimbra were unlikely to be foraging in the waters west of the British Isles as larvae and small juveniles.

Back –calculated length estimates associated with intermediate lens tissue reflects the size range of fish observed in the Rockall Trough. However, the isotopic composition of this tissue is elevated relative to the muscle tissue of individuals caught in the region (Figure 6.1). This may be due to species-specific muscle-lens discrimination factor, driven by differences in the biochemical composition of lens protein and white muscle collagen. Whilst tissue-specific spacing is not addressed in this study, these offsets are discussed at length in Chapter 3.

Life history isotopic traits recovered from individual *A. carbo* caught as adults west of Sesimbra, Portugal, are therefore strongly supportive of the ontogenetic migratory model for *A. carbo* in the northeast Atlantic. Individual *A. carbo* between c.700 and 1000mm body length process isotopically positive resources (enriched in the heavier isotope), likely migrating to northern waters to exploit the southern limits of the blue whiting migration (Ribeiro Santos *et al.* 2013).

The rapid increase in lens $\delta^{13}C$ values with increasing size suggests large-scale movement across strong isotopic gradients during early life history. However, the increasing trend in $\delta^{13}C$ values observed in sequential eye lens samples is unexpected given the ontogenetic migration hypothesis for this species. Spawning is believed to occur in the waters surrounding Maderia (Morales-Nin & Sena-Carvalho, 1996;

Figueiredo *et al*. 2003; Neves *et al*. 2009; Ribeiro Santos *et al*. 2013) followed by the northward migration of larvae and juveniles. Thus, one would anticipate that a systematic decline in $\delta^{13}C$ values would be recorded in incrementally formed tissues, associated with movement through isotopic provinces characterised by decreasing baseline carbon isotope ratios. However, the reverse is observed, and the eye lenses of all but one black scabbard specimen caught off Sesmibra record increasing $\delta^{13}C$ values with increasing size. We attribute the very negative lens core $\delta^{13}C$ values to this to confounding effect of depth migration. The very negative $\delta^{13}C$ values observed in the lens core may reflect surface dwelling during very early life history. This is also supported by the findings of Longmore *et al*. (2014) who suggested that the isotopic composition of the otolith core was representative of *A.carbo* larvae occupying relatively southerly, shallow waters.

The stable isotope lens transect of one individual *Aphanopus carbo* specimen examined within the scope of this study presents very different trends compared to the remaining 17 individuals. In Figure 6.4(p), relatively stable cross-lens $\delta^{13}C$ and $\delta^{15}N$ values are observed. This suggests that the individual in question may not be moving over large distances over it's lifetime, potentially feeding in regions characterised by similar baseline isotope ratios throughout ontogeny. One possible explanation for this is the misidentification of the individual. *Aphonopus intermedius* is closely related to *A. carbo*, and is morphometrically similar (Ribeiro Santos *et al*. 2013). Co-occurring in the southernmost waters of *A.carbo* distribution, misidentification of *A. intermedius* can be problematic, and genetic analysis is often used in order to confidently differentiate between the two (Stefanni & Knutsen, 2007; Stafanni *et al*. 2009; Farias *et al.* 2014; Longmore *et al*. 2014). Genetic analysis was beyond the scope of this study, and it is therefore possible that the individual in question has been misidentified as *A. carbo*, when it is in fact *A. intermedius*. Moreover, this would also explain why cross-lens stable isotope variability is low in Figure 6.5(p), as *A. intermedius* do not undertake large-scale movements, and thus, would be exposed to relatively stable isotope ratios throughout life history, subject to some temporal variability. Whilst *A. intermedius* are not generally believed to occur in the waters of continental Portugal, this may again reflect the difficulties associated with distinguishing between the two species (Nakamura & Parin, 1993). It is therefore possible that the apparent absence of *A. intermedius* in the region may be an

artefact of misidentification. This individual is therefore excluded from the following discussion.

Due to the growth dynamics of the eye lens, successive migratory patterns are unlikely to be recorded within the lens tissue of mature *A. carbo*. Lens laminae form in linear proportion to somatic growth (Figure 6.2). At the onset of sexual maturity, as somatic growth rate decreases and energy is focused toward gonadal development, the amount of lens tissue formed is dramatically reduced. Outer lens samples, with a comparable diameter to core samples, therefore represent foraging over a longer time frame. Fine-scale isotopic variability relating to spatial and trophic ecology of the individual is therefore averaged out within the outer lens tissue. Thus, recovery of high-resolution time-series data is only possible from the fast-growing region of the lens (due to the mass requirements of stable isotope analysis). Black scabbardfish lenses are therefore unlikely to record successive migratory cycles at sufficient resolution to be studied retrospectively.

To summarise, the isotopic composition of lens nucleus tissue of black scabbardfish caught off the coast of continental Portugal (Sesimbra) is too low, with regards to both carbon and nitrogen, to reflect foraging in the Rockall Trough (based upon characterisation of the itotopic niche of teleosts caught off the west coast of Scotland). This reflects the anecdotal evidence that suggests that no small juveniles and larvae occur west of the British Isles. Moreover, the isotopic composition of lens core tissue is also indicative of relatively warm, shallow waters, which agrees with the findings of Longmore *et al.* (2014) who examined the chemistry of *A. carbo* otoliths, revealing that the oxygen isotopes recorded in the otolith core reflected a warm, shallow environment, relative to the recently formed outer otolith tissue, which resembles foraging in cold, deep waters in later life. These findings provide further support for the ontogentic migration theory, which assumes that spawning occurs in the waters surrounding Madeira (and, to a lesser extent, the Canary Islands and further south (Figueiredo *et al.* 2003; Pajuelo *et al.* 2008; Neves *et al.* 2009; Ribeiro Santos *et al.* 2013)) followed by a northward (and vertical) migration towards the cooler, deeper waters of the Rockall Trough. Lens tissue with an associated total length estimate that exceeds the size range of *A. carbo* recovered from Rockall also records $\delta^{13}C$ and $\delta^{15}N$ values that fall beyond the isotopic niche of teleosts caught in the area, arguably

reflecting movement away from the sub-adult feeding ground to the capture location of continental Portugal, where fish are believed to continue to grow and attain size at first maturity (Farias *et al*. 2013).

6.6 Conclusion

To conclude, isotopic data recovered from sequentially formed eye lens tissue supports the ontogenetic clockwise migration of black scabbardfish. The chemical composition of core lens samples from fish from both capture locations reflects movement from warm, shallow waters as larvae, to cooler waters during early juvenile life history. Furthermore, lens tissue samples with corresponding size estimates equivalent to the range of fish observed in the Rockall Trough record $\delta^{13}C$ and $\delta^{15}N$ values representative of the isotopic niche of teleosts in the area (estimated from muscle tissue data). Outer lens samples from the larger Sesimbra-caught specimens, which fall beyond the isotopic niche of the Rockall teleost muscle, arguably record isotopic ratios that reflect foraging off the coast of continental Portugal around the onset of maturity (~100cm TL).

Chapter 7: Conclusion

The primary purpose of this project was to expand upon the current literature relating to the suitability of the fish eye lens as a target tissue allowing retrospective investigation of spatial and trophic ecology. In order to achieve this, specific aims were outlined in Chapter 1. These include:

- Applying novel and established lens-based protocols to investigate isotopic variability in incrementally formed eye lenses. Comparing and contrasting lens data from the spiny dogfish (*Squalus acanthias*), the northeast Atlantic porbeagle shark (*Lamna nasus*) and the deep-water teleosts, *Aphanopus carbo* and *Coryphaenoides rupestris*. Preliminary ontogenetic data are also discussed in relation to the known spatial and trophic ecology of one case-study species (*A. carbo*) (Chapter 2).

- Corroborate lens data with the known spatial and trophic ecology of case study species (*S. acanthias*, *L. nasus* & *A. carbo*) in order to examine whether the lens records "sensible" trends in isotope composition (Chapter 2, 4, 5 & 6, respectively).

- Examine species-specific tissue isotopic offsets (i.e. lens-muscle spacing) (Chapter 2 & 3).

- Examine maternal-offspring tissue isotopic spacing, and address the impact that reproductive (placental vs. aplacental viviparity) strategy has upon the chemical composition of lens tissue formed in utero (elasmobranchs only) (Chapter 4).

Chapter 2 serves as a detailed review of the structure and formation of the lens, in relation to its suitability of the tissue a target for retrospective isotope analysis. Whilst Wallace *et al*. (2014) presented a comprehensive methodology for lens sub-sampling, this technique is not suitable for all lenses as their highly gelatinous or, conversely, highly crystelline structure prevents the removal of individual laminae. Chapter 2 therefore presents and alternative, embedding approach (Epoxy resin) to lens sampling. However, not all lenses are well suited to resin embedding, due to their

permeability, which results in varying susceptibility to resin contamination. Thus, this method should only be applied where the peeling approach introduced by Parry (2003) and developed upon by Wallace *et al*. (2014), is unsuitable. Evolving from the work of Wallace *et al*. (2014), Chapter 2 presents bilateral symmetry in across-lens isotope transects, revealing that locations of equal radial distance from the core record analogous chemical signals, which is consistent with the growth and formation of the lens. Growth relationships between lens and body size were also identified for 4 case study species: *Coryphaenoides rupestris*, *Squalus acanthias*, *Lamna nasus* & *Aphanopus carbo*. These relationships confirm that lens growth and somatic size are closely coupled, allowing back-calculation of an estimate of total length from lens diameter measurements. Crucially, these relationships allow reconstruction of size-based ontogenetic trends in lens chemistry.

The isotopic composition of the lens nucleus of three of the four aforementioned study species, relating to larval and *in utero* development for teleosts and aplacentally viviparous sharks respectively, display differences consistent with their known trophic ecology; $\delta^{15}N$ values increase from the zooplanktivorous *C. rupestris* to the piscivorous *A. carbo*, with the highest values observed in the lenses of the vivaporous shark, *L. nasus*. This provides some corroboration as eye lens chemistry reflects anticipated differences in trophic level and foraging. Sadly, resin contamination limited recovery of high-resolution lens transects from *C. rupestris* and *L. nasus*.

Having identified clear inter-specific differences in lens core chemistry (Chapter 2), high-resolution lens transects were produced for the spiny dogfish (*S. acanthias*), porbeagle shark (*L. nasus*) and black scabbardfish (*A. carbo*). Spiny dogfish lens data were subsequently geographically assigned to feeding locations within the North Sea, using a spatially stable, validated isoscape (Trueman *et al*. 2016), revealing an ontogenetic shift from nutrient assimilation in the northern to southern North Sea (Chapter 4). However, one key assumption made during this study is that the formation and remodelling of all spiny dogfish samples assigned were fuelled by foraging within the North Sea. Given the potential dispersal of the species, and its known migratory behaviour, this caveat must be considered when interpreting assignment results.

The isotopic variability of lenses from 53 juvenile and sub-adult porbeagle sharks (*L. nasus*) indicates that the mothers individuals caught in the Celtic Sea region demonstrate high variability in foraging behaviour (Chapter 5). Suggesting that this proposed nursery attracts mothers from a wide geographical area, the Celtic Sea is likely to be important for the conservation of the endangered northeast Atlantic porbeagle population.

Similarly, black scabbardfish (*A. carbo*) lens tissue from specimens caught in the Rockall Trough and off the coast of Sesimbra (Portugal) formed during juvenile life history is isotopically comparable, suggesting that individuals from both locations occupied waters characterised by similar baseline isotope signatures as larvae and small juveniles (Chapter 6). Similarly, outer lens samples from larger specimens caught off the coast off Sesimbra record isotopic ratios that are beyond the isotopic niche of Rockall teleosts and elasmobranchs. These findings support the ontogenetic migration theory of black scabbardfish.

7.1 Future work

Whilst beyond the scope of this study, there are several areas of research that could be pursued in order to improve and develop upon the work presented in this thesis. First and foremost, development of a universal sampling protocol that can be applied to all spherical lenses, including problematic gelatinous lenses, would allow recovery of whole life history ontogenetic data from all teleosts and elasmobranchs. Moreover, given that gelatinous lenses pose the greatest sampling challenges, and that these are generally associated with large pelagic sharks, such a protocol would allow access to invaluable movement and foraging data from these elusive animals.

An essential assumption made in this process of the geographical assignment of spiny dogfish tissues is that all samples were fuelled by foraging within the North Sea, which, as previously discussed, may not be the case. Extension of the underlying isoscape to the English Channel, the Irish and Celtic Seas and beyond, would therefore improve the accuracy of the reassignment.

Tissue-specific offsets for the roundnose grenadier (*C. rupestris*) and spiny dogfish (*S. acanthias*) were examined within this study. Whilst lens-muscle isotope spacing

appears to differ between the two species, the comparability of the tissues remains in question. In the case of *C. rupestris*, paired samples were unavailable, and thus the differences in the isotopic values recorded may be driven by individual and temporal variability. In order to confidently quantify lens-muscle offsets, controlled feeding experiments are necessary. Furthermore, given the potential for species-specific variability in lens-muscle isotope spacing, driven by taxon-specific variability in crystalline protein composition, this isotopic spacing must be address on a case-by-case basis.

Having identified the potential for considerable temporal de-coupling between nutrient assimilation fuelling maternal tissue turnover and yolk sac provisioning, the temporal comparability of maternal and embryonic tissues of placental species must also be addressed.

Appendix – Raw Data

Table A1 – Total length (mm) and lens diameter (mm) measurements for *Squalus acanthias* (SA), *Lamna nasus* (LN), *Coryphaenoides rupestris* (CR) and *Aphanopus carbo* (AC) specimens used to establish growth relationships.

Total Length (mm)	Lens Diameter (mm)	Species	Total Length (mm)	Lens Diameter (mm)	Species
870	9	SA	830	9	SA
1100	13	SA	820	10	SA
770	9.5	SA	790	8.5	SA
840	10	SA	980	10	SA
650	8	SA	1070	12.5	SA
1070	11.75	SA	1030	11	SA
780	10	SA	1030	11.5	SA
830	10.25	SA	990	10.5	SA
400	4.75	SA	1050	11.5	SA
530	7.5	SA	1050	12.5	SA
930	10	SA	740	9	SA
1000	11.5	SA	1000	12	SA
730	10	SA	1040	12	SA
1040	12.25	SA	710	8	SA
830	11	SA	1060	11.25	SA
890	10	SA	1000	11	SA
560	6.5	SA	1060	12.75	SA
870	9.5	SA	1080	11.5	SA
780	9.5	SA	1050	11.5	SA
800	11	SA	990	11.5	SA
790	8	SA	980	11.5	SA
910	8.5	SA	940	10	SA
810	8	SA	1110	12.5	SA
900	10	SA	910	10.5	SA
810	10.5	SA	1000	12	SA
700	7.5	SA	990	12	SA
880	10	SA	560	8	SA
1070	13	SA	1090	11.5	SA
960	10.5	SA	1110	13	SA
1000	10.5	SA	1020	11.5	SA
950	9.75	SA	1080	13	SA
1000	10.5	SA	980	11	SA
1030	12	SA	850	10	SA
1030	11	SA	1120	13.5	SA
950	11	SA	1110	13	SA
980	11	SA	1080	11.5	SA
1030	11.5	SA	1000	11.25	SA
950	11	SA	820	10	SA

1060	11.5	SA	750	9	SA
990	11.5	SA	810	8.5	SA
910	11	SA	750	9	SA
1090	10.5	SA	840	9	SA
850	10	SA	1140	13.5	SA
710	9.5	SA	1010	12	SA
750	10	SA	1000	11	SA
740	9	SA	860	8.5	SA
860	10	SA	870	11	SA
810	9	SA	1050	13	SA
820	10	SA	770	9.25	SA
910	11	SA	1576	16.5	LN
840	10	SA	1850	17.5	LN
840	10	SA	130	1.2	CR
1050	12.5	SA	164	1.4	CR
155.5	2	SA	180	1.5	CR
142	1.5	SA	170	1.4	CR
155	2.2	SA	200	1.6	CR
142	1.5	SA	170	1.4	CR
120	1	SA	190	1.5	CR
126	1	SA	180	1.5	CR
141	2	SA	210	1.7	CR
137	1.5	SA	185	1.5	CR
155	2	SA	210	1.75	CR
120.5	1.5	SA	700	7	CR
153	2.25	SA	640	7.5	CR
137	2	SA	750	7	CR
150.5	2.25	SA	660	7	CR
158.5	2.25	SA	670	7	CR
162.5	2	SA	640	6.5	CR
152.5	2.5	SA	580	6	CR
134	2	SA	460	5	CR
149	2.25	SA	440	4	CR
19480	18.5	LN	470	5	CR
1480	15.25	LN	480	5	CR
1360	14.5	LN	490	4.5	CR
1396	13.5	LN	420	4	CR
1130	12	LN	360	3.5	CR
1940	18.5	LN	250	3	CR
1660	16	LN	190	2.5	CR
2160	19.5	LN	205	1.6	CR
1980	17.5	LN	220	1.8	CR
2180	20	LN	930	14	AC
1446	14	LN	1010	16	AC
1948	16.5	LN	990	14	AC
1860	17	LN	830	13	AC
1400	14	LN	1180	18	AC

1738	17.25	LN	1020	15	AC
1400	14	LN	970	14.5	AC
1825	18	LN	1190	19	AC
1410	13	LN	930	14	AC
1822	18	LN	1050	16	AC
1845	17.5	LN	820	11	AC
1885	18	LN	770	10	AC
1370	14.5	LN	1200	18	AC
1750	16.75	LN	910	13	AC
1440	14.5	LN	1040	15	AC
1554	15	LN	950	13	AC
2214	19.5	LN	870	11	AC
1593	15.5	LN	810	12	AC
1410	15.5	LN	870	12.5	AC

Table A2 – Stable carbon ($\delta^{13}C$) and nitrogen ($\delta^{15}N$) values of lens nucleus tissue from *Coryphaenoides rupestris* (CR), *Lamna nasus* (LN) and *Aphanopus carbo* (AC) specimens, corrected for resin contamination. Estimated resin contamination also presented.

Species	**$\delta^{13}C$**	**$\delta^{15}N$**
CR	-20.56	4.72
CR	-17.89	6.74
CR	-19.90	6.06
CR	-19.53	7.46
CR	-19.73	6.49
CR	-18.32	4.62
CR	-19.47	7.97
CR	-19.62	6.74
CR	-19.09	5.89
CR	-20.51	6.36
CR	-18.03	9.71
LN	-19.95	14.09
LN	-20.95	12.19
LN	-20.93	12.77
LN	-21.38	12.69
LN	-21.56	11.91
LN	-20.55	13.87
LN	-20.69	11.12
AC	-19.98	8.42
AC	-19.78	8.95
AC	-19.47	9.77
AC	-19.67	9.59
AC	-19.64	10.04
AC	-19.97	8.55
AC	-21.10	9.02
AC	-20.49	10.4

AC	-18.14	13.56
AC	-19.84	10.5
AC	-19.18	10.93

Table A3 – Isotopic composition ($\delta^{13}C$ and $\delta^{15}N$ values) of sequential lens *Aphanopus carbo* samples (corrected for resin contamination) and corresponding radial distance from lens nucleus.

Fish ID	Sub-sample	$\delta^{13}C$	$\delta^{15}N$	Radial distance (mm)
a	1	-18.47	15.65	2.6
a	2	-18.27	14.71	2.1
a	3	-18.06	14.17	1.6
a	4	-18.52	12.87	1.1
a	5	-19.05	8.40	0.6
a	6	-20.27	10.31	0
a	7	-19.29	8.49	0.6
a	8	-18.68	12.23	1.1
a	9	-18.45	14.75	1.6
a	10	-18.59	16.00	2.1
b	1	-17.89	13.02	1.9
b	2	-18.20	12.46	1
b	3	-19.97	10.86	0
b	4	-17.98	12.83	1
b	5	-18.01	14.63	1.9
b	6	-18.08	14.80	2.8
c	1	-18.02	15.01	3.7
c	2	-18.17	12.81	3.1
c	3	-18.09	12.48	2.5
c	4	-18.42	11.98	1.9
c	5	-18.60	12.81	1.3
c	6	-18.02	12.70	0.7
c	7	-20.27	10.22	0
c	8	-18.33	12.15	0.7
c	9	-18.62	13.13	1.3
c	10	-18.26	12.98	1.9
c	11	-17.98	14.00	2.5
c	12	-17.98	14.48	3.1
e	1	-18.30	15.69	4.2
e	2	-18.37	16.06	3.5
e	3	-18.43	13.76	2.8
e	4	-20.06	15.04	2.1
e	5	-20.44	13.20	1.4
e	6	-21.36	11.90	0.7
e	7	-19.24	14.78	0
e	8	-18.04	13.83	0.7
e	9	-18.61	14.55	1.4

e	10	-18.88	14.90	2.1
f	1	-18.74	14.88	3.5
f	2	-19.06	15.68	2.8
f	3	-19.32	15.80	2.1
f	4	-19.33	14.49	1.4
f	5	-19.74	13.47	0.7
f	6	-20.14	12.28	0
f	7	-19.68	14.05	0.7
f	8	-19.02	15.36	1.4
f	9	-19.30	16.98	2.1
g	1	-17.97	14.61	3.1
g	2	-19.23	14.05	2.1
g	3	-19.50	13.69	1.1
g	4	-19.78	11.11	0
g	5	-19.12	13.75	1.1
g	6	-18.68	14.12	2.1
g	7	-18.73	14.42	3.1
h	1	-18.47	19.34	3.7
h	2	-18.49	15.82	2.4
h	3	-18.93	13.73	1.3
h	4	-19.50	11.21	0
h	5	-18.97	13.11	1.3
h	6	-18.38	16.63	2.4

Table A4 – Isotopic composition ($\delta^{13}C$ and $\delta^{15}N$) of larval muscle and lens nucleus tissue from unpaired *Coryphaenoides rupestris* samples caught during the 2012 and 2013 deep-water surveys of the west Scotland continental slope onboard the MRV Scotia (survey methods reported in Neat *et al*. 2010). Isotopic composition of lens and muscle tissue from paired *Squalus acanthias* embryos by-caught in a seized catch by Marine Management Organisation off Southwold (long-liners <10m) from June-September, 2014.

Species	**Tissue**	**ID**	**$\delta^{13}C$**	**$\delta^{15}N$**
CR	Lens	NA	-20.56	4.93
CR	Lens	NA	-17.89	6.63
CR	Lens	NA	-19.90	6.20
CR	Lens	NA	-19.53	7.55
CR	Lens	NA	-19.73	6.60
CR	Lens	NA	-18.32	4.57
CR	Lens	NA	-19.47	8.05
CR	Lens	NA	-19.62	6.84
CR	Lens	NA	-19.09	5.93
CR	Lens	NA	-20.51	6.57
CR	Lens	NA	-18.03	9.62
CR	Muscle	NA	-18.71	7.37
CR	Muscle	NA	-18.42	7.71
CR	Muscle	NA	-18.93	7.14

CR	Muscle	NA	-18.46	8.17
CR	Muscle	NA	-19.65	8.03
SA	Muscle	NA	-16.20	12.38
SA	Lens	11	-16.34	12.28
SA	Lens	16	-16.92	10.56
SA	Lens	28	-16.77	12.14
SA	Lens	32	-17.56	10.81
SA	Lens	36	-16.06	13.60
SA	Lens	38	-16.18	11.57
SA	Lens	58	-16.59	12.65
SA	Lens	68	-16.82	11.75
SA	Lens	81	-16.29	13.30
SA	Lens	86	-15.79	13.09
SA	Lens	88	-16.85	10.91
SA	Muscle	11	-16.82	13.24
SA	Muscle	16	-17.11	12.14
SA	Muscle	28	-16.88	13.54
SA	Muscle	32	-17.32	12.75
SA	Muscle	36	-17.35	12.73
SA	Muscle	38	-17.07	12.60
SA	Muscle	58	-16.80	13.70
SA	Muscle	68	-16.94	12.65
SA	Muscle	81	-16.87	12.83
SA	Muscle	86	-16.38	13.61
SA	Muscle	88	-17.15	12.38

Table A5 – $\delta^{13}C$ and $\delta^{15}N$ values of embryonic and maternal muscle and lens tissue from *Squalus acanthias*, including chemical composition of muscle tissue from 5 embryos from 5 gravid females. All muscle data corrected to account for lipid content.

Shark ID	**Embryo/Adult**	**Embryo ID**	**Tissue**	**$\delta^{15}N$**	**$\delta^{13}C$**
11	E	a	Muscle	12.38	-16.20
11	E	b	Muscle	12.72	-16.15
11	E	c	Muscle	12.48	-16.24
11	E	d	Muscle	12.81	-16.34
11	E	e	Muscle	13.08	-15.99
37	E	a	Muscle	12.02	-16.83
37	E	b	Muscle	12.51	-16.90
37	E	c	Muscle	11.62	-16.71
37	E	d	Muscle	11.84	-16.75
37	E	e	Muscle	11.77	-16.78
81	E	a	Muscle	13.99	-16.52
81	E	b	Muscle	14.19	-16.23
81	E	c	Muscle	14.23	-16.38
81	E	d	Muscle	14.26	-16.27

81	E	e	Muscle	14.12	-16.15
86	E	a	Muscle	14.10	-15.67
86	E	b	Muscle	14.29	-15.84
86	E	c	Muscle	14.00	-15.76
86	E	d	Muscle	14.32	-15.69
86	E	e	Muscle	14.21	-15.77
89	E	a	Muscle	14.27	-16.29
89	E	b	Muscle	14.35	-16.34
89	E	c	Muscle	14.41	-16.25
89	E	d	Muscle	14.50	-16.31
89	E	e	Muscle	14.51	-16.32
11	E	NA	Lens	-16.34	12.28
16	E	NA	Lens	-16.92	10.56
28	E	NA	Lens	-16.77	12.14
32	E	NA	Lens	-17.56	10.81
36	E	NA	Lens	-16.06	13.60
38	E	NA	Lens	-16.18	11.57
58	E	NA	Lens	-16.59	12.65
68	E	NA	Lens	-16.82	11.75
81	E	NA	Lens	-16.29	13.30
86	E	NA	Lens	-15.79	13.09
88	E	NA	Lens	-16.85	10.91
11	A	NA	Muscle	-16.82	13.24
16	A	NA	Muscle	-17.11	12.14
28	A	NA	Muscle	-16.88	13.54
32	A	NA	Muscle	-17.32	12.75
36	A	NA	Muscle	-17.35	12.73
38	A	NA	Muscle	-17.07	12.60
58	A	NA	Muscle	-16.80	13.70
68	A	NA	Muscle	-16.94	12.65
81	A	NA	Muscle	-16.87	12.83
86	A	NA	Muscle	-16.38	13.61
88	A	NA	Muscle	-17.15	12.38
11	A	NA	Lens - Outer	-16.82	12.49
16	A	NA	Lens - Outer	-17.68	11.71
28	A	NA	Lens - Outer	-16.45	13.79
32	A	NA	Lens - Outer	-16.99	12.98
36	A	NA	Lens - Outer	-17.21	12.75
38	A	NA	Lens - Outer	-17.00	12.44
58	A	NA	Lens - Outer	-17.09	12.96
68	A	NA	Lens - Outer	-17.23	13.06
81	A	NA	Lens - Outer	-16.50	13.96
86	A	NA	Lens - Outer	-16.66	13.10
88	A	NA	Lens - Outer	-17.36	12.35
1	A	NA	Lens - Core	-15.92	15.03
2	A	NA	Lens - Core	-16.43	13.36
3	A	NA	Lens - Core	-16.22	15.26

5	A	NA	Lens - Core	-16.45	14.44
10	A	NA	Lens - Core	-17.27	12.30
11	A	NA	Lens - Core	-16.82	12.49
13	A	NA	Lens - Core	-16.61	15.31
14	A	NA	Lens - Core	-16.90	12.32
16	A	NA	Lens - Core	-17.68	11.71
17	A	NA	Lens - Core	-17.46	11.57
19	A	NA	Lens - Core	-17.38	12.18
20	A	NA	Lens - Core	-16.35	15.64
21	A	NA	Lens - Core	-17.52	11.99
22	A	NA	Lens - Core	-17.43	12.43
24	A	NA	Lens - Core	-17.27	11.54
25	A	NA	Lens - Core	-18.04	12.89
26	A	NA	Lens - Core	-17.75	14.17
26	A	NA	Lens - Core	-16.11	14.36
26	A	NA	Lens - Core	-14.91	14.63
26	A	NA	Lens - Core	-15.48	15.06
26	A	NA	Lens - Core	-15.08	14.41
26	A	NA	Lens - Core	-15.53	14.27
26	A	NA	Lens - Core	-15.21	13.94
27	A	NA	Lens - Core	-17.52	12.09
27	A	NA	Lens - Core	-17.91	11.28
27	A	NA	Lens - Core	-16.35	11.86
28	A	NA	Lens - Core	-16.45	13.79
28	A	NA	Lens - Core	-16.95	12.90
28	A	NA	Lens - Core	-16.83	10.81
28	A	NA	Lens - Core	-16.00	12.80
29	A	NA	Lens - Core	-17.26	12.21
30	A	NA	Lens - Core	-16.69	13.89
32	A	NA	Lens - Core	-16.99	12.98
33	A	NA	Lens - Core	-16.34	14.33
35	A	NA	Lens - Core	-16.89	11.53
36	A	NA	Lens - Core	-17.21	12.75
38	A	NA	Lens - Core	-17.00	12.44
39	A	NA	Lens - Core	-17.40	11.11
42	A	NA	Lens - Core	-16.35	13.96
43	A	NA	Lens - Core	-18.03	11.75
45	A	NA	Lens - Core	-18.09	12.11
46	A	NA	Lens - Core	-16.64	11.74
48	A	NA	Lens - Core	-16.78	12.41
49	A	NA	Lens - Core	-16.06	14.78
50	A	NA	Lens - Core	-16.40	12.80
51	A	NA	Lens - Core	-18.54	11.04
52	A	NA	Lens - Core	-17.64	11.47
53	A	NA	Lens - Core	-17.82	11.04
58	A	NA	Lens - Core	-17.09	12.96
59	A	NA	Lens - Core	-17.07	13.18

60	A	NA	Lens - Core	-16.54	15.02
66	A	NA	Lens - Core	-16.29	12.98
80	A	NA	Lens - Core	-16.14	14.80
88	A	NA	Lens - Core	-17.51	11.64
90	A	NA	Lens - Core	-17.49	12.10
91	A	NA	Lens - Core	-17.93	10.94
93	A	NA	Lens - Core	-16.84	10.80
97	A	NA	Lens - Core	-16.46	12.02
98	A	NA	Lens - Core	-16.43	15.05
108	A	NA	Lens - Core	-17.49	12.58
110	A	NA	Lens - Core	-17.70	11.86

Table A5 – Isotopic composition ($\delta^{13}C$ and $\delta^{15}N$ values) of sequential *Lamna nasus* eye lens samples.

Shark ID	**Sub ID**	**$\delta^{15}N$**	**$\delta^{13}C$**	**Lens Diameter (mm)**
1	I	15.79	-15.17	2.25
1	H	15.66	-14.98	4
1	F	16.07	-15.19	6.5
1	E	14.21	-16.05	8
1	D	12.29	-16.78	10
1	C	12.03	-16.7	13.25
1	B	12.07	-16.77	16
1	A	12.32	-16.71	19.5
2	J	11.1	-16.39	2
2	I	10.94	-16.65	4.5
2	H	10.8	-17.06	5.5
2	G	10.74	-17.15	6
2	F	11.51	-17.14	7.5
2	E	12.71	-16.62	9
2	D	12.66	-16.69	11
2	C	12.03	-16.48	13.5
2	B	11.31	-16.71	18
2	A	12.13	-16.28	20
3	F	16.11	-15.18	2
3	E	15.78	-15.31	4
3	D	15.96	-15.31	6
3	C	15.6	-15.47	8
3	B	11.98	-17.53	11.5
3	A	11.59	-17.44	15
4	E	11.73	-17.39	2
4	D	12.96	-17.73	6
4	C	12.85	-17.73	7.25
4	A	11.11	-17.32	13.5
5	E	11.4	-16.99	2.5

5	D	11.19	-17.08	5.25
5	C	10.72	-17.3	6.5
5	B	10.94	-17.38	9.5
5	A	10.73	-17.21	11
6	D	12.26	-17.93	3
6	C	12.39	-18.1	6.25
6	B	12.55	-18	7.25
6	A	11.33	-17.7	10
8	D	10.76	-17.47	3
8	C	10.41	-16.9	6.5
8	B	10.48	-17.39	9.5
8	A	10.24	-17.39	13
9	G	12.9	-16.95	2
9	F	12.76	-18	4
9	E	12.55	-18.18	6
9	D	11.77	-18.05	7.5
9	C	11.43	-17.81	9
9	B	11.48	-17.44	13.5
9	A	11.66	-17.37	15.5
10	E	10.76	-16.64	2
10	D	10.61	-17.02	4.25
10	C	10.75	-17.32	6
10	B	10.23	-17.36	9.25
10	A	11.1	-17.47	13
11	E	12.27	-17.47	2.75
11	D	12.7	-17.78	5
11	C	12.6	-17.82	6.5
11	B	11.45	-17.58	9.75
11	A	11.34	-17.25	13.25
12	F	12.92	-17.51	2.5
12	E	12.64	-17.96	5
12	D	12.35	-18.32	7
12	C	12.44	-18.27	7.75
12	B	11.77	-18.03	10
12	A	11.44	-18.01	12
13	E	12.13	-16.82	2
13	D	11.72	-16.66	3.5
13	C	12.17	-16.79	6.25
13	B	11.66	-17.37	7.5
13	A	11.15	-17.6	11.5
14	D	15.7	-15.59	4.5
14	C	15.26	-16.04	5.5
14	B	13.87	-16.45	7
14	A	13.28	-16.87	12.5
15	F	10.61	-16.73	2
15	E	10.92	-17.05	4.5
15	D	10.69	-17.26	5.5

15	C	10.76	-17.34	8.5
15	B	11.29	-17.24	10
15	A	11.6	-17.15	15
16	I	12.35	-15.84	2
16	H	12.21	-15.98	4.75
16	G	12.14	-16.06	6
16	F	11.76	-16.35	6.5
16	E	11.98	-16.33	8
16	D	10.97	-17.16	8.75
16	C	11.68	-16.86	11.5
16	B	11.96	-16.7	15
16	A	11.47	-16.75	17.75
17	G	13.13	-16.32	2
17	F	12.83	-16.63	3
17	E	12.89	-16.78	5
17	D	12.58	-16.76	6.5
17	C	11.09	-17.14	9
17	B	11.2	-17.42	11
17	A	11.98	-16.85	15.5
18	I	12.86	-17.28	2
18	H	13.22	-17.68	4.75
18	G	13.36	-17.8	5.25
18	E	12.6	-17.88	6.5
18	F	12.96	-17.71	6.5
18	D	11.47	-17.67	8.5
18	C	12.25	-17.27	11.5
18	B	12.92	-16.66	13.75
18	A	13.03	-16.33	16
19	I	10.45	-16.7	1.5
19	H	10.59	-16.97	3.5
19	G	10.01	-17.2	4
19	F	10.12	-17.44	5
19	E	10.04	-17.36	7
19	D	10.08	-17.35	9
19	C	11.49	-17.12	11.5
19	B	11.93	-17.15	15
19	A	11.14	-16.98	17
20	G	10.55	-16.91	1.5
20	F	10.54	-17.12	3.5
20	E	10.37	-17.39	5
20	D	9.96	-17.63	6.75
20	C	11.16	-17.23	8.5
20	A	12.52	-16.61	17
21	N	15.28	-14.72	1.5
21	M	14.9	-14.9	3
21	L	14.49	-15.12	3.5
21	K	13.91	-15.13	4.25

21	J	13.97	-15.11	4.75
21	I	13.36	-15.44	5.25
21	H	13.48	-15.59	6
21	G	12.61	-16.05	7.25
21	F	11.1	-16.66	7.75
21	E	11.56	-16.81	9
21	D	12.67	-16.43	10.5
21	C	12.96	-16.08	12.5
21	B	12.34	-16.24	15.75
21	A	11.67	-16.34	17.25
22	G	12.8	-16.11	2
22	F	11.82	-16.64	4
22	E	11.37	-16.9	5.5
22	D	11.41	-17.58	7.25
22	C	11.43	-17.65	9
22	B	11.49	-17.26	11
22	A	11.67	-17.26	15.25
24	F	13.59	-16.48	2
24	E	13.5	-16.59	3.75
24	D	13.28	-17.02	6
24	C	12.25	-17.24	6.5
24	B	11.15	-17.48	10.5
24	A	11.29	-17.23	13.5
25	F	14.63	-15.51	3
25	E	14.18	-15.8	5.5
25	D	13.85	-16.16	7.25
25	C	11.4	-17.16	9.75
25	B	11.75	-16.95	12
25	A	11.7	-16.9	14.5
26	H	13.37	-16.66	2.5
26	G	13.25	-16.82	4.5
26	F	13.11	-16.83	5.25
26	E	13.12	-16.83	6
26	D	12.26	-17.12	7
26	C	11.62	-17.43	9.5
26	B	11.06	-17.4	11.75
26	A	11.16	-17.31	16
28	F	11.25	-16.56	3
28	E	10.9	-17.01	4.5
28	D	10.75	-17.31	5.75
28	C	10.7	-17.36	7.7
28	B	10.91	-17.26	11.5
28	A	10.75	-17.38	15.5
29	G	11.31	-16.81	2
29	F	11.07	-17.05	3.75
29	E	11.04	-17.05	5.75
29	D	10.95	-17.07	7

29	C	11.25	-17.17	8.5
29	B	11.42	-17.32	10.5
29	A	11.23	-17.23	12.5
30	H	16.14	-15.04	2.5
30	G	16.26	-15.27	4.25
30	F	16.48	-15.3	5.5
30	E	16.79	-15.56	6
30	D	16.7	-15.82	7
30	C	15.37	-16.36	8.5
30	B	13.88	-16.8	10
31	I	13.2	-17.37	2
31	H	12.6	-17.85	4
31	G	12.13	-17.75	4.75
31	F	12.97	-17.81	5.75
31	E	12.74	-16.84	6
31	D	12.23	-17.64	7
31	C	12.47	-16.76	8
31	B	12.62	-16.73	10.25
31	A	12.63	-16.61	12.75
32	F	11.52	-17.09	2
32	E	11.48	-17.19	4.5
32	D	11.35	-17.65	7.25
32	C	10.92	-17.72	9
32	B	11.56	-17.32	12.5
32	A	12.04	-17.06	16.75
33	D	11.55	-17.19	3
33	C	11.5	-17.49	5.5
33	B	10.92	-17.71	7.5
33	A	10.74	-17.66	10.5
34	G	13.94	-16.7	2
34	F	13.2	-16.96	4
34	E	12.71	-17.22	6
34	D	12.54	-17.18	7
34	C	11.98	-17.54	9
34	B	11.61	-17.63	12.5
34	A	11.65	-17.23	15
35	F	10.99	-17.05	3
35	E	10.85	-17.07	5
35	D	10.85	-17.25	6
35	C	10.77	-17.43	8
35	B	11.07	-17.37	10
35	A	11.55	-17.33	23
36	G	15.93	-15.31	1
36	F	12.91	-16.46	2
36	E	13.05	-16.62	4.5
36	D	13.43	-16.65	5.75
36	C	11.42	-17.13	7.5

36	B	11.67	-17.01	9.25
36	A	11.29	-17.33	11.5
37	G	12.59	-17.57	3
37	F	12.55	-17.91	4
37	E	12.15	-18.09	6
37	D	11.94	-17.42	8.25
37	C	12.05	-17.28	10
37	B	12.05	-17.3	11.25
37	A	11.84	-16.89	15
39	F	10.94	-16.89	2.5
39	E	11.03	-17.17	5
39	D	10.84	-17.2	7.5
39	C	10.81	-17.78	10.5
39	B	12.76	-16.55	13.5
39	A	11.65	-16.62	16.25
40	G	11.21	-16.36	3
40	F	11.16	-16.39	4.5
40	E	11.16	-16.57	6
40	D	11.64	-17.36	9
40	C	11.81	-16.91	10
40	B	11.65	-17	12
40	A	11.81	-16.94	16
41	F	12.52	-17.09	2
41	E	12.68	-17.43	4
41	D	12.36	-17.63	5.5
41	C	12.3	-17.68	6.5
41	B	11.72	-17.59	9
41	A	11.2	-17.43	12
42	G	13.74	-15.91	2
42	F	13.74	-16.25	3.5
42	E	13.51	-16.74	5
42	D	13.28	-16.86	6
42	C	11.67	-17.47	8
42	B	10.9	-17.64	9
42	A	11.02	-17.53	12
43	F	11.8	-16.91	3
43	E	11.78	-17.44	5
43	D	11.46	-17.55	8
43	C	11.09	-17.64	9
43	B	11.28	-17.47	11.5
43	A	11.58	-17.07	12.5
44	F	14.12	-17.33	4
44	E	13.71	-17.52	5
44	D	13.95	-17.86	6.5
44	C	12.5	-17.61	9
44	B	12.38	-16.86	12
44	A	12.68	-16.74	15

45	D	10.49	-16.76	3
45	C	10.42	-16.85	6
45	B	10.18	-17.25	10.5
45	A	10.62	-17.38	12.75
46	F	12.64	-17.18	2
46	E	12.77	-17.58	4
46	D	12.45	-17.77	5.5
46	C	12.38	-17.8	7.5
46	B	10.91	-17.6	10
46	A	11.34	-17.43	13
47	G	10.48	-16.62	3
47	F	10.26	-16.99	5
47	E	10.08	-17.19	6
47	D	10.19	-17.45	7
47	C	11.74	-17.29	9
47	B	12.25	-17.06	13
47	A	12.58	-16.76	18
48	H	12.59	-17.88	2
48	G	12.73	-17.59	4.5
48	F	12.31	-18.18	5
48	D	12.48	-18.19	7
48	C	12.11	-17.7	9
48	B	11.98	-17.22	11.5
48	A	12.38	-17.08	14
49	D	13.34	-15.7	2
49	C	12.85	-16.73	6
49	B	11.55	-17.28	10
49	A	11.08	-17.46	12
50	E	14.22	-16.61	3
50	D	13.71	-16.61	5
50	C	13.36	-16.77	7
50	B	12.41	-17.14	10.5
50	A	11.98	-17.36	12.5
51	D	10.31	-17.09	3
51	C	10.29	-17.29	4.5
51	B	10.25	-17.37	6
51	A	10.24	-17.61	8
52	I	12.94	-17.8	2
52	H	12.82	-17.87	4
52	G	12.22	-18.08	6
52	F	12.44	-18.07	7.5
52	E	11.48	-17.64	9
52	D	11.45	-17.37	10.5
52	C	11.98	-16.87	12
52	B	12.13	-16.74	13
52	A	11.98	-16.74	16
100	E	10.38	-16.97	1.5

100	D	10.36	-17.12	3
100	C	10.17	-17.4	6.75
100	B	10.14	-17.55	9.5
100	A	10.1	-17.56	12.5
666	F	14.22	-15.55	2
666	E	13.51	-16.08	4.5
666	D	13.61	-16.24	6
666	C	12.07	-17.06	7.5
666	B	11.47	-17.27	10
666	A	11.06	-16.68	13
999	N	13.47	-17.57	1.5
999	M	13.82	-17.26	4.5
999	L	13.63	-17.67	5
999	K	13.24	-17.78	6
999	J	13.2	-17.68	6.75
999	I	12.28	-17.68	7
999	H	11.29	-17.51	7.75
999	G	10.96	-17.29	9
999	F	11.09	-16.76	9.5
999	E	11.31	-16.87	11
999	D	11.25	-16.92	14
999	C	10.67	-17	15.5
999	B	10.71	-17.1	18.5
999	A	10.49	-17.55	20
NOID	F	13.25	-17.35	4
NOID	E	13.13	-17.57	5.25
NOID	D	12.98	-17.69	7
NOID	C	11.48	-17.56	8.5
NOID	B	11.6	-17.32	11
NOID	A	11.7	-17.19	15.5

Literature Cited

Aasen, O. 1960. The Norwegian taggings of spiny dogfish (*Squalus acanthias*). *Annales Biologiques* **17**, pp. 85–95.

Aasen, O. 1963. Length and growth of the porbeagle (*Lamna nasus*) in the North West Atlantic. *Fiskeridirektoratets Skrifter Serie Havundersøkelser* **13**, pp. 20–37.

Aasen, O. 1964. .The Exploitation of the Spiny Dogfish (*Squalus acanathias* L.) in European Waters. *Fiskeridirektoratets Skrifter Serie Havundersøkelser* **13**(7).

Abrahams, M. V. and Dill, L. M. 1989. A determination of the energetic equivalence of the risk of predation. *Ecology* **70**, pp. 999–1007.

Allain, V., Biseau, A. and Kergoat, B. 2003. Preliminary estimates of French deepwater fishery discards in the Northeast Atlantic Ocean. *Fisheries Research* **60**(1), pp. 185–192.

Arrington, D. A., Winemiller, K. O., Loftus, W. F. and Akin, S. 2002. How often do fishes "run on empty"? *Ecology* **83**(8), pp. 2145–2151.

Augusteyn, R. C. 2010. On the growth and internal structure of the human lens. *Experimental eye research* **90**(6), pp. 643–54.

Bada, J. L., Schoeninger, M. J. and Schimmelmann, A. 1989. Isotopic fractionation during peptide bond hydrolysis. *Geochimica et Cosmochimica Acta* **53**, pp. 3337–3341.

Ball, L. E., Garland, D. L., Crouch, R. K. and Schey, K. L. 2004. Post-translational modifications of aquaporin 0 (AQP0) in the normal human lens: spatial and temporal occurrence. *Biochemistry* **43**(30), pp. 9856–65.

Bamstedt, U., Ishii, H. and Martinussen, M. B. 1997. Is the scyphomedusa *Cyanea capillata* (L.) dependent on gelatinous prey for its early development? *Sarsia* **82**(), pp. 269–273. doi: 10.1080/00364827.1997.10413654.

Barnes, C., Jennings, S. and Barry, J. T. 2009. Environmental correlates of large scale spatial variation in the $\delta^{13}C$ of marine animals. *Estuarine, Coastal and Shelf Science* **81**, pp. 368–374.

Bassnett, S. 2002. Lens organelle degradation. *Experimental Eye Research* **74**, pp. 1–6.

Bassnett, S. and Beebe, D. C. 1992. Coincident loss of mitochondria and nuclei during lens fiber cell differentiation. *Developmental Dynamics* **194**, pp. 85–93.

Bauer, S. and Hoye, B. J. 2014. Migratory animals couple biodiversity and ecosystem functioning worldwide. *Science* **344**, p. 1242552.

Baum, J. K. and Worm, B. 2009. Cascading top-down effects of changing oceanic predator abundances. *Journal of Animal Ecology*,**78**(4), pp. 699–714. doi: 10.1111/j.1365-2656.2009.01531.x.

Bearhop, S., Adams, C. E., Waldron, S., Fuller, R. A. and Macleod, H. 2004. Determining trophic niche width: a novel approach using stable isotope analysis. *Journal of Animal Ecology* **73**, pp. 1007–1012.

Beebe, D. C. 2003. 'The Lens', in Kaufman, P. L. and Alm, A. (eds) *Adler's Physioogy of the Eye*. *Mosby Inc*., pp. 117–158.

Bendall, V. A., Hetherington, S. J., Ellis, J. R., Smith, S. F., Ives, M. J., Gregson, J. and Riley, A. A. 2012. *Spurdog, porbeagle and common skate bycatch and discard reduction*, *Fisheries Science Partnership 2011-2012 Final Report*.

Bendall, V. A, Barber, J. L., Papachlimitzou, A., Bolam, T., Warford, L., Hetherington, S. J., Silva, J. F., McCully, S. R., Losada, S., Maes, T., Ellis, J. R. and Law, R. J. 2014. Organohalogen contaminants and trace metals in North-East Atlantic porbeagle shark (*Lamna nasus*)., *Marine pollution bulletin*. Elsevier Ltd. doi: 10.1016/j.marpolbul.2014.05.054.

Bergstad, O. A., Gjelsvik, G., Schander, C. and Høines, A. S. 2010. Feeding Ecology of *Coryphaenoides rupestris* from the Mid-Atlantic Ridge. *PLoS ONE* **5**(5), pp. 1–10.

Bergstad, O. A., Wik, A. D. and Hildre, O. 2003. Predator–prey relationships and food sources of the Skagerrak deep-water fish assemblage. *Journal of Northwest Atlantic Fishery Science*. **31**, pp. 165–180.

Best, P. B. and Schell, D. M. 1996. Stable isotopes in southern right whale (*Eubalaena australis*) baleen as indicators of seasonal movements, feeding and growth. *Marine Biology* **124**, pp. 483–494.

Biais, G., Coupeau, Y., Seret, B., Calmettes, B., Lopez, R., Hetherington, S. and Righton, D. 2017. Return migration patterns of porbeagle shark (*Lamna nasus*) in the Northeast Atlantic: implications for stock range and structure. *ICES Journal of Marine Science* **74**(5), pp.1268-1276.

Block, B. A., Jonsen, I. D., Jorensen, S. J., Winship, A. J., Shaffer, S. A., Bograd, S. J., Hazen, E. L., Foley, D. G., Breed, G. A., Harrison, A.-L., Ganong, J. E., Swithenbank, A., Castleton, M., Dewar, H., Mate, B. R., Shillinger, G. L., Schaefer, K. M., Benson, S. R., Weise, M. J., Henry, R. W. and Costa, D. P. 2011. Tracking apex marine predator movements in a dynamic ocean. *Nature* **475**, pp. 86–90.

Bloemendal, H., de Jong, W., Jaenicke, R., Lubsen, N. H., Slingsby, C. and Tardieu, A. 2004. Ageing and vision: structure, stability and function of lens crystallins. *Progress in biophysics and molecular biology* **86**, pp. 407–85.

Blundell, T., Lindley, P., Miller, L., Moss, D., Slingsby, C., Tickle, I., Turnell, B. and Wistow, G. 1981. The molecular structure and stability of the eye lens: X-ray analysis of γ-crystallin II. *Nature* **289**, pp. 771–777.

Bolle, L. J., Hunter, E., Rijnsdorp, A. D., Pastoors, M. A., Metcalfe, J. D. and Reynolds, J. D. 2005. Do tagging experiments tell the truth? Using electronic tags to evaluate conventional tagging data. *ICES Journal of Marine Science* **62**(2), pp. 236–246.

Bordalo-Machado, P., Fernandes, A. C., Figueiredo, I., Moura, O., Reis, S., Pestana, G. and Serrano Gordo, L. (2009) 'The black scabbardfish (*Aphanopus carbo*; Lowe, 1839) fisheries from the Portuguese mainland and Madeira Island', *Scientia Marina*, 73(S2), pp. 63–76.

Le Bourg, B., Kiszka, J. and Bustamante, P. 2014. Mother-embryo isotope ($\delta^{15}N$, $\delta^{13}C$) fractionation and mercury (Hg) transfer in aplacental deep-water sharks. *Journal of Fish Biology* **84**, pp. 1574–1581.

Brewer, R. H. 1989. The Annual Pattern of Feeding , Growth , and Sexual in *Cyanea* (Cnidaria : Scyphozoa) Reproduction in the Niantic River Estuary , Connecticut', *Biological Bulletin* **176**, pp. 272–281.

Bidigare, R. R., A. Fluegge, K. H. Freeman, K. L. Hanson, J. M. Hayes, D. Hollander, J. P. Jasper, L.

L. King, E. A. Laws, J. Milder, F. J. Millero, R. Pancost, B. N. Popp, P. A. Steinberg, and S. G. Wakeham. 1997. Consistent fractionation of C-13 in nature and in the laboratory: growth-rate effects in some haptophytae algae. *Global Biogeochemical Cycles* **11**:279-292.

Bowen, G. J. 2010. Isoscapes: spatial pattern in isotopic biogeochemistry. Annual Review of Earth and Planetary Sciences **38**:161-187.

Bowen, G. J., Wassenaar, L. I. and K. A. Hobson. 2005. Global application of stable hydrogen and oxygen isotopes to wildlife forensics. Oecologia **143**:337-348.

Bowen, G. J. and West, J. B. 2008. Isotope landscapes for terrestrial migration research *in* K. A. Hobson and L. I. Wassenaar, editors. Tracking Animal Migration with Stable Isotopes.

Brennan, J. S. and G. M. Cailliet. 1989. Comparative age-determination techniques for white sturgeon in California. *Transactions of the American Fisheries Society* **118**:296-310.

Bron, A. J., Versen, G. F. J. M., Kortez, J., Maraini, G. and Harding, J. J. 2000. 'The Ageing Lens', in Lütjen-Drecoll, E. (ed.) *Ophthalmologica*. Erlangen-Nürnberg: Kargen.

Brown, J. S. 1988. Patch use as an indicator of habitat preference, predation risk, and competition. *Behavioural Ecology and Sociobiology* **22**, pp. 37–47.

Brown, J. S. 1992. Patch use under predation risk I. Models and predictions. *Annales Zoologici Fennici* **29**, pp. 301–309.

Brown, S. J., Laundre, J. W. and Gurung, M. 1999. The ecology of fear: optimal foraging, game theory and trophic interactions. *Journal of Mammology* **80**, pp. 385–399.

Du Buit, M.-H. 1978. Alimentation de quelques poissons teleost ens de profondeur dans la zone du seuil de Wyville Thomson. *Oceanologica Acta* **1**(2), pp. 129–134.

Burgess, G. H. 2002. 'Spiny dogfishes: Family Squalidae' in Bigelow and Schroeder's fishes of the Gulf of Maine in Collette. B. B. and Klein-MacPhee, G. (eds). Smithsonian Institution Press, Washington, D.C., pp. 48–57.

de Busserolles, F., Fitzpatrick, J. L., Paxton, J. R., Marshall, N. J. and Collin, S. P. 2013. Eye-size variability in deep-sea lanternfishes (myctophidae): an ecological and phylogenetic study. *PloS ONE* **8**(3), pp. 1–14.

Cabana, G. and Rasmussen, J. B. 1996. Comparison of aquatic food chains using nitrogen isotopes. *Proceedings of the National Academy of Sciences of the United States of America* **93**(20), pp. 10844–7.

Cailliet, G. M. 1990. Elasmobranch age determination and verification: an updated review. NOAA Technical Report. *National Marine Fisheries Service* **90**:157–165.

Cailliet, G. M., Goldman, K. J. and Heithaus, M. R. 2004. Age determination and validation in chondrichthyan fishes. Pages 399-447 *in* J. C. Jeffrey, J. A. Musick, and M. R. Heithaus, editors. Biology of Sharks and Their Relatives. CRC Press, Boca Raton, FL.

Campana, S. E. 1999. Chemistry and composition of fish otoliths: pathways, mechanisms and applications. *Marine Ecology Progress Series* **188**, pp. 263–297.

Campana, S. E., Gibson, A. J. F., Fowler, M., Dorey, A. and Joyce, W. 2013. *Population dynamics of Northwest Atlantic porbeagle (Lamna nasus), with an assessment of status and projections for recovery. Research Document 2012/096, Canadian Science Advisory Secretariat, Fisheries*

and Ocean, Ottawa, Canada.
Campana, S. E., Jones, C., McFarlane, G. a. and Myklevoll, S. 2006. Bomb dating and age validation using the spines of spiny dogfish (*Squalus acanthias*). *Environmental Biology of Fishes* **77**(3–4), pp. 327–336.

Campana, S. E. and Joyce, W. 2004. Temperature and depth association of porbeagle shark (*Lamna nasus*) in the northwest Atlantic. *Fisheries Oceanography* **13**(1), pp. 52–64.

Campana, S. E., Joyce, W., Marks, L., Hurley, P., Natanson, L. J., Kohler, N. E., Jensen, C. F., Mello, J. J., Pratt Jr., H. L., Mykelvoll, S. and Harley, S. 2008. The rise and fall (again) of the porbeagle shark population in the Northwest Atlantic, in Camhi, M. D., Pikitch, E. K., and Babcock, E. A. (eds) *Sharks of the Open Ocean: Biology, Fisheries and Conservation*. Blackwell Publishing. Pp. 445-461.

Campana, S. E., Natanson, L. J. and Mykelvoll, S. 2002. Bomb dating and age determination of large pelagic sharks. *Canadian Journal of Fisheries and Aquatic Sciences* **59**, pp. 450–455.

Campana, S. E. and Thorrold, S. R. 2001. Otoliths, increments, and elements: keys to a comprehensive understanding of fish populations? *Canadian Journal of Fisheries and Aquatic Sciences* **58**(1), pp. 30–38.

Carlisle, A. B., Goldman, K. J., Litvin, S. Y., Madigan, D. J., Bigman, J. S., Swithenbank, A. M., Jr, T. C. K. and Block, B. A. 2015. Stable isotope analysis of vertebrae reveals ontogenetic changes in habitat in an endothermic pelagic shark. *Royal Society of London B: Biological Sciences* 282.1799 (2015): 20141446.

Carlisle, A. B., Kim, S. L., Semmens, B. X., Madigan, D. J., Jorgensen, S. J., Perle, C. R., Anderson, S. D., Chapple, T. K., Kanive, P. E. and Block, B. A. 2012. Using stable isotope analysis to understand the migration and trophic ecology of Northeastern Pacific white sharks (*Carcharodon carcharias*). *PLoS ONE* **7**(2), pp. 1–5.

Carraro, R. & Gladstone, W. 2006. Habitat preferences and site fidelity of the ornate wobbegong shark (*Orectolobus ornatus*) on rocky reefs of New South Wales. *Pacific Science* **60**, 207–223. doi:10.1016/j.biocon.2006.11.013

Cherel, Y., K. A. Hobson, and H. Weimerskirch. 2000. Using stable-isotope analysis of feathers to distinguish moulting and breeding origins of seabirds. Oecologia **122**:155–162.

Cherel, Y., Hobson, K. A. and Weimerskirch, H. 2005. Using stable isotopes to study resource acquisition and allocation in procellariiform seabirds. *Oecologia* **145**, pp. 533–540.

Cherel, Y., Kernaleguen, L., Richard, P. and Guinet, C. 2009. Whisker isotopic signature depicts migration patterns and multi-year intra- and inter-individual foraging strategies in fur seals. *Biology Letters* **5**, pp. 830–832.

Cheung, W. W. L., Pitcher, T. J. and Pauly, D. 2005. Fuzzy logic expert system to estimate intrinsice extinction vunerabilities of marine fishes to fishing. *Biological Conservation* **124**(1), pp. 97–111.

Christensen, K., Guenette, S., Heymans, J. J., Walters, C. J., Watson, R., Zeller, D. and Pauly, D. 2003. Hundred-year decline of North Atlantic predatory fishes. *Fish and Fisheries* **4**, pp. 1–24.

Christiansen, H. M., Hussey, N. E., Wintner, S. P., Cliff, G., Dudley, S. F. J. and Fisk, A. T. 2014. Effect of sample preparation techniques for carbon and nitrogen stable isotope analysis of hydroxyapatite structures in the form of elasmobranch vertebral centra. *Rapid communications in mass spectrometry* **28**(5), pp. 448–56.

Clark, M. R., Althaus, F., Schlacher, T. A., Williams, A., Bowden, D. A. and Rowden, A. A. 2016. The impacts of deep-sea fisheries on benthic communities: A review. *ICES Journal of Marine Science* **73**, pp. i51–i69.

Cole, M. L., Valiela, I., Kroeger, K. D., Tomasky, G. L., Cebrian, J., Wigand, C., Mckinney, R. A., Grady, S. P. and Carvalho da Silva, M. H. 2004. Assessment of $\delta^{15}N$ Isotopic Method to Indicate Anthropogenic Eutrophication in Aquatic Ecosystems. *Journal of Environmental Quality* **33**, pp. 124–132.

Compagno L. J. V., Dando M, Fowler, S. L. 2005. *Sharks of the World*. Princeton University Press, Princeton, NJ.

Conradt, L. 2005. 'Definitions, hypotheses, models, and measures in the study of animal segregation' in Sexual segregation in vertebrates: ecology of the two sexes, Ruckstuhl, K. E. and Neuhaus, P. (eds). Cambridge University Press, Cambridge, pp. 11–32.

Cortes, E. 1999. Standardized diet compositions and trophic levels of sharks. *ICES Journal of Marine Science* **56**, pp. 707–717.

Compagno, L. J. V., Dando, M., Fowler, S. 2005. *Sharks of the World*. Princeton University Press, Princeton, NJ.

Degens, E. T., Deuser, W. G. and Haedrich, R. L. 1969. Molecular structure and composition of fish otoliths. *Marine Biology* **2**(2214), pp. 105–113.

Dell'Apa, A., Cudney-Burch, J., Kimmel, D. G. and Rulifson, R. A. 2014. Sexual Segregation of Spiny Dogfish in Fishery-Dependent Surveys in Cape Cod, Massachusetts: Potential Management Benefits. *Transactions of the American Fisheries Society* **143**(4), pp. 833–844.

DeNiro, M. J. and Epstein, S. 1978. Influence of diet on the distribution of carbon isotopes in animals. *Geochimica et Cosmochimica Acta* **42**, pp. 495–506.

DeNiro, M. J. and Epstein, S. 1981. Influence of diet on the distribution of nitrogen isotopes in animals. *Geochimica et Cosmochimica Acta* **45**, pp. 341–351.

Devine, J. A., Baker, K. D. & Haedrich, R. L. 2006. Fisheries: deep-sea fishes qualify as endangered. Nature 439, 29.

DFO (2005) *Stock Assessment Report on NAFO Subareas 3-6 Porbeagle Shark*, *DFO. Can. Sci. Advis. Sec. Sci. Advis. Rep. 2005/044*.

Dove, S. G. and Kingsford, M. J. 1998. Use of otoliths and eye lenses for measuring trace-metal incorporation in fishes: a biogeographic study. *Marine Biology* **130**, pp. 377–387.

Dugdale, R. C. and Goering, J. J. 1967. Uptake of new and regenerated forms of nitrogen in primary productivity. *Limnology and Oceanography* **12**, pp. 196–206.

Ebert, D. A. 1991(a). Diet of the seven gill shark *Notorynchus cepedianus* in the temperate coastal waters of southern Africa. *South African Journal of Marine Science*, **11,** pp. 565–572.

Ebert, D. A. 1991(b). Observations on the Predatory Behavior of the Sevengill Shark *Notorynchus Cepedianus*. *South African Journal of Marine Science-Suid-Afrikaanse Tydskrif Vir Seewetenskap* **11**, pp. 455–465.

Ebert, D. A. 2002. Ontogenetic changes in the diet of the sevengill shark. *Marine and*

Freshwater Research **53**, pp. 517–523.

Ebert, D., Fowler, S. and Compagno, L. 2013. *Sharks of the World*. Wild Nature Press.

Ehrich, S. 1983. On the occurrence of some fish species at the slopes of the Rockall Trough. *Archiv für Fischereiwissenschaft* **33**, pp. 105–150.

Ellis, J. R., Milligan, S. P., Readdy, L., Taylor, N. and Brown, M. J. 2012. Spawning and nursery grounds of selected fish species in UK waters. *Scientific Series Technical Report* **147**, 56 pp.

Ellis, J. R., Cruz-Martinez, A., Rackham, B. D. and Rogers, S. I. 2005. The distribution of chondrichthyan fishes around the British Isles and implications for conservation. *Journal of Northwest Atlantic Fishery Science* **35**: 195–213.

Eppley, R. W. and Peterson, B. J. 1979. Particulate organic matter flux and planktonic new production in the deep ocean. *Nature* **282**:677–680

Espinoza, M., Farrugia, T. J. & Lowe, C. G. 2011. Habitat use, movements and site fidelity of the gray smooth-hound shark (*Mustelus californicus* Gill 1863) in a newly restored southern California estuary. *Journal of Experimental Marine Biology and Ecology* **401**, 63–74. doi:10.1016/j.jembe.2011.03.001

Estes, J. A., Terborgh, J., Brashares, J. S., Power, M. E., Berger, J., Bond, W. J., Carpenter, S. R., Essington, T. E., Holt, R. D., Jackson, J. B. C., Marquis, R. J., Oksanen, L., Oksanen, T., Paine, R. T., Pikitch, E. K., Ripple, W. J., Sandin, S. a, Scheffer, M., Schoener, T. W., Shurin, J. B., Sinclair, A. R. E., Soulé, M. E., Virtanen, R. and Wardle, D. A. 2011. Trophic downgrading of planet Earth. *Science* **333**(6040), pp. 301–306. doi: 10.1126/science.1205106.

Estrada, J. A., Rice, A. N., Natanson, L. J. and Skomal, G. B. 2006. Use of isotopic analysis of vertebrae in reconstructing ontogenetic feeding ecology in white sharks. *Ecology* **87**(4), pp. 829–834.

Fancett, M. S. 1988. Diet and prey selectivity of scyphomedusae from Port Phillip Bay, Australia. *Marine Biology* **509**, pp. 503–509.

Fancett, M. S. and Jenkins, G. P. 1988. Predatory impact of scyphomedusae on ichthyoplankton and other zooplankton in Port Phillip Bay. *Journal of Experimental Marine Biology and Ecology* **116**(1), pp. 63–77. doi: 10.1016/0022-0981(88)90246-8.

Farias, I., Figueiredo, I., Janeiro, A. I., Bandarra, N. M., Batista, I. and Morales-Nin, B. 2014. Reproductive and feeding spatial dynamics of the black scabbardfish, *Aphanopus carbo* Lowe, 1839, in NE Atlantic inferred from fatty acid and stable isotope analyses. *Deep-Sea Research Part I: Oceanographic Research Papers* **89**, pp. 84–93.

Farias, I., Morales-Nin, B., Lorance, P. and Figueiredo, I. 2013. Black scabbardfish, *Aphanopus carbo*, in the northeast Atlantic: distribution and hypothetical migratory cycle. *Aquatic Living Resources* **26**(4), pp. 333–342.

Fernald, R. D. 1985. Growth of the teleost eye: novel solutions to complex constraints. *Environmental Biology of Fishes* **13**(2), pp. 113–123.

Field, C. B., Behrenfeld, M. J., Randerson, J. T. and Falkowski, P. 1998. Primary production of the biosphere: integrating terrestrial and oceanic components. *Science* **281**(5374), pp.237-240.

Figueiredo, I., Reis, S., Blasdale, T., Newton, A. and Gordo, L. S. 2003. Short communication:

Observations on the reproductive cycle of the black scabbardfish (*Aphanopus carbo* Lowe , 1839) in the NE Atlantic. *ICES Journal of Marine Science* **60**, pp. 774–779.

Fordham, S., Fowler, S.L., Coelho, R., Goldman, K.J., Francis, M. 2006. *Squalus acanthias*. IUCN 2006: 2006 IUCN Red List of Threatened Species. http//www.ucnredlist.org/.

Francis, M. P., Campana, S. E. and Jones, C. M. 2007. Age under-estimation in New Zealand porbeagle sharks (*Lamna nasus*): is there and upper limit to ages that can be determined from shark vertebrae. *Marine and Freshwater Research* **58**, pp. 10–23.

Francis, M. P., Natanson, L. J. and Campana, S. E. 2008. *The biology and ecology of the porbeagle shark, Lamna nasus*, *Sharks of the Open Ocean, Biology, Fisheries and Conservation*. Edited by M. D. Camhi, E. K. Pikitch, and E. A. Babcock. Blackwell Publishing.

Francois, R., M. A. Altabet, R. Goericke, D. C. McCorkle, C. Brunet, and A. Poisson. 1993. Changes in the $\delta^{13}C$ of surface water particulate organic matter across the subtropical convergence in the South West Indian Ocean. *Global Biogeochemical Cycles* **7**:627-644.

Frankel, N., Vander Zanden, H., Reich, K., Williams, K. and Bjorndal, K. 2012. Mother–offspring stable isotope discrimination in loggerhead sea turtles *Caretta caretta*. *Endangered Species Research* **17**(2), pp. 133–138. doi: 10.3354/esr00412.

Freeman, K. H., and J. M. Hayes. 1992. Fractionation of carbon isotopes by phytoplankton and estimates of ancient carbon dioxide levels. *Global Biogeochemical Cycles* **6**:185-198.

Fretwell, S. D. and Lucas, H. L. J. 1970. On territorial behavior and other factors influencing habitat distribution in birds. *Acta Biotheoretica* **14**, pp. 16–36.

Fry, B. 1991. Stable Isotope Diagrams of Freshwater Food Webs. *Ecology* **72**(6), pp. 2293–2297.

Fry, B. 2002. Stable isotopic indicators of habitat use by Mississippi River fish. *North American Benthological Society* **21**, pp. 676–685.

Fry, B., Joern, A. and Parker, P. L. 1978. Grasshopper Food Web Analysis: Use of Carbon Isotope Ratios to Examine Feeding Relationships Among Terrestrial Herbivores. *Ecology* **59**(3).

Fry, B. and Sherr, E. B. 1984. 13C measurements as indicators of carbon flow in marine and freshwater ecosystems. *Contributions in Marine Science* **27**, pp. 13–47.

Fry, B., and S. C. Wainright. 1991. Diatom sources of C-13 rich carbon in marine food webs. *Marine Ecology Progress Series* **76**:149-157.

Gaebler, H., Vitti, T. G. and Vukmirovich, R. 1966. Isotope effects in metabolism of 14N and 15N from unlabeled dietary proteins. *Canadian Journal of Biochemistry* **44**, pp. 1249–1257.

Gannes, L. Z., O'brien, D. M. and Martinez Del Rio, C. 1997. Stable isotopes in animal ecology: Assumptions, caveats, and a call for more laboratory experiments. *Ecology* **78**, pp. 1271–1276.

Gauld, J. 1979. *Reproduction and fecundity of the Scottish–Norwegian stock of spurdogs, Squalus acanthias (L.). ICES CM Document.*

Gauld, J. A. 1989. Records of Porbeagles Landed in Scotland, with observtopns on the biology, distribution and exploitation of the species. *Department of Agriculture and Fisheries for*

Scotland. Scottish Fisheries Research Report **45.**

Gauld, J. A. and MacDonald, W. S. (1982) 'The Results of Tagging Experiments on Spurdogs *Squalus acanthias* L. around Scotland', *ICES CM Document.*

Genner, M. J., Turner, G. F., Barker, S. and Hawkins, S. J. 1999. Niche segregation among Lake Malawi cichlid fishes? Evidence from stable isotope signatures. *Ecology Letters* **2**, pp. 185–190.

Gianni, M. 2004. High seas bottom trawl fisheries and their impacts on the biodiversity of vulnerable deep-sea ecosystems, Options for International Action. *International Union for Conservation of Nature and Natural Resources.*

Gillanders, B. M. 2001. Trace metals in four structures of fish and their use for estimates of stock structure. *Fisheries Bulletin* **99**, pp. 410–419.

Goericke, R., J. P. Montaya, and B. Fry. 1993. Physiology of isotope fractionation in algae and cyanobacteria.*in* K. Lajtha and B. Michener, editors. Stable Isotopes in Ecology.

Goericke, R., and B. Fry. 1994. Variations of marine plankton $\delta^{13}C$ with latitude, temperature, and dissolved CO_2 in the world ocean. *Global Biogeochemical Cycles* **8**:85-90.

Goering, J., Alexander, V. and Haubenstock, N. 1990. Seasonal variability of stable carbon and nitrogen isotope ratios of organisms in a North Pacific bay. *Estuarine, Coastal and Shelf Science* **30**, pp. 239–260.

Graham, B. S., Koch, P. L., Newsome, S. D., McMahon, K. W. and Aurioles, D. 2010. *Using Isoscapes to Trace the Movements and Foraging Behaviour of Top Predators in Oceanic Ecosystems*, *Isoscapes: Understanding Movement, Pattern, and Process on Earth Through Isotope Mapping*. Edited by J. B. West, G. J. Bowen, and T. E. Dawson. Springer Science.

Grainger, R. M. 1992. Embryonic lens induction: shedding light on vertebrate tissue determination. *Trends in Genetics* **8**, pp. 349–355.

Grønkjær, P., Pedersen, J. B., Ankjærø, T. T., Kjeldsen, H., Heinemeier, J., Steingrund, P., Nielsen, J. M. and Christensen, J. T. 2013. Stable N and C isotopes in the organic matrix of fish otoliths: validation of a new approach for studying spatial and temporal changes in the trophic structure of aquatic ecosystems. *Canadian Journal of Fisheries and Aquatic Sciences* **146**, pp. 143–146.

Grubbs, R. D. 2010. Ontogenetic shifts in movements and habitat use. Pages 319-350 *in* J. C. Carrier, J. A. Musick, and M. R. Heithaus, editors. Sharks and Their Relatives II: Biodiversity, Adaptive Physiology, and Conservation. CRC Press, Boca Raton, FL.

Grubbs, R. D., Carlson, J. K., Romine, J. G., Curtis, T. H., McElroy, W. D., McCandless, C. T., Cotton, C. F. and Musik, J. A. 2016. Critical assessment and ramifications of a purported marine trophic cascade. *Scientific Reports* **6**(20970).

Gutierrez, D. B., Garland, D. and Schey, K. L. 2011. Spatial analysis of human lens aquaporin-0 post-translational modifications by MALDI mass spectrometry tissue profiling. *Experimental eye research* **93**(6), pp. 912–20.

Haines, A. H. 1976. Relative Reactivities of Hydroxyl Groups in Carbohydrates. *Advances in Carbohydrate Chemistry and Biochemistry* **33**, pp. 11–109.

Hamady, L. L., Natanson, L. J., Skomal, G. B. and Thorrold, S. R. 2014. Vertebral bomb

radiocarbon suggests extreme longevity in white sharks. *PloS one* **9**(1), p. e84006.

Hamlett, W. C. & Koob, T. J. 1999. Female reproductive system. In: Hamlett WC, editor. Sharks, skates and rays: the biology of elasmobranch fishes. Baltimore, MD: Johns Hopkins University Press. p 398–443.

Hamlett, W. C. & Hysell, M. K. 1998. Uterine specializations in elasmobranchs. *Journal of Experimental Zoology* **282**, pp. 438-459.

Hammond, T. R. and Ellis, J. R. 2004. Bayesian Assessment of Northeast Atlantic Spurdog Using a Stock Production Model, with Prior for Intrinsic Population Growth Rate Set by Demographic Methods. *Journal of Northwest Atlantic Fishery Science* **37**(November 2004), pp. 299–308.

Hanson, N., Wurster, C. and Todd, C. 2013. Reconstructing marine life-history strategies of wild Atlantic salmon from the stable isotope composition of otoliths. *Marine Ecology Progress Series* **475**, pp. 249–266.

Hansson, L. J. 1997. Capture and digestion of the scyphozoan jellyfish *Aurelia aurita* by *Cyanea capillata* and prey response to predator contact. *Journal of Plankton Research* **19**(2), pp. 195–208. doi: 10.1093/plankt/19.2.195.

Hare, P. E., Fogel, M. L., Stafford, T. W., Mitchell, A. D. and Hoering, T. C. 1991. The isotopic composition of carbon and nitrogen in individual amino acids isolated from modern and fossil proteins. *Journal of Archaeological Science* **18**, pp. 277–292.

Hastings, A., Petrovskii, S., Morozov, A., Hastings, A. and Petrovskii, S. 2011. Spatial ecology across scales. *Biology Letters* **7**, pp. 163–165.

Hedfalk, K., Törnroth-Horsefield, S., Nyblom, M., Johanson, U., Kjellbom, P. and Neutze, R. 2006. Aquaporin gating. *Current opinion in structural biology* **16**, pp. 447–56.

Heithaus, M. R., Frid, A. J. and Wirsing, A. J.Worm, B. 2008. Predicting ecological consequences of marine top predator declines. *Trends in Ecology and Evolution* **23**, pp. 202–210.

Heithaus, M. R., Frid, A., Wirsing, A. J., Dill, L. M., Fourgurean, J. W., Burkholder, D., Thomson, J. and Beider, L. 2007. State-dependent risk taking by green sea turtles mediates top-down effects of tiger shark intimidation in a marine ecosystem. *Journal of Animal Ecology* **76**, pp. 837–844.

Hennache, C. and Jung, A. 2010. *Etude de la pêche palangrière de requin-taupe de l'île d'Yeu. Association pour l'étude et la conservation des sélaciens (APECS), Brest, France*.

Heupel, M. R., Carlson, J. K. and Simpendorfen, C. A. 2007. Shark nursery areas: concepts, definition, characterization and assumptions. *Marine Ecology Progress Series* **337**, pp. 287–297.

Heupel, M. R., Simpfendorfer, C. A. & Hueter, R. E. 2004. Estimation of shark home ranges using passive monitoring techniques. Environmental Biology of Fishes **71**, 135–142. doi:10.1023/B:EBFI.0000045710.18997.f7

Heupel, M. R., Knip, D. M., Simpfendorfer, C. A. and Dulvy, N. K. 2014. Sizing up the ecological role of sharks as predators. *Marine Ecology Progress Series* **495**, pp. 291–298.

Hisaw, F., K and Albert, A. 1947. Observations on the reproduction of the spiny dogfish, *Squalus acanthias*. *Biological Bulletin* **92**, pp. 187–199.

Hjertenes, P. O. 1980. The spurdogs (*Squalus acanthias*) in the North Sea area: The Norwegian fishery and observations on changes in migration pattern. ICES C.M. Doc., No. 1980/H:60',

Hobson, K. A. 1999. Tracing origins and migration of wildlife using stable isotopes: a review. *Oecologica* **120**, pp. 314–326.

Hobson, K. A., R. Barnett-Johnson, and T. Cerling. 2010. Using isoscapes to track animal migration *in* B. West, G. J. Bowen, T. E. Dawson, and K. P. Tu, editors. Isoscapes: Understanding Movement, Pattern, and Process on Earth through Isotope Mapping. Springer Science, Berlin.

Hobson, K. A. and Schell, D. M. 1998. Stable carbon and nitrogen isotope patterns in baleen from eastern Arctic bowhead whales (*Balaena mysticetus*). *Canadian Journal of Fisheries and Aquatic Sciences* **55**, pp. 2601–2607.

Hobson, K. A. and Smith, R. J. F. 2007. 'Applications of Stable Isotope Analysis to Tracing Nutrient Sources to Hawaiian Gobioid Fishes and Other Stream Organisms' in Evenhuis, N. L. and Fitzsimons, J. M. (eds) *Biology of Hawaiian Streams and Estuaries*. Honolulu, Hawai'i.: Bishop Museum Bulletin in Cultural and Environmental Studies.

Hobson, K. A. and Welch, H. E. 1992. Determination of trophic relationships within a high Arctic marine food web using δ13C and δ15N analysis. *Marine Ecology Progress Series* **84**, pp. 9–18.

Hofmann, M., Wolf-Gladrow, D. a, Takahashi, T., Sutherland, S. C., Six, K. D. and Maier-Reimer, E. 2000. Stable carbon isotope distribution of particulate organic matter in the ocean: a model study. *Marine Chemistry* **72**(2–4), pp. 131–150.

Hogberg, P. 1997. Tansley review No. 95 - ^{15}N natural abundance in soil-plant systems. *New Phytologist* **139**(595).

Hoie, H., Otterlei, E. and Folkvord, A. 2004. Temperature-dependant fractionation of stable oxygen isotopes in juvenile cod (*Gadus morhua* L.). *ICES Journal of Marine Science* **61**, pp. 243–251.

Holden, M. J. 1965. The stocks of spurdogs (*Squalus acanthias* L.) in British waters and their migrations. *Fish. Invest., Land. Ser.* ***2***, 24(4).

Holden, M. J. 1967. Transatlantic movement of a tagged spurdogfish. *Nature* **214**(5093), pp. 1140–1141.

Holden, M. J. and Meadows, P. S. 1962. The Structure of the Spine of the Spur Dogfish (*Squalus acanthias* L.) and its use for Age Determinations. *Journal of the Marina Biological Association of the UK* **42**, pp. 179–197.

Holdo, R. M., Holt, R. D., Sinclair, A. R. E., Godley, B. J. and Thirgood, S. 2011. 'Migration impacts on communities and ecosystems: empirical evidence and theoretical insights', in Milner-Gulland, E. J., Fryxell, J. M., and Sinclair, A. R. E. (eds) *Animal Migration: A Synthesis.* Oxford University Press, Oxford.

Holt, R. E., Foggo, A., Neat, F. C. and Howell, K. L. 2013. Distribution patterns and sexual segregation in chimeras: implications for conservation and management. *ICES Journal of Marine Science* **70**(6), pp. 1198–1205.

Holmes, E. E., Lewis, M. A., Banks, J. E. and Veit, R. R., 1994. Partial differential equations in ecology: spatial interactions and population dynamics. *Ecology* **75**(1), pp.17-29.

Howell, K.L., Heymans, J.J., Gordon, J. D. M., Duncan, J., Ayers, M. and Jones, E.G. 2009 DEEPFISH Project: Applying an ecosystem approach to the sustainable management of deep-water fisheries. Part 1: Development of the Ecopath with Ecosim model', *Scottish Association for Marine Science, Oban, UK*, (259a).

Howey-Jordan, L. A., Brooks, E. J., Abercrombie, D. L., Jordan, L. K., Brooks, A., Williams, S., Gospodarczyk, E. and Chapman, D. D., 2013. Complex movements, philopatry and expanded depth range of a severely threatened pelagic shark, the oceanic whitetip (*Carcharhinus longimanus*) in the western North Atlantic. *PloS one* ***8***(2), p.e56588

Hunsicker, M. E., Essington, T. E., Aydin, K. Y. and Ishida, B. 2010. Predatory role of the commander squid *Berryteuthis magister* in the eastern Bering Sea: insights from stable isotopes and food habits. *Marine Ecology Progress Series* **415**, pp. 91–108.

Hussey, N. E., Dudley, S. F. J., McCarthy, I. D., Cliff, G. and Fisk, A. T. 2011. Stable isotope profiles of large marine predators: viable indicators of trophic position, diet, and movement in sharks? *Canadian Journal of Fisheries and Aquatic Sciences* **68**, pp. 2029–2045.

Hüssy, K., Mosegaard, H. and Jessen, F. 2004. Effect of age and temperature on amino acid composition and the content of different protein types of juvenile Atlantic cod (*Gadus morhua*) otoliths. *Canadian Journal of Fisheries and Aquatic Sciences* **61**, pp. 1012–1020. Hutchings, J. A. and Baum, J. K. 2005. Measuring marine fish biodiversity : temporal changes in abundance , life history and demography Measuring marine fish biodiversity : temporal changes in abundance , life history and demography. *Philosophical Transactions of the Royal Society B* **360**(1454), pp. 315–338. doi: 10.1098/rstb.2004.1586.

Hyslop, E. J. 1980. Stomach contents analysis—a review of methods and their application. *Journal of Fish Biology* **17**(4), pp. 411–429.

ICES. 2009a. *Report of the Joint Meeting between ICES Working Group on Elasmobranch Fishes (WGEF) and ICCAT Shark Subgroup, 22 – 29 June 2009, Copenhagen, Denmark. ICES Document CM 2009/ ACOM: 16.*

ICES. 2009b. *Report of the Workshop on Learning from Salmon Tagging Records (WKLUS-TRE). Copenhagen: ICES.*

ICES. 2012. *Report of the Working Group on the Biology and Assessment of Deep-Sea Fisheries Resources (WGDEEP). ICES CM 2012/ACOM:17.*

Iken, K., Brey, T., Wand, U., Voigt, J., Junghans, P. 2001. Food web structure of the benthic community at the Porcupine Abyssal Plain (NE Atlantic): a stable isotope analysis. *Progress in Oceanography* **50**, 383–405.

Jackson, J. R. 2007. Earliest References to Age Determination of Fishes and Their Early Application. *Fisheries* **32**(7), pp. 321-328.

Jaeger, A., Lecomte, V. J., Weimerskirch, H., Richard, P. and Cherel, Y. 2010. Seabird satellite tracking validates the use of latitudinal isoscapes to depict predators' foraging areas in the Southern Ocean, *Rapid Communications in Mass Spectrometry* **24**, pp. 3456–3460.

Jenkins, S. G., Partridge, S. T., Stephenson, T. R., Farley, S. D. and Robbins, C. T. 2001. Nitrogen and carbon isotope fractionation between mothers, neonates, and nurseing offspring.

Oecologia **129**(3), pp. 336–341.

Jennings, S., Barnes, C., Sweeting, C. J. and Polunin, N. V. C. 2008. Application of nitrogen stable isotope analysis in size-based marine food web and macroecological research. *Rapid Communications in Mass Spectrometry* **22**, pp. 1673–1680.

Jennings, S. and Van Der Molen, J. 2015. Trophic levels of marine consumers from nitrogen stable isotope analysis: estimation and uncertainty.*ICES Journal of Marine Science* **72**(8), pp. 2289–2300.

Jennings, S. and Warr, K. J. 2003. Environmental correlates of large-scale spatial variation in the $\delta^{15}N$ of marine animals. *Marine Biology* **142,** pp. 1131–1140.

Jensen, C. F., Natanson, L. J., Pratt Jr., H. L., Kohler, N. E. and Campana, S. E. 2002. The reproductive biology of the porbeagle shark (*Lamna nasus*) in the western North Atlantic Ocean. *Fisheries Bulletin* **100**, pp. 727–738.

Jones, T. S. and Ugland, K. I. 2001. Reproduction of female spiny dogfish, S*qualus acanthias*, in the Oslofjord. *Fishery Bulletin* **99**, pp. 685–690.

Jorgensen, S. J., Reeb, C. A., Chapple, T. K., Anderson, S., Perle, C., Van Sommeran, S. R., Fritz-Cope, C., Brown, A. C., Klimley, A.P. and Block, B.A. 2009. Philopatry and migration of Pacific white sharks. *Proceedings of the Royal Society of London B: Biological Sciences*, p.rspb20091155.

Junk G, Svec HV. 1958. The absolute abundance of the nitrogen isotopes in the atmosphere and compressed gas from various sources. *Geochimica et Cosmocliimica Acta* **14**: 23-1—243.

Kalish, J. M. 1991. ^{13}C and ^{18}O isotopic disequilibria in fish otoliths: metabolic and kinetic effects. *Marine Ecology Progress Series* **75**, pp. 191–203.

Karasov, W. H. and Martínez del Rio, C. 2007. Physiological Ecology. *Princeton University Press, Princeton, NJ.*

Kelly, C. J., Connolly, P. L. and Clarke, M. W. 1998. The deep water fisheries of the Rockall trough; some insights gleaned from Irish survey data. *International Council for the Exploitation of the Seas*

Kerr, L. A., Andrews, A. H., Cailliet, G. M., Brown, T. A. and Coale, K. H. 2006. Investigations of Δ 14C, δ 13C, and δ 15N in vertebrae of white shark (*Carcharodon carcharias*) from the eastern North Pacific Ocean. *Environmental Biology of Fishes* **77**(3–4), pp. 337–353. doi: 10.1007/s10641-006-9125-1.

Ketchen, K. S. 1972. Size at Maturity, Fecundity, and Embryonic Growth of the Spiny Dogfish (*Squalus acanthias*) in British Columbia Waters. *Journal of the Fisheries Research Board of Canada* **29**(12), pp. 1717–1723.

Kim, S. L., del Rio, C. M., Casper, D. and Koch, P. L. 2012(a). Isotopic incorporation rates for shark tissues from a long-term captive feeding study. *The Journal of Experimental Biology* **215**, pp. 2495–2500.

Kim, S. L., Tinker, M. T., Estes, J. A. and Kock, P. L. 2012(b). Ontogenetic and Among-Individuals Variation in Foraging Strategies of Northeast Pacific White Sharks Based on Stable Isotope Analysis. *PLoS ONE* **7**(9), pp. 1–11.

Kim S. L. and Koch, P. L. 2012. Methods to collect, preserve, and prepare elasmobranch

tissues for stable isotope analysis. *Environmental Biology of Fishes* **95**, pp. 53–63.

Kingsford, M. J. and Gillanders, B. M. 2000. Variation in concentrations of trace elements in otoliths and eye lenses of a temperate reef fish, *Parma microlepis*, as a function of depth, spation scale, and age. *Marine Biology* **137**, pp. 403–414.

Kjeldsen, Heinemeier, J., Heegaard, S., Jacobsen, C. and Lynnerup, N., H. 2010. Dating the time of birth: A radiocarbon calibration curve of human eye-lens crystallines. *Nuclear Instruments and Methods in Physics Research B* **286**, pp. 1303–1306.

Knip, D. M., Heupel, M. R., Simpfendorfer, C. A. 2010. Sharks in nearshore environments: models, importance, and consequences. *Marine Ecology Progress Series* **402**, 1–11. doi:10.3354/meps08498

Koob, T. J. and Callard, I. P. 1999. Reproductive endocrinology of female elasmobranchs: lessons from the little skate (*Raja erinacea*) and spiny dogfish (*Squalus acanthias*). *The Journal of Experimental Zoology* **284**(5), pp. 557–74.

Koslow, J. A., Boehlert, G. W., Gordon, J. D. M., Haedrich, R. L., Lorance, P. and Parin, N. 2000. Continental slope and deep-sea fisheries: Implications for a fragile ecosystem. *ICES Journal of Marine Science* **57**, pp. 548–557.

Kotler, B. P. and Blaustein, L. 1995. Titrating food and safety in heterogeneous environments: when are the risky and safe patches of equal value? *Oikos* **74**, pp. 251–258.

Kröger, R. H. H. 2013. Optical plasticity in fish lenses. *Progress in Retinal and Eye Research* **34**, pp. 78–88.

Lallemand-Lemoine, L. 1991. Analysis of the French fishery for porbeagle *Lamma nasus*. (Bonnaterre, 1788). ICES CM /G:71. Mejuto', *ICES Document C.M*, 10, p. 71pp.

Lara, R. J., Alder, V., Franzosi, C. A. and Kattner, G. 2010. Characteristics of suspended particulate organic matter in the southwestern Atlantic: Influence of temperature, nutrient and phytoplankton features on the stable isotope signature. *Journal of Marine Systems* **79**(1–2), pp. 199–209.

Laws, E. A., B. N. Popp, R. R. Bidigare, M. C. Kennicutt, and S. A. Macko. 1995. Dependence of phytoplankton carbon isotopic composition on growth rate and $CO_{2(aq)}$ – theoretical considerations and experimental results. *Geochimica Et Cosmochimica Acta* **59**:1131-1138.

Lee, S. H., Schell, D. M., McDonald, T. L. and Richardson, W. J. 2005. Regional and seasonal feeding by bowhead whales *Balaena mysticetus* as indicated by stable isotope ratios. *Marine Ecology Progress Series* **285**, pp. 271–287.

Legendre, P. and Fortin, M.-J. 1989. Spatial pattern and ecological analysis. *Vegetatio* **80**, pp. 107–138.

Levin, S. A. 1992. The Problem of Pattern and Scale in Ecology. *Ecology* **73**(6), pp. 1943–1967.

Lima, S. L. and Dill, L. M. 1990. Behavioral decisions made under the risk of predation: a review and prospectus. *Canadian Journal of Zoology* **68**, pp. 619–640.

Longmore, C., Trueman, C. N., Neat, F., Jorde, P. E., Knutsen, H., Stefanni, S., Catarino, D., Milton, J. A. and Mariani, S. 2014. Ocean-scale connectivity and life cycle reconstruction in a deep-sea fish. *Canadian Journal of Fisheries and Aquaculture Science* **71**, pp. 1312–1323.

Longmore, C., Trueman, C. N., Neat, F., O'Gorman, E. J., Milton, J. A. and Mariani, S. 2011. Otolith geochemstry indicates life-long spatial population structuring in a deep-sea fish, *Coryphaenoides rupestris*. *Marine Ecology Progress Series* **435**, pp. 209–224.

Lorance, P., Garren, F. and Vigneau, J. 2003. Age estimation of Roundnose Grenadier (*Coryphaenoides rupestris*), Effects of Uncertainties on Ages. *Journal of Northwest Atlantic Fishery Science* **31**, pp. 387–399.

Lorrain, A., Graham, B., Menard, F., Popp, B., Bouillon, S., van Breugel, P. and Cherel, Y. 2009. Nitrogen and carbon isotope values of individual amino acids: a tool to study foraging ecology of penguins in the Southern Ocean. *Marine Ecology Progress Series* **391**, pp. 293–306.

Lorrain, A., Paulet, Y. M., Chauvaud, L., Savoye, N., Donval, A. and Saout, C. 2002. Differential δ13C and δ15N signatures among scallop tissues: implications for ecology and physiology. *Journal of Experimental Marine Biology and Ecology* **257**, pp. 47–61.

Lundberg, J. and Moberg, F. 2003. Mobile link organisms and ecosystem functioning: implications for ecosystem resilience and management. *Ecosystems* **6**, pp. 87–98.

Lynnerup, N., Kjeldsen, H., Heegaard, S., Jocobsen, C. and Heinmeier, J. 2008. Radiocarbon Dating of the Human Eye Lens Crystallines Reveal Proteins without Carbon Turnover throughout Life. *PLoS ONE* **1**, p. e1529.

MacKenzie, K. M. 2010. *The marine life of Atlantic salmon: evidence from the chemistry of scales*, *School of Ocean and Earth Science*. University of Southampton.

MacKenzie, K. M., Longmore, C., Preece, C., Lucas, C. H. and Trueman, C. N. 2014. Testing the long-term stability of marine isoscapes in shelf seas using jellyfish tissues. *Biogeochemistry* **121**(2), pp. 441–454.

MacKenzie, K. M., Palmer, M. R., Moore, A., Ibbotson, A. T., Beaumont, W. R. C., Poulter, D. J. S. and Trueman, C. N. 2011. Locations of marine animals revealed by carbon isotopes. *Scientific Reports* **1**(21), pp. 1–6.

Mackinson, S. and Daskalov, G. 2007. Science Series Technical Report no.142', *Cefas*, (142).

Magozzi, S., Yool, A, Vander Zanden, H. B., Wunder, M. B., Trueman, C. N. Using ocean models to predict spatial and temporal variation in marine carbon isotopes (*in press*) *Ecosphere.*

Maillet, G. L. and Checkley, S. M. 1990. Effects of starvation on the frequency of formaion and width of growth increments in sagittae of laboratory reared Atlantic menhaden (*Brevoortia tyrannus*) larvae. *Fishery Bulletin* **88**, pp. 155–165.

Mann, K. H. and Lazier, J. R. N. 1996. Dynamics of marine ecosystems. Blackwell, London.

Maranon, E. 2009. Phytoplankton size structure. Encyclopedia of Ocean Sciences (2nd Edition), 445-452pp.

Mariotti A. 1983**.** Atmospheric nitrogen is a reliable standard for natural $\delta^{15}N$ abundance measurements, .*Nature* **303:** 685-687.

Martins, M. R., Leite, A. M. and Nunes, M. L. 1987. 'Peixe-espada-preto. Algumas notas acerca da pescaria do peixe-espada-preto (in Portuguese). Instituto Nacional de Investigaco das Pescas a (publicaces avulsas)', in. Instituto Nacional de Investigaco das Pescas a (publicaces avulsas), p. 14pp.

Mauchline, J. and Gordon, J. D. M. 1984. Occurrence and feeding of berycomorphid and percomorphid teleost fish in the Rockall Trough. *ICES Journal of Marine Science* **41**(3), pp. 239–247.

McCann, K. S., Rasmussen, J. B. and Umbanhowar, J. 2005. The dynamics of spatially coupled food webs. *Ecology Letters* **8**, pp. 513–523.

McCauley, D. J., Young, H. S., Dunbar, R. B., Estes, J. A., Semmens, B. X. and Micheli, F. 2012. Assessing the effects of large mobile predators on ecosystem connectivity. *Ecological Applications* **22**, pp. 1711–1717.

McClelland, J. W. and Montoya, J. P. 2002. Trophic Relationships and the Nitrogen Isotopic Composition of Amino Acids in Plankton. *Ecology* **83**(8), pp. 2173–2180.

McClelland, J. W., Valiela, I. and Michener, R. H. 1997. Nitrogen-stable isotope signatures in estuarine food webs: A record of increasing urbanization in coastal watersheds. *Limnology and Oceanography* **42**(5), pp. 930–937.

McFarlane, G. A. and King, J. R. 1979. Migration patterns of spiny dogfish (*Squalus acanthias*) in the North Pacific Ocean. *Fisheries Bulletin* **101**, pp. 358–367.

McMahon, K. W., Hamady, L. L. and Thorrold, S. R. 2013. A review of ecogeochemistry approaches to estimating movements of marine animals. *Limnology and Oceanography* **58**, pp. 697–714.

McMahon, K. W., Polito, M. J., Abel, S., McCarthy, M. D. and Thorrold, S. R. 2015. Carbon and nitrogen isotope fractionation of amino acids in an avian marine predator, the gentoo penguin (*Pygoscelis papua*). *Ecology and Evolution* **5**, pp. 1278–1290.

McMeans, B. C., Olin, J. A. and Benz, G. W. 2009. Stable-isotope comparisons between embryos and mothers of a placentatrophic shark species. *Journal of Fish Biology* **75**(10), pp. 2464–2474.

McNamara, J. M. and Houston, A. I. 1992. State-dependent life-history theory and its implications for optimal clutch size. *Evolutionary Ecology* **6**, pp. 70–185.

Mejuto, J. 1985. *Associated catches of Sharks, Prionace glauca, Isurus oxyrinchus, and Lamna nasus, with NW and N Spain Swordfish Fishery, in 1984*, *International Council for the Exploration of the Sea*. Edited by ICES. Copenhagen, Denmark.

Michener, R.H., Kaufman, L. 2007. Stable isotope ratios as tracers in marine food webs: an updateIn: Michener, R., Lajtha, K. (Eds.), Stable Isotopes in Ecology and Environmental Science, second ed. Blackwell Publishing Ltd., Oxford, pp. 238–278.

Minagawa, M. and Wada, E. 1984. Stepwise enrichment of ^{15}N along food chains: Further evidence and the relation between $\delta^{15}N$ and animal age. *Geochimica et Cosmochimica Acta* **48**(5), pp. 1135–1140.

Minson, D. J., Ludlow, M. M. and Troughton, J. H. 1975. Differences in natural carbon isotope ratios of milk and hair from cattle grazing tropical and temperate pastures. *Nature* **265**(602).

Morales-Nin, B. and Sena-Carvalho, D. 1996. Age and growth of the black scabbard fish (*Aphanopus carbo*) off Madeira. *Fisheries Research* **25**(3–4), pp. 239–251.

Morato, T., Watson, R., Pitcher, T. J. and Pauly, D. 2006. Fishing down the deep. *Fish and*

Fisheries **7**(1), pp. 24–34.

Morris, D. W. 1988. Habitat-dependent population regulation and community structure. *Evolutionary Ecology* **2**, pp. 253–269.

Morris, D. W. 1998. State dependent optimization of litter size. *Oikos* **83**, pp. 518–528.

Morris, D. W. 2003. Toward an ecological synthesis: A case for habitat selection. *Oecologia* **136**(1), pp. 1–13.

Mucientes, G. R., Queiroz, N., Sousa, L. L., Tarroso, P. and Sims, D. W. 2009. Sexual segregation of pelagic sharks and the potential threat from fisheries. *Biology letters* **5**(2), pp. 156–159.

Mullin, M. M., Rau, G. H. and Eppley, R. W. 1984. Stable nitrogen isotopes in zooplankton: some geographic and temporal variations in the North Pacific. *Limnology and Oceanography* **29**, pp. 1267–1273.

Munoz-Chapuli, R. 1984. Ethology of reproduction in some sharks from northern Atlantic. *Cybium* **8**(4), pp. 1–14.

Myers, R. A., Baum, J. K., Shepherd, T. D., Powers, S. P. and Peterson, C. H. 2007. Cascading effects of the loss of apex predatory sharks from a costal ocean. *Science* **315**, pp. 1846–1850.

Myers, R. A. and Worm, B. 2003. Rapid worldwide depletion of predatory fish communities. *Nature* **423**(6937), pp. 280–283.

Nakamura, I. and Parin, N. 1993. *Snake Mackerels and Cutlassfishes of the World (families Gempylidae and Trichiuridae): An Annotated and Illustrated Catalogue of the Snake Mackerels, Snoeks, Escolars, Gemfishes, Sackfishes, Domine, Oilfish, Cutlassfishes, Scabbardfishes, Hairtails, and F*. Food and Agriculture Organization of the United Nations.

Nammack, M. F. 1982. *Life History and Management of Spiny Dogfish, Squalus acanthias, off the Northeastern United States. Master's Thesis. College of William and Mary, Williamsburg, VA.*

Natanson, L. J., Gervelis, B. J., Winton, M. V., Hamady, L. L., Gulak, S. J. B. and Carlson, J. K. 2013. Validated age and growth estimates for *Carcharhinus obscurus* in the northwestern Atlantic Ocean, with pre- and post management growth comparisons. *Environmental Biology of Fishes* **97**(8), pp. 881–896. doi: 10.1007/s10641-013-0189-4.

Natanson, L. J., Mello, J. J. and Campana, S. E. 2002. Validated age and growh of the porbeagle shark, *Lamna nasus*, in the wester North Atlantic Ocean. *Collective Volume of Scientific Papers - ICCAT* **54**(4), pp. 1261–1279.

National Marine Fisheries Service. 2008. *Recovery Plan for the Steller Sea Lion (Eumetopias jubatus). Revision.*, *National Marine Fisheries Service, Silver Spring, MD. 325 pages.*

National Marine Fisheries Service. 2009. Endangered and Threatened Species; Designation of Critical Habitat for Atlantic Salmon (*Salmo salar*) Gulf of Maine Distinct Population Segment', pp. 1–37. *National Marine Fisheries Service, Silver Spring, MD. 62 pages*

Neat, F., Kynoch, R., Drewery, J. and Burns, F. 2010. *Deepwater trawl survey manual. Marine Scotland - Science Report 03/10*.

Neves, A., Vieira, A. R., Farias, I., Figueiredo, I., Sequeira, V. and Serrano Gordo, L. 2009. Reproductive strategies in black scabbardfish (*Aphanopus carbo* Lowe, 1839) from the NE Atlantic. *Scientia Marina* **73**(S2), pp. 19–31.

Newsome, S. D., Clementz, M. T. and Koch, P. L. 2010. Using stable isotope biogeochemistry to study marine mammal ecology. *Marine Mammal Science* **26**, pp. 509–572.

Newsome, S. D., Martinez del Rio, C., Bearhop, S. and Phillips, D. L. 2007. A niche for isotopic ecology. *Frontiers in Ecology and the Environment* **5**, pp. 429–436.

Ngochera, M. J. and Bootsma, H. A. 2011. Temporal trends of phytoplankton and zooplankton stable isotope composition in tropical Lake Malawi. *Journal of Great Lakes Research* **1**, pp. 45–53.

Nicol, J. A. C. 1989. *The Eyes of Fishes*. Oxford University Press.

Nielsen, J., Hedeholm, R. B., Heinemeier, J., Bushnell, P. G., Christiansen, J. S., Olsen, J., Ramsey, C. B., Brill, R. W., Simon, M., Steffensen, K. F. and Steffensen, J. F. 2016. Eye lens radiocarbon reveals centuries of longevity in the Greenland shark *Somniosus microcephalus*. *Science* **353**(6300), pp. 702–704.

Norton, S. L., Wiley, T. R., Carlson, J. K., Frick, A. L., Poulakis, G. R. and Simpfendorfer, C. A. 2012. Designating critical habitat for juvenile endangered smalltooth sawfish in the United States. *Marine and Coastal Fisheries* **4**(1), pp. 473–480.

O'Brien, D. M., Schrag, D. P. and Martinez del Rio, C. 2000. Allocation to reproduction in a hawkmoth: a quantitative analysis using stable carbon isotopes. *Ecology* **81**, pp. 2822–2831.

O'Leary, M. H. 1981. Carbon isotope fractionation in plants. *Phytochemistry* **20**:553-567.

Officer, R. A, Gason, A. S., Walker, T. I. and Clement, J. G. 1996. Sources of variation in counts of growth increments in vertebrae from gummy shark, (*Mustelus antarcticus*, and school shark, *Galeorhinus galeus*): implications for age determination. *Canadian Journal of Fisheries and Aquatic Sciences* **53**(8), pp. 1765–1777.

Oliveira, A. A. De, Ellis, J. R. and Dobby, H. 2013. Incorporating density dependence in pup production in a stock assessment of NE Atlantic spurdog *Squalus acanthias*. *ICES Journal of Marine Science* **70**(7), pp. 1341–1353.

Onthank, K. L. 2013. *Exploring the life histories of Cephalopods using stable isotope analysis of an archival tissue*. Washington State Univerity.

Owens, N. J. P. 1985. Variations in the natural abundance of $\delta^{15}N$ in estuarine suspended particulate matter: a specific indicator of biological processing. *Estuarine, Coastal and Shelf Science* **20**, pp. 505–510.

Owens, N. J. P. 1987. Natural variations in ^{15}N in the marine environment. *Advances Marine Biology* **24**, pp. 389–451.

Pade, N. G., Queiroz, N., Humphries, N. E., Witt, M. J., Jones, C. S., Noble, L. R. and Sims, D. W. 2009. First results from satellite-linked archival tagging of porbeagle shark, *Lamna nasus*: Area fidelity, wider-scale movements and plasticity in diel depth changes. *Experimental Marine Biology and Ecology* **370**(1–2), pp. 64–74.

Pajuelo, J. G., González, J. a., Santana, J. I., Lorenzo, J. M., García-Mederos, A. and Tuset, V. 2008. Biological parameters of the bathyal fish black scabbardfish (*Aphanopus carbo* Lowe, 1839) off the Canary Islands, Central-east Atlantic. *Fisheries Research* **92**(2–3), pp. 140–147.

Pannella, G. 1971. Fish Otoliths : Daily Growth Layers and Periodical Patterns. *American*

Association for the Advancement of Science **173**(4002), pp. 1124–1127.

Parry, M. 2003. *The trophic ecology of two Ommastrephid squid species, Ommastrephes bartramii and Sthenotheuthis oualaniensis, in the North Pacific sub-tropical gyre*, *PhD dissertation*. University of Hawaii-Manoa, Honolulu, HI.

Pauly, D., Christensen, V., Dalsgaard, J., Froese, R. and Torres Jr, F. 1998. Fishing down marine food webs. *Science* **279**(5352), pp. 860–863.

Pawson M. G. 1995. Biogeographical identification of English Channel fish and shellfish stocks. *Fisheries Research Technical Report Number 99*.

Pawson, M. G. and Ellis, J. R. 2005. Stock identity of elasmobranchs in the Northeast Atlantic in relation to assessment and management. *Journal of Northwest Atlantic Fishery Science* **35**, pp. 173–193.

Pawson, M. G., Ellis, J. R. and Dobby, H. 2009. 'The evolution and management of spiny dogfish (spurdog) fisheries in the Northeast Atlantic' in Biology and Management of Dogfish Sharks. Eds. Gallucci, V. F., Bargmann, G. G., McFarlane, G. American Fisheries Society: Bethesda, MD., pp. 373–390.

Perera, C. B. 2008. Distribution and Biology of black scabbardfish (*Aphanopus carbo* Lowe , 1839) in the Northwest of Africa. *Universidade de Lisboa, Faculdade de Ciencias, Departmento de Bioliga Animal*.

Perry, J. N., Liebhold, A. M., Rosenberg, M. S., Dungan, D., Miriti, M., Jakomulska, A. and Citron-Pousty, S. 2002. Illustrations and guidelines for selecting statistical methods for quantifying spatial pattern in ecological data. *Ecography* **25**(5), pp. 578–600.

Peterson, B. and Fry, B. 1987. Stable Isotopes in Ecosystem Studies. *Annual Review of Ecolog,, Evolution, and Systematics* **18**, pp. 293–320.

Philipson, B. 1969. Distribution of protein within the normal rat lens. *Investigative Ophthalmology and Visual Science* **8**(3), pp. 258–270.

Pilgrim, M. A. 2007. Expression of maternal isotopes in offspring: implications for interpreting ontogenetic shifts in isotopic composition of consumer tissues. *Isotopes in Environmental Health Studies* **43**, pp. 155–163.

Pinnegar, J. K. and Polunin, N. V. C. 1999. Differential fractionation of $\delta^{13}C$ and $\delta^{15}N$ among fish tissues : implications for the study of trophic interactions. *Functional Ecology* **13**, pp. 225–231.

Polis, G. A., Anderson, W. B. and Holt, R. D. 1997. Toward an integration of landscape and food web ecology: the dynamics of spatially subsidized food webs. *Annual Review of Ecology and Systematics* **28**, pp. 289–316.

Polunin, N.V.C., Morales-Nin, B., Pawsey,W.E., Cartes, J.E., Pinnegar, J.K., Moranta, J. 2001. Feeding relationships in Mediterranean bathyal assemblages elucidated by stable nitrogen and carbon isotope data. *Marine Ecology Progress Series* **220**, 13–23.

Popp, B. N., Takigiku, R., Hayes, J. M., Louda, J. W. and Baker, E. W. 1989. The Post-Paleozoic Chronology and Mechanism of 13C Depletion in Primary Marine Organic Matter. *American Journal of Science* **289**, pp. 436–454.

Popp, B. N., Laws, E. A., Bidigare, R. R., Dore, J. E., Hanson, K. L. and Wakeham, S. G. 1998.

Effect of phytoplankton cell geometry on carbon isotopic fractionation. *Geochimica et Cosmochimica Acta* **62**(1), pp. 69–77.

Popp, B. N., T. Trull, F. Kenig, S. G. Wakeham, T. M. Rust, B. Tilbrook, F. B. Griffiths, S. W. Wright, H. J. Marchant, R. R. Bidigare, and E. A. Laws. 1999. Controls on the carbon isotopic composition of Southern Ocean phytoplankton. *Global Biogeochemical Cycles* **13**:827-843.

Porter, M. E., Beltrán, J. L., Koob, T. J. and Summers, A. P. 2006. Material properties and biochemical composition of mineralized vertebral cartilage in seven elasmobranch species (Chondrichthyes). *Journal of Experimental Biology* **209**(15), pp. 2920–2928.

Post, D. M. 2002. Using stable isotopes to estimate trophic position: models, methods, and assumptions. *Ecology* **83**(3), pp. 703–718.

Purcell, J. E. 2003. Predation on zooplankton by large jellyfish, *Aurelia labiata*, *Cyanea capillata* and *Aequorea aequorea*, in Prince William Sound, Alaska. *Marine Ecology Progress Series*, **246**, pp. 137–152. doi: 10.3354/meps246137.

Purcell, J. E., Purcell, J. E., Sturdevant, M. V and Sturdevant, M. V. 2001. Prey selection and dietary overlap among zooplanktivorours jellyfish and juvenile fishes in Prince William Sound, Alaska. *Marine Ecology Progress Series*, **210**, pp. 67–83. doi: 10.3354/meps210067.

Rau, G. H., T. Takahashi, and D. J. D. Marais. 1989. Latitudinal variations in plankton $\delta_{13}C$ – implications for CO_2 and productivity in past oceans. *Nature* **341**:516-518.

Reum, J. C. P. 2011. Lipid correction model of carbon stable isotopes for a cosmopolitan predator, spiny dogfish *Squalus acanthias*. *Journal of fish biology* **79**, pp. 2060–6.

Ribeiro Santos, A., Trueman, C., Connolly, P. and Rogan, E. 2013. Trophic ecology of black scabbardfish, *Aphanopus carbo* in the NE Atlantic—Assessment through stomach content and stable isotope analyses. *Deep Sea Research Part I: Oceanographic Research Papers* **77**, pp. 1–10.

Richardson, A. J. and Schoeman, D. S. 2004. Climate impact on plankton ecosystems in the Northeast Atlantic. *Science* **305**(5690), pp. 1609–1612.

Riley, S. P. 2006. Spatial ecology of bobcats and gray foxes in urban and rural zones of a national park. *Journal of Wildlife Management* **70**(5), pp.1425-1435.

Roff, G., Doropoulos, C., Rogers, A., Bozec, Y., Krueck, N. C., Aurellado, E., Priest, M., Birrell, C. and Mumby, P. J. 2016. The Ecological Role of Sharks on Coral Reefs. *Trends in Ecology & Evolution,* pp. 1–13.

Rolff, C. 2000. Seasonal variation in $\delta^{13}C$ and $\delta^{15}N$ of size-fractionated plankton at a coastal station in the northern Baltic proper. *Marine Ecology Progress Series* **203**(1990), pp. 47–65.

Rosenfeld, J. S. and Hatfield, T. 2006. Information needs for assessing critical habitat of freshwater fish. *Canadian Journal of Fisheries and Aquatic Sciences* **63**(3), pp. 683–698. doi: 10.1139/f05-242.

Rosenzweig, M. L. 1981. A theory of habitat selection. *Ecology* **62**, pp. 327–335.

Rubenstein, D. R. and Hobson, K. A. 2004. From birds to butterflies: animal movement patterns and stable isotopes. *Trends in Ecology and Evolution* **19**, pp. 256–263.

Ruppert, J. L. W., Fortin, M. and Meekan, M. G. 2016. The Ecological Role of Sharks on Coral

Reefs : Response to Roff *et al*. *Trends in Ecology & Evolution* **31**, pp. 586–587.

Sackett, W. M., Eckelman.Wr, M. L. Bender, and A. W. H. Be. 1965. Temperature dependence of carbon isotope composition in marine plankton and sediments. *Science* **148**.

Salzman, J. 1990. Evolution and application of critical habitat under the Endangered Species Act. *Harvard Environmental Law Review* **14**(311), pp. 311–342.

Samelius, G., Alisauskas, R. T., Hobson, K. A. and Lariviere, S. 2007. Prolonging the arctic pulse: long-term exploitation of cached eggs by arctic foxes when lemmings are scarce. *Journal of Animal Ecology* **76**, pp. 873–8.

Saunders, R. A., Royer, F. and Clarke, M. W. 2011. Winter migration and diving behaviour of porbeagle shark, *Lamna nasus*, in the Northeast Atlantic. *ICES Journal of Marine Science* **68**(1), pp. 166–174.

Schartau, J. M., Sjögreen, B., Gagnon, Y. L. and Kröger, R. H. H. 2009. Optical plasticity in the crystalline lenses of the cichlid fish *Aequidens pulcher*. *Current biology* **19**(2), pp. 122–6.

Schell, D. M., Saupe, S. M. and Haubenstock, N. 1989. 'Natural Isotope Abundances in Bowhead Whale (*Balaena mysticetus*) Baleen: Markers of Aging and Habitat Usage' in *Stable Isotopes in Ecological Research*, pp. 260–269.

Schloesser, R. W., Neilson, J. D., Secor, D. H. and Rooker, J. R. 2010. Natal origin of Atlantic bluefin tuna (*Thunnus thynnus*) from Canadian waters based on otolith d13C and d18O. *Canadian Journal of Fisheries and Aquatic Sciences* **67**, pp. 563–569.

Secor, D. H., Enderson-Arzapalo, A. and Piccoli, P. M. 1995. Can otolith microchemistry and habitat utilization chart patterns of migration in anadromous fishes? *Journal of Experimental Marine Biology and Ecology* **192**(1), pp. 15–33.

Secor, D. H. and Piccoli, P. M. 2007. Oceanic migration rates of Upper Chesapeake Bay striped bass (*Morone saxatilis*), determined by otolith microchemical analysis. *Fishery Bulletin* **105**, pp. 62–73.

Shepherd, T., Page, F. and Macdonald, B. 2002. Length and sex-specific associations between spiny dogfish (*Squalus acanthias*) and hydrographic variables in the Bay of Fundy and Scotian Shelf. *Fisheries Oceanography* **11**(2), pp. 78–89.

Sigman, D. M., and K. L. Casciotti. 2001. Nitrogen isotopes in the ocean. Page 2449 *in* J. H. Steele, K. K. Turekian, and S. A. Thorpe, editors. Encyclopedia of Ocean Sciences. Academic, London, UK.

Smit, A. J. 2001. Source identification in marine ecosystems: food web studies using $d^{13}C$ and $d^{15}N$., in Unkovich MJ, Pate JS, McNeil AM, G. J. (eds) (ed.) *Stable isotope techniques in the study of biological processes and functioning of ecosystems*. Kluwer Academic, Dordrecht, pp. 219–245.

Smith, B. N. and Epstein, S. 1970. Biogeochemistry of the Stable Isotopes of Hydrogen and Carbon in Salt Marsh Biota. *Plant Physiology* **46**, pp. 738–742.

Stafanni, S., Bettencourt, R., Knutsen, H. and Menezes, G. 2009. Rapid polymerase chain reaction–restriction fragment length polymorphism method for discrimination of the two Atlantic cryptic deep-sea species of scabbardfish. *Molecular Ecology Resources* **9**(2).

Stefanni, S. and Knutsen, H. 2007. Phylogeography and demographic history of the deep-sea

fish *Aphanopus carbo* (Lowe, 1839) in the NE Atlantic: vicariance followed by secondary contact or speciation? *Molecular Phylogenetics and Evolution* **41**(1), pp. 38–46.

Stenberg, C. 2005. Life history of the piked dogfish (*Squalus acanthias* L.) in Swedish waters. *Journal of Northwest Atlantic Fishery Science* **35**, pp. 155–164.

Sturrock, A. M., Trueman, C. N., Darnaude, A., M and Hunter, E. 2012. Can otolith elemental chemistry retrospectively track migrations in fully marine fishes? *Journal of fish biology* **81**(2), pp. 766–95.

Swan, S. C., Gordon, J. D. M. and Shimmield, T. 2003. Preliminary Investigations on the Uses of Otolith Microchemistry for Stock Discrimination of the Deep-water Black Scabbardfish (*Aphanopus carbo*) in the North East Atlantic. *Journal of Northwest Atlantic Fishery Science* **31**, pp. 221–231.

Switzer, P. V. 1993 Site fidelity in predictable and unpredictable habitats. *Evolutionary Ecology* **7**, 533–555.

Tagliabue, A. and Bopp, L. 2008. Towards understanding global variability in ocean carbon-13. *Global Biogeochemical Cycles* **22**, pp. 1–13.

Tallack, S. M. L. and Mandelman, J. W. 2009. Do rare-earth metals deter spiny dogfish? A feasibility study on the use of electropositive "mischmetal" to reduce the bycatch of *Squalus acanthias* by hook gear in the Gulf of Maine. *ICES Journal of Marine Science* **66**(2), pp. 315–322.

Templeman, W. 1976. Transatlantic migrations of spiny dogfish (*Squalus acanthias*). *Journal of the Fisheries Research Board of Canada* **33**(11), pp. 2605–2609.

Thorrold, S. R., Campana, S. E., Jones, C. M. and Swart, P. K. 1997. Factors determining $\delta^{13}C$ and $\delta^{18}O$ fractionation in aragonitic otoliths of marine fish. *Geochimica et Cosmochimica Acta* **61**, pp. 2909–2919.

Tieszen, L. L., Boutton, T. W., Tesdahl, K. G. and Slade, N. A. 1983. Fractionation and turnover of stable carbon isotopes in animal tissues: implications for $\delta^{13}C$ analysis of diet. *Oecologia* **57**, pp. 32–37.

Tilman, D. and Kareiva, P.M. eds., 1997. *Spatial ecology: the role of space in population dynamics and interspecific interactions* (Vol. 30). Princeton University Press.

Törnroth-Horsefield, S., Hedfalk, K., Fischer, G., Lindkvist-Petersson, K. and Neutze, R. 2010. Structural insights into eukaryotic aquaporin regulation. *Federation of European Biochemical Societies Letter*s **584**(12), pp. 2580–8.

Trueman, C. N., Johnston, G., Hea, B. O. and Mackenzie, K. M. 2014. Trophic interactions of fish communities at midwater depths enhance long-term carbon storage and benthic production on continental slopes. *Proceedings of the Royal Society B* **281**(1787)

Trueman, C. N., MacKenzie, K. M. and Palmer, M. R. 2012. Identifying migrations in marine fishes through stable-isotope analysis. *Journal of Fish Biology* **87**(2), pp. 826–847.

Trueman, C. N., MacKenzie, K. M. and St John Glew, K. 2016. Stable isotope-based location in a shelf sea setting: accuracy and precision are comparable to light-based location methods. *Methods in Ecology & Evolution* **8**(2), pp. 232-240.

Trueman, C. N., Rickaby, R. E. M. and Shephard, S. 2013. Thermal, trophic and metabolic life

histories of inaccessible fishes revealed from stable-isotope analyses: a case study using orange roughy *Hoplostethus atlanticus*. *Journal of Fish Biology* **83**(6), pp. 1613–36.

Tucker, R. 1985. Age validation studies on the spines of the spurdog (*Squalus acanthias*) using tetracyclined. *Journal of the Marine Biological Association of the United Kingdom* **65**(3), pp. 641–651.

Tuross, N., Fogel, M. L. and Hare, P. 1988. Variability in the preservation of the isotopic composition of collagen from fossil bone. *Geochimica et Cosmochimica Acta* **52**(4), pp. 929–935.

Vaghefi, E., Walker, K., Pontre, B.P., Jacobs, M.D., Donaldson, P. J. 2012. Magnetic resonance and confocal imaging of solute penetration into the lens reveals a zone of restricted extracellular space diffusion. *American Journal of Physiology - Regulatory, Integrative and Comparative Physiology* **302**(11).

Vandeperre, F., Aires-da-Silva, A., Fontes, J., Santos, M., Serrão Santos, R. and Afonso, P. 2014. 'Movements of Blue Sharks (*Prionace glauca*) across their life history. *PloS one* **9**(8), e103538.

Vandeperre, F., Aires-da-Silva, A., Lennert-Cody, C. E., Serrão Santos, R. and Afonso, P. 2016. Essential pelagic habitat of juvenile blue shark (*Prionace glauca*) inferred from telemetry data. *Limnology and Oceanography* **61**, pp. 1605–1625.

Vander Zanden, M. J., Clayton, M. K., Moody, E. K., Solomon, C. T. and Weidel, B. C. 2015. Stable Isotope Turnover and Half-Life in Animal Tissues : A Literature Synthesis. *PLoS ONE* pp. 1–16, e0116182.

Vander Zanden, M. J. and Rasmussen, J. B. 1999. Primary consumer $\delta^{13}C$ and $\delta^{15}N$ and the trophic position of aquatic consumers. *Ecology* **80**, p. 139501404.

Vanderklift, M. a and Ponsard, S. 2003. Sources of variation in consumer-diet delta ^{15}N enrichment: a meta-analysis. *Oecologia* **136**(2), pp. 169–82.

Vaudo, J. J., Matich, P. and Heithaus, M. R. 2010. Mother-offspring isotope fractionation in two species of placentatrophic sharks. *Journal of Fish Biology* **77**(7), pp. 1724–7.

Veríssimo, A., McDowell, J. R. and Graves, J. E. 2010. Global population structure of the spiny dogfish *Squalus acanthias*, a temperate shark with an antitropical distribution. *Molecular ecology* **19**(8), pp. 1651–62. doi: 10.1111/j.1365-294X.2010.04598.x.

Vince, M. R. 1991. Stock identity in spurdog (*Squalus acanthias* L.) around the British Isles. *Fisheries Research* **12**, pp. 341–354.

Vinogradov, M. E. 1997. Some problems of vertical distribution of meso- and macroplankton in the ocean. *Advances in Marine Biology* **32**, pp. 1–92.

Voss, M., Dippner, J. W. and Montoya, J. P. 2001. Nitrogen isotope patterns in the oxygen-deficient waters of the Eastern Tropical North Pacific Ocean. *Deep-Sea Research* **48**:1905–1921.

Waas, S., Werner, R. A. and Starch, J. M. 2010. Fuel switching and energy partitioning during the postprandial metabolic response in the ball python (*Python regius*). *Journal of Experimental Biology* **213**, pp. 1266–1271.

Wada, E., Mizutani, H. and Minagawa, M. 1991. The use of stable isotopes for food web

analysis. *Critical reviews in Food Science and Nutrition* **30**(4), pp. 361–371.

Wallace, A. A., Hollander, D. J. and Peebles, E. B. 2014. Stable isotopes in fish eye lenses as potential recorders of trophic and geographic history. *PloS one* **9**(10), p. e108935.

Werner, E. E. and Gillam, J. F. 1984. The ontogenetic niche and species interactions in size-structured populations. *Review of Ecology, Evolution and Systematics* **15**, pp. 393–425.

Werry, J. M., Lee, S. Y., Otway, N. M., Hu, Y. and Sumpton, W. 2011. A multi-faceted approach for quantifying the estuarine - nearshore transition in the life cycle of the bull shark, *Carcharhinus leucas*. *Marine and Freshwater Research* **62**(12), p. 1421.

West, J. B., G. J. Bowen, T. E. Dawson, and K. P. Tu, editors. 2010. Isoscapes: Understanding Movement, Pattern, and Process on Earth through Isotope Mapping. Springer Science, Berlin.

Wiley, T. R. and Simpfendorfer, C. A. 2007. The ecology of elasmobranchs occurring in the Everglades National Park, Florida: implications for conservation and management. *Bulletin of Marine Science* **80**, 171–189.

Wong, W. W. and W. M. Sackett. 1978. Fractionation of stable carbon isotopes by marine phytoplankton. *Geochimica Et Cosmochimica Acta* **42**:1809-1815.

Wood, C. C., Ketchen, K. S. and Beamish, R. J. 1979. Population Dynamics of Spiny Dogfish (*Squalus acanthias*) in British Columbia Waters. *Journal of the Fisheries Research Board of Canada* **36**, pp. 647–656.

Wourms, J. P. 1977. Reproduction and development in Chondrichthyan fishes. *American Zoologist* **17**:379–410.

Wourms, J. P. 1981. Viviparity: maternal-fetal relationships in fishes. *American Zoologist* **21**:473–515.

Wourms, J. P., Grove, B. D., Lombardi, J. 1988. The maternal-embryonic relationship in viviparous fishes. In: Hoar WS, Randall DJ, editors. Fish physiology, vol. IXB. San Diego: Academic Press. p 1–134.

Wunder, M. B. 2010. Using isoscapes to model probability surfaces for determining geographic origins. Pages 251-270 *in* J. B. West, G. J. Bowen, T. E. Dawson, and K. P. Tu, editors. Isoscapes: Understanding Movement, Pattern, and Process on Earth through Isotope Mapping. Springer Science, Berlin.

Wunder, M. B., and Norris, D. R. 2008. Analysis and design for isotope-based studies of migratory animals *in* K. A. Hobson and L. I. Wassenaar, editors. Tracking Animal Migration with Stable Isotopes

Yahner, R. H., 1988. Changes in wildlife communities near edges. *Conservation biology* **2**(4), pp.333-339.

Zilanov, V. K. and Shepel, L. I. 1975. Notes on the ecology of black scabbardfish *Aphanopus carbo*, of the North Atlantic. *Journal of Ichthyology* **51**(4), pp. 661–663.

Zohary, T., Erez, J., Gophen, M., Berman-Frank, I. and Stiller, M. 1994. Seasonality of stable carbon isotopes within the pelagic food web of Lake Kinneret. *Limnology and Oceanography* **39**(5), pp. 1030–1043.